DEVELOPMENT OF A PASSIVE SAMPLING STRATEGY FOR MONITORING OF ORGANIC POLLUTANTS AND THEIR IMPACTS IN AQUATIC SYSTEMS

A Thesis Submitted to the
College of Graduate and Postdoctoral Studies
In Partial Fulfillment of the Requirements
For the Degree of Doctor of Philosophy
In the School of Environmental and Sustainability of
the University of Saskatchewan
Saskatoon, Saskatchewan, Canada

BY

XIAOWEN JI

PERMISSION TO USE

In presenting this thesis in partial fulfillment of the requirements for a Postgraduate degree from the University of Saskatchewan, I agree that the Libraries of this University may make it freely available for inspection. I further agree that permission for copying of this thesis/dissertation in any manner, in whole or in part, for scholarly purposes may be granted by the professor or the Dean of the College in which my thesis work was done. It is understood that any copying or publication or use of this thesis or parts thereof for financial gain shall be given to me and to the University of Saskatchewan in any scholarly use which may be made of any material in my thesis.

DISCLAIMER

This thesis was exclusively created to meet the thesis and/or exhibition requirements for the degree of Doctor of Environment and Sustainability at the University of Saskatchewan. Any reference in this thesis to any specific commercial products, process, or service by trade name, trademark, manufacturer, or otherwise, does not constitute or imply its endorsement, recommendation, or favoring by the University of Saskatchewan. The views ad opinions of the author expressed herein do not state or reflect those of the University of Saskatchewan and shall not be used for advertising or product endorsement purposes. Requests for permission to copy or to make other uses of materials in this thesis/dissertation in whole or part should be addressed to:

Chair of the School of Environment and Sustainability Program
117 Science Place
University of Saskatchewan
Saskatoon, Saskatchewan, S7N 5B3, Canada

OR

Dean
College of Graduate and Postdoctoral Studies
University of Saskatchewan
116 Thorvaldson Building, 110 Science Place
Saskatoon, Saskatchewan S7N 5C9 Canada

ABSTRACT

Anthropogenic organic compounds are constantly released into the freshwater environment, demanding a better knowledge of the chemical status of our Earth's surface waters and sediments. Conventional water quality monitoring only provides "snapshots" of information in time and space. Passive sampling has been proposed as an *in-situ* time integrative sampling technique to offer better monitoring of the chemical status of our environment. In this thesis, the diffusive gradient in thin films (DGT) technique is introduced because the DGT passive sampler allows for assessing time-weighted average concentrations of various organic contaminants with minimal hydrodynamic influence.

This thesis first reviewed the available literature on the potential limitations of DGT samplers. This review summarized the current configurations of the DGT samplers for organics, storage stability of analytes in DGT samplers, kinetic desorption of organic contaminants in sediments and at the interface of water and sediment, and combinations of DGT samplers and bioassays. This review identified two critical gaps: (*i*) there are only limited studies for desorption kinetics of organic contaminants, especially for hydrophilic to moderately hydrophobic compounds, at the interface of water and sediment; and (*ii*) there are no studies so far for predicting bioavailability in aquatic biota by *in situ* DGT technique. Based on these gaps, the objectives of this thesis are to (1) develop DGT samplers that can be applied for the monitoring of organic contaminants across the water-sediment interface in the field with an efficient time; (2) describe the kinetic equilibrium of compounds between sediments and overlying water using a dynamic model; and (3) use DGT-derived concentrations to predict bioaccumulation of organic

contaminants by invertebrates through *in-situ* and laboratory-controlled experiments.

First, this research conducted a 30-day laboratory simulation experiment, where DGT samplers were tested for adsorption performance and then were deployed in sediments spiked with nine model antipsychotic compounds, i.e., amitriptyline, bupropion, carbamazepine, citalopram, clozapine, duloxetine, fluoxetine, lamotrigine, and venlafaxine. A dynamic model, DGT-induced fluxes in soils and sediments (DIFS), was used to reveal the dynamic resupply processes of organic contaminants from the solid phase to the aqueous phase. This experiment showed that antipsychotics could be continuously depleted from the sediment aqueous phase and captured by the DGT binding gel. The highest resupply ability was observed for lamotrigine and carbamazepine. The adsorption process took control of the spiked sediments under laboratory conditions during incubation time.

Second, DGT devices were *in situ* deployed at the sediment−water interface and in sediments, downstream of the Saskatoon Wastewater Treatment Plant, on the South Saskatchewan River. Apart from the DIFS model, a dynamic fraction transfer model was also developed to consider the real status of organic contaminants in sediments during field deployment. The field experiment revealed that positive fluxes of antipsychotics were found from sediment to overlying water and the desorption process was dominant within a 15 cm depth of sediments. The results from the three-fraction transfer model can be auxiliary to further explain dynamic desorption kinetics calculated by the DIFS model.

Third, another 30-day laboratory-controlled experiment, where the benthic oligochaete *Lumbriculus variegatus* was exposed to freshwater sediments spiked with nine antipsychotic compounds, and DGT samplers were synchronously deployed, was conducted to develop a

numerical model for passive bioaccumulation using DGT-derived concentrations. Passive uptake of antipsychotic compounds by the benthic oligochaetes could be successfully modeled by inputting the diffusion-induced concentrations measured by DGT samplers in water and sediments. Fast desorption to the labile fraction of analytes in a short response time accounted for the process of uptake by oligochaetes.

Fourth, DGT devices were *in situ* deployed at a wastewater-impacted site for 20 days to develop a predictive bioaccumulation model by comparison between the modeled concentration using DGT-derived concentrations in water and those in resident benthic invertebrates, specifically crayfish (*Faxonius virilis*). The results showed that targeted antipsychotics could be constantly resupplied to the interstitial water and absorbed by crayfish. DGT techniques with a steady-state uptake model in the current study for crayfish could provide a close prediction compared to the measured concentrations for some compounds while it still needs further developments to predict different organic compounds. This thesis has the potential to transform the DGT technique to efficiently monitor emerging contaminants and evaluate their bioavailability in the aquatic cycle, and help protect the safety of our water resources for human and environmental health.

Keywords: Organic contaminants, passive sampling, in-situ monitoring, aquatic environment, diffusive gradient in thin films, DGT

ACKNOWLEDGEMENT

Finally, I would like to thank God, my parents, and all my friends who have sustained me through all my study time, the best and toughest years of my life. Also, thanks to pastor George Hind from Lutheran Campus Centre, for good prayers, meetings, and generous food every Tuesday evening.

TABLE OF CONTENTS

CHAPTER 4: DGT technique and sequential extraction approach to investigate *in situ*

desorption kinetics of emerging organic contaminants at the sediment−water interface

LIST OF TABLES

LIST OF FIGURES

LIST OF ABBREVIATIONS

WWTPs: Wastewater Treatment Plants

CECs: Contaminants of Emerging Concern

LLE: Liquid-liquid extraction

GC: Gas Chromatography

LC: Liquid Chromatography

MS: Mass Spectrometer

SDGs: Sustainable Development Goals

TWACs: Time-Weighted Average Concentrations

DGT: Diffusive Gradient in Thin Films

DET: Diffusion Equilibrium in Thin Films

Log K_{ow}: Log Octanol/Water Partition Coefficient

PES: Polyethersulfone

PTFE: Polytetrafluoroethylene

MCE: Mixed Cellulose Ester

GHP: Hydrophilic Polypropylene

PC: 0.2 μm Nucleopore Track-Etched Polycarbonate

PC1: 0.2 μm Cyclopore Track-Etched Polycarbonate

PC2: 0.015 μm Nucleopore Track-Etched Polycarbonate

CN: Cellulose Nitrate

CA: Cellulose Acetate

NL: Nylon

PVDF: Polyvinylidene Fluoride

POCIS: Polar Chemical Integrative Sampler

DIFS: DGT-Induced Fluxes in Soils/Sediments

R: Ratio

MDLs: Method Detection Limits

LOQ: Limits of Quantitation

LOD: Limits of Detection

S/N: Signal/Noise

DO: Dissolved Oxygen

DOC: Dissolved Organic Carbon

UHPLC: Ultra High Pressure Liquid Chromatography

TCEP: Tris(2 chloroethyl) Phosphate

TCPP: Tris(chloropropyl) Phosphate

TPrP: Tripropyl Phosphate

TDCPP: Tris(1,3-dichloro-2-propyl) Phosphate

TBP: Tributyl Phosphate

QSARs: Quantitative Structure–Activity Relationships

ERE: Estrogen Responsive Element

CALUX: Chemically Activated LUciferase Gene eXpression

MWHC: Maximum Water Holding Capacity

ABS: Acrylonitrile Butadiene Styrene

IS: Internal Standard

LIST OF APPENDICES

PREFACE

This thesis is organized and formatted to follow the University of Saskatchewan College of Graduate Studies and Postdoctoral Research guidelines for a manuscript-style thesis. Therefore, there is some repetition between the content presented in each chapter. Chapter 1 contains general information about the research background and current problems. Chapter 2 is a critical review for a general introduction and to analyze current published data for current study gaps that were set as the objectives of the current study. Chapters 2−6 are organized as a manuscript for publication in a peer-reviewed scientific journal and a description of author contributions is provided in the preface of each chapter. Chapters 2−6 have already been published. All published supplementary materials to Chapters 2 to 6 have been included in the Appendix section at the end of this thesis. Chapter 7 is a general discussion about the study gaps filled by this study, the application of this study, and further needed study. References cited were included at the end of this thesis.

CHAPTER 1: General introduction

1.1 Introduction and background

Water quality has been impacted by point and nonpoint sources of contamination in urban and rural regions. Some of these sources are wastewater effluents, agricultural runoff, and industrial discharges that often contain chemicals that can adversely affect aquatic ecosystems and human health (Khatri and Tyagi, 2015). Many of these chemicals are present in the environment at trace concentrations ranging from ng L^{-1} to μg L^{-1}, also known as micropollutants. However, some of these micropollutants can accumulate in the aquatic environment over time with latently adverse effects on aquatic ecosystems and human health (Vasquez et al., 2014; Ribeiro et al., 2016). Some organic micropollutants in the aquatic environment have become a concern due to their low volatility, lipophilicity, low biodegradation, and high bioaccumulation potential (Chen et al., 2011; Valili et al., 2013). Although most industrial and domestic wastewater can be treated in wastewater treatment plants (WWTPs) before discharge, many of these micropollutants were poorly removed (Deblonde et al., 2011). Because many of these micropollutants cannot be easily degraded in the water body, these micropollutants are persistent in aquatic ecosystems (Boreen et al., 2003). Exposure to some of these organic micropollutants (e.g., estrogens) can lead to aquatic system degradation and human health issues such as endocrine disruption and cancer (Nanseu-Njiki et al., 2010). Therefore, continuous monitoring of organic micropollutants is crucial for policymakers to take precautionary actions to prevent the potential risk to the environment and

human health.

The number of studies concerning the environmental analysis of organic pollutants, e.g., pesticides, pharmaceuticals, and personal care products in the aquatic environment, is continually increasing (Godoy et al., 2015; Sorensen et al., 2015; Barbosa et al., 2016). However, environmental analysis of micropollutants is a complex issue due to the complexity of different matrices, various chemical properties of the analytes, and their occurrence at trace levels (Ribeiro et al., 2015). Therefore, reliable quantification of micropollutants in environmental samples often demands that sample concentrations need to be increased before analysis (i.e., pre-concentration by extraction from bulk water samples). As opposed to more traditional methods to achieve this, passive sampling techniques are based on an *in-situ* accumulation of analytes within a binding phase during an environmental medium exposure. Passive sampling strategies are particularly suitable because they are simple to use and have low costs, compared to grab sampling with high costs of labor and energy, to determine a wide variety of compounds of interest (Vrana et al., 2005; Kot-Wasik et al., 2007). Besides, passive sampling methods minimize sample treatment procedures and save energy (Armenta et al., 2017). However, each passive technique also has its drawbacks to overcome and can be combined with other approaches to assess the chemical effects on the aquatic ecosystem.

1.2 Water quality threats

Water quality concerns are linked to many problems that humankind is encountering (UN-Water, 2009). Industrial and agricultural activities, as well as urban developments, significantly impact aquatic ecosystems. These activities can cause pollution of water by releasing various

synthetic and organic chemical substances into the environment. Chemical contamination of the natural aquatic environment has now become a significant threat globally (Raghav et al., 2019). Water bodies polluted by agricultural, industrial, and urban runoff, as well as municipal wastewater, can endanger drinking water security and negatively affect aquatic organisms (Verhougstraete et al., 2015; Beiras, 2018). The levels of pesticides (e.g., commonly detected triazines in US rivers) can exceed ecotoxicological effect thresholds for aquatic biota and maximum allowable levels for surface waters (Gilliom, 2007). Therefore, an effective monitoring system for pollutants in water over time is key to better controlling pollution sources and ensuring water security.

In addition to some of the well-studied chemicals, contaminants of emerging concern (CECs) have only recently been detected in the aquatic environment and are continuously being released due to various anthropogenic activities (Patel et al., 2020). Toxicity information for many CECs, e.g., pharmaceuticals, personal care products, pesticides, etc., is often unavailable, and they enter the aquatic environment predominantly because WWTPs cannot effectively eliminate them (Wilkinson et al., 2017). Furthermore, CECs are often found in the environment yet biologically active at low concentrations, usually in the ng L^{-1} range, making them practically untraceable using conventional analytical methods (Wilkinson et al., 2017). Therefore, establishing better strategies for monitoring these micropollutants in the aquatic environment is essential to protect ecosystems and human health (Geissen et al., 2015).

1.3 Strategies for monitoring pollution

1.3.1 Chemical analysis

To measure the occurrence of organic micropollutants that typically occur at low concentrations in the aquatic environment, high-precision instruments, e.g., gas or liquid chromatography with mass spectrometry (GC-MS or LC-MS), are required (Bucheli et al., 1997; Öllers et al., 2001; Vanderford et al., 2003; Benotti et al., 2009). These instruments have been reported to be able to   detect trace organic contaminants concentrated from different matrices at the ng L^{-1} level (Hao et al., 2007). Both GC-MS and LC-MS have advantages and disadvantages; knowing this is of central significance for selecting the applicable analysis techniques to acquire the best data. The superior method is highly dependent on the sample's complexity (Hao et al., 2007). Polar organic compounds are soluble either in water or polar organic solvents (e.g., methanol), which merits LC-MS analysis. Nonpolar organic compounds are more soluble and better extracted in nonpolar organic solvents (e.g., dichloromethane). GC-MS is highly effective in analyzing nonpolar organic compounds at very low levels present in different environmental media.

Reliable sample preparation is indispensable for both GC-MS and LC-MS analysis. The vital first step in the sample preparation procedure is extraction. Liquid-liquid extraction (LLE) and solid-phase extraction (SPE) are effective means of extracting water samples. LLE is a reliable (Mottaleb, 2015) yet time and reagent-consuming procedure and cannot easily be automated. Thus, SPE has been developed as an alternative technique. Compared to other pre-extraction methods, SPE requires fewer reagents and provides better recoveries with minimal mass

transfer (Rezaee et al., 2006). Although SPE has advantages, it does not always perform well because some compounds can significantly adhere to the surfaces of sample containers and glassware due to their physicochemical characteristics. This adherence may lead to a certain loss of the analyte (Płotka-Wasylka et al., 2015). On the contrary, LLE allows that solvent can directly come into contact with the laboratory container walls. Thus, analytes that adhere to the sample container walls are rinsed and captured in this method.

1.3.2 Conventional sampling strategies

The majority of aquatic monitoring methods are based on grab or spot sampling of water at a fixed time (Vrana et al., 2005). Often, where pollutants are present at only trace levels, large volumes of water need to be collected. The subsequent laboratory analysis of the obtained water samples will only provide a snapshot of pollutant levels at a single sampling time. However, pollutant concentrations can vary considerably over time. Therefore, accidental pollution events, such as spills, may get missed. One way to solve this problem is to sample water frequently or set up automatic sampling systems to obtain and ideally refrigerate multiple water samples over long periods. This solution is expensive and impractical in many conditions. A safe and accessible location and pre-treatment of water are required before chemical analysis. Consequently, such systems are hardly applied in comprehensive monitoring campaigns. Last, the detected concentrations of contaminants using spot sampling may be different between methodologies because of variations in the applied pre-treatments before chemical analysis (e.g., filtration and concentration) (Madrid and Zayas, 2007) and do not provide data on the dissolved or bioavailable fraction of the pollutants.

1.3.3 Time-integrated sampling

In the last two decades, another option has been proposed to avoid many of the problems outlined above for traditional monitoring strategies: the application of passive samplers, i.e., devices that passively sample dissolved chemicals from bulk water. Passive sampling techniques can offer *in situ* pre-concentrated samples and derive time-weighted average concentrations (TWACs) rather than snapshots in time. Generally, passive samplers consist of a binding phase that allows for the binding and concentration of targeted chemicals within a device safely deployed in the environment. Passive samplers have three advantages: they (1) have little or no moving parts, (2) require no power to operate, and (3) can sample over prolonged durations (hours to days to months).

Organic contaminants in the aquatic environment have been sampled by various devices, including the Membrane-Enclosed Sorptive Coating (MESCO) (Vrana et al., 2001), Semi-Permeable Membrane Device (SPMD) (Sabaliūnas and Södergren, 1997), Polar Organic Chemical Integrative Sampler (POCIS) (Alvarez et al., 2004), and Chemcatcher (Charriau et al., 2016). These sampling devices differ predominantly in the sorbent of the binding phase. However, many passive samplers (such as SPMD and POCIS) are affected by environmental factors, e.g., water temperature, flow velocity, and biofouling (Harman et al., 2012; Fauvelle et al., 2017). Thus, sampling rates required for the estimation of TWACs can vary among different waterbodies sampled (Alvarez et al., 2004; Buzier et al., 2006; Li et al., 2010; Guibal et al., 2017). Calibration of sampling rates is time-consuming and costly, and their measurement cannot usually be optimized for each passive sampling system. For example, the sampling rate of different compounds depends not only on environmental conditions (e.g., water temperature

and salinity range) but also on their chemical structures (Togola and Budzinski, 2007). As a result, sampling rates measured in the laboratory only consider "normal" conditions for TWAC estimation, while significant inaccuracies may arise when deployed in the field (Challis et al., 2018b; Buzier et al., 2019). Previous research indicates that an increase in water flow velocity might result in a 2-fold increase in the sampling rate of the POCIS sampler (Alvarez et al., 2004). Other studies reported a similar increase in the POCIS sampling rate when the temperature increased from 5 to 25 °C (Togola and Budzinski, 2007; Harman et al., 2012).

To overcome the problem of variable sampling rates, a new passive sampling technique, the diffusive gradient in thin films (DGT) technique (**Figure 1.1**), was developed and first applied for inorganic compounds by integrating a diffusive layer into the sampling device (Davison and Zhang, 1994). Bondarenko et al. (2011) first adapted this design for organic compounds in soils. This diffusive layer (hydrogel) limits the chemical mass transfer rate from the environment into the sampler to the diffusive flux across this layer. Therefore, the device's sampling rate is dominated by the compound's mass transfer rate imposed by this limiting phase. The DGT technique can be further developed as a tool for risk assessment in aquatic systems. Detailed information on the DGT technique can be found in Chapter 2.
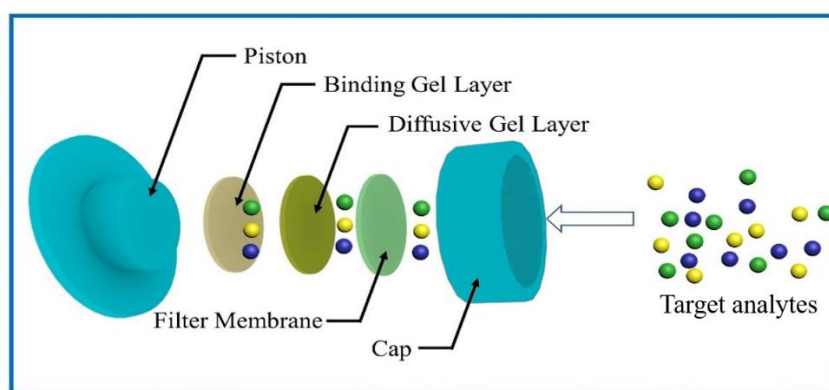
Figure 1.1 Structural sketch of a DGT device. Left: exploded diagram, consisting of an outer shell (a piston and a cap), a binding gel, a diffusive gel, and a filter membrane.

1.4 Objectives of the current thesis

Developing an advanced passive sampling approach to support future monitoring of emerging contaminants in water and sediment is a key goal, as currently, various references employ different methodologies for sampling and analysis with a wide range of performances. This makes it difficult for environmental decision-makers to use published monitoring data to decide which new candidate substances may be included in forthcoming proposals for water and sediment monitoring or need to be controlled. To solve this issue, this thesis aims to fill gaps in our knowledge and address important challenges in efficiently and reliably monitoring water quality and conducting protective chemical risk assessments in a simple and economical way. The major objective of this thesis was to develop the DGT technique to *in situ* assess the dynamic fate of emerging contaminants and the magnitude of bioaccumulation by aquatic biota. Specifically, this objective contained (1) a summary and analysis of all accessible data from current publications concerning the DGT technique used for organic contaminants in aquatic environments in order to better focus on current significant gaps of DGT deployment for monitoring emerging contaminants from a perspective of whole aquatic system; (2) development of DGT devices for water and sediments, spiking with nine analytes, i.e., antipsychotic compounds (amitriptyline, bupropion, carbamazepine, citalopram, clozapine, duloxetine, fluoxetine, lamotrigine, and venlafaxine) that were previously detected in water and sediments in South Saskatchewan River and present different ionization states in different pH water environments, to test first in laboratory-controlled condition; (3) the deployment of tested DGT devices in natural river and establishment of a model to quantify desorption kinetics of different physically binding states of contaminants with sediments; (4) establishment of a model

to predict bioaccumulation of contaminants by aquatic organisms through the DGT-derived concentrations in water and sediments.

Objectives 1-4 correspond to chapters 2-6 that have been published, listed below:

- **Objective 1, Chapter 2:**

Xiaowen Ji, Catherine Estefany Davila Arenas, Ana Sharelys Cardenas Perez, John P. Giesy, Markus Brinkmann. Predicting kinetics of resupply of organic pollutants from sediments, using diffusive gradients in thin films (DGT) samplers and their bioavailability to aquatic invertebrates. *Environmental Toxicology and Chemistry*, 2023, 42, 1696-1708. Published: 7 June 2023. DOI: https://doi.org/10.1002/etc.5681

- **Objective 2, Chapter 3:**

Xiaowen Ji, Jenna Cantin, Ana S. Cardenas Perez, Yufeng Gong, John P.Giesy, Markus Brinkmann. Combining passive sampling with fraction transfer and toxicokinetic modeling to assess bioavailability of organic pollutants in a benthic invertebrate, *Lumbriculus variegatus*. *Journal of Hazardous Materials*, 2023, 441, 129986. Published: 5 January 2023. DOI: https://doi.org/10.1016/j.jhazmat.2022.129986

- **Objective 3, Chapter 4:**

Xiaowen Ji, Jonathan K. Challis, Jenna Cantin, Ana S. Cardenas Perez, Yufeng Gong, John P. Giesy, Markus Brinkmann. A novel passive sampling and sequential extraction approach to investigate desorption kinetics of emerging organic contaminants at the sediment−water interface. *Water Research,* 2022, 217, 118455. Published: 15 June 2022. DOI: https://doi.org/10.1016/j.watres.2022.118455

- **Objective 4, Chapters 4&5:**

Xiaowen Ji, Jonathan K. Challis, Jenna Cantin, Ana S. Cardenas Perez, Yufeng Gong, John P. Giesy, Markus Brinkmann. Desorption kinetics of antipsychotic drugs from sandy sediments by diffusive gradients in thin-films technique. *Science of The Total Environment*, 2022, 832, 155104. Published: 1 August 2022. DOI: https://doi.org/10.1016/j.scitotenv.2022.155104

Xiaowen Ji, Jonathan K. Challis, Markus Brinkmann. A critical review of diffusive gradients in thin films technique for measuring organic pollutants: Potential limitations, application to solid phases, and combination with bioassays. *Chemosphere*, 2022, 287, Part 3, 132352. Published: January 2022. DOI: https://doi.org/10.1016/j.chemosphere.2021.132352

1.5 Contributions to environment and sustainability

Water security has become a major global challenge in the 21st century. The United Nations defines water security as "the capacity of a population to safeguard sustainable access to adequate quantities of acceptable quality water for sustaining livelihoods, human well-being, and socio-economic development, for ensuring protection against water-borne pollution and water-related disasters, and for preserving ecosystems in a climate of peace and political stability, Page vi" (UN-Water, 2009). Moreover, securing water for humans and the environment is crucial for sustainable development and achieving the United Nations Sustainable Development Goals (SDGs), e.g., Goal 3–Good Health, Goal 6–Clean Water and Sanitation, and Goal 14–Life Below Water (https://sdgs.un.org/goals). Although most aquatic ecosystems possess the natural tendency to dilute contamination to some extent, severe contamination of water bodies can cause changes in flora and fauna in the local communities (Bashir et al., 2020). In addition, water contamination did not receive enough attention until the negative consequences appeared on aquatic ecosystems and human health when exceeding the threshold levels (Halpern et al., 2008). For example, the discharge of chemical contaminants into the aquatic environment at levels below their individual thresholds for acute effects, which often form the basis of guideline values, can still have long-term or chronic effects, e.g., endocrine-disrupting effects (Diamanti-Kandarakis et al., 2009). Such contamination may pose a risk to water security, with non-identifiable effects on the ecosystems, or secondary damage to food webs in the form of minor disturbances that can be observed over a long period. Therefore, solutions to address the challenges of water security cannot be based on a single shared concept or perception.

So far, over 350,000 chemicals have been registered for production and use worldwide (Wang et al., 2020b). The majority of these emerging contaminants are not under government regulation and might have long-term effects with chronic exposures to the aquatic biota at low concentrations when they are released into the aquatic environment (Diamanti-Kandarakis et al., 2009). This causes a great challenge to obtaining water security and the SDGs of the United Nations for sustainable use of water resources. Currently, grab sampling is still the most common way to sample samples from water bodies and bottom sediments for monitoring water contamination. However, when it comes to environmental impacts and socio-economic issues, this method requires a large amount of manpower resources, and costs to analyze samples, and disturbs the samples themselves (e.g., sediment cores). With these limitations, this method often cannot reflect a time-dependent result in an economic way. The advantages of the DGT passive sampling technique can significantly contribute to SDGs and water security for humans and the environment and can be a useful tool for water security. Specifically, the developed DGT technique in this thesis can better assess the presence of emerging contaminants in the aquatic environment with several advantages of (*i*) contamination situations over time, (*ii*) commercially accessible and low cost, (*iii*) easy use in water and sediments, e.g., DGT devices can be deployed in remote regions, where residents do not need specific training, for monitoring episodic changes in contaminant concentrations, (*iv*) minimum interferences during the deployment in the field, and (*v*) DGT-derived models to predict bioaccumulation and potential second-release from sediments. This technique can partially overcome economic scarcity for monitoring water security, particularly in areas where contaminant concentration is not constant or an integrated measurement is needed for water monitoring and regulatory purposes.

CHAPTER 2: A critical review of diffusive gradients in thin films technique for measuring organic pollutants: potential limitations, application to solid phases, and combination with bioassays

Overview

A version of this chapter has been published in *Chemosphere* with the following details:

Contributions

Xiaowen Ji: Summary and analysis references and manuscript writing.

Jonathan K. Challis: Providing suggestions, offering raw data from one of his publications, and editing the manuscript.

Markus Brinkmann: Revising the manuscript.

Abstract

The diffusive gradient in thin films (DGT) for organics has received considerable attention for studying the chemical dynamics of various organic pollutants in the environment. This review investigates the current limitations of DGT for organics and identifies several research gaps for future studies. The application of a protective outer filter membrane has been recommended for most DGT applications, however, important questions regarding longer lag times due to significant interaction or adsorption of specific groups of compounds on the outer membrane remain. A modified DGT configuration has been developed that uses the diffusive gel as the outer membrane without the use of an extra filter membrane, however use of this configuration, while largely successful, remains limited. Biofouling has been a concern when using DGT for metals; however, the effect on the performance of DGT for organics needs to be systemically studied. Storage stability of compounds on intact DGT samplers has been assessed in select studies and that data is synthesized here. DGT has been used to describe the kinetic desorption of antibiotics from soils and biosolids based on the soil/biosolid physical-chemical characteristics, yet applications remain limited and require further research before wide-scale adoption is recommended. Finally, DGT for organics has only rarely, albeit successfully, been combined with bioassays as well as *in vivo* bioaccumulation studies in zebrafish. Studies using DGT combined with bioassays to predict the adverse effects of environmental mixtures on aquatic or terrestrial biota are discussed here and should be considered for future research.

Keywords: Diffusive gradients in thin films (DGT), organic-DGT, organic pollutants, limitations, bioassays

2.1 Introduction

Anthropogenic activities have led to significant contamination in the aquatic and terrestrial environment (Rhind, 2009; Khatri and Tyagi, 2015). Some trace metal species and micropollutants such as pharmaceuticals and personal care products, pesticides, and flame retardants, to name only a few, have been shown to pose a threat to environmental and human health (Rainbow, 2002; Kim and Zoh, 2016). Conventional wastewater treatment plants (WWTPs) are typically not designed to remove organic micropollutants, and thus, their elimination by WWTPs is often limited (Larsen et al., 2004). Consequently, these degradation-resistant micropollutants are frequently detected in WWTP effluents, surface waters, drinking water, sediments, and irrigated soils (Vieno and Sillanpää, 2014; Vodyanitskii and Yakovlev, 2016). Due to the low levels of these compounds present in environmental samples and the complexity of environmental matrices, appropriate pre-concentration is required prior to chemical analysis. Additionally, their emission patterns are often highly dynamic, making traditional grab or spot sampling of water at a fixed time challenging. To overcome these limitations, passive sampling strategies have been developed. These are based on the *in situ* accumulation of analytes within a binding phase during exposure to bulk environmental media and can be used to derive time-weighted average concentrations (TWACs). Another advantage is that they are simple to use and have relatively low associated costs (Kot-Wasik et al., 2007).

Organic micropollutants in the aquatic environment can be sampled using a wide variety of passive sampling devices (Guibal et al., 2019). There has been an increasing interest in developing diffusive gradients in thin films (DGT) samplers since the concept was initially

15

described in the 1990s (Davison and Zhang, 1994; Zhang and Davison, 1995). There are now more than 1,100 peer-reviewed publications concerning the configuration, calibration, and field application of DGT samplers for environmental monitoring and research in water, soils, and sediments, and 42 publications concerning DGT for organic compounds. In comparison to other passive samplers for organic compounds such as Polar Chemical Integrative Sampler (POCIS) and Chemcatcher®, chemical uptake (sampling rates) in DGT is typically less influenced by temperature or water flow velocity (Bondarenko et al., 2011). This has resulted in an organic-DGT sampler with more accurate *in situ* sampling rates and therefore smaller uncertainties compared to POCIS and Chemcatcher® (Poulier et al., 2014; Buzier et al., 2019). Although the majority of these publications address heavy metals or other inorganic substances, the DGT sampler or DGT-based passive probe for soil or sediment has recently been adapted to sample various organic compounds from the aqueous phase of soil (Bondarenko et al., 2011) and in natural waters (Chen et al., 2012). Since these initial publications, DGT samplers have been applied to sample an extensive range of organic compound classes (Challis et al., 2016; Guibal et al., 2017; Guo et al., 2017a; Chen et al., 2018; Wang et al., 2019), including personal care products, household chemicals, pesticides, pharmaceuticals, illicit drugs, hormones, organophosphorus flame retardants, bisphenols, perfluoroalkyl substances, and endocrine-disrupting chemicals. Among 142 compounds tested so far, pharmaceuticals are the most frequently studied compounds.

To date, several review papers have been published covering the various available passive sampling techniques. Vrana et al. (2005) reviewed passive sampling technologies for environmental monitoring of waterborne inorganic and organic pollutants (6 and 21 devices,

respectively) and put forward several future trends for organic compounds, including: (*i*) miniaturization of passive sampling devices to decrease consumption of solvents during sample processing and for deployment applications with limited space and volume of water (e.g., in groundwater borehole); (*ii*) passive samplers need to be adapted to a wider range of chemicals (e.g., low to high polarity); (*iii*) reduction or control of the effects of environmental conditions and biofouling on the sampler performance; (*iv*) development of quality assurance, quality control, and method validation schemes for acceptance in regulatory programs. Davison and Zhang (2012) systematically reviewed the progress regarding DGT development and limitations. Recently, Taylor et al. (2020) reviewed passive samplers for monitoring polar pesticides in water and compared DGT with POCIS and Chemcatcher®. The authors highlighted major advantages of DGT including the utilization of the thick hydrogel diffusive layer to reduce the impact of an aqueous boundary layer on sampling rates and the hydrogel binding layer that maintains a constant distribution of sorbent material across the surface area of the sampler. The authors discussed two major drawbacks to be addressed in future research: (*i*) reducing the influence of environmental conditions (e.g., water flow rate) on the performance of DGT can sacrifice sensitivity (i.e., lower sampling rates) compared to Chemcatcher® and POCIS; (*ii*) enlarging the sampler to increase sampling rates will be limited by the strength of the hydrogels. Additionally, Guibal et al. (2019) provided a detailed review of DGT for organic compounds concerning theory, configuration, robustness, and field applications. Common among these reviews is the concern around DGT sensitivity as a result of the comparatively small sampling rates, often resulting in calls to scale up DGT samplers. While these concerns are valid in theory, to our knowledge there is no study to systematically demonstrate fewer

analyte detections in situ by DGT compared to other co-deployed samplers (e.g., POCIS and Chemcatcher®). On the contrary, many studies have demonstrated sufficient sensitivity and comparable analyte detections in DGT compared to POCIS and grab sampling (Challis et al., 2016; Challis et al., 2018b; Chen et al., 2018; Stroski et al., 2018; Challis et al., 2020; Wang et al., 2021). Further research is needed to address the concerns regarding sensitivity and the need to scale up DGT to increase sampling rates.

The present review focuses on the limitations of DGT for organic compounds that have not yet been reviewed in other review articles, specifically focusing on issues regarding the potential adsorption of compounds to the outer filter membrane, the deployment of DGT for organic contaminants in environmental media (e.g., soils, biosolids, and sediments), storage of DGT samplers, and the potential for combining DGT with biological test methods. Papers concerning DGT for organic compounds were selected according to the focused questions outlined above.

2.2 DGT basic configuration

The DGT device is an evolution of a similar device named the diffusion equilibrium in thin-films (DET) device introduced by Davison and Zhang (1994). The DGT device comprises (*i*) a gel layer containing a binding adsorbent that serves as a solute sink, (*ii*) a hydrated diffusion gel segregating it from the water phase, and (*iii*) a filter membrane for protection (**Figure 1.1**). The standard DGT device has an exposure area of 3.1 cm^2, while some studies have expanded the area to 12.6 cm^2 (Mechelke et al., 2019) and 22.7 cm^2 (Urík and Vrana, 2019). This device creates a hydrogel (diffusion layer) with a well-defined thickness (e.g., 0.75–2.00 mm for

agarose gel) (Guibal et al., 2019), which is significantly thicker than the thickness of the diffusive boundary layer (e.g., for polar organic compounds, 0.22 ± 0.11 mm at 2.4 cm/s flow velocity and 0.75 ± 0.19 mm under static condition) (Challis et al., 2016) and the filter membrane (e.g., PES membrane ≈ 0.16 mm), allowing DGT measurements to be quite insensitive to hydrodynamic fluctuations in the water. A number of subsequent refinements of this basic configuration can extend the application domain of DGT to various groups of organic pollutants by embedding suitable binding agents into the receiving phase gel and optimizing outer filter membranes.

2.3 Potential limitations of current DGT configurations for organic compounds

2.3.1 Uptake of organic compounds by the filter membrane

The filter membrane physically holds the diffusive gel and binding gel in place and is designed to minimize the adhesion of particles, physical damage, biological interference, and biofouling. However, a range of filter membrane materials used for DGT have been observed to suppress or slow the uptake of organic compounds in water (Guibal et al., 2019; Taylor et al., 2020). Therefore, the choice of filter membrane material needs to consider two aspects: (*i*) the potential interaction between target analytes and the filter membrane; and (*ii*) the impact biofouling and field conditions may have on the outer membrane. Some filter membranes used in DGT for hydrophilic and hydrophobic organic compounds (log octanol/water partition coefficient, log K_{ow} = 0.8–9.5) have been tested for potential interactions with target analytes, including polyethersulfone (PES), hydrophilic polytetrafluoroethylene (PTFE), mixed cellulose

ester (MCE), hydrophilic polypropylene (GHP), 0.2 μm nucleopore track-etched polycarbonate (PC), 0.2 μm cyclopore track-etched polycarbonate (PC1), 0.015 μm nucleopore track-etched polycarbonate (PC2), cellulose nitrate (CN), cellulose acetate (CA), nylon (NL) and polyvinylidene fluoride (PVDF). The most frequently used filter membrane configuration for DGT is PES, followed by PTFE. The number of analytes tested with different DGT filter membranes is shown in order (Chen et al., 2012; Zheng et al., 2015; Challis et al., 2016; Chen et al., 2017; Guo et al., 2017a; Guo et al., 2017b; Chen et al., 2018; Guan et al., 2018; Zhang et al., 2018; Zou et al., 2018; Wang et al., 2019; You et al., 2019; Fang et al., 2021; Iuele et al., 2021; Li et al., 2021a; Liu et al., 2021): PES (45) > PTFE (41) > NL (34) > GHP (19) > CA / PC (18) > MCE (13) > CN / PC1 / PC2 (11) > PVDF (1). Most studies determined the fraction adsorbed (%), i.e., the ratio between mass of analytes in the membrane and total mass in the initial solution and mass adsorbed (μg) per filter membrane area; these results are summarized in **Figure 2.1–2.5** for different filter membrane materials.

2.3.2 PES membrane

PES membranes are polymeric membranes widely used for separation applications because of their mechanical strength, thermal stability, and chemical inertness (Ran, 2015). PES membrane behaves as an inert and stable membrane in water and acts only as a barrier in the separation process. Therefore, PES has been widely used in the early development of other passive samplers, such as POCIS (Alvarez et al., 2004) and Chemcatcher (Kingston et al., 2000). The main drawback of the PES membrane is its relatively hydrophobic character (Omidvar et al., 2015). Thus, PES membranes may have a potential influence on more hydrophobic

compounds when it is used as an outer filter membrane. However, some relatively hydrophilic

compounds, e.g., atrazine and diazinon (Log K_{ow} = 2.60 and 3.81, respectively), accumulated

in the PES membrane at double the amount compared to the adsorbent of Chemcatcher after 7-

day exposures (Alvarez et al., 2004) and significantly high amounts of diuron (Log K_{ow} = 2.68)

was found in the PES membrane of Chemcatcher (Tran et al., 2007). Similarly, significant

absorption of PES membranes for various organic chemicals used in DGT was observed

(**Figure 2.1A**).

Although PES membranes appeared to be more likely to adsorb hydrophobic compounds

(fraction adsorbed > 20%), high fractions adsorbed were shown for some hydrophilic

compounds, e.g., norfloxacin, ofloxacin, pefloxacin, ciprofloxacin, enrofloxacin, tris(2-

chloroethyl) phosphate, methylparaben, estriol, tris(2-chloroisopropyl) phosphate, and tri-*n*-

propyl phosphate (**Figure 2.1A**). Liu et al. (2021) found that five fluoroquinolones (norfloxacin,

ofloxacin, pefloxacin, ciprofloxacin, and enrofloxacin) have over 28% fraction adsorbed to the

PES membrane, which brings into question the accuracy of results obtained by Chen et al. (2013)

who used the DGT device with the PES membrane for the same fluoroquinolones. However,

Chen et al. (2013) did not conduct adsorption experiments for the PES membrane but followed

the previous DGT configuration that was only checked for adsorption of sulfamethoxazole on

the PES membrane (Chen et al., 2012). Liu et al. (2021) mentioned that the contradiction of

results for adsorption by membranes might also be caused by differences in membrane

fabrication when obtaining them from different manufacturers. These results highlight

difficulties in using previously published adsorption results and suggest that the usability of

filter membranes in DGT configurations for different organic compounds needs to be verified.

More notably, significant differences in fractions adsorbed of ~10% and ~58% for tris(2-chloroethyl) phosphate were observed by Wang et al. (2019) and Zou et al. (2018), respectively. Interestingly, similar sorption experiments were conducted for both studies allowing comparisons between the two. Wang et al. (2019) measured PES adsorption of analytes in 25 mL 0.01 M NaCl solutions containing 200 µg L^{-1} analytes for 6 h with horizontal shaking. The differences in methods used by Zou et al. (2018) were volume (10 mL), spiking concentration (100 μg L^{-1}), and experimental duration (24 h). Wang et al. (2019) observed the sorption equilibrium of tris(2-chloroethyl) phosphate within 6 h. However, different results observed by Zou et al. (2018) showed 50-60% adsorption of tris(2-chloroethyl) phosphate to PES after 24 h. For further discussion of the two studies and comparison of the same tested analytes, we assume that both datasets were allowed to reach equilibrium and that no other losses occurred during the experiments so that mass only partitioned between filter membrane and water. The mass concentration on the filter (q) can be calculated as

$$q = \frac{V\,(C_i - C_f)}{m_s} \quad (2.1)$$

where V is the solution volume (L), C_i and C_f are the initial and final aqueous concentrations (μg L^{-1}), and m_s is the mass of the filter (μg). It should be noted that m_s is not given in the current studies. Assuming the mass loss was only from the solution to the filter membrane, the equation can be converted to Eq. (2.2):

$$q = \frac{V \times C_i \times adsorption\ rate}{m_s} \quad (2.2)$$

The equilibrium partition coefficient can be determined as

$$K_{eq} = \frac{q}{C_f} \quad (2.3)$$

A Langmuir isotherm can be written as

$$K_{eq} = \frac{q}{c_f} = \frac{q_{max}K_L}{1+K_LC_e} \quad (2.4)$$

Where q_{max} is the maximum adsorption capacity and K_L is the Langmuir equilibrium constant.

For reaching equilibrium, assuming $C_f = C_e$. When $K_LC_e \ll 1$, the Langmuir isotherm approximates linear partitioning, whereas $K_LC_e \gg 1$, a maximum adsorption plateau is reached.

$$K_{eq} = \frac{q}{c_f} = \frac{q_{max}K_L}{1+K_LC_e}$$
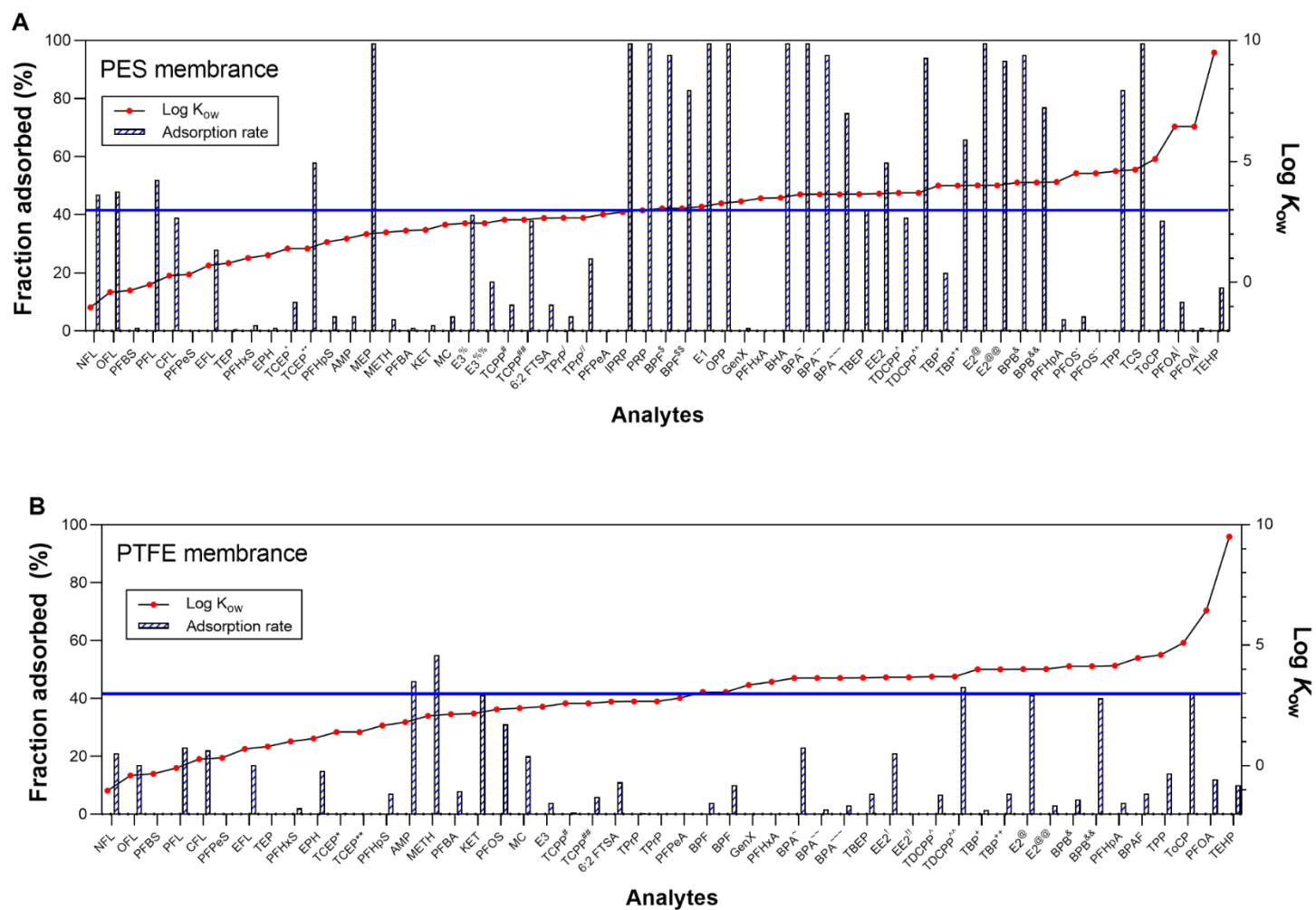
Figure 2.1 Summarized fraction adsorbed (%) of tested organic compounds by polyethersulfone (PES) membrane (**A**) and polytetrafluoroethylene (PTFE) membrane (**B**) used in the DGT devices. It is plotted as increasing log octanol-water partition coefficient (log K_{ow}) values of tested analytes. The blue line represents the Log K_{ow} value of 3.

Abbreviations for analytes: NFL[1]: norfloxacin, OFL[1]: ofloxacin, PFBS[2]: perfluorobutane sulfonate, PFL[1]: pefloxacin, CFL[1]: ciprofloxacin, PFPeS[2]: perfluoropentane sulfonate, EFL[1]: enrofloxacin, TEP[3]: triethyl phosphate, PFHxS[2]: perfluorohexane sulfonate, EPH[4]: ephedrine, TCEP[*]/ TCEP[**3/5]: tris(2-chloroethyl) phosphate, PFHpS[2]: perfluoroheptane sulfonate, AMP[6]: amphetamine, MEP[7]: methylparaben, METH[6]: methamphetamine, PFBA[2]: perfluorobutanoic acid, KET[6]: ketamine, MC[4]: methcathinone, E3[%]/E3[%%8/9]: estriol, TCPP[#]/TCPP[##3/5]: tris(2-chloropropyl) phosphate, 6:2 FTSA[2]: 6:2 fluorotelomer sulfonic acid, TPrP[/]/ TPrP[//3/5]: tri-n-propyl phosphate, PFPeA[2]: perfluoropentanoic acid, IPRP[7]: isopropylparaben, PRP[7]: propylparaben, BPF[$]/BPF[$$10/9]: bisphenol F, E1[8]: estrone, OPP[7]: ortho-phenylphenol, GenX[2]: hexafluoropropylene oxide dimer ammonium salt, PFHxA[2]: prerfluorohexanoic acid, BHA[7]: butylated hydroxyanisole, BPA[~]/ BPA[~~]/ BPA[~~~9/8/10]: bisphenol-A, TBEP [5]:Tris(2-butoxyethyl) phosphate, EE2[9]: 17α-ethinylestradiol, TDCPP[^]/ TDCPP[^^3/5]: Tris(1,3-dichloro-2-propyl) phosphate, TBP[+]/TBP[++3/5]: tributyl phosphate, E2[@]/ E2[@@8/9]: β-estradiol, BPB[&]/BPB[&&10/9]: bisphenol B, PFHpA[2]: perfluoroheptanoic acid, PFOS[-]/ PFOS[--2/11]: perfluorooctane sulfonate, TPP[3]: triphenyl phosphate, TCS[7]: triclosan, ToCP[3]: tri-o-cresyl phosphate, PFOA[‖]/ PFOA[‖2/11]: perfluorooctanoic acid, TEHP[3]: tris(2-ethylhexyl) phosphate, and BPAF[12]: bisphenol AF. It should be noted that log K_{ow} values of PFOA and PFOS originated from Rodea-Palomares et al. (2012) whereas they are surface-active compounds. In a biphasic system, these surfactants will aggregate in multi-layers or micellar structures yielding colloidal dispersed solutions rather than a partition equilibrium. Therefore, log K_{ow} values of PFOA and PFOS may have uncertainties. The data were collected by [1]Liu et al. (2021), [2]Fang et al. (2021), [3]Wang et al. (2019), [4]Zhang et al. (2018), [5]Zou et al. (2018), [6]Guo et al. (2017a), [7]Chen et al. (2017), [8]Chen et al. (2018), [9]Li et al. (2021a), [10]Zheng et al. (2015), [11]Guan et al. (2018), and [12]Iuele et al. (2021).

Because the 0.45 μm PES membrane used by Wang et al. (2019) and Zou et al. (2018) was

obtained from Pall Corporation (NY, US), the mass of the filter membrane can be assumed to

be equal. Thus, simply plotting the mass adsorbed per mass of filter membrane *vs.* C_f can reveal

more information on the adsorption isotherm for the two studies (**Figure 2.2**). From **Figure 2.2**,

several pieces of information can be obtained: (*i*) contact time for tri(2-chloroethyl) phosphate

and tris(chloropropyl) phosphate could reach equilibrium within 6 h due to the comparable

adsorbed masses for 24 h (Zou et al., 2018) and 6 h (Wang et al., 2019) and might follow a

Langmuir isotherm with $q_{max} \approx 0.5$ μg and $K_L \approx 0.7$ L μg^{-1}. (*ii*) The q values of tri(1,3-

dichloro-2propyl) phosphate and tributyl phosphate calculated by Wang et al. (2019) were

apparently higher than those calculated by Zou et al. (2018), which might be because

equilibrium was not reached for Wang et al. (2019). (*iii*) The equilibrium status was reached in

6 h for tripropyl phosphate with $q_{max} = 0.25$ μg. Even though these studies compared the same

set of analytes, direct comparisons are still difficult based on the chemical fraction adsorbed

(%) since the adsorption tests had different parameters, e.g., the volume of spiked solution, and

the equilibrium aqueous concentration (C_f). C_f can be obtained by rearranging Eq. (2.2) and

(2.4) to Eq. (2.5), written as

$$Fraction\ adsorbed\ (\%) = \frac{q_{max}m_s}{q_{max}m_s + \frac{V}{K_L} + VC_f} \quad (2.5)$$

where the fraction adsorbed is dependent on the Langmuir isotherm values (q_{max} and K_L), the

aqueous volume (V), and the equilibrium aqueous concentration (C_f). If the filter membrane is

the same type from the same manufacturer, the values of q_{max} and K_L can be assumed to be

constant. Therefore, the larger value of V and C_f used in Wang et al. (2019) led to a lower

fraction adsorbed compared to that in Zou et al. (2018). Considering this, part of the data (some

studies did not give all parameters for calculation) has been replotted by mass adsorbed normalized by filter area (**Figure 2.3A**). From **Figure 2.3A**, q values of bisphenol-A (0.99 μg) and β-estradiol (0.99 μg) tested for 24 h from Chen et al. (2018) were lower than those of bisphenol-A (2.25 μg) and β-estradiol (2.79 μg) tested for 36 h from Li et al. (2021a). The q value of bisphenol (0.95 μg) tested for 6 h from Zheng et al. (2015) was similar to that from Chen et al. (2018). These data showed that both bisphenol-A and β-estradiol did not reach adsorption equilibrium within at least 24 h.
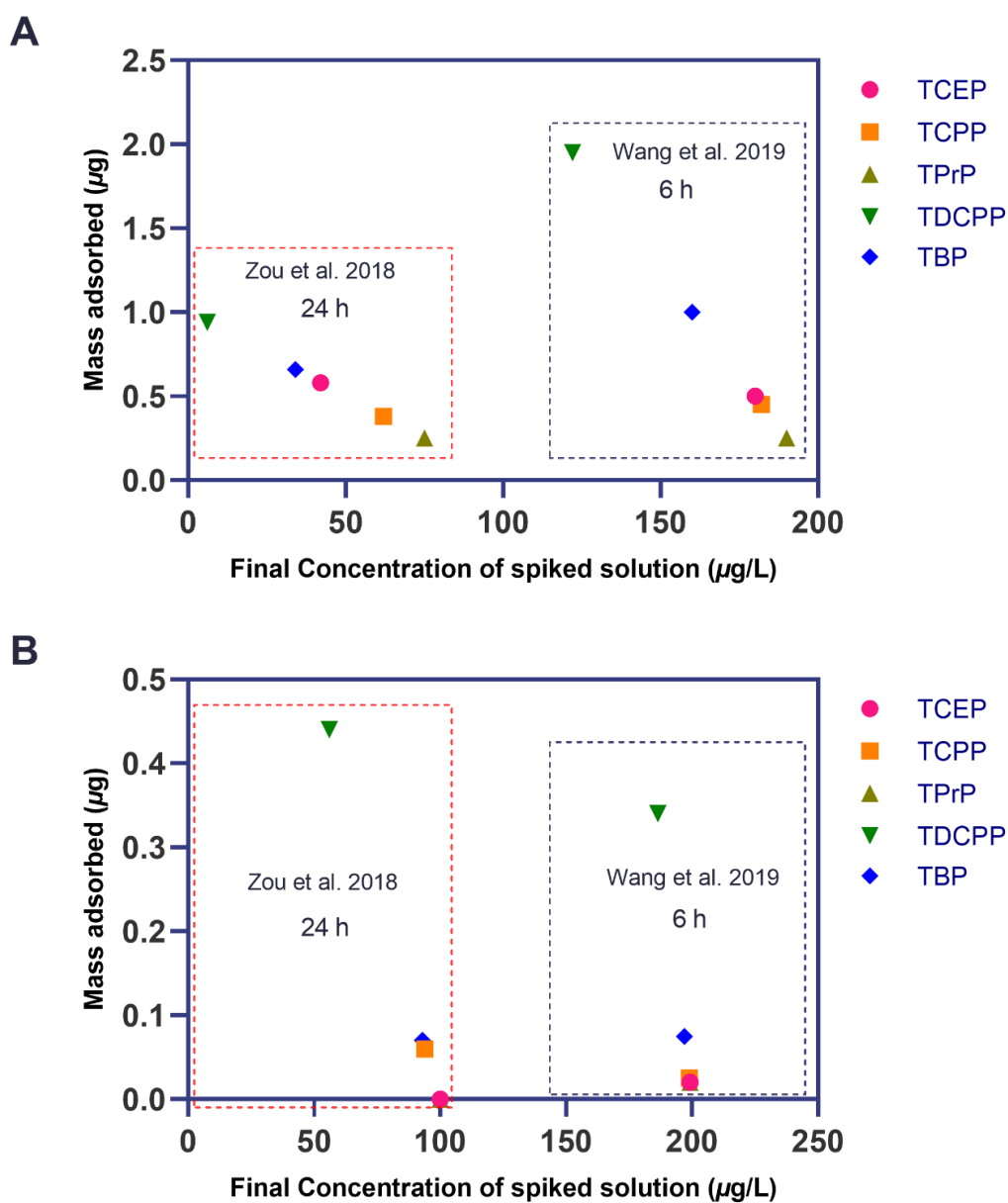
Figure 2.2 The plot of mass adsorbed by PES/PTFE filter membrane (**A/B**) vs. the final aqueous concentrations for tris(2 chloroethyl) phosphate (TCEP), tris(chloropropyl) phosphate (TCPP), tripropyl phosphate (TPrP), tris(1,3-dichloro-2-propyl) phosphate (TDCPP), and tributyl phosphate (TBP). The data were obtained from Zou et al. (2018) and (Wang et al., 2019).
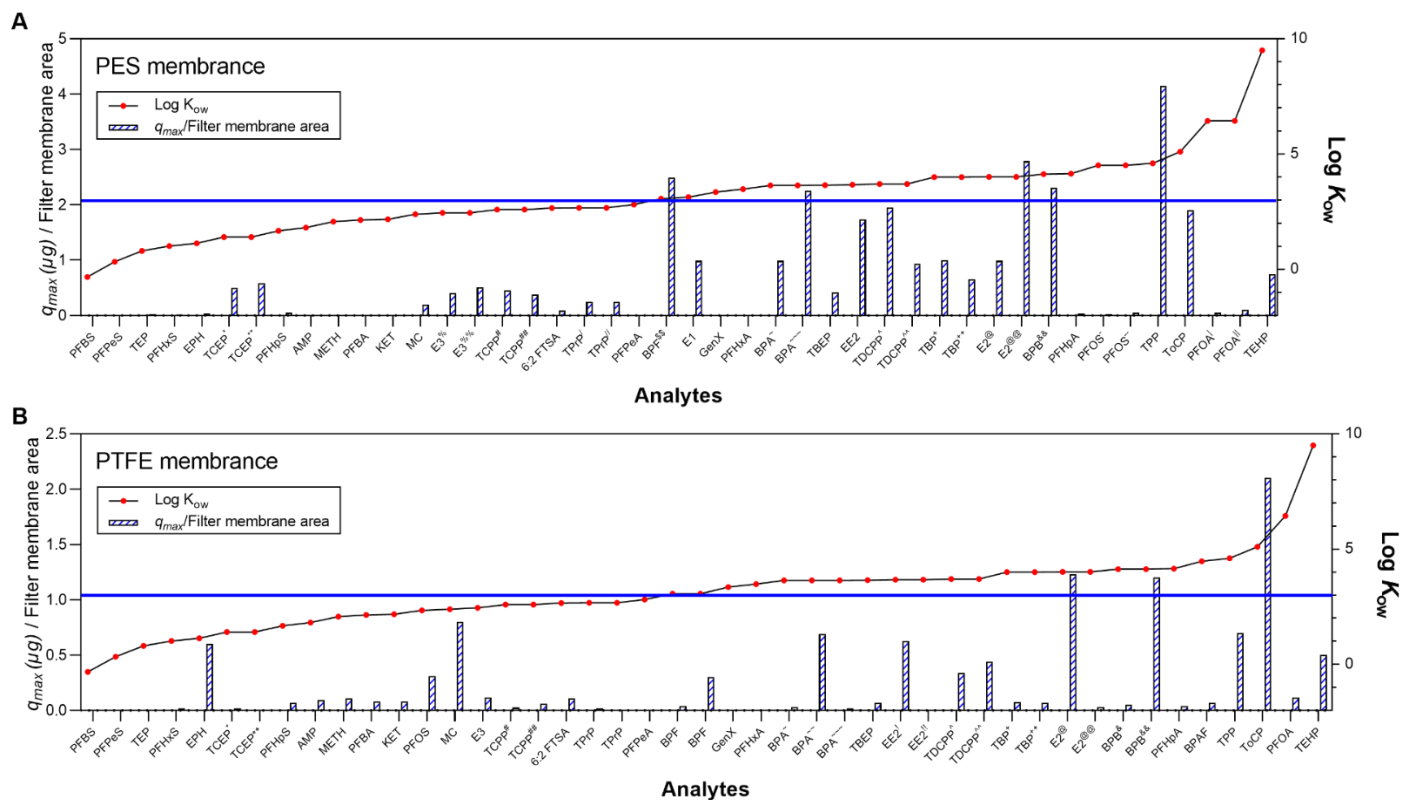
Figure 2.3 The maximum adsorbed mass (q_{max}) per area of PES membrane (**A**) and PTFE membrane (**B**). Abbreviations for analytes and data sources follow those listed in Figure 2.1. It should be noted that some publications in Figure 2.1 were not included here due to the lack of value for the volume of spiked solution for the adsorption test.

Lipophilic chemicals appeared in the sorbent after a lag phase when they were retained in the PES membrane (Vermeirssen et al., 2012). Endo and Matsuura (2018) conducted a batch experiment with 14 neutral chemicals (log K_{ow}: -0.07–3.48), showing that $K_{PES/W}$ values (the ratio of the concentration of the analyte in the filter membrane and that in the water at equilibrium at 25 °C) are 2–3 log units greater than K_{ow}. This result showed strong sorption of the PES filter membrane not only to hydrophobic compounds but also highly hydrophilic ones (e.g., caffeine), which is in agreement with previous studies for a suite of 34 pharmaceuticals and pesticides (Challis et al., 2016), household and personal care products (Chen et al., 2017), bisphenols (Zheng et al., 2015; Xie et al., 2018), and organophosphorus flame retardants (Zou et al., 2018). The high $K_{PES/W}$ may also be the result of the large surface area of the porous membrane, offering high surface adsorption. Additionally, Zhang et al. (2018) found that the PES membrane gave the least adsorption (<5 %) of polar organic compounds (methcathinone and ephedrine) compared to PTFE (>20 %), cellulose ester (>30 %), and nylon (>10 %). Similar results were also reported by Alvarez et al. (2004) and Kingston et al. (2000).

Except for the polarity of compounds, Endo and Matsuura (2018) pointed out that significant sorption of various compounds by PES membranes may be a result of their molecular structure with phenyl and sulfonate groups (e.g., 2-methoxynaphthalene and 2-naphthalene sulfonate), which provide hydrophobic molecular conditions to adsorb hydrophobic compounds while the latter may have strong polar-polar interactions. However, there are exceptions to this finding, including perfluorooctanoic acid and perfluorooctane sulfonate which showed minimal retention on the PES membrane (**Figure 2.1A**). This may relate to issues with assessing K_{ow} of surface-active compounds (anionic compounds). The lipophilicity difference is based on the

charged head group ($-CO_2^-$ or $-SO_3^-$) and the effect of electron-withdrawing through the displacement of fluorine on the alky chain (Jing et al., 2009). However, for surface-active compounds, this can cause discrepancies in K_{ow} determination. However, no studies to date have compared the adsorption of compounds with different polarities/structures or elucidated adsorption mechanisms for particular categories of compounds.

2.3.3 PTFE membrane

PTFE membranes were developed as a new product with the advent of the second generation of Gore-Tex membranes in the 1970s (Zeng et al., 2019). PTFE is an inherently hydrophobic material, which can be treated with ethanol or isopropanol to become hydrophilic. Hydrophilic PTFE membranes can be used as outer protection membranes for passive samplers in the aqueous environment. Generally, PTFE material is highly resistant to compounds, and it is theoretically unlikely to react with chemicals. Some authors have recommended PTFE as a better filter membrane to reduce the potential for adsorption used in DGT configurations compared to PES (Zheng et al., 2015; Zou et al., 2018; Wang et al., 2019), GHP (Wang et al., 2019), CA (Zou et al., 2018), NL (Zheng et al., 2015), and MCE (Zheng et al., 2015). Although PTFE membranes showed high adsorption for some compounds, low adsorption (< 20%) was found for most tested compounds, especially for hydrophobic compounds (**Figure 2.1B**). The highest adsorbed mass was ~2.1μg per filter membrane area ($\approx$ 4.91 cm^2) for tri-o-cresyl phosphate (**Figure 2.3B**). Moreover, it is similar to the finding for bisphenol-A and β-estradiol through the comparison of data from Zheng et al. (2015), Li et al. (2021a), and Iuele et al. (2021), where both compounds did not reach the adsorption equilibrium within 6 h.

There are some studies reporting discrepancies related to the sorption of analytes by the PTFE membrane. Endo and Matsuura (2018) reported that PTFE had no significant sorption for target analytes and recommended PTFE as a promising candidate as a filter membrane material that prevents lag times and lag responses to fluctuating concentrations. The significantly higher fraction adsorbed of some hydrophilic compounds (20%–55%), e.g., methcathinone, ephedrine, ketamine, methamphetamine, and amphetamine, was observed, which have a benzene structure (**Figure 2.1B**). The results of this study suggest that the PTFE filter membrane of the DGT sampler may only be reliable when sampling hydrophilic (log K_{ow}: 0.8–2.6) and non-aromatic compounds. Interestingly, for tris(1,3-dichloro-2-propyl) phosphate (log K_{ow}: 3.7), the different fractions adsorbed reported were 6.8% (Wang et al., 2019) and 44% (Zou et al., 2018), which were determined using similar experimental methods (discussed in section 2.2.1). From the plot of mass adsorbed vs. C_f (**Figure 2.2B**), 6 h contact time was likely sufficient to reach equilibrium for tris(2 chloroethyl) phosphate ($q_{max} \approx 0.02$), tris(chloropropyl) phosphate ($q_{max} \approx 0.025$), tripropyl phosphate ($q_{max} \approx 0.02$), and tributyl phosphate ($q_{max} \approx 0.07$) due to similar mass sorbed from two studies, while tris(1,3-dichloro-2-propyl) phosphate (TDCPP) is similar to the finding for PES membrane, showing higher value for 6 h in equilibrium experiment done by Wang et al. (2019) (the data from Zou et al. (2018) could potentially be even higher if equilibrium was not attained). However, Zou et al. (2018) did not point out whether 24 hours was sufficient to reach equilibrium for membranes tested for the sorption experiments. For $K_{PTFE/W}$ values (the ratio of analyte concentration retained in PTFE membrane and water at equilibrium), Wang et al. (2019) reported a larger log $K_{PTFE/W}$ of 4.61 (tri-o-cresyl phosphate) compared to other studied compounds with log $K_{PTFE/W}$

values of < 1.65 (Endo and Matsuura, 2018) and 1.78 (tetrachloroethene) (Leggett and Parker, 1994). Therefore, hydrophobicity reflected by log K_{ow} appears to be one important factor affecting the adsorption of compounds to the PTFE polymer filter membrane and slow equilibration.

2.3.4 PC membranes

Nuclepore and cyclopore PC membranes are made from polycarbonate film, which is typically used for size-based filtration (Shindell et al., 2015). Hydrophilic PC membranes have been introduced as outer protection membranes in several DGT configurations (Chen et al., 2017; Chen et al., 2018). The polarity of compounds tested for fraction adsorbed ranged from hydrophilic to moderately hydrophobic (Log K_{ow} = 2.00–4.66) (**Figure 2.4A**). The adsorption by PC membranes did not show a regular pattern of increase/decrease with increasing log K_{ow} values based on current studies. However, an apparent pattern was observed for nuclepore PC (0.2 μm) and PC2 membranes (0.015 μm) showing lower adsorption of all analytes compared to cyclopore PC1 (0.2 μm) membrane (**Figure 2.4A**). This may be due to the microporous structure of cyclopore PC1 membrane capturing more compounds compared to the sharply defined pore size of nuclepore PC and PC2 membranes providing less resistance. Furthermore, Chen et al. (2017) reported minimal adsorption of all tested chemicals (log K_{ow}: 2.0–3.5) by the PC membrane (<5%), PC2 membrane (12%), and PC1 membrane (34%) in comparison to PES membrane (almost 100%) and CNM membrane (50%). Chen et al. (2018) further showed little adsorption of endocrine-disrupting chemicals (log K_{ow}: 2.45–4.01) by PC (< 5%), PC2 (10%), and PC1 (20%), which is comparable to the results for PC membranes obtained by Li et al.

(2021a) for endocrine-disrupting chemicals (log K_{ow}: 2.81–4.13) with less than 5% of fraction adsorbed. Li et al. (2021a) also reported that washing PC membranes with pure water showed negligible adsorption (< 1%) of all targeted endocrine-disrupting chemicals. Apparent differences in q_{max} values for the same analytes were found for estriol (0.13 μg for Chen et al. (2018) and 0.03 μg for Li et al. (2021a)) and 17α-ethinylestradiol (0.005 μg for Chen et al. (2018) and 0.18 μg for Li et al. (2021a)) for PC membrane (**Figure 2.5A**). Both studies used the same spiked concentration, volume, and PC membrane purchased from Whatman, while the only difference was tested time with 24 h used by Chen et al. (2018) and 36 h by Li et al. (2021a). This implies that a reversible chemical equilibrium might occur after 24 h for estriol and 17α-ethinylestradiol did not reach the maximum adsorption equilibrium within 24 h. However, there are currently no studies examining the compatibility of a wide range of organic compounds with PC or PC2 filter membranes. The adsorption mechanism of different porous structures and pore sizes of membranes, as well as washing processes should be further examined for development of new membranes or selection of proper membranes for targeted compounds.
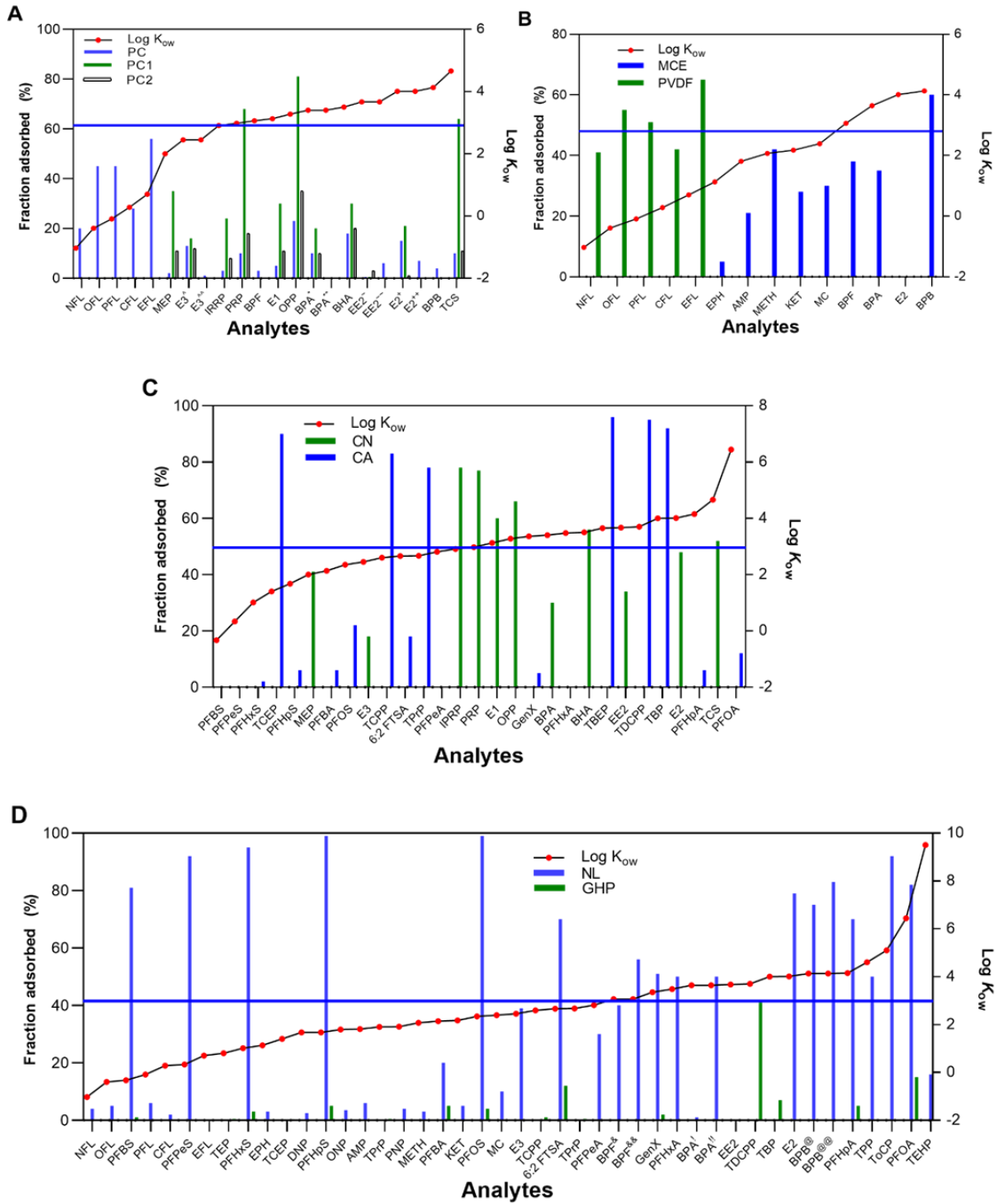
Figure 2.4 Summarized fraction adsorbed (%) of tested organic compounds by different filter membranes. **(A)**: 0.2 μm nucleopore track-etched polycarbonate (PC), 0.2 μm cyclopore track-etched polycarbonate (PC1), and 0.015 μm nucleopore track-etched polycarbonate (PC2). **(B)**: mixed cellulose ester (MCE) and polyvinylidene fluoride (PVDF). **(C)**: cellulose nitrate (CN) and cellulose acetate (CA). **(D)**: hydrophilic polypropylene (GHP) and nylon (NL). Data are plotted as increasing log octanol-water partition coefficient (log K_{ow}) values of tested analytes. The blue line represents the Log K_{ow} value of 3.

Abbreviations for analytes: NFL[1]: norfloxacin, OFL[1]: ofloxacin, PFL[1]: pefloxacin, CFL[1]: ciprofloxacin, EFL[1]: enrofloxacin, MEP[2]: methylparaben, E3ˆ/ E3^[3/4]: estriol, IPRP[2]: isopropylparaben, PRP[2]: propylparaben, TPrP: tripropyl phosphate for **C**[5] and **D**[6], TPP[6]: triphenyl phosphate, ToCP[6]: tri-*o*-cresyl phosphate, TEP[6]: triethyl phosphate, TEHP[6]: tris(2-ethylhexyl) phosphate, TDCPP: tris(1,3-dichloro-2-propyl) phosphate for **C**[5] and **D**[6], TCS [2]: triclosan, TCPP: tris(2-chloropropyl) phosphate for **C**[5] and **D**[6], TCEP: tris(2-chloroethyl) phosphate for **C**[5] and **D**[6], TBP: tri-n-butyl phosphate for **B**[5] and **C**[6], TBEP[5]: Tris(2-butoxyethyl) phosphate, PNP[7]: *p*-nitrophenol, PFPeS[8]: perfluoropentane sulfonate, PFPeA[8]: perfluoropentanoic acid, PFOS [8]: perfluorooctane sulfonate, PFOA [8]: perfluorooctanoic acid, PFHxS[8]: prerfluorohexanoic acid, PFHxA[8]: prerfluorohexanoic acid, PFHpS[8]: perfluoroheptane sulfonate, PFHpA[8]: perfluoroheptanoic acid, PFBS[8]: perfluorobutane sulfonate, PFBA[8]: perfluorobutanoic acid, OPP[2]: ortho-phenylphenol, ONP[7]: *o*-nitrophenol, METH[9]: methamphetamine, MC[10]: methcathinone, KET[9]: ketamine, GenX[8]: hexafluoropropylene oxide dimer ammonium salt, EPH[10]: ephedrine, EE2~/EE2~[3/4]: 17α-ethinylestradiol, E2: β-estradiol for E2$^+$/E2^{++} in **A**[3/4], **B**[11], C[3], and **D**[3], E1[3]: estrone, DNP[7]: 2,4-dinitrophenol, BPF: bisphenol F in **A**[4], **B**[12], and in **D** for BPF$^&$/BPF$^{&&}$[4/12], BPB[8]: bisphenol B in **A**[4], **B**[12], and in **D** for BPB$^@$/BPF$^{@@}$[4/12], BPA: bisphenol-A for BPA*/BPA**[3/4] in **A**, in **B**[14], in **C**[3], and for BPA*/BPA** in **D**[4/12], BHA[2]: butylated hydroxyanisole, AMP[9]: amphetamine, and 6:2 FTSA[8]: 6:2 fluorotelomer sulfonic acid. The data collected from [1]Liu et al. (2021), [2]Chen et al. (2017), [3]Chen et al. (2018), [4]Li et al. (2021a), [5]Zou et al. (2018), [6]Wang et al. (2019), [7]You et al. (2019), [8]Fang et al. (2021), [9]Guo et al. (2017a), [10]Zhang et al. (2018), [11]Guo et al. (2017b), and [12]Zheng et al. (2015).
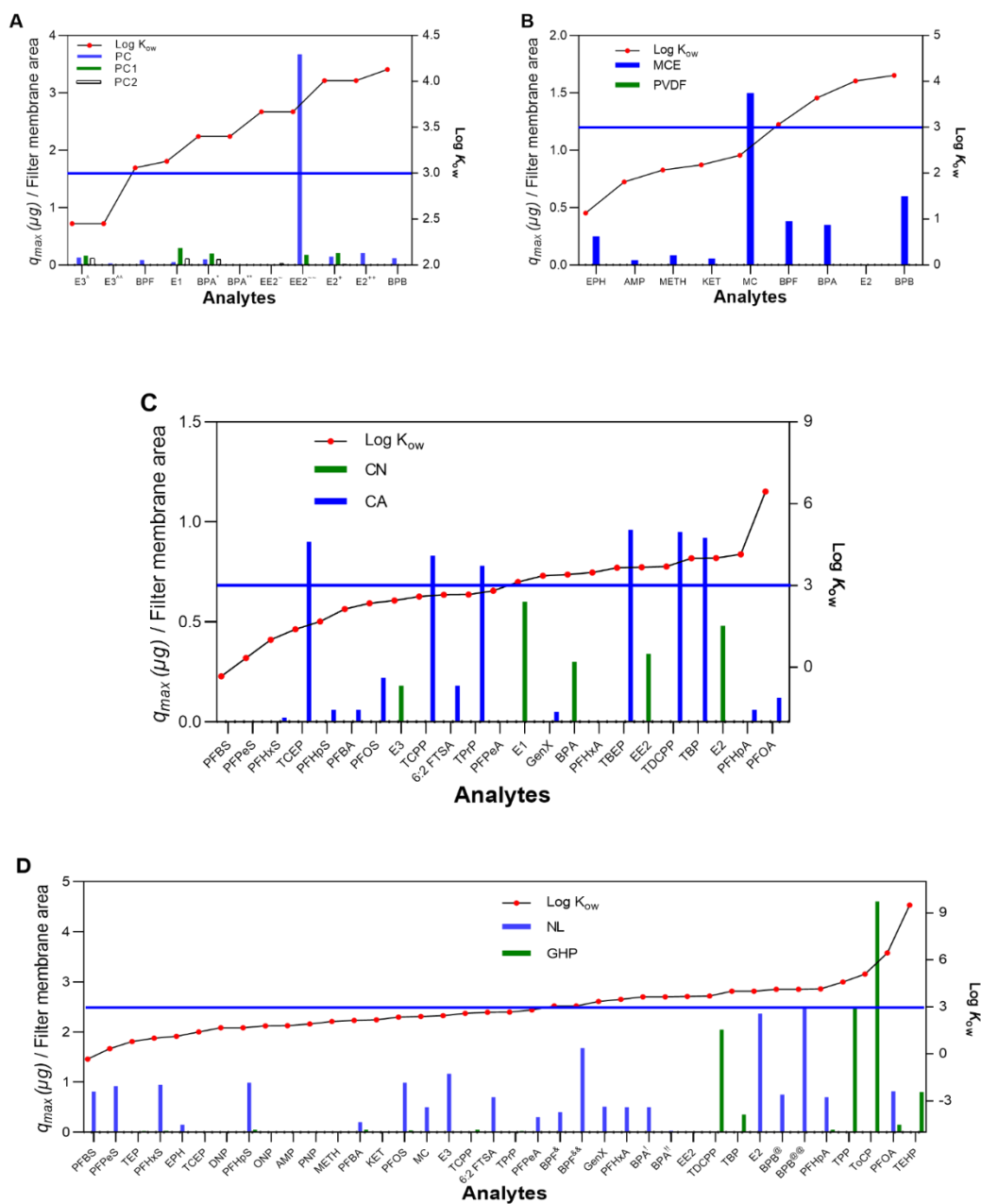
Figure 2.5 The maximum adsorbed mass (q_{max}) per area of **(A)**: PC, PC1, and PC2, **(B)**: MCE and PVDF, **(C)**: CN and CA. (**D**): GHP and NL. Abbreviations for analytes and data sources follow those listed in Figure 2.4. It should be noted that some publications in Figure 2.4 were not included here due to the lack of value for the volume of spiked solution for the adsorption test.

2.3.5 Other membranes

MCE membrane is a mixture of CN and CA. In comparison to the fraction adsorbed (18-95%) of CA and CN for hydrophilic compounds, MCE showed less adsorption (5-35%) for the tested compounds, with the exception of bisphenol B (60%) (**Figure 2.4B**). Guo et al. (2017b) first used PVDF membranes in a DGT configuration for detecting β-estradiol in water and there was negligible adsorption after 48 h (2.4%). PVDF has been widely used as an ultrafiltration membrane material in different applications (Wang et al., 2016). The external hydrophilic and intrinsic hydrophobic structure might make it a suitable filter membrane material for DGT configurations for organics. However, some studies pointed out the low surface energy of PVDF, which leads to poor wettability and aggregation of organic material on the membrane surface (Gaw et al., 2017). From the perspective of mass adsorbed, the mass adsorption of methcathinone by MCE is three times higher than that of other compounds (**Figure 2.4B**). Therefore, PVDF needs to be tested for a larger range of organic chemicals to confirm its performance.

CN and CA are similar polymer membranes having many microscopic pores. CN is made by the reaction of cellulose and nitric acid while CA is made of the mixture of cellulose diacetate and triacetate. Both CN and CA have been screened for potential use as a DGT filter membrane (Chen et al., 2017; Chen et al., 2018; Zou et al., 2018). The tested compounds ranging from hydrophilic to relatively hydrophobic (log K_{ow}: 1.4–4.5), showed quite low fractions adsorbed for most analytes (**Figure 2.4C**) except for perfluorobutane sulfonic acid, perfluoropentane sulfonate, prerfluorohexanoic acid, and tri-npropyl phosphate. However, this pattern did not correspond to the mass adsorbed (**Figure 2.4C**), which could be owing to many factors (e.g.,

spiked concentrations, time, and difference of filter membrane mass from different manufacturers). Since there was no information on equilibrium adsorption, we did not further analyze this dataset. Simply comparing to mass adsorbed (ranging from $0-0.95$ μg) by CA and CN, it is still comparable to that by other filter membranes (**Figures 2.3** and **2.4**). Therefore, whether CN and CA membranes can be efficiently used as the outer filter membrane requires further dedicated research.

NL membrane is naturally hydrophilic. The adsorption of compounds was similar to the results shown for PES membranes, where apparent lesser adsorption was found for hydrophilic compounds ($0-10\%$) compared to that in hydrophobic compounds ($40-75\%$) (**Figure 2.4D**). You et al. (2019) studied the interaction between NL membranes and nitrophenols, e.g., *o*-nitrophenol, *p*-nitrophenol, and 2,4-dinitrophenol (log K_{ow} of 1.79, 1.91 and 1.13, respectively) in detail. The authors used scanning electron microscopy and showed that membranes were macroscopically identical and showed no visible cracks or differences in pore structure before and after soaking in spiked solutions. For GHP membranes, Wang et al. (2019) conducted a sorption experiment with 9 model chemicals (log K_{ow} = $0.8-9.5$, molecular weight =$182-435$ Da) and found that GHP efficiently absorbed hydrophobic compounds that did not reach equilibrium after 6 h, which is similar as PES and NL membranes. Furthermore, the q_{max} values of bisphenol A (0.5 μg for 6 h and 0.03 μg for 36 h) and bisphenol B (0.75μg for 6 h and 2.49 μg for 36 h) using NL membranes from the same manufacturer (Shanghai Anpel) (**Figure 2.5C**), implied that both compounds did not reach adsorption equilibrium for 6 h while the maximum adsorption capacity for bisphenol B occurred within 36 h.

Only one study applied glass fiber membranes to DGT for measuring triclocarban, triclosan,

and methyl triclosan (log K_{ow} = 4.32, 4.76, and 5.22, respectively) with adsorption tests showing less than 4% of the total mass for the three targeted compounds (Wei et al., 2019). Even though glass fiber filters are widely used in the filtration of the water grab samples for organics, glass fiber adsorption tests are lacking. Testing the filter membrane for wider groups of organic compounds should be carried out, which is beneficial for both the DGT and water grab sampling communities. Therefore, even though numerous adsorption tests have been conducted for different organic chemicals and different filter membranes, caution needs to be applied and the adsorption potentials of filter membranes for targeted analytes need to be determined.

2.3.6 Other influences of filter membranes

Other influences of outer filter membranes on the accuracy of DGT concentrations have also been reported. For example, Challis et al. (2016) extracted PES membranes after laboratory exposures and compared the results with the HLB binding gel itself, concluding that PES adsorbed a significant amount of some compounds (chlorpyrifos, diazinon, fluoxetine, paroxetine, roxithromycin, estrone, 17β-estradiol,17α-ethynylestradiol, fenoprofen, and gemfibrozil). Since the thick diffusive gel in DGT devices strictly controls an analyte's uptake rate, this will cause a serious issue concerning the accuracy of diffusion coefficients for the calculation of C_{DGT}. However, to the best of our knowledge, no other DGT studies have checked the analytes' masses on the filter membrane after deployment and determined the diffusion coefficient of a combination of the filter membrane and diffusive gel. Another concern may be the diffusive boundary layer (δ). Some studies deployed multiple DGT samplers with varying diffusive gel thicknesses to estimate the δ values and the results showed field-measured δ values

of 0.034 $\pm$ 0.032 cm (Challis et al., 2018b), 0.043 $\pm$ 0.039 cm (Challis et al., 2016), and 0.023 cm (Chen et al., 2013) were significantly higher than the thickness of the PES membrane (100 μm) (Harman et al., 2012). This suggests that DGT for organic is still controlled by the diffusive layer. Therefore, the analyte mass accumulated on the filter membrane (if used) in a completely assembled DGT device should be tested to decide whether the current filter membrane is suitable to use.

2.3.7 Filter membrane studies outside of DGT devices

The filter membranes currently used for DGT devices for organics are also used in other research areas. Considering the application of filter membranes in other fields may be useful for further consideration of filter membrane selection for DGT devices. Hebig et al. (2014) examined the mass loss of compounds (43 basic, neutral, and acidic organic micropollutants) in spiked solutions (methanol concentration < 0.1%, v/v) after filtration through several filter membranes, i.e., CA, PC, glass fiber, CA, NL, and cellulose. The batch experiments of this study showed that most of the analytes were not influenced by any filter membrane (mass loss < 20%) whereas only three compounds (loratadine, fluoxetine, and sertraline) showed significant mass loss for most of the tested filter membranes. Specifically, several discussions were provided by Hebig et al. (2014): (*i*) mass loss of fluoxetine and sertraline was not a result of cation exchange because no effect was observed for atenolol. (*ii*) Loratadine presented its neutral form under experimental conditions (pH = 8.2), whereas no significant interactions for other neutral compounds (except for diuron) were found. (*iii*) Identical charges and identical filter membranes did not result in similar mass losses. This result is similar to previous

adsorption tests done in DGT studies discussed above. The behavior of each compound through the filter membranes is specific and not always obviously related to ionic character and partitioning (e.g., log K_{ow}).

Apart from the behavior of each compound, the different structures of filter membranes may also lead to different mechanisms of binding to analytes. For example, Gasch et al. (2011) measured the mass loss of low doses of drugs filtered by PES^+ and PES^0 (positively charged and uncharged polyethersulfone) membranes, showing that anionic drugs in saltless solutions were more easily retained by charged filter membrane (PES^+). The adsorption of a single compound, estrone, was tested with a variety of microfiltration membrane filters, e.g., NL, polypropylene, PTFE, and CA (Han et al., 2010), which showed that estrone could be retained in NL filters at almost 100% during the filtration process and losses remained substantial (42%) after the filter capacity was reached. Han et al. (2010) used Fourier transform infrared spectroscopy to demonstrate the hydrogen bonding between NL membranes and estrone and further found deprotonation of the estrone molecule by increasing the pH could greatly reduce the estrone adsorption by NL membranes. Furthermore, Han et al. (2010) found that only glass microfiber filters showed consistently low adsorption (< 2.3%) for estrone. Although most of these studies used low volumes (10–25 mL) of spiked solution, some possible mechanisms occurring between organic compounds and filter membranes may be considered: (*i*) the highly porous structures of membranes may exhibit physical adsorption to analyte; (*ii*) charge interactions between membranes and analyte; (*iii*) analyte molecules binding with membranes through the reaction with specific functional groups within filter membranes.

2.4 DGT configuration without filter membrane

As highlighted above, many studies have shown that filter membranes can result in lag times in the initial mass transfer rate, especially for some higher log K_{ow} compounds due to the potential for membrane adsorption, resulting in some studies to study and recommend using DGT without a membrane filter altogether. Challis et al. (2016) first introduced the configuration of DGT without a filter membrane for polar organics and showed good agreement with grab samples in a wastewater treatment plant, demonstrated less impact by the boundary layer compared to that of co-deployed POCIS, and despite the visible formation of biofilms on the surface of the outer hydrogel, reported limited impact of biofouling on sampler performance. This DGT configuration without a filter membrane was found to be comparably insensitive to the diffusive boundary layer under slow flow rates (2.4 cm s^{-1}), which largely reduces the need for sampler calibration of sampling rates. Moreover, field evaluation of the same DGT sampler has been explored in several representative conditions, e.g., an agriculturally-influenced fast-flowing river, a dilute lake for long-term sampling (> 40 days), wastewaters, and under ice at near-freezing point temperatures (Challis et al., 2018b; Challis et al., 2020). The results of these field evaluations of this DGT configuration were more accurate water concentrations for a suite of polar pharmaceuticals and pesticides compared to that measured by simultaneously deployed POCIS. Comparisons were assessed against select grab (Challis et al., 2018b) and active sampling (Challis et al., 2020), and the authors concluded that the more accurate DGT concentrations were largely due to significant minimization of *in-situ* boundary layer effects, similar to what is found for applications of filter-DGT configurations. In other words, the authors concluded that DGT configurations without a filter membrane remove many of the

uncertainties associated with compound sorption to the filters and lag times while maintaining both sampler performance, and, with few exceptions (detailed below), sampler durability.

Similar configurations omitting the outer filter membrane and relying on the diffusive gel to protect the inner binding gel have also been used to sample antibiotics (Chen et al., 2012) and determine metal speciation (Li et al., 2005). Agarose has been the most widely used diffusive hydrogel material in DGT samplers for various organic pollutants (Belles et al., 2017; Xie et al., 2018; Buzier et al., 2019). However, Challis et al. (2018b) found that DGT diffusive gels made from 1.5% agarose could be damaged with scarred surfaces or completely destroyed by grazing aquatic insects. Although Challis et al. (2018b) reported only one set of destroyed agarose diffusive gels in a specific field site, it may be assumed that agarose as a polysaccharide may serve as a potential food source for particular aquatic insects (Gustavsson and Son, 2003). Additionally, in these specific circumstances of gel degradation, the absence of the protective outer membrane would certainly lead to faster degradation of exposed diffusion gel. For instance, Urík and Vrana (2019) reported that the agarose diffusive layer as the outer membrane of DGT became visually thinner after exposure to natural water for 4 weeks. In light of these limitations, short deployment of DGT without an outer protective membrane may be required.

To solve this issue, Urík and Vrana (2019) put forward a new design where two binding gels (diameter of 3.8 cm) were placed between two larger agarose diffusive layers (diameter of 5.5 cm) embedded by a nylon mesh (similar to the POCIS design) for increasing sampling rates and enhancing resistance to mechanical damages. The measured average sampling rate of compounds (11 perfluoroalkyl substances and 12 pharmaceuticals and personal care products) was estimated to be over an order of magnitude higher than that controlled by the hydrogel,

clearly suggesting that the diffusion layer acts as a rate-limiting barrier for analytes, with little influence of the variable thickness of diffusive boundary layer on it. However, the surface-specific sampling rate measured by Urík and Vrana (2019) was lower than those measured by Challis et al. (2016) for the same compounds with differences: 37% for clofibric acid, 23% for diclofenac, 51% for ibuprofen, 71% for ketoprofen, and 61% for naproxen. Urík and Vrana (2019) stated that this difference may be caused by higher pH (2.5 units) and lower temperature by 1−5 °C. The uptake of organic compounds could be influenced by the pH of water when the pKa values of the target compounds are similar to the water pH (Stroski et al., 2018). Although Urík and Vrana (2019) increased the resilience of agarose gel, the thickness and diffusion pathway length were also increased. A recent study showed that nylon netting agarose gel does not influence polar organic pollutants by testing 12 perfluoroalkyl substances, 14 pharmaceuticals and personal care products and 33 currently used pesticides with three methods, e.g., the diffusion cell method, stack method, and Taylor dispersion method (Urík et al., 2020). Therefore, using or evaluating sampling rates calculated using diffusion coefficients determined in gels without the incorporated mesh can be used widely in the future, and further studies concerning the net effect on diffusion coefficients of nonpolar compounds should be conducted.

Another solution to solve the current issues with agarose gels is to explore other diffusive gel materials when no filter membrane is used. Polyacrylamide has been used as a viable alternative to agarose. Ideally, optimal hydrogel materials for DGT should include resistance, low toxicity, low cost, and easy preparation procedures. Polyacrylamide has been widely used in DGT samplers for metals (Scally et al., 2006). Stroski et al. (2018) reported that polyacrylamide diffusive gels were more resistant to degradation and grazing invertebrates in

natural water bodies and recommended its use over agarose. Additionally, polyacrylamide diffusive gels have also been shown to be more suitable for the sampling of anionic pesticides (Guibal et al., 2017) and per- and polyfluoroalkyl substances (Wang et al., 2021). However, the current drawback of polyacrylamide gel is having smaller pore sizes (estimated < 20 nm) compared to agarose (estimated pore size of > 100 nm) (Zhang and Davison, 1999), limiting the sampling rates. Another material, advanced ceramic (made of synthetic inorganic substances with high purity) (Liang and Dutta, 2001), was introduced to function as a single outer diffusive layer in DGT device for organic micropollutants by Xie et al. (2021). This idea originated from another passive sampler–ceramic dosimeter (Martin et al., 2003; Bonifacio et al., 2017). The ceramic tube functions as a diffusion barrier and serves as a container to hold a solid sorbent, and the process of diffusion for organic compounds through the ceramic membrane can meet the principle of the DGT theory. Xie et al. (2021) found that the fraction adsorbed to the ceramic membrane for ten organic micropollutants (log K_{ow} = -1.48–3.05) was < 10%, whereas other organic polymer filter membranes showed higher adsorption, e.g., PES and PC adsorbed > 50% and PVDF exceed 20%. This is consistent with the previous studies that ceramic membrane is free of adsorption to organic compounds, e.g., dioxin-like polychlorinated biphenyls (Addeck et al., 2014), flame retardants (Cristale et al., 2013), and cytostatic drugs (Franquet-Griell et al., 2017). However, the pore size of the ceramic membrane (range from 10 to 15 nm) reported by Xie et al. (2021) was similar to that of polyacrylamide membrane, which is lower than that of agarose membrane. More studies on robust materials with larger or tunable (e.g., % crosslinker for polyacrylamide) pore sizes and negligible adsorption of organic compounds should be further studied.

2.5 Biofouling

In natural water, DGT samplers deployed can be prone to the accumulation and colonization of microorganisms, which causes the formation of biofilms on the surface (Feng et al., 2016). Some studies reported that periphyton colonizing the surface of passive samplers might affect the sampling rates (Huckins et al., 2002; Björklund Blom et al., 2003). This biofilm comprises various types of fouling, including colloidal particles (flocs and clays), organics (humic substances and polyelectrolytes), biota (bacteria, fungi, microalgae, and their extracellular polymeric secretions), and scales (precipitation of minerals) (Donlan, 2002). Furthermore, the composition of biofilms varies broadly and depends on the local environments.

Long-term deployments of passive samplers may not produce accurate quantitative data when the influence of biofouling increases, especially in eutrophic waters (Harman et al., 2009). The presence of biofilms may impact the diffusive layer thickness and/or the target analyte diffusion coefficient. Several DGT studies for inorganic substances showed that biofilms might act as an additional layer on the surface of the outer gel (Zhang et al., 1998a; Chlot et al., 2013), or it may have interactions with the analyte (Uher et al., 2012). Davison (2016) recommended that DGT samplers should be carefully checked for fouling upon retrieval, and data derived from samplers with significant biofouling should be interpreted cautiously. Biofouling may be a potential source of uncertainty for DGT measurements. For example, Pichette et al. (2009) found that the DGT technique was only able to reliably measure reactive phosphorous in freshwater aquaculture within four days of deployment before biofilm buildup began interfering with sampling. To prevent biofilm growth, the outer filter membranes and diffusive gels were soaked in different anti-microbial agents. Silver iodide appeared to affect the diffusive gel, and

iodide and chloramphenicol were partially effective in preventing the formation of algal growth (Pichette et al., 2007). An additional Whatman Nuclepore™ polycarbonate membrane was used to limit biofilm growth on the surface of DGT samplers, and the results showed that this membrane could be problematic for the measurement of some metals (Cr and Co) following a 10-day deployment (Uher et al., 2012).

Chen et al. (2018) discussed that an observed plateau or decline in the concentrations of endocrine-disrupting chemicals after 18 days might have been due to biofouling. Chen et al. (2013) reported that a 7-day deployment of DGT samplers in wastewater treatment plants for ambient antibiotic concentrations was recommended before significant occurrence of biofouling, whereas some antibiotics required longer deployment times. Assuming the presence of biofilms can negatively impact the performance of DGT samplers, the deployment time should be kept to a minimum to prevent the generation of biofilm. Alternatively, the deployment of DGT samplers with a thicker diffusion layer (> 1 mm) can minimize the influence of the diffusive boundary layer (DBL) and biofilm layer, however, a trade-off needs to be made between reducing the impact of the biofilm and analytical sensitivity.

Since DGT sampling of organic chemicals at trace levels is still a relatively recent development, only a few studies so far have investigated the impact of biofouling on DGT performance for organic chemicals (**Table 2.1**). To our knowledge, the report of Wang et al. (2020a) is the only study to date to specifically study the impacts of biofilm formation on organic DGT uptake for a wide range of emerging organic pollutants. This study investigated two factors potentially impacting DGT performance: (*i*) bio-fouled diffusive gels versus clean diffusive gels; and (*ii*) bio-fouled filter membrane versus clean filter membrane. Test 1 showed

that the two groups of DGT samplers accumulated similar amounts of all targeted analytes, with

the exception of a marginally significant ($p < 0.05$) 20% decrease in estriol observed in bio-

fouled versus clean diffusive gels. No analytes were detected in the fouled diffusive gel. Test 2

showed that, even though filter membranes were severely bio-fouled (for 8 and 15 days) and

the diffusion distance increased, biofilms did not affect the uptake of most target compounds at

different biofilm formation times. Other studies also found little effect of biofilm formation on

organic DGT uptake during field deployments. Challis et al. (2016) conducted DGT

deployment for polar organic pollutants in wastewater for a longer period (21 days), and the

results showed that no analytes were detectable in the fouled outer diffusive gel; the same

observation was made for the same DGT configuration and organic pollutants in a

comprehensive field evaluation of natural surface waters as described in Challis et al. (2018b).

Additionally, no degradation of the diffusive gel was found despite the presence of a significant

biofilm. Nominally, an increased field diffusive boundary layer (0.043 ± 0.039 cm) compared

to that determined in the laboratory (0.022 cm) was observed (Challis et al., 2016). This study

concluded that biofilms formed on the diffusive gel did not sequester organic pollutants.

Table 2.1 The summary comments on the influences of biofouling on DGT measurement of organic compounds in water.

Targeted compounds	Outer membrane	Application field	Deployment time	Influences of biofouling	References
Antibiotics	0.14 mm PES filter membrane	The influent and effluent of the wastewater treatment plant	18 days	Some antibiotics could not be detected within 4 days whereas it can experience biofouling for longer deployment time.	(Chen et al., 2013)
Pharmaceuticals and pesticides	1.00 mm 1.5% agarose diffusive gel	The influent and effluent of the wastewater treatment plant	21 days	Biofouling showed no influence because of (1) the similar concentrations obtained from significantly biofouled DGT and grab sampling; and (2) no analytes found in the biofouled diffusive gels.	(Challis et al., 2016)
Pharmaceuticals and pesticides	0.75 mm 1.5% agarose diffusive gel	An agriculturally influenced fast-flowing river, a large dilute lake system, wastewaters, and river under ice	21 days >40 days in the dilute lake	Degradation of agarose gel was not relevant to biofilm formation on its surface in the tested field. The significant biofouled-DGT TWA concentrations agreed well with POCIS TWA concentrations.	(Challis et al., 2018b)
Chemicals in household and personal, antibiotics, endocrine-disrupting chemicals	0.80 mm 1.5% agarose diffusive gel	The influent and effluent of the wastewater treatment plant.	8–15 days	No differences in analytes' mass accumulation were found in biofouled diffusive gel (previously exposed in wastewater) and clean diffusive gel.	(Wang et al., 2020a)
	0.11 mm hydrophilic polypropylene filter membrane	This study only applied DGT in the field of biofilm generation where uptake tests were carried out in the laboratory.	8–15 days	No differences in analytes' mass accumulation were found in the biofouled filter membrane and clean filter membrane even if the diffusive distance increased by 10−20%.	

2.6 Storage of DGT samplers

A large number of DGT samplers can be collected during a field sampling season. These field-deployed DGT devices require proper handling and storage for accurate measurement of sampled compounds. There have been concerns that analytes could be lost or degraded within the DGT samplers during deployment and storage. Theoretically, this might result from photolysis, adsorption, hydrolysis, biodegradation, and redox reactions, previously reported in water samples (Barceló and Alpendurada, 1996; Lin et al., 2019). Misleading results would be obtained when any degradation of analytes present within the sampler occurred, particularly for those compounds that are highly labile during prolonged sampling and storage. The DGT sampler is considered to show minimal loss due to photolysis because of the nontransparent holder (Chen et al., 2017). Most studies disassembled DGT samplers once the samplers were retrieved and transported to the laboratory, i.e., transport and retrieval on the same day (Chen et al., 2013; Chen et al., 2017; Guo et al., 2017a; Challis et al., 2018a; Stroski et al., 2018). However, most published studies did not mention how long DGT samplers were stored.

Only two studies emphasized the storage protocol of DGT samplers for organic pollutants. Challis et al. (2018a) first tested the cold temperature stability of 30 organic pollutants (pharmaceuticals and pesticides) for short-term (28 days) and long-term (563 days) storage in DGT samplers. They found no significant change in the analytes' concentrations in both assembled DGT and detached binding gel under 4 °C in the fridge after 28 days compared to the initial concentration (day 0), with an average variation of 5%. Exceptions were observed for paroxetine (binding gel) and 17β-estradiol (fully assembled DGT) with a maximum change

of 15% and 28%, respectively. For 563 days at -20 °C in the freezer, the results showed that the variation on laboratory-loaded DGT was 9% with a range of 1–37% compared to initial mass and certain analytes revealed small increases in mass after 563 days. Challis et al. (2018a) concluded that the observed variation during the storage period was an outcome of experimental and instrumental uncertainties (10-20%) and analytes were stable on DGT for at least one year.

Monitoring projects often cover large areas, and freezer/fridge access for a large number of samplers is not always granted. Wang et al. (2020a) studied four storage methods to test within-sampler degradation loss for up to 2 months. Four storage methods were considered: (*i*) entire DGT devices were sealed in a polyethylene bag at 18–26 °C after field deployment; (*ii*) total DGT devices were stored in a refrigerator (at 4 °C); (*iii*) DGT devices were disassembled, and binding gels were stored in acetonitrile at 18–26 °C; and (*iv*) binding gels were stored in acetonitrile at 4 °C. The results showed that (1) most compounds in intact samplers stored in polyethylene bags were stable (mass loss < 20%) at room temperature (18–26 °C) for 30 days, and at 4 °C for 60 days (**Figure 2.6A and B**); (2) good recoveries of most chemicals were found in the binding gel at room temperature and 4 °C for 60 days (**Figure 2.6A and B**). One exception, norfloxacin, showed a significant loss compared to the initial mass loading in all four storage methods, and ethylparaben had > 20% mass loss in all binding gels storage (**Figure 2.6**). Wang et al. (2020a) explained that fluoroquinolones (norfloxacin and ofloxacin) are prone to hydrolysis under normal conditions due to their carboxyl groups. Llorca et al. (2014) observed that norfloxacin and ofloxacin exhibited low stability in the first week after sampling at -20 °C and Fedorova et al. (2014) also found norfloxacin concentrations declining with time in spiked wastewater samples at -18 °C. However, Wang et al. (2020a) showed a relatively good recovery

(>80%) for ofloxacin in both intact samplers and binding gels at 4 °C (**Figure 2.6**). The addition

of acid into the maintenance solvent for stabilizing these unstable compounds needs further

study. In summary, based on the results of Challis et al. (2018a) and Wang et al. (2020a), the

most convenient and stable storage for preserving intact DGT devices is in a refrigerator (4 °C)

or a freezer (-20 °C), with most chemicals being stable for at least one year.
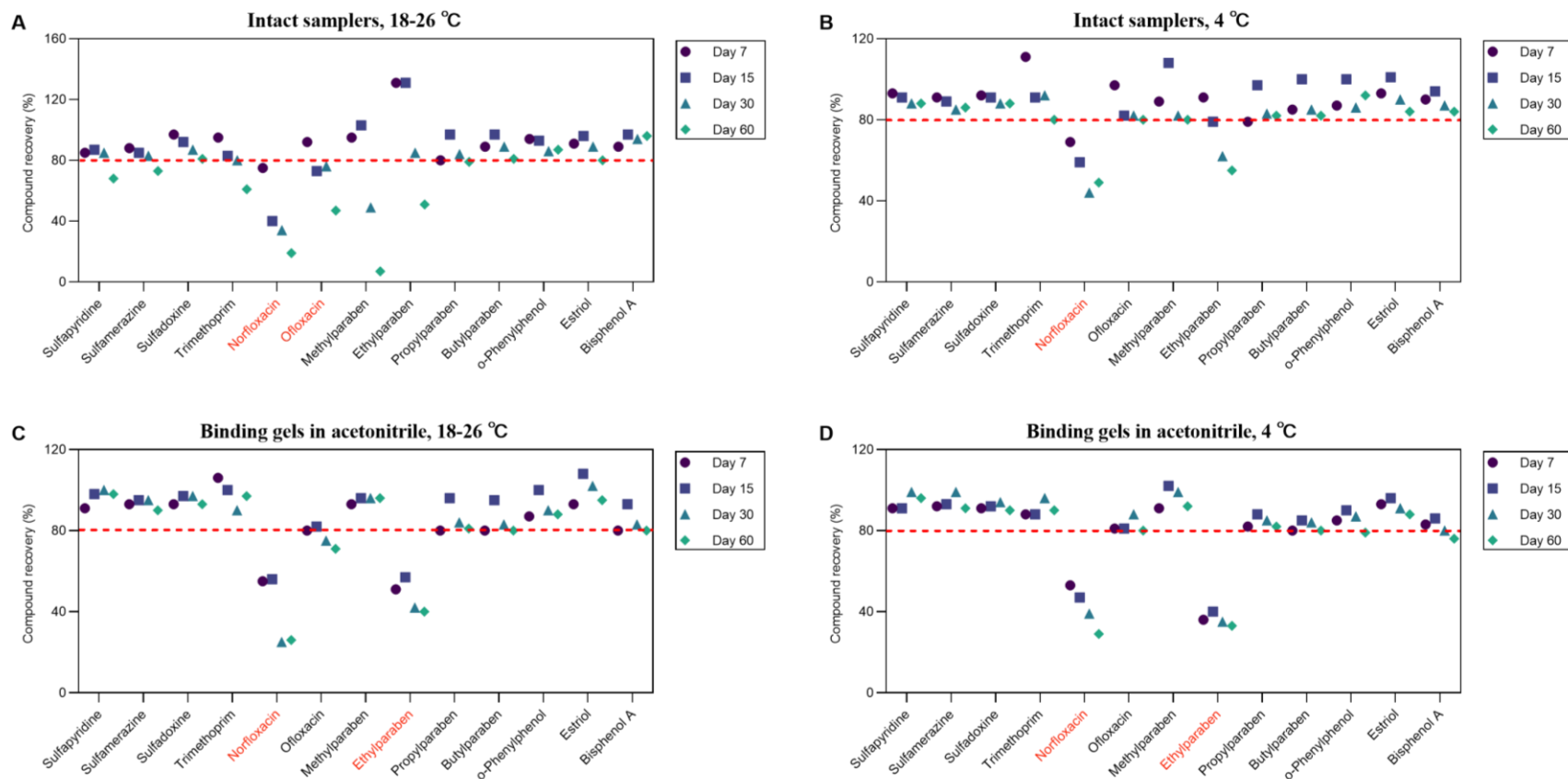
Figure 2.6 Recoveries of tested organic pollutants from the four storage strategies. The red dashed line represents < 20% difference between the recovered mass after a storage time and initial mass loading. The analyte in red indicated the significant mass loss of this compound (> 20%). The data originates from Wang et al. (2020a).

2.7 Application to environmental media

The DGT technique was initially developed to measure metal concentrations in water (Davison and Zhang, 1994) and was later extended to measure the fluxes of metals in soils and sediments (Harper et al., 1998; Ernstberger et al., 2005). Although DGT samplers have been widely adapted to measure trace organic pollutants in waters, recently reviewed by Guibal et al. (2019), few studies have applied DGT for organic compounds in soil and sediments. The results of these studies are summarized in this section.

2.7.1 Theory of the DIFS model

Some studies recently have used the DIFS model (DGT-Induced Fluxes in Soils/Sediments) to mechanistically describe the desorption kinetics of organic pollutants in soils (Chen et al., 2014; Chen et al., 2015) and biosolids (D'Angelo and Starnes, 2016; D'Angelo and Martin, 2018). Organic contaminants are usually distributed heterogeneously in solids, such as soils and sediments, which results in a dispersed but highly concentrated distribution of chemicals (Guan, 2019). When DGT samplers are deployed in soil slurries or sediments, the sustained transfer of solutes from the soil solution or sediment porewater to the binding gel leads to the formation of a concentration gradient within the diffusive layer of the DGT sampler and the immediately adjacent solid phase of soil or sediment (**Figure 2.7**). The concentration induced *via* the DGT diffusive layer, determined by the diffusive layer's thickness (Δ_g) and the labile solute concentration at the interface between DGT and soil/sediment, is the time-integrated interfacial concentration (C_{DGT}). The DGT technique combined with the DIFS model can predict the release of trace metals in soils and offer better insights into the size of the labile

pool, as well as the kinetics of metal resupply from the solid phase (Ernstberger et al., 2005).

Ernstberger et al. (2005) determined the exchange rates of trace metals between soil porewater

and solid phase in soils of different textures using the DIFS model. The concentration of labile

analytes in the solid phase available for analyte release, and the kinetics of adsorption and

desorption processes will control the extent to which the concentrations of analytes are

maintained in the porewater of soil/sediment in comparison to the initial level. The ratio (R) of

C_{DGT} to the independently measured initial soil/sediment solution concentration (C_d) can

provide an estimate as to the extent of the depletion of the porewater concentration at the

interface between DGT/porewater of the solid phase (Ernstberger et al., 2005) (Eq. 2.6):

$$R\ (t) = \frac{C_{DGT}(t)}{C_d}\ (2.6)$$

The DIFS model quantifies the dependence of R on the resupply of labile compound from

solid particles to porewater, coupled to diffusive transfer to the DGT interface and across the

diffusion layer to the binding gel, by solving a pair of linked partial differential equations (Eqs.

2.7–2.8), demonstrating dissolved/sorbed concentrations of the labile compound in the

porewater or the DGT diffusion layer.

$$\frac{\partial C}{\partial t} = -k_1 C + k_{-1} P_c C_s + D_s \frac{\partial^2 C}{\partial x^2} \qquad (2.7)$$

$$\frac{\partial C_s}{\partial t} = \frac{k_1 C}{P_c} - k_1 C_s \qquad (2.8)$$

A one-dimensional DIFS model simulates analytes consumed by DGT which induces a flux

from solid phase to solution. It uses K_{dl} (the distribution coefficient of the labile analyte) (Eq.

1.9) and the response time (T_c) (Eq. 1.10) to quantify the fraction adsorbed constant (k_1) and

desorption rate constant (k_{-1}) in the solid-phase porewater. K_{dl} values may be lower than the

corresponding k_d values ($K_d = \frac{C_s}{C_{total}}$, depending on the total measured analyte concentrations

in the solid phase. T_c defines the time for the partitioning of K_d to reach 63% of its equilibrium value (Ernstberger et al., 2005).

$$K_{dl} = \frac{C_s}{C_d} = \frac{k_1}{P_c k_{-1}} \tag{2.9}$$

$$T_c = \frac{1}{k_1 + k_{-1}} = \frac{1}{k_{-1}(1 + k_{dl}P_c)} \approx \frac{1}{k_{-1}k_{dl}P_c} \tag{2.10}$$

where C_s represents the concentration of the labile analyte in the solid phase; C_d represents the initial sediment pore water concentration.
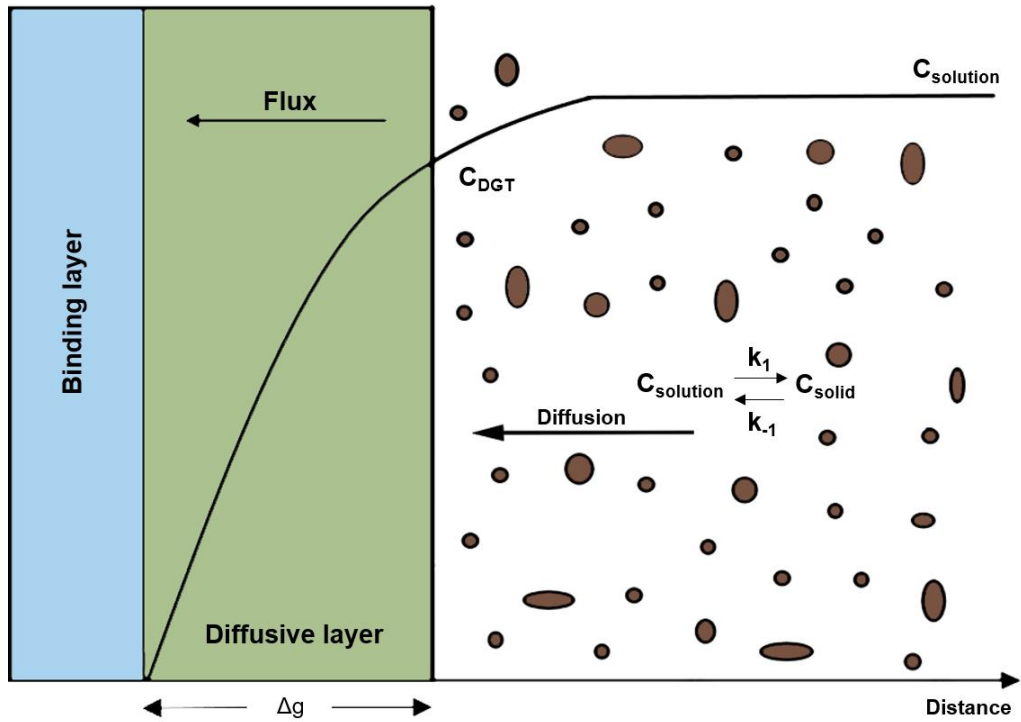
Figure 2.7 Processes induced by the deployment of a DGT sampler in a solid environment. The mass of the analyte in solution ($C_{solution}$) is accumulated in the binding layer by diffusion across the diffusion layer (Δg) of the exposed interfacial area. The DGT-measured concentration of the analyte (C_{DGT}) can be determined according to the linear concentration gradient between the DGT sampler surface and the binding layer. When the analytes are continuously depleted by DGT, the analytes in the solid phase (C_{solid}) will be induced to resupply the solution. k_1 represents the fraction adsorbed constant and k_{-1} represents the desorption rate constant.

Based on this model, R can be calculated using inputs of K_{dl} and T_c, or the model can be fitted

to R versus time to estimate K_{dl} and T_c. DIFS requires data for C_{DGT}, C_d, sediment porosity (ϕ_d),

diffusion layer porosity (ϕ_s), particle concentration (P_c), effective diffusion coefficient in the

solid phase (D_s), diffusion coefficient in the diffusion layer (D_d), and deployment time (t).

Irrespective of the operation mode, DIFS can be used to estimate the analyte concentrations in

solution and solid-phase spatially and temporally within DGT–solid phase systems such as soils

and sediments. A well-developed software, 2D_DIFS, that is freely available can be used to

obtain K_{dl} and $T_{c,}$ and 1D_DIFS can be used to simulate analyte distribution in solid phases and

solutions (Harper et al., 2000; Lehto et al., 2008). The summary of the solution and labile

concentrations of organic contaminants in soil/biosolids (C_d and C_s), and parameters derived

using the DIFS model, are shown in **Table 2.2**.

Table 2.2 Parameters for tested organic pollutants derived from the DIFS model in different soils and biosolids.

Analyte	Soil / Biosolid parameters / description				DIFS-derived parameters						
	Particle distribution	MWHC (%)	pH	SOM (%)	C_d (ng mL^{-1})	C_s (ng g^{-1})	k_d (mL g^{-1})	k_{dl} (mL g^{-1})	T_c (s)	k_l (s^{-1})	k_{-l} (s^{-1})
Sulfamethoxazole[1]	Sand: 56% Silt: 25% Clay: 19%	46	5.2	4.8	1511 ± 363	916 ± 116	0.68	0.54	13244	4.0×10^{-5}	35×10^{-6}
	Sand: 55% Silt: 27% Clay: 18%	51	5.0	9.3	1118 ± 171	841 ± 56	0.78	0.80	4864	13×10^{-5}	77×10^{-6}
Sulfamethazine[1]	Sand: 56% Silt: 25% Clay: 19%	46	5.2	4.8	739 ± 61	903 ± 115	1.3	1.4	1847	41×10^{-5}	135×10^{-6}
	Sand: 56% Silt: 25% Clay: 19%	51	5.0	9.3	558 ± 80	743 ± 67	1.3	1.8	1636	48×10^{-5}	126×10^{-6}
Sulfadimethoxine[1]	Sand: 56% Silt: 25% Clay: 19%	46	5.2	4.8	582 ± 136	761 ± 150	1.5	0.41	18465	2.5×10^{-5}	29×10^{-6}
	Sand: 56% Silt: 25% Clay: 19%	51	5.0	9.3	332 ± 78	691 ± 77	2.3	1.0	14179	48×10^{-5}	228×10^{-6}
Trimethoprim[1]	Sand: 56% Silt: 25% Clay: 19%	46	5.2	4.8	54 ± 7.8	759 ± 61	15	74	1091	91×10^{-5}	5.9×10^{-6}
	Sand: 56% Silt: 25% Clay: 19%	51	5.0	9.3	85 ± 12	1281 ± 41	16	50	127	780×10^{-5}	74×10^{-6}
Tetracycline hydrochloride[2]	Sand: 27.8% Silt: 66.6% Clay: 5.6%	56.3	7.19	N.A.	290 ± 53	19 ± 4.0	15	4.1	5700	27.3×10^{-5}	31.4×10^{-6}
	Sand: 18.5% Silt: 79.6% Clay: 4.6%	60.3	7.99	N.A.	637 ± 135	24 ± 5.2	26	0.6	10200	14.9×10^{-5}	121×10^{-6}
	Sand: 42.6% Silt: 47.5% Clay: 9.9%	26.6	7.54	N.A.	85 ± 19	15 ± 3.2	5.7	4.3	2300	39.1×10^{-5}	43.3×10^{-6}
	Sand: 27.8% Silt: 66.9% Clay: 5.3%	53.0	6.95	N.A.	324 ± 156	17.7 ± 4.1	18	1.7	3300	13.8×10^{-5}	38.5×10^{-6}

	Sand: 19.3% Silt: 74.2% Clay: 6.5%	48.8	8.33	N.A.	785 ± 101	20 ± 3.0	39	0.8	3700	6.11×10^{-5}	36.8×10^{-6}
Oxytetracycline hydrochloride[2]	Sand: 27.8% Silt: 66.6% Clay: 5.6%	56.3	7.19	N.A.	576 ± 183	39 ± 2.8	15	2.8	3400	25.1×10^{-5}	43.4×10^{-6}
	Sand: 18.5% Silt: 79.6% Clay: 4.6%	60.3	7.99	N.A.	1115 ± 373	37 ± 3.7	30	2.3	4000	25.2×10^{-5}	43×10^{-6}
	Sand: 42.6% Silt: 47.5% Clay: 9.9%	26.6	7.54	N.A.	102 ± 44	37 ± 2.5	2.7	8.6	2100	45.6×10^{-5}	25.2×10^{-6}
	Sand: 27.8% Silt: 66.9% Clay: 5.3%	53.0	6.95	N.A.	590 ± 84	37 ± 8.6	16	2.3	6500	12.7×10^{-5}	26.5×10^{-6}
	Sand: 19.3% Silt: 74.2% Clay: 6.5%	48.8	8.33	N.A.	1122 ± 393	37 ± 3.0	30	2.8	4100	20.8×10^{-5}	25.5×10^{-6}
chlortetracycline hydrochloride[2]	Sand: 27.8% Silt: 66.6% Clay: 5.6%	56.3	7.19	N.A.	N.A.	22 ± 2.6	N.A.	N.A.	N.A.	N.A.	N.A.
	Sand: 18.5% Silt: 79.6% Clay: 4.6%	60.3	7.99	N.A.	97 ± 14	25 ± 5.1	4	59	6300	1.58×10^{-5}	1.26×10^{-6}
	Sand: 19.3% Silt: 74.2% Clay: 6.5%	48.8	8.33	N.A.	71 ± 34	22 ± 2.6	3	173	300	315×10^{-5}	8.67×10^{-6}
Atrazine[3]	Malpas soil	Spiked 5 mg kg^{-1}	4.8	3.9		2.91	NA	1.20	N.A.	1.4	3.64	1.4×10^{-1}
		Spiked 10 mg kg^{-1}				77.2	NA	3.05	N.A.	320	3.5×10^{-2}	2.8×10^{-4}
	Dares soil	Spiked 5 mg kg^{-1}	5.7	5.4		2.76	NA	2.46	N.A.	0.021	348	6.5
		Spiked 10 mg kg^{-1}				64.7	NA	2.81	N.A.	0.064	128	1.9
	Reddish soil	Spiked 5 mg	6.7	4.8		3.04	NA	2.64	N.A.	10000	1×10^{-3}	1.6×10^{-5}

	kg⁻¹ Spiked 10 mg kg⁻¹			69.9	NA	1.38	N.A.	2000	2×10^{-3}	1.3×10^{-4}
	Spiked 5 mg kg⁻¹			3.21	NA	1.77	N.A.	0.37	9.7	0.75
Kettering soil	Spiked 10 mg kg⁻¹	7.7	8.1	64.1	NA	1.50	N.A.	6500	5×10^{-4}	4.8×10^{-5}
Ciprofloxacin[4]	Dry solid: 96% Spherical average diameter:1.5 mm Dense pellets 0.7–0.8 g cm⁻³ Production: anaerobic digestion, centrifuge dewatering, and thermal drying of primary sludge			0.19 ± 0.125	2.17	12428	13	22270	4×10^{-5}	4×10^{-6}
Tetracycline[5]	pH: 5.78 Dissolved organic carbon: 9.5% Volumetric water content: 0.66 cm³ water cm⁻³ total Porosity: 0.66 cm³ pores cm⁻³ total Particle concentration: 0.70 g cm⁻³ solution Bulk density: 0.48 g cm⁻³			2700	1590	12	0.59	678	4×10^{-4}	10×10^{-4}
	pH: 6.36 Dissolved organic carbon: 11.8% Volumetric water content: 0.84 cm³ water cm⁻³ total Porosity: 0.84 cm³ pores cm⁻³ total Particle concentration: 0.31 g cm⁻³ solution Bulk density: 0.26 g cm⁻³			4100	3800	15	0.95	299	8×10^{-4}	25×10^{-4}
	pH: 5.31 Dissolved organic carbon: 14.5% Volumetric water content: 0.76 cm³ water cm⁻³ total Porosity: 0.76 cm³ pores cm⁻³ total Particle concentration: 0.44 g cm⁻³ solution Bulk density: 0.38 g cm⁻³			4800	1510	9	0.32	978	1×10^{-4}	9×10^{-4}
	pH: 6.36 Dissolved organic carbon: 6.2% Volumetric water content: 0.86 cm³ water cm⁻³ total			1500	2870	46	2.0	445	9×10^{-4}	14×10^{-4}

Porosity: 0.86 cm^3 pores cm^{-3} total
Particle concentration: 0.31 g cm^{-3} solution
Bulk density: 0.28 g cm^{-3}

N.A.: not available

K_d values were calculated by dividing measured concentrations of an analyte in soil by its dissolved concentrations (C_d) at equilibrium. C_s is the labile concentration of analyte calculated using Eq. (4) with DIFS-derived K_{dl} values. It should be noted that measured concentrations of an analyte in soil were determined by acetonitrile extraction for ref 1& 3 and by 1 M NaCl/1 M oxalic acid/methanol extraction for ref 2. For ref 3, the parameters were only taken at the end of incubation experiment (at 23 day).

[1]Chen et al. (2014), [2]Ren et al. (2020), [3]Li et al. (2021b), [4]D'Angelo and Starnes (2016), [5]D'Angelo and Martin (2018).

When DGT is deployed in soils and sediments, the binding layer binds the chemicals that diffuse through the diffusion layer, establishing a linear concentration gradient in the diffusive layer with increasing deployment time, (**Figure 2.8**). The flux of DGT (F_{DGT}) can be calculated by Fick's first law (Eq. 2.11):

$$F_{DGT}(t) = \frac{D C_{DGT}(t)}{\Delta g} \quad (2.11)$$

where D is the diffusion coefficient (cm^2 s^{-1}) of the analyte and t is the deployment time. When the porewater solute concentration is equal to that of resupply to the solid phase ($C_{DGT} = C_d$), C_{DGT} represents the DGT interfacial concentration of the compound. However, in soils/sediments, most compounds can be strongly adsorbed to soil mineral or organic particles (Kleber et al., 2015). With increasing deployment time, solute progressively accumulates in the binding gel of DGT, leading to a change of C_d. Due to the different properties of the solid phase of soils/sediments, the DGT-induced solid phase to solution flux, F_{SS}, and the maximum potential flux from the solid phase to the solution, F_{MAX}, are not equivalent. F_{SS} may be a fraction of or infinitely close to F_{MAX}. Therefore, three scenarios among the direct DGT-measured flux (F_{DGT}), the partial flux (F_{SS}), and potential flux (F_{MAX}) of compounds from the solid phase to the solution can occur (Zhang et al., 1998b) (**Figure 2.8**):

(*i*) Fully supplied: When the compounds accumulate in the DGT sampler, solid particles quickly resupply analytes to the solution, keeping their freely dissolved concentration constant. This case indicates that the partial flux of compounds from the solid phase to the solution is much less than the local potential flux ($F_{DGT} = F_{SS} < F_{MAX}$).

(*ii*) Partially supplied: The solid phase can only partially supply compounds to the solution, and this supply cannot meet the adsorption requirements of DGT so that the concentration of

compounds progressively decreases. The flux sampled by the DGT is almost equal to the partial

flux of compounds from the solid phase to the solution that is close to the local potential flux

($F_{\mathrm{DGT}} \approx F_{\mathrm{SS}} \sim F_{\mathrm{MAX}}$).

(*iii*) Diffusion only: This is another extreme case where the solid phase cannot supply

compounds to the solution ($F_{\mathrm{DGT}} = F_{\mathrm{SS}} = 0$). The adsorption of compounds by DGT only

depends on the solution diffusion. In this case, the supply to DGT sampler becomes gradually

depleted, initially in the DGT sampler's vicinity, then extending into the solution. After a certain

deployment time, a declining concentration gradient is generated in the solution.
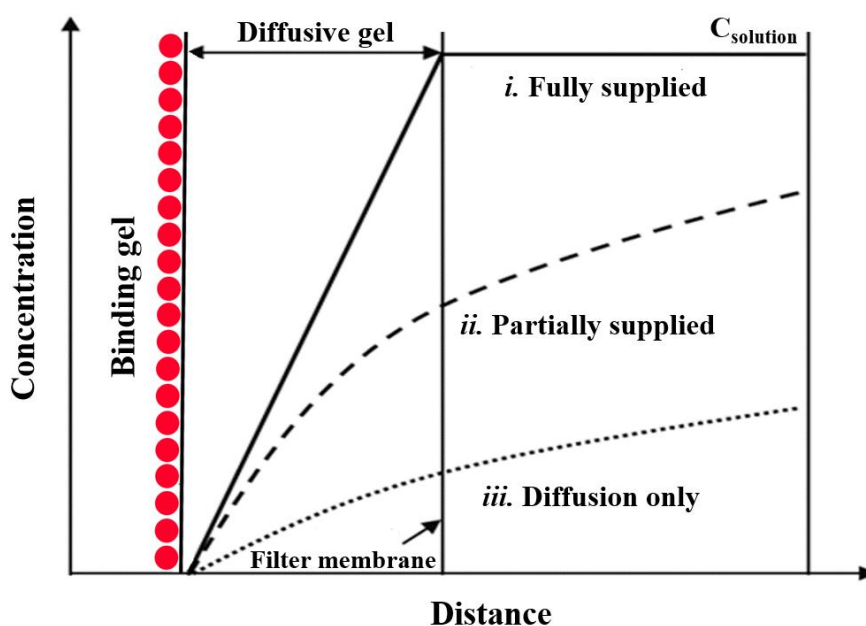
Figure 2.8 Schematic diagram of the solid phase's supply types. This picture is modified from Zhang et al. (1998b). C_{solution}: the initial concentration of analyte in the solid (soil/sediment) solution. With continuous depletion of the analytes by the DGT sampler, the capability of the analytes to be remobilized from the solid phase into solution can be reflected by the ratio (R) of C_{DGT} and the metal concentrations in solid solution (C_{solution}), indicating the extent of depletion of soil solution concentrations at the interface of DGT (Eq. 2.1). Fully supplied: resupply to solution can meet DGT adsorption ($R = 1$, reality: $R > 0.95$). Partially supplied: resupply is insufficient to sustain the initial bulk concentration and to satisfy DGT demands fully ($0 < R < 0.95$). If $R < 0.1$, it is diffusion only that supply to the DGT sampler is solely by diffusion from the soil solution.

Since the DIFS model is highly dependent on input data, there are inherent uncertainties involved in the application of the DIFS model. All studies using 2D-DIFS for organics so far considered the standard soil/sediment parameters, e.g., flux from solution to DGT device, ϕ_s, and P_c, which would cause uncertainties in output data. Lehto et al. (2008) assessed the quantitative output value of K_{dl} and T_c for metals using an error function and indicated that T_c could significantly vary under different conditions (e.g., different soil porosities). Additionally, the output of T_c and k_{-1} values can only provide the general kinetic resupply information in soils and sediments, while these cannot interpret the mechanism of desorption processes, which will need further development of this model. In addition, Ciffroy et al. (2011) highlighted two drawbacks of the DIFS model for geochemical behaviors, (*i*) accumulation kinetics in DGT show multiple kinetic stages; (*ii*) many combinations of K_{dl} and T_c are likely to be fitted to an experimental data set with equivalent results, raising a question of how to choose the most appropriate combinations. The probabilistic approach recommended by Ciffroy et al. (2011) for metals can be used to describe two or more labile particle pools that organic compounds are associated with, e.g., easily accessible or weak interaction compounds and an "inert" or "bound" pool characterized by stronger interactions (less accessible). In summary, the uncertainties of 2D-DIFS model for organic compounds are unknown and the relative values cannot provide a detailed information of intrinsic kinetic resupply in soils/sediments.

2.7.2 Soils

Soils are a sink for numerous organic pollutants through various pathways, e.g., sludge or manure application, air transport, pesticide application, and effluent irrigation (Hayat et al.,

2010). The risk assessment of these contaminants requires a thorough understanding of the interactions between these compounds and soils. Most studies have used batch extraction experiments to study the dynamics of organic compounds in soils, which consume a large volume of solvents (Collins et al., 2013; Zhang et al., 2020). These methods cannot directly reflect the *in situ* transfer of compounds between solids and solution or describe their mobility or bioavailability. Traditional methods such as solvent extraction and dynamic column techniques can affect a compound's distribution in soil solution and alter soil structures. *In situ* passive measurement approaches can minimize disturbance or perturbation of soil solutions in a controlled manner (Zhang et al., 1998b), offering an alternative method. DGT approaches have been successfully used to efficiently assess the availability, mobility, and lability of inorganic substances in soils and sediments (Roulier et al., 2008; Zhang et al., 2014; Sun et al., 2019).

DGT for organics with an XAD binding gel was first used in soil systems (sandy clay and loam soils) to provide insight into the mobility and lability of four antibiotics, including three sulfonamides (sulfamethoxazole, sulfamethazine, sulfadimethoxine) and trimethoprim (Chen et al., 2015). Chen et al. (2015) observed that the uptake of these antibiotics by DGT from soil solution could, to some extent, be sustained by resupply from the solid phase. Different thicknesses of diffusive gels (0.8 mm and 0.5 mm) were used in this study to characterize the ability of resupply from soils, which showed that the desorption from solid soil phases partially resupplied the concentrations of these antibiotics. Furthermore, increasing soil organic matter and ionic strength appeared to increase the fluxes of trimethoprim, whereas the sulfonamides were slightly suppressed. This observation might have been due to the declining thickness of

the electrical bilayer of the charged surface (Białk-Bielińska et al., 2012) and competition between preferentially sorbed dissolved organic matter moieties (such as carboxyl and phenol) and sulfonamides (Haham et al., 2012). This phenomenon may be impacted by different soil properties, and more studies with different soils should be carried out.

Chen et al. (2014) further studied the dynamics of these four antibiotics' sorption and desorption processes using the DIFS model. DGT samplers continuously adsorbed the antibiotics in soils, and correspondingly, the depletion of concentrations of antibiotics was observed in the adjacent soils. DIFS results showed that trimethoprim had the largest R values, indicating the greatest capability of the soil to maintain the original soil solution of trimethoprim concentrations. Furthermore, the higher labile solid phase pools (k_{dl}) for trimethoprim compared to sulfonamides showed a larger labile trimethoprim reservoir to resupply to the soil solution. With regard to T_c values, trimethoprim (> 3 h) appeared to be longer than sulfonamides (> 27 min), showing more rapid supply of trimethoprim to the soil solution. Similar results were observed for other antibiotics, namely tetracyclines (tetracycline, oxytetracycline, and chlortetracycline), in five farmland silt loam soils (wetted to 100% maximum water holding capacity) where DGT was deployed for 20 days (Ren et al., 2020). Three tetracyclines reached the steady state within 0.5 to 3 h, suggesting a quick initial resupply occurred for all three compounds. Although the greatest accumulated masses in DGT samplers were oxytetracycline > tetracycline > chlortetracycline, the fastest desorption rate with the largest values of response time derived from DIFS model was observed for chlortetracycline. Interestingly, Ren et al. (2020) found that chlortetracycline is highly bound to the soil solid phase as shown by the largest K_{dl} value, whereas continuous desorption from soil particles was

still substantial, a result attributed to soil textures. A positive Pearson correlation between the fraction adsorbers and clay portion (r = 0.901, $p < 0.05$) for oxytetracycline, and sand portion for tetracycline (r = 0.891, $p < 0.05$) was observed. To compare with more sandy texture soils studied by Chen et al. (2014), the fastest desorption rate found ($5.9 \times 10^{-6}\,s^{-1}$ for trimethoprim) was higher than that ($1.26 \times 10^{-6}\,s^{-1}$) reported by Ren et al. (2020). Recently, Li et al. (2021b) deployed DGT samplers to measure atrazine in four agricultural aging soils for 23 days and DIFS-derived results showed soil porewater was partially resupplied by the solid phase of the soils with less labile pool and slow desorption rate. Li et al. (2021b) related this phenomenon to soil pH, i.e., atrazine in its cationic form will have an affinity to negatively charged colloids in soils. However, the mechanism of the continuous and substantial supply of soil solution for certain compounds that interacted with soil properties needs to be further explored to understand the transport and uptakes by plant roots in the rhizosphere and other soil organisms.

Bialk-Bielinksa et al. (2012) used traditional solvent extraction methods and reported soils with higher organic matter and lower pH limited the desorption of sulfonamides and consequently caused lower soil solution concentrations (lesser values of C_d and C_s), findings similar to Chen et al. (2015). These two studies (Chen et al., 2014; Chen et al., 2015) showed that organic pollutants (e.g., antibiotics) could be released from the solid phase into solution under some circumstances, which controls the supply rates to the DGT sampler. This limited uptake by DGT samplers can be similar to uptake into soil biota if uptake by biota is initially fast. Therefore, the DGT device may mimic the constraint supply experienced by biota in soils. It was previously reported that DGT measurements of metals in soils were strongly correlated with their concentrations in soil biota (Zhang et al., 2001; Bade et al., 2012).

DGT samplers with HLB binding resin were recently deployed to different soils in the field after wetting with water to measure atrazine and its metabolites (Li et al., 2019). The results showed that the DGT sampler could be successfully used to measure the metabolites and revealed different degradation pathways (chemical and biological) for atrazine. Li et al. (2019) also reported that soil pH (range: 4.8−7.7) had more influence on atrazine degradation compared to previously reported impacts of soil organic matter content (Gavrilescu, 2005). Increasing soil pH increased the concentrations of atrazine metabolites, which may be due to hydrolysis of atrazine (Armstrong et al., 1967). Li et al. (2021b) further compared the adsorption processes of atrazine in neutral and acidic soils, showing that atrazine tended to be protonated to the cationic form that has a greater affinity to negatively charged colloids in soils when the soil pH is decreased. This proves that soil pH (compared to the analyte's pK_a) is an important controlling factor for the kinetics processes of organic compounds. Pesticides can be anionic, cationic, neutral, or zwitterionic, and dependent on pH values; thus, changing soil physicochemical properties depending on environmental conditions can affect the performance of DGT, as Chen et al. (2015) reported for the sulfonamides discussed above. Therefore, DGT performance for different organic contaminants and their possible metabolites in different soils under both controlled laboratory and field conditions should be further examined.

2.7.3 Sediments/biosolids

Passive samplers such as DGT measure the concentration of freely dissolved compounds (Booij et al., 2016), and therefore the diffusion of compounds is a key transport process in aquatic systems. Polymeric passive samplers have been used in sediments extensively to

estimate freely-dissolved concentrations and bioavailability of hydrophobic organic contaminants, e.g., polychlorinated biphenyls (Gschwend et al., 2011). More hydrophilic compounds may be more likely to assess the bioavailability with the DGT device. The scale of diffusion time through diffusion layers in mildly stirred media (e.g., sediments) can be similar to the chronic accumulation of pollutants by an organism over a short or long time (van Leeuwen et al., 2005). For example, if a benthic organism removes organic pollutants slowly in the sediment system, it can be resupplied by diffusion. In such a case, the depletion at the biological cell membrane can be negligible, revealing the uptake limiting condition and fitting the equilibrium models such as quantitative structure–activity relationships (QSARs). On the other hand, if the flux of bio-medium is larger than the diffusional supply, the concentration of compounds will be depleted at the biota-medium interface where a resupply from porewater of the solid phase in the sediment is limited (Fernandez et al., 2014). This supply limitation is equivalent to the principle of DGT and DIFS dynamic model. Therefore, the DIFS model may be suitable to describe the bio-uptake of organic pollutants in sediment or at the sediment/water interface, which will be a useful tool to assess bioavailability and toxicity of sediment-borne contaminants.

The flux of organic contaminants between the sediment and water column may occur *via* several mechanisms (Lick, 2006). There are only two studies using DGT for organic pollutants in sediment. Mechelke et al. (2019) used DGT with a larger exposed surface area (12.6 cm^2 versus 3.1 cm^2 for the standard configuration of DGT) to measure polar and semi-polar organic contaminants across the water-sediment interface in urban streams (hyporheic zones) with very low flow velocities (0.1 and 0.4 m s^{-1}). This new DGT configuration successfully measured the

attenuation patterns of 104 organic pollutants within different depths of sediments in hyporheic zones. Li et al. (2021b) first used both DGT probes for metals and organic compounds *in situ* in an intact lake sediment core and deployed the DIFS model for resupply kinetics and labile pool. This study found that atrazine can be resupplied from solid phase to solution and observed a greater labile size at the top layer of sediments due to the reduction of Fe/Mn oxides. The spatial resolution was 5 mm scale for ng L^{-1} in intact sediment cores in this study. Finer spatial scales for processes in different sediment layers of oxic/anoxic and water-sediment surface microlayers can be further studied.

Organic contaminants can remain in sewage sludge (biosolids) from municipal wastewater plants even after treatment (McClellan and Halden, 2010). Biosolids are applied to agricultural soils to improve soil fertility and other soil properties in many countries (White et al., 2011; Torri et al., 2017). An antibiotic, ciprofloxacin, was examined for its diffusion coefficient and sorption/desorption exchange processes in biosolids using a DGT sampler under laboratory-controlled conditions (D'Angelo and Starnes, 2016). The mass accumulation of ciprofloxacin in the DGT sampler over time was fitted to the DIFS model to successfully derive K_{dl} and sorption/desorption rate constant in the biosolids. DIFS results in this study suggested that there was more labile ciprofloxacin in the solid phase (~16% of total concentration) than was estimated by acetonitrile extraction (< 3%), which was the opposite trend observed for labile antibiotics (mean = 25%) and those extracted by acetonitrile (mean = 34%) in soils measured by Chen et al. (2014). Moreover, D'Angelo and Starnes (2016) observed that DGT could effectively measure the release of ciprofloxacin from the solid phase controlled by the effective diffusion coefficient over longer deployments (300 h). However, this diffusion coefficient can

be affected by environmental conditions, e.g., pH, ionic strength, and organic matter content. Therefore, D'Angelo and Martin (2018) further conducted an isotherm experiment to study the desorption kinetics of another antibiotic (tetracycline) in biosolids with organic amendments (poultry manure, wood chips litter, and rice hull litter) using the DGT-DIFS method. The results showed that high dissolved organic carbon content inhibited tetracycline partitioning, causing desorption and diffusion to be slow and transitory (<3 day) due to the small values of the effective diffusion coefficient ($< 8 \times 10^{-8}$ cm^2 s^{-1}) and the low labile pool (< 5% of the total concentration). D'Angelo and Martin (2018) recommend further studies concerning the uptake of tetracycline by root interception and microbial colonization from organic amendments, which may help to explain mechanisms of adsorption of organic pollutants in biosolids.

2.8 Combination with bioassays

The concentrated mass of organic pollutants extracted from receiving phases of passive samplers can be combined with various bioassay procedures to simultaneously estimate both pollutant concentrations and the resulting biological effects (Sabaliūnas et al., 1999). Conducting traditional toxicity tests and *in vitro* bioassays using bulk water samples is particularly challenging for most hydrophobic organic contaminants that are present at trace levels (i.e., < 1 µg L^{-1}). Thus, extraction and reconstitution are often required to yield sufficient analyte for subsequent bioassays. Using "bio-mimetically" derived extracts from passive samplers may solve this issue (Budzinski and Dévier, 2013).

The DGT technique has previously been combined with the Estrogen Responsive Element (ERE)-Chemically Activated LUciferase gene eXpression (CALUX) bioassay to determine

estrogenic activity, with 17β-estradiol as the model steroid hormone. The results demonstrated that this combination was a sensitive tool to determine estrogenic activities at very low concentrations (0.026 ± 0.003 ng 17β-estradiol-equivalents L^{-1}) from one-day *in situ* samplings in the discharge from three types of urban WWTPs, e.g., activated sludge with biological filtration (1,000,000 m^3 day^{-1}), activated sludge with ultrafiltration and ozone oxidation (550,000 m^3 day^{-1}), and sand filtration with oxidation ditch (90,000 m^3 day^{-1}) (Guo et al., 2017b). In a subsequent study, Guo et al. (2019) investigated various exposure times of DGT and assessed *in situ* the thickness of the diffusive boundary layer and its influence on the calculation of estrogenic activity. This study found that if the diffusive boundary layer thickness (0.010–0.023 cm) is negligible, the estrogenic activity estimated from DGT-derived concentrations would be underestimated by 10–20%. These two studies showed that time-averaged estrogenic activities could be determined by DGT coupled with the ERE-CALUX bioassay.

Another recent study was conducted to expose zebrafish and DGT samplers in water spiked with different concentrations of methamphetamine and its metabolite (amphetamine) (Yin et al., 2019). Interestingly, despite *in vivo* bioaccumulation and biotransformation of organic contaminants in fish being complex, strong positive relationships between the DGT-derived concentrations and whole-body concentrations of methamphetamine ($R^2 = 0.97$–1.00, $p < 0.001$) and amphetamine ($R^2 = 0.95$, $p < 0.001$) in zebrafish were observed at a methamphetamine exposure concentration of 1.00 μg L^{-1}. This was the first, but promising attempt to use the DGT technique to assess the bioavailability of organic compounds in zebrafish. More applications should be carried out for the combination of specific organic pollutants bioassays and DGT-derived concentrations, and predicting of bioavailability of organic pollutants by DGT

technique with various aquatic biota.

2.9 Conclusions and future recommendations

The DGT sampler has been a useful passive sampling tool for monitoring contaminants in aquatic and terrestrial systems because it is economical and easy to deploy at many sites simultaneously. It offers an average time-integrated concentration of the dissolved fraction of chemicals in water or soil/sediment porewater. This review discussed several current concerns in DGT passive samplers that need to be further examined for the applicability domain of DGT passive samplers for organics.

The original DGT configuration for metals included a protective filter membrane, yet the current materials used for filter membranes show retention of organic analytes. The most widely used PES membrane and PTFE membrane are not suitable for various organic compounds. A significant issue occurs in most currently used filter membranes concerning the initial mass of compounds taking longer time to reach adsorption equilibrium. Generally, individual compound behaves differently in different filter membranes. Although Wang et al. (2019) reported that the lag time caused by a PTFE membrane before linear mass accumulation can be calibrated through linear mass accumulation (steady state) experiments in the laboratory or can be negligible if the environmental concentrations are very high (> 10 μg L^{-1}). Current studies did not conduct a real equilibrium adsorption test to determine the maximum adsorption capacity for analytes.

Using the diffusive gel as the outer membrane may be an alternative approach to solve this issue. Although polyacrylamide and ceramic gels showed more resistance to grazing by aquatic

insects and general degradation in natural aquatic systems, both gels face the issue concerning the smaller pore size, and thus smaller sampling rates. Nylon netting agarose gel can be more robust with the same pore size as agarose gel, which may be a new option for DGT configuration for organic compounds. Besides, the fixing device for DGT samplers is usually not clearly mentioned in the studies. To some extent, different fixing devices will lead outer diffusive gels to face different environmental situations, which needs to be considered in future studies. Furthermore, using the diffusive gel as the outer membrane for sediment/soil systems should be further examined since it may be problematic due to a greater chance of physical damage during deployment into the solid phase.

Most studies are consistent that biofilms have minimal to no effect on DGT uptake for hydrophilic and hydrophobic compounds in the short term (7–8 days) and long term (15–21 days). However, very few publications have studied this systematically. The mechanisms controlling biofilm formation on DGT hydrogels for organic compounds should be further studied.

Currently, studies on DGT deployments in the solid phase (e.g., soils and sediments) are quite limited. DGT performance for more compounds (especially for hydrophobic compounds) and their metabolites should be investigated in different physical-chemical characterizations and exchange kinetics processes, especially at sediment and water interfaces. The uncertainty output from the DIFS model caused by input parameters should be systemically studied and DIFS should be further developed to explain mechanisms of dynamic exchange processes between the solid phase and the solution by quantitative values.

Limited evidence suggests promising possibilities for DGT to be combined with bioassays,

including with ERE-CALUX and *in vivo* bioaccumulation in zebrafish. Further studies considering using DGT coupled with bioassays to predict bioavailable fractions or reveal toxic/adverse effects on aquatic or terrestrial biota should be further developed. Moreover, the combination of the dynamic models in soils and sediments (e.g., DIFS model) with bioavailability is also recommended to predict the bio-uptake of organic contaminants in different desorption stages.

CHAPTER 3: Desorption kinetics of emerging organic contaminants from sandy sediments by diffusive gradients in thin-films technique

Overview

A version of this chapter has been published in *Science of The Total Environment* with the following details:

Xiaowen Ji, Jonathan K. Challis, Jenna Cantin, Ana S. Cardenas Perez, Yufeng Gong, John P. Giesy, Markus Brinkmann. Desorption kinetics of antipsychotic drugs from sandy sediments by diffusive gradients in thin-films technique. Science of The Total Environment, 2022, 832, 155104. Published: 1 August 2022. DOI: https://doi.org/10.1016/j.scitotenv.2022.155104

Contributions

Xiaowen Ji: conducted the entire experiment and wrote the manuscript.

Jonathan K. Challis: set up the LC-MS methods for nine antipsychotics and revised the manuscript.

Jenna Cantin: Ran part of samples.

Ana S. Cardenas Perez: spiked the sediments.

Yufeng Gong: revised the manuscript.

John P. Giesy: revised the manuscript.

Markus Brinkmann: designed the experiment, secured funding, and revised the manuscript.

Transition

The previous review chapter reviewed the current development of the DGT technique and potential gaps in the current deployment. One of the significant gaps was that DGT performance for hydrophobic contaminants and DGT deployment in sediment and water interfaces for exchange kinetic processes were rarely reported. To solve this gap, this chapter aimed to test and deploy DGT samplers both in laboratory-controlled conditions and natural rivers for desorption kinetics of nine selected organic contaminants in water and sediments. Briefly, DGT configuration, including protection filter membrane, shell molding, and diffusive gel, was checked for potential adsorption of analytes. Furthermore, the efficiency of contact time and adsorption capacity for binding gel was also checked to meet the adaptability to detect concentrations of analytes in the aquatic environment. The sampling rates in the diffusive gel of analytes were measured before the DGT deployment. Based on the results obtained from both laboratory-controlled conditions and the natural field (South Saskatchewan River), resupply processes and kinetics of exchange of analytes in water–sediment system were modeled, compared, and explained.

Abstract

Dynamic processes of organic contaminants in sediments can have important toxicological implications in aquatic systems. The current study used diffusive gradients in thin-films (DGT) devices in sandy sediments spiked with nine antipsychotics and in field sandy sediments. Samplers were deployed for 1 to 30 days to determine the flux of these compounds to DGT devices and the exchange rates between the porewater and sediment solid phase. The results showed a continuous removal of antipsychotics to a binding gel and induced a mobile flux from the DGT device to the adjacent sediment solution. A dynamic model, DGT−induced fluxes in soils and sediments, was used to derive rate constants of resupply of antipsychotics from the solid phase to the aqueous phase (response time, T_c) and distribution coefficients for labile antipsychotics. The largest labile pool was found for lamotrigine and carbamazepine in spiked sediments. Carbamazepine, clozapine, citalopram, and lamotrigine were resupplied rapidly by sediments with T_c (25−30 min). T_c values of bupropion and amitriptyline were the longest ($\approx$ 5 h), which exhibited slow desorption rates in sediments. In field sediments, high resupply was found for carbamazepine and lamotrigine, which did not show a higher labile pool. The T_c values were obviously higher in the filed sediments (52−171 h). Although the adsorption process is dominant for most studied antipsychotics in both spiked sediments and field sediments, the kinetic resupply of antipsychotic compounds may not be accurately estimated by laboratory-controlled incubation experiments. More studies are needed to explore the mechanisms of desorption kinetics by using *in situ* DGT technique in the field.

Keywords: Antipsychotics, DGT, desorption kinetics, sediments, DIFS-model

3.1 Introduction

Due to the treatment of aging-related, chronic, and emerging diseases, as well as alterations in clinical practice, the consumption of pharmaceutical drugs continues to increase globally (Kümmerer, 2008). Global use of human pharmaceutical drugs was estimated to be approximately 100,000 metric tons annually (Kümmerer, 2008). In particular, consumption of antipsychotic drugs to treat or manage, e.g., schizophrenia, severe depression, and autism, continues to increase globally (López-García et al., 2018; Kuroda et al., 2019). Drugs excreted from our bodies enter wastewater treatment plants through municipal sewage. Common technologies applied for treating domestic sewage are not designed to remove these pharmaceutical compounds or their metabolites, which results in the occurrence of pharmaceuticals in the environment (Escudero et al., 2021). For instance, The occurrence of several antipsychotic drugs, e.g., venlafaxine (0.526–1.115 μg L^{-1}), citalopram (0.136–0.223 μg L^{-1}), fluoxetine (0.020–0.091 μg L^{-1}), and bupropion (0.070–0.191 μg L^{-1}) was observed in Canadian untreated wastewater with ~40% removal rate in the outlet (Metcalfe et al., 2010). Additionally, various psychoactive drugs and their metabolites have been detected in surface and drinking water (Silveira et al., 2013; Nannou et al., 2015; Caldas et al., 2016), wastewater (Bollmann et al., 2016; Reichert et al., 2019), offshore seawater (Alygizakis et al., 2016), river sediment (Nunes et al., 2019), and fish (Kalichak et al., 2017). These compounds have the potential to cause effects in aquatic ecosystems. For example, exposure to venlafaxine and citalopram could cause significant foot detachment from the substrate for two freshwater snails (*Leptoxis carinata* and *Stagnicola elodes*) (Fong and Hoy, 2012). Fluoxetine was found to significantly affect the mating behavior of male fathead minnow (*Pimephales promelas*) at

relatively small concentrations (1 µg L^{-1}) (Weinberger and Klaper, 2014).

After entering aquatic environments, these bioactive compounds can be dissolved in the aqueous phase or sorbed to organic material and particles, where they can settle in sediments (Stein et al., 2008). However, the sorption of organic compounds onto sediments is influenced by various factors, including chemical structure, ionization state, and sorbent properties. Extensive H-bond interactions between sorbents and antipsychotic compounds are possible, given the polarity of these compounds (Stein et al., 2008). Therefore, cationic species of antipsychotic compounds are likely to interact electrostatically with negatively charged sorption sites of sorbents. Strong sorption caused by electrostatics was observed for some polar pharmaceuticals, such as sulfonamides and trimethoprim to soils (Chen et al., 2015), and ciprofloxacin to biosolid (D'Angelo and Starnes, 2016). Results of previous studies are consistent and indicate that most cationic species of antipsychotic compounds will bind to negatively charged sorption sites on/in the surfaces of clay and silt minerals, sediment organic matter, and clay mineral-humic complexes (Gao and Pedersen, 2005; Stein et al., 2008; Styszko, 2016; Azuma, 2018; Nunes et al., 2019). However, to date, the dynamics of these compounds have been studied mostly in batch or dynamic column experiments, and the kinetic exchange of antipsychotics has received less attention. Kinetic controls of antipsychotic resupply in the sediment environment can affect the mobility of these compounds in the water−sediment continuum and the availability of these compounds to aquatic organisms.

A passive sampling technology, DGT (diffusive gradients in thin films) for organics, was initially designed for sampling from water (Chen et al., 2012) but has been recently used for *in-situ* measurement of desorption kinetics of antibiotics in soils (Chen et al., 2014; Chen et al.,

2015; Ren et al., 2020) and biosolids (D'Angelo and Starnes, 2016; D'Angelo and Martin, 2018).

Information on the distributions of contaminants between solution and sediment is essential for understanding their environmental behaviors, which is usually expressed as the sediment-water distribution coefficient (K_d) (Martín et al., 2012; Nunes et al., 2019). However, most traditional methods cannot measure the dynamics of compounds while minimally disturbing the sediments. A dynamic model (DGT-Induced Fluxes in Sediments and Soils, DIFS) can be used to describe the release of solutes in sediments and offer better insights into the labile pool size and kinetics of solute resupply from the solid phase (Harper et al., 1998). DGTs are limited in their ability to provide quantitative results, primarily due to issues with knowledge of their sampling rate (Yao et al., 2019). Pseudo-first-order models work well because the slowest kinetic process is generally near-surface diffusion, which is by definition first-order and generally rate-limiting (Noh et al., 2019). If more accurate information is available for the kinetics of diffusion and if the duration of exposure is known, then rates of sampling can be calibrated for various compounds, and quantitative estimates of the available fraction and concentrations can be determined (Dunn et al., 2003). Only one study used the DGT and DIFS model for the remobilization of organic pollutants (pesticide atrazine) in an intact sediment core for an *in situ* fine scale (Li et al., 2021b). The hypothesis of this study is that the DIFS model can quantitatively estimate the dynamic processes of antipsychotics in either spiked sediment systems or *in situ* field sediments.

Here, the DIFS model was adapted to describe the dynamics of antipsychotics in sediments in two different environments with quantitative parameters to describe kinetics and partitioning. The DGT samplers were deployed both in spiked sediments, which were well-equilibrated (~60%

equilibrium) with nine representative and environmentally relevant antipsychotics (amitriptyline, bupropion, carbamazepine, citalopram, clozapine, duloxetine, fluoxetine, lamotrigine, and venlafaxine), and *in situ* surficial sediments from a natural river for various time periods up to 30 days. The concentrations accumulated in DGT samplers over time were fitted to the DIFS models to estimate desorption rate constants and labile pool sizes of antipsychotics in the solid phase of sediments.

3.2 Materials and methods

3.2.1 Standards, reagents, and chemicals

Nine high purity (> 98%) antipsychotics (amitriptyline, bupropion, carbamazepine, citalopram, clozapine, duloxetine, fluoxetine, lamotrigine, and venlafaxine) and the corresponding nine mass-labeled internal standards (amitriptyline-d_6, bupropion-d_9, carbamazepine-d_{10}, citalopram-d_6, clozapine-d_4, duloxetine-d_7, fluoxetine-d_5, lamotrigine-$[^{13}C;^{15}N_4]$, and venlafaxine-d_6) were used. The details on standards, reagents, and chemicals are shown in **Appendix 1** and **Table A1**.

3.2.2 Theory of DGT and DIFS model in sediments

The DGT sampler for organics is composed of a binding layer, a diffusive layer, and a filter membrane for protection (Chen et al., 2012; Challis et al., 2016). External analyte diffuses through the diffusion layer with a certain diffusion coefficient (D) and is promptly bound by the adsorbent in the binding layer. After an initial period needed to reach steady-state diffusion dynamics, a constant concentration gradient is maintained in the diffusion layer.

DGT *in situ* passive sampling is based on Fick's first law of diffusion (Davison and Zhang, 1994). After an initial period that is needed to reach steady-state diffusion dynamics, a constant concentration gradient is maintained in the diffusion layer. This gradient is determined by the thickness of the diffusion gel (Δg) and the interfacial concentration of labile analytes between the DGT device and sediments (C_i). The flux of antipsychotics (F, mol cm^{-2} s^{-1}) through the diffusion phase to the binding phase can be calculated based on Fick's first law (Eq. 3.1). As deployment time increases, the compound concentrations in the sediment solution are gradually depleted from increasingly further distances from the interface between sediments and the DGT sampler. This can induce a resupply of compounds through diffusive transport from the particle phase (Harper et al., 2000). Since the binding gel functions as an infinite sink (for the trace concentration in the aquatic environment) that is consistently adsorbing compounds from sediment solution during deployment, the total mass of bound compounds can be determined after retrieval of the device. Meanwhile, the flux of compounds can be expressed as Eq. (3.2).

$$F(x,t) = \varepsilon D \frac{C_i(x,t)}{\Delta g}, 0 < t < T, x \in (-r,r) \quad (3.1)$$

$$m = \frac{\varepsilon D}{\Delta g} \int_{-r}^{r} \int_{0}^{T} C_i(x,t)dtdx \quad (3.2)$$

where ε is the porosity of the agarose diffusion gel, D (cm^2 s^{-1}) is the diffusion coefficient of each analyte in the diffusion layer, t (s) is the deployment time, r represents the radius of the circular exposure window, and m (mg) is the accumulated mass of compounds in the binding gel. The porosity of the gel ($\varepsilon = 1 - \emptyset$, $\emptyset$ is the volume fraction of fibers) can be defined as an estimate of the pore size determined by using a hydrodynamic model that links permeability to the structural properties of the fibril matrix (Levick, 1987). The Carman Kozeny equation

(Carman, 1937) offers the relation between permeability, average hydraulic radius (r_H), and hydrodynamic screening distance (κ), explained as Eq (3.3).

$$\kappa = \varepsilon \cdot \frac{r^2_H}{k} \quad (3.3)$$

where k represents the Kozeny factor, depending on the channel shape and tortuosity. Pluen et al. (1999) used this model for 2 % agarose gel with results $\varepsilon = 0.9805, \varnothing = 0.0195$, which were also used in our study.

The time-averaged interfacial concentration (C_{DGT}) of targeted solutes accumulated on the binding gel can be determined according to m shown in Eq. (3.4) (Lehto et al., 2008).

$$C_{DGT} = \frac{\int_{-r}^{r} \int_{0}^{T} C_i(x,t) d_t d_x}{T} = \frac{m \Delta g}{\varepsilon ADT} \quad (3.4)$$

where A is the area of exposure surface (2.54 cm^2). m can be determined with HPLC−Orbitrap MS after extraction of antipsychotics from the binding gel.

A ratio (R) between C_{DGT} and the independently measured initial concentration ($C_{porewater}$) in interstitial water (porewater) of sediment can explain the extent of depletion of concentrations at the interface of the DGT device (Eq. 3.5) (Ernstberger et al., 2002).

$$R = \frac{C_{DGT}}{C_{porewater}} \quad (3.5)$$

The magnitude of the value of R depends on the kinetics of adsorption−desorption in sediments. Kinetic parameters can be derived from inputting R to the DIFS model. The one-dimensional DIFS model is used for describing processes in only the sediment solution, while the two-dimensional DIFS model is used for simulating the DGT behavior within sediments (Lehto et al., 2008). In the sediment system, the flux from the solid phase to the solution induced by DGT (F_{ss}) might not be equivalent to the maximum potential flux from the solid phase to

the solution (F_{pm}), which depends on DGT characteristics and the sediment properties. There are three possibilities for the relationship between F_{ss} and F_{pm}: (*i*) fully supplied–compounds adsorbed by the DGT device from sediment solutions can be replenished instantly from the solid phase supplied by a labile pool size, which efficiently maintains a constant concentration in the solution; (*ii*) diffusion only–no resupply from solid phase to the sediment solution ($F_{ss} \approx$ 0). Concentrations of compounds in porewater at the interface of the device will gradually decrease, with this decline of concentration progressively extending to the sediments situated further away from the interface of the DGT device; (*iii*) there is partial resupply of compounds from the solid phase to sediment porewater whereas this supply is not enough to maintain the initial concentration in the porewater that can be taken up by the DGT device ($F_{ss} \approx F_{pm}$). Generally, the most probable condition for most organic compounds in sediments is case (*iii*) due to the supply of organic compounds from the solid phase to solution through the release of several forces, e.g., surface complexation, electrostatic interaction, and hydrogen bonding (Delle Site, 2001).

Values of R (Eq. 3.5) can be used to differentiate the three cases stated above. When $R \geq 0.95$, the compounds in porewater are completely replenished from the solid phase. When $0.1 < R < 0.95$ and $R < 0.1$, indicates scenarios of partially supplied and diffusion only, respectively. In general, larger values of R indicate larger sizes of labile pools and more rapid rates of replenishment. Another approach that does not rely on measurements of R to identify these cases is by simultaneously deploying DGT samplers with different thicknesses of diffusive layers (different Δg), that can be used to plot F against $1/\Delta g$. If there is a linear increase of

fluxes with $1/\Delta g$ or time, it would be fully supplied, whereas the curved increase would be partially supplied or diffusion only.

The DIFS model can describe quantitatively the distribution ratio (K_{dl}, cm^3 g^{-1}) between concentrations of labile compounds associated with the solid phase (C_s) to concentrations in sediment porewater ($C_{porewater}$) at steady state (Harper et al., 2000) (Eq. 3.6) and the exchange rate of the sediment response time, T_c (s), which is the characteristic time in the disturbed system (after DGT deployment) to approach 63% of its steady-state (Eq. 3.7) (Jannasch et al., 1988).

$$k_{dl} = \frac{C_s}{C_{porewater}} = \frac{k_f}{P_c k_b} \quad (3.6)$$

$$T_c = \frac{1}{k_f + k_b} = \frac{1}{k_b + (k_{dl} P_c + 1)} \quad (3.7)$$

where k_f and k_b represent adsorption and desorption rate constant (s^{-1}), and P_c is the particle concentration ($P_c = M/V$, g cm^{-3}, where M represents the gross mass of the solid particles and V represents the volume of porewater of the gross volume of sediment). Key parameters required by the DIFS model are listed in **Table A2**, hypothesizing a particle density of 2.56 g cm^{-3} (Chen et al., 2014) since the soil/sediment particle density generally ranges from 2.40 to 2.75 g cm^{-3}, often assumed as the average value of 2.65 g cm^{-3} (density of quartz) (Amoozegar et al., 2023). In the present study, DGT samplers with different diffusion layer thicknesses were deployed at different times. In each interval, C_{DGT} was calculated with Eq. (3.4) and $C_{porewater}$ was directly measured, and the corresponding R value was calculated (Eq. 3.5). K_{dl} and T_c values were derived from the best-fit model of a plot of R versus t. Finally, k_b and k_f were derived from K_{dl} and T_c (Eq. 3.6 and Eq. 3.7).

3.2.3 Sediment preparation and spiking

Sediment for spiking was collected from an urban area of the South Saskatchewan River (52°09'22.8"N 106°38'08.2" W), in Saskatoon, Canada (**Figure A1**), upstream of Saskatoon's wastewater treatment plant. Surface sandy-loam sediments (<5 cm, avoiding the inhomogeneous texture of sediments) were sampled with a shovel and stored in a PVC bucket that was previously rinsed with river water, then immediately transferred to a thermostatic chamber (4 ± 1 °C) in the dark for 1 day. Afterward, the sediments were transferred to a freezer (-20 °C) before lyophilization (Dura-Dry MP FD2085, Stone Ridge, NY). The dried sediments were passed through a 2-mm sieve to remove large fragments and roots before the spiking experiment and determination of the sediment's physicochemical properties. The pH of sediment was potentiometrically measured in a 1:2.4 sediment-liquid mixture containing either ultrapure water or 0.01 M $CaCl_2$ solution. Maximum water holding capacity (MWHC) was determined by soaking the sediments in water and draining them for 2 h (Priha and Smolander, 1999). Distributions of particle sizes, organic matter, and TOC (total organic carbon) were measured by hydrometer and federal standard method (MMFSPA Ch6 1991 m), respectively, which were conducted by Bureau Veritas Laboratory (Edmonton, AB). Characteristics of this sediment are: pH-H_2O 7.13, pH-$CaCl_2$ 6.69, MWHC 65%, sand 54%, silt 35%, clay 11%, organic matter 1%, and TOC 0.59%.

Before spiking, dried sediment was extracted and analyzed using high-performance liquid chromatography–Orbitrap™ mass spectrometry (HPLC–Orbitrap MS) (details in section 3.2.8) to ensure that tested analytes did not pre-exist in our sediments. Approximately 2 mg of each antipsychotic compound was dissolved using a small volume of methanol (~2 mL), diluted in

50 mL ultrapure water, and added to 800 g of sediments (total in the tank). To do this, a small portion of the sediment was placed in a mortar, and the spiking solution was gradually added and mixed thoroughly to minimize solvent effects. Finally, all sediment portions were mixed and stirred together using an Omni Mixer Homogenizer (PerkinElmer, Waltham, MA) to reach a concentration of 2.5 mg kg^{-1} for each antipsychotic compound in order to be adequate supply to sediment solution following a previous study (Chen et al., 2015). The well-mixed sediments were then placed in a glass tank (length: 12 cm, height: 7 cm, and width: 6 cm), and the overall weight (sediment + glass tank) was measured each day until the weight remained stable ($\pm$ 0.1 g) over three days at room temperature (21 $\pm$ 0.5 °C). Blank sediment was prepared using the same amount of methanol and ultrapure water without antipsychotic compounds following the same protocol. Afterward, the sediments were submerged under ~ 3.5 cm of ultrapure water and kept at the same water level for 24 h at room temperature before the deployment of DGT devices.

3.2.4 DGT preparation

Standard size of DGT devices (made from polytetrafluoroethylene) with 0.75 mm Sepra^{TM} ZT (surface modified styrene-divinylbenzene, Phenomenex, Torrance, CA) resin gels, 0.75 mm agarose diffusive gels, and 0.45 μm pore size polyethersulfone (PES) filter membranes (Sartorius Stedim Biotech GmbH, Gottingen, Germany) were prepared following the protocols of Challis et al. (2016). This study still used a traditional DGT configuration that contains an agarose gel and a protection filter because the pore sizes of agarose (>100 nm) are far larger than those of polyacrylamide (<20 nm) commonly used as an outer membrane (detailed

discussion in Review Chapter 2.4). Additionally, DGT units were assembled with several thicknesses of diffusive gels (0.75, 1.0, 1.2, 1.5, 1.8, 2, and 3 mm). These different thicknesses of the diffusive gel can provide information on the characteristics of the transport ability of analytes from the sediment particle phase to the aqueous phase. Briefly, a 2% dissolved agarose was cast between vertical glass sheets using the Mini-Protean® casting system (BioRad, Mississauga, ON). The gels were cut into corresponding disks and stored at room temperature in ultrapure water. The binding gels were cast horizontally to make the sorbent powder settle on one side of the gel. Eventually, cut gels contained ~ 25 mg of sorbent per gel disk. Both diffusive gels and binding gels were rinsed with ultrapure water before the preparation of the DGT device. The binding gel was placed on the standard polytetrafluoroethylene DGT base (sorbent side pointed up), covered with the diffusive gel and PES filter membrane layered on top, and sealed with the DGT cap. To test the performance of DGT samplers, the potential adsorption of the targeted antipsychotics to the diffusive gel, DGT molding, and PES filter membrane, as well as the sorption efficiency of Sepra™ ZT binding gel were assessed (Details in **Appendix 2**).

3.2.5 DGT deployment

3.2.5.1 Deployment in laboratory-controlled spiked sediments

DGT devices were assembled before deployment in sediments. DGT devices with various thicknesses of diffusive gels (triplicate) were then pressed firmly onto the sediment in order to achieve close contact between the sediment and DGT devices (**Figure 3.1**). A digital thermometer was inserted into the tank water to ensure a constant temperature during the

experiment. DGT devices were deployed for 1, 3, 5, 8, 11, 16, 20, 25, or 30 days in the laboratory at a water temperature of 21 ± 0.5 °C to obtain information about the extent of depletion of sediment solution concentrations of antipsychotics at the DGT interface.
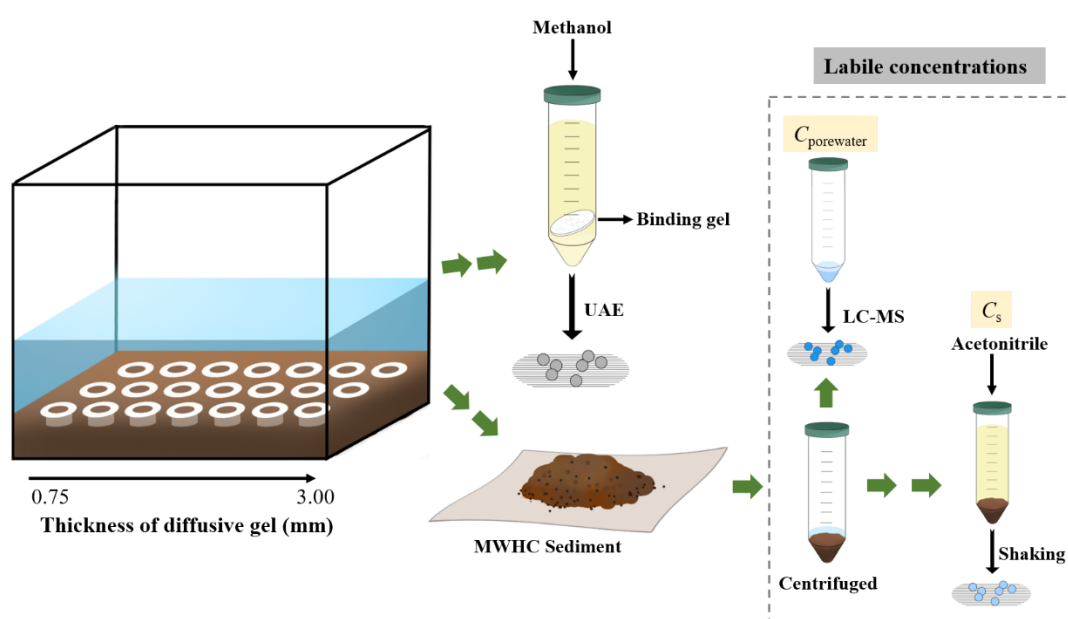
Figure 3.1 Schematic representation of the deployment of DGT samplers with different diffusive gel thicknesses (0.75, 1.0, 1.2, 1.5, 1.8, 2.0, and 3.0 mm) in sediments. Three DGT devices in a row represent triplicate samplers, while the thickness of diffusive gels progressively increases. Additionally, the procedure used to obtain concentrations in the sediment porewater ($C_{porewater}$), and extract the labile concentration with the solid phase (C_s) as shown in Eq. (3.6), and the concentration of binding gel is depicted.

3.2.5.2 Deployment in field

One DGT probe (length: 170 mm and width: 40 mm), constructed from acrylonitrile butadiene styrene (ABS) polymer and contained the same three layers as the DGT device, with different dimensions of binding gel (~250 mg per gel), diffusive gel, and PES membrane (length: 150.3 mm and width: 20.4 mm), and a temperature logger was attached in the bottom on a perforated stainless-steel profile (thickness: 3.18 cm, width: 3.18 cm, length: 183 cm). Three separate profiles with attached samplers were slowly inserted into sediments, with 2 cm of the

probe board exposed out of sediments (15 cm was put into the sediment), and were supported by three cement blocks (height: 19 cm, width: 27 cm) for protection (**Figure A2**). DGT setup for sediments was deployed from a natural area (Fred Heal Canoe Launch, 51°59'04.8" N 106°44'13.9" W) of the South Saskatchewan River, in Saskatoon, Canada, downstream of Saskatoon's wastewater treatment plant. Characteristics of field sediment were: pH-H_2O 7.43, pH-$CaCl_2$ 6.21, MWHC 61%, sand 46%, silt 32%, clay 22%, organic matter 2%, and TOC 0.63%. The nine antipsychotic compounds were detected at this sampling site in a previous investigation (unpublished data). Three extra DGT probes were brought to the field as the field blanks. DGT probes were deployed for 1, 3,6, 9, 12, 15, and 21 days.

3.2.6 DGT retrieval, sediment sampling, and extraction

DGT devices/probes were retrieved after each duration of deployment in triplicate. Sediment attached to DGT devices was rinsed off using ultrapure water, and the devices were disassembled to remove the binding gel and transfer them into glass vials immediately. The cleaned DGT probes were covered by aluminum foil and delivered to the laboratory immediately. The procedure of extraction of binding gel and labile concentration is shown in **Figure 3.1**. For binding gel disassembled from the DGT device, fifty microliters of 1 mg L^{-1} internal standards were added. Five milliliters of methanol were added into the vial for ultrasonic extraction for 10 min, and the same procedure was repeated three times. Extracts were combined and reduced to near dryness with a gentle flow of nitrogen gas (purity > 99%), reconstituted in 1 mL of methanol, and filtered through Target2™ 0.2 μm polytetrafluoroethylene syringe filters (Waltham, MA) into 2 mL LC vials.

Once DGT devices/probes were retrieved, approximately 5 g of wet sediment (adjacent to DGT probes in the field, depth: ~5 cm) was sampled and drained for 2 h (for maximum water-holding capacity) and then centrifuged at 1,280× g for 40 min to obtain sediment porewater. The sediments sampled from the field were stored in amber bottles which were covered by ice bags until delivered to the laboratory. Fifty microliters of internal standards were added to 950 µL of this solution and filtered through a 0.2 µm polytetrafluoroethylene syringe filter into 2 mL LC vials for analysis of $C_{porewater}$. The remaining sediment was lyophilized, extracted twice with 5 mL of acetonitrile for 10 min on a shaker, fortified with internal standards, and then followed the same procedure above for analysis of C_s.

3.2.7 Agarose diffusion coefficient (D)

Diffusion coefficients of analytes were measured using a diaphragm diffusion cell in pseudo-steady-state mode (**Figure A3**), which is the most accurate method to determine diffusion coefficients in agarose gel (Westrin et al., 1994; Zhang and Davison, 1999). Each cell (made of clear acrylic) held ca. 50 mL and had a 2.3 cm^2 circular connecting window. A diffusive gel was placed on the window (a spacer was made based on the gel thickness) between the two cells and gently sealed together with clamps. Each cell was full with 40 mL solution. To each cell, 20 mL of 10 mM NaCl was added, followed by a spike of the 9-analyte stock mixture (1,000 μg L^{-1}) prepared in 5% methanol into the source cell at a target concentration of 500 μg L^{-1}. Meanwhile, 20 mL of 5% methanol spike was added to the receiving cell. Both cells were stirred gently on stir plates. The water temperature was kept at 21±0.5 °C during the experiment. Triplicate samples (195 μL) were taken from the receiving cell and source cell at ten different

time points spread out over the experimental duration (5 to 140 min). Samples were pipetted directly into LC vials and spiked with 5 μL of 1,000 μg L^{-1} internal standards before instrumental analysis.

The mass of the analyte from the receiving cell was plotted as a function of time to acquire a slope (k) from the first-order diffusion rate constant, D can be calculated as Eq. (3.8).

$$D = k \frac{\Delta g}{CA} \quad (3.8)$$

Where Δg is the thickness of the agarose gel, C is the concentrations of nine antipsychotics in the source cell, and A is the area of the window between two cells.

For D calculation for different temperatures, they were calculated from D values for 25 °C (D_{25}) using an empirical formula established by Yuan-Hui and Gregory (1974) (Eq. 3.9):

$$\log \frac{D_{25}(273+T)}{298} = \log D_T - \frac{1.37023(T-25) + 0.000836(T-25)^2}{109+T} \quad (3.9)$$

3.2.8 Instrumental analysis

Analysis of nine antipsychotic compounds from all samples was conducted using a Vanquish UHPLC and Q-Exactive^{TM} HF Quadrupole-Orbitrap^{TM} hybrid mass spectrometer (Thermo-Fisher, Mississauga, ON). LC separation was achieved with a Kinetex 1.7 μm XB-C$_{18}$ LC column (100 × 2.1 mm) (Phenomenex, Torrance, CA) by gradient elution with 95% water + 5% methanol (A) and 100% methanol (B), both containing 0.1% formic acid (Optima MS grade) at a flow rate of 0.2 mL min^{-1} and a column temperature of 40 °C. The gradient method started at 10% B, ramping linearly to 100% B over 7 min, was held for 1.5 min, and returned to starting conditions for column re-equilibration between 8.5 – 11 min.

Samples were ionized using positive mode heated electrospray ionization (HESI). The Q-

Exactive Orbitrap method used the following source parameters: sheath gas flow = 35; aux gas flow = 10; sweep gas flow = 1; aux gas heater = 400 °C; spray voltage = 3.8 kV; S-lens RF = 60; capillary temperature = 350 °C. A Full MS/parallel reaction monitoring (PRM) method was used with the following scan settings: 120,000/15,000 resolution, AGC target = $1\times10^6/2\times10^5$, max injection time = 50 ms/50 ms, full MS scan range of 80-500 m/z and PRM isolation window of 2.0 m/z and multiplexing count of 4.

Batch analyses of samples were conducted by running calibration standards at the beginning and end of each sample batch along with blanks run between replicate treatment sets and 50 μg L^{-1} single calibration standards after running calibration standards and every 20 samples as a QA/QC protocol. A nine-point calibration curve ranging from 0.01 – 950 μg L^{-1} and spiked with 50 µg/L IS was used for quantification by isotope dilution (linearity > 0.99 for all analytes). All data acquisition and processing were conducted using Xcalibur v. 4.2 (Qual and Quan browser). The quantification of each analyte was according to precursor and product ions, and retention time (**Table A3** and **Figure A4**). The calibration curves (**Table A4**), method detection limits (MDL), limits of quantitation (LOQ), and limits of detection (LOD) are reported (**Table A5**). When the concentrations of analytes were below the detection limit, the substitution method (LOD/square root of 2) was used(Ganser and Hewett, 2010). MDL was calculated using the average blank DGT concentration plus three times the standard deviation (3σ). The extraction and processing procedures of DGT laboratory blanks were the same as described in the main text. The instrumental LOD and LOQ were regarded as the low concentration of analyte with a measured signal/noise (S/N) of 3 and 10, respectively (LOD = 3σ$_{blank}$/slope, LOQ = 10σ$_{blank}$/slope). Slopes were obtained from 9-point calibration curve.

3.2.9 Statistical analyses

Kolmogorov-Smirnov test and Shapiro-Wilk test were used to check the normality of datasets. Hartley's Fmax test was used for data homoscedasticity. Then, a one-way ANOVA with a Tukey's posthoc test was conducted to compare diffusion coefficients at various thicknesses of diffusive gels and to compare concentrations measured by DGT and porewater concentrations directly analyzed by LC-MS. Significant differences were defined as $p \leq 0.05$. Statistical analysis was conducted using IBM SPSS 26.

3.3 Results and discussion

3.3.1 DGT performance and diffusion coefficient

3.3.1.1 Sorption to DGT materials

Sorption steady-state concentrations of the nine antipsychotics were quickly reached (< 0.5 h) for DGT molding and diffusive gel. Concentrations remained consistent for 168 h with a negligible fraction (< 0.01% total mass of the standard solution) adsorbed to DGT moldings and diffusive gels. This observation is consistent with tests for other organic compounds (e.g., pharmaceuticals, hormones, and pesticides) (Zheng et al., 2015; Chen et al., 2018; Guan et al., 2018; Zhang et al., 2018; Zou et al., 2018; Wang et al., 2019).

Concentrations of all compounds on the PES filter membrane increased within an hour and reached steady-state sorption within 2 h (**Figure 3.2**). Proportions of analytes sorbed were negligible (< 1% of the total mass of the standard solution) for all durations. This result is consistent with the results of previous studies, which confirms that PES filter membranes can

support long deployment times, high sampling rates, and minimal adsorption of hydrophilic

organic compounds (log K_{ow} < 3) (Alvarez et al., 2004; Zhang et al., 2018). Large amounts of

sorption (>30% of the total mass of the standard solution) of some hydrophobic compounds

(log K_{ow} =3.7−5.1) by the PES filter membrane has been previously reported by Wang et al.

(2019), which did not reach sorption equilibrium after as long as 6 h, thereby potentially

resulting in a lag time for uptake into binding gels for short deployment periods. Among

analytes studied here, log K_{ow} values of amitriptyline, bupropion, duloxetine, and fluoxetine

were in a range similar to that of the previous study by Wang et al. (2019) (3.85 to 4.95) but did

not show similarly elevated sorption. By plotting the equilibrium mass adsorbed *vs.* the final

aqueous solution (**Figure 3.3**), the adsorption trends did not follow log K_{ow} values.
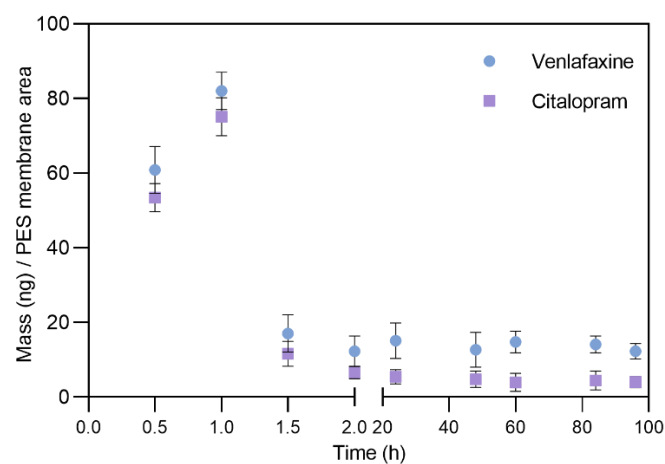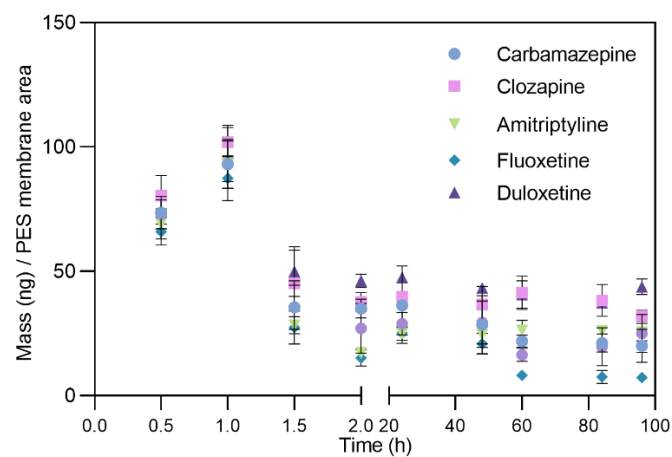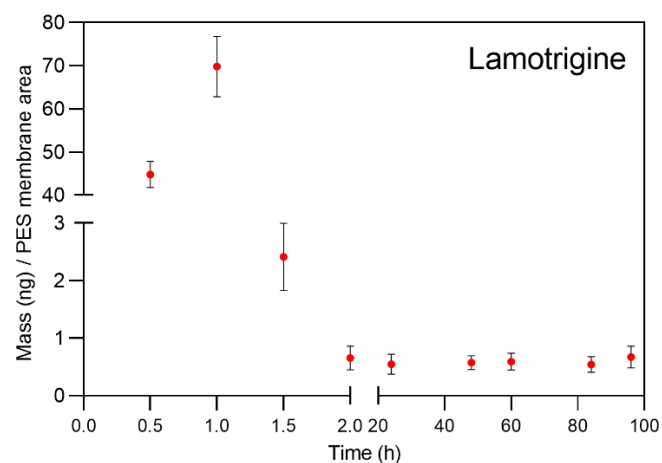
Figure 3.2 Dependence of the mass of nine antipsychotics accumulated per the polyethersulfone (PES) filter membrane area (4.91 cm^2) was determined over time in a 250 µg L^{-1} standard solution at a water temperature of 21±0.5 °C. Circles represent mean values, error bars the standard deviation of measurements from triplicate samples.
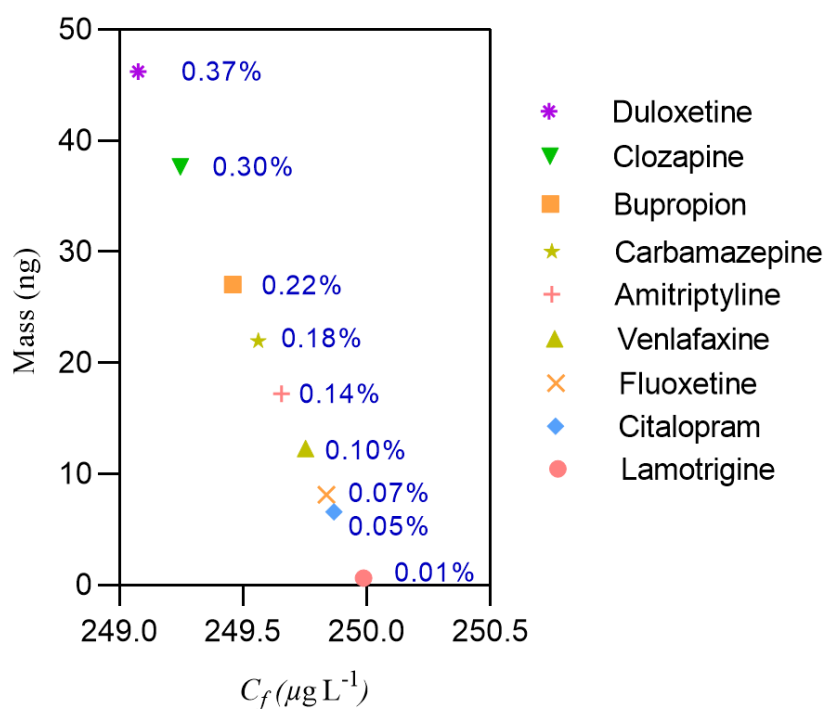
Figure 3.3 The plot of the maximum equilibrium mass adsorbed by PES filter membrane *vs.* the final aqueous concentrations (C_f) for nine antipsychotic compounds. The blue numbers represent the adsorbed fraction (%, adsorbed mass by PES membrane/total mass in the solution).

3.3.1.2 Effect of contact time and adsorption capacity for binding gel

Adsorption of the nine antipsychotics to Sepra™ ZT binding gel was rapid, within four hours, and became slower as it reached a steady-state and the available surface binding sites became saturated (**Figure 3.4**). To quantify the adsorption capacity of a Sepra™ ZT binding gel for the analytes from a given solution, amounts of each analyte adsorbed by Sepra™ ZT binding gel *vs.* the original concentration of each analyte in the solution were plotted (**Figure 3.5**). An increasing trend of the adsorption amount with solute concentration was observed for all nine compounds, ranging from 200 to 2,000 μg L^{-1} without a significant deviation from linearity. At a solute concentration of 5,000 μg L^{-1}, the amounts adsorbed were not significantly different from that at 2,000 μg L^{-1}, which indicated that binding sites of the Sepra™ ZT adsorbents were

saturated. Adsorption by Sepra^{TM} ZT binding gel at a 2,000 μg L^{-1} solute concentration was 0.23 μg mg^{-1} for lamotrigine, 0.06 μg mg^{-1} for bupropion, 0.15 μg mg^{-1} for venlafaxine, 0.25 μg mg^{-1} for clozapine, 0.07 μg mg^{-1} for citalopram, 0.10 μg mg^{-1} for duloxetine, 0.14 μg mg^{-1} for amitriptyline, 0.36 μg mg^{-1} for fluoxetine, and 0.30 μg mg^{-1} for carbamazepine. Taking 7 days as deployment time, the calculated time-average concentration is 58.19 μg L^{-1} for lamotrigine, 18.53 μg L^{-1} for bupropion, 58.80 μg L^{-1} for venlafaxine, 66.78 μg L^{-1} for clozapine, 14.47 μg L^{-1} for citalopram, 38.07 μg L^{-1} for duloxetine, 29.19 μg L^{-1} for amitriptyline, 105.69 μg L^{-1} for fluoxetine, and 74.99 μg L^{-1} for carbamazepine, which is adequate to detect concentrations in aquatic environment (<1 μg L^{-1}) (Metcalfe et al., 2010).
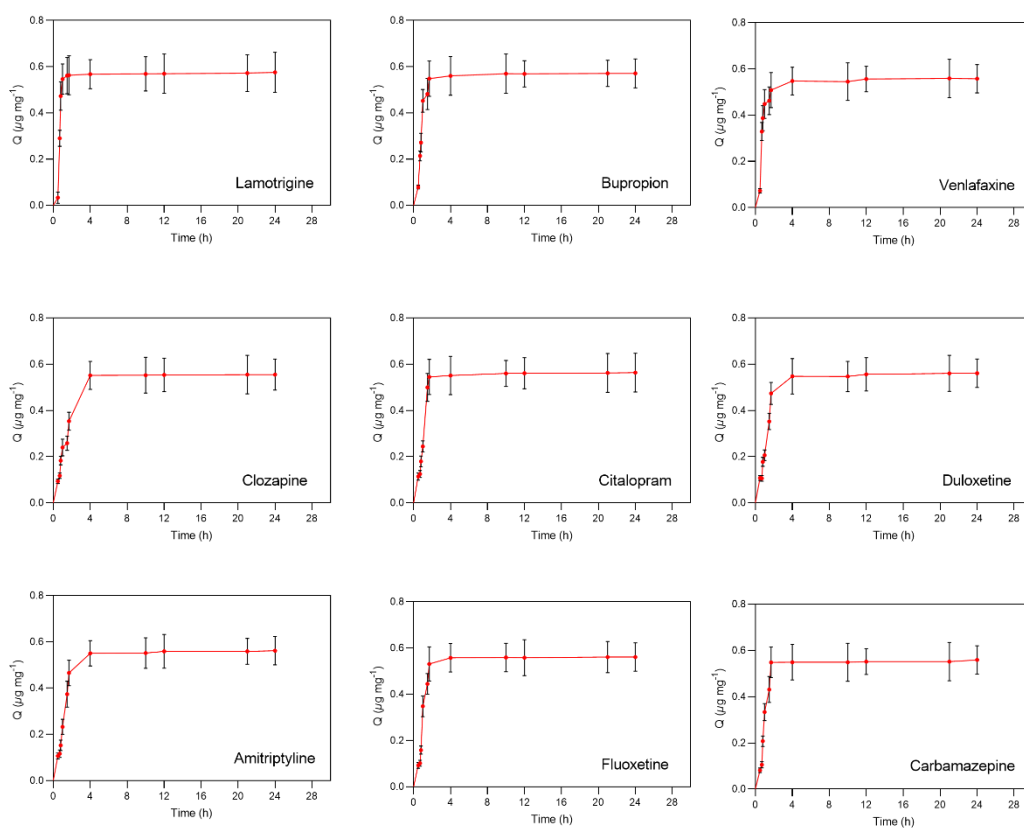
Figure 3.4 Adsorption of nine antipsychotic compounds on Sepra^{TM} ZT binding gel was observed at pH = 7 over 24 h at a temperature of 21 ± 0.5°C. Circles represent mean values, and error bars are the standard deviation of measurements from triplicate samplers. The adsorption amount (Q, μg mg^{-1}) was calculated from $Q = \frac{(C_0 - C_i) \times V}{1000m}$. C_0 and C_i represent the initial concentration and concentration from each sampling time, respectively. V and m represent the volume of the standard solution (mL) and the mass of adsorbents in the binding gel (mg), respectively.
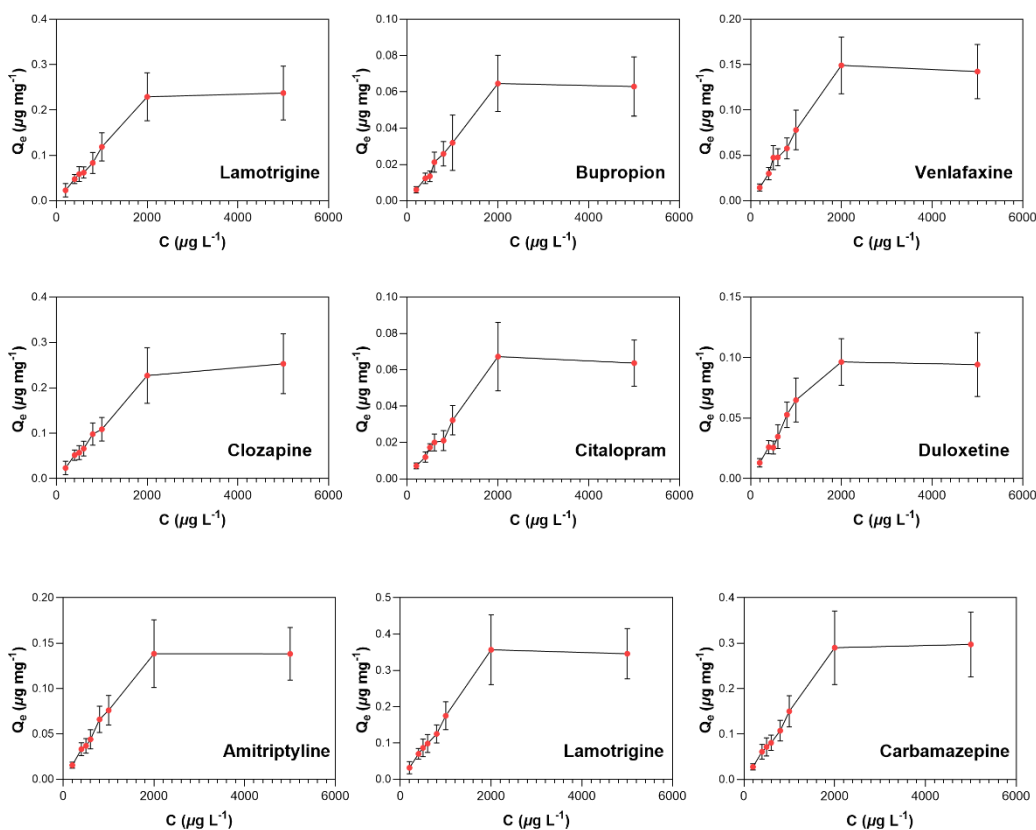
Figure 3.5 Steady-state adsorption isotherms of nine antipsychotic compounds on Sepra^{TM} ZT binding gel at pH 7 at 24 hrs and a temperature of $21 \pm 0.5°C$. Circles represent mean values, error bars the standard deviation of measurements from triplicate samplers. C (μg L^{-1}) represents different concentrations of analyte standard solution. The steady-state adsorption amount (Q, μg mg^{-1}) was calculated from $Q_e = \frac{(C_0 - C_e) \times V}{1000m}$. C_0 and C_e represent the initial concentration and the reached steady-state concentration, respectively. V and m represent the volume of the standard solution (mL) and the mass of adsorbents in the binding gel (mg), respectively.

3.3.1.3 Diffusion coefficients

Diffusion coefficients (D) of nine antipsychotics were measured using the diaphragm diffusion cell and are summarized in **Table A6**. Linear correlations (R^2 from 0.96 to 0.99) between diffused masses and deployment time were observed (**Figure A5**). The concentration of amitriptyline in the source compartment was observed to be unstable due to its water solubility. Issues with low-aqueous-solubility chemicals were previously reported for similar

diffusion cell systems (Wang et al., 2019). The exact comparison of diffusion properties for such analytes in hydrogel and water could be conducted to confirm the diffusion coefficients. However, D_w is difficult to measure and requires specialized equipment. Most studies to date have used either the Wike-Change equation (Wilke and Chang, 1955) or the Hayduk-Laudie equation (Hayduk and Laudie, 1974) to estimate D_w values rather than experimentally determining them.

The values of diffusion coefficients at 21°C of 0.75-mm gels did not show a statistically significant difference compared to gels of other thicknesses (1–3 mm; $p > 0.05$). D values of 2 and 3-mm gels showed an overall slight decrease (1–2%) compared to those in 0.75 mm since the slope from plotting between the mass of analytes and time for thicker gels became smaller (**Table A6**). These results also demonstrated values of D that were not strictly dependent on molecular mass according to Archie's Law (Chen et al., 2013), which is consistent with previous results (Liu et al., 2020). The diffusion coefficients (cm^2 s^{-1}) at 21°C (0.75 mm) were 4.98×10^{-6} for carbamazepine, 4.03×10^{-6} for bupropion, 4.92×10^{-6} for lamotrigine, 5.97×10^{-6} for amitriptyline, 3.17×10^{-6} for venlafaxine, 3.27×10^{-6} for duloxetine, 4.24×10^{-6} for fluoxetine, 6.02×10^{-6} for citalopram, and 4.66×10^{-6} clozapine. Values for D determined in this study were similar to previously reported values for carbamazepine (5.01×10^{-6}) and fluoxetine (4.38×10^{-6}) at 25 °C (Challis et al., 2016), while D for bupropion was slightly lower than that determined in a previous study (5.21×10^{-6}) at 25 °C (Fang et al., 2019).

3.3.2 Distributions in spiked sediment and concentrations measured by DGT

Concentrations in sediment porewater ($C_{porewater}$) and solid phase (C_s) did not change ($p >$

0.05) after 11 days of aging (**Table 3.1)**. Non-extractable fractions ranged from 75 to 87% for all compounds except lamotrigine, for which it was 57%. This might be due to lesser organic carbon-water partitioning coefficients for lamotrigine (2.1) (Golovko et al., 2020) with small organic content of sediments (< 0.6%). Decreasing concentrations of antipsychotics in sediment porewater were: carbamazepine > lamotrigine > bupropion > clozapine > amitriptyline > citalopram > duloxetine > venlafaxine > fluoxetine, which is dependent on kinetics of desorption from sediment.

Table 3.1 Concentrations (mean ± standard deviation, $n = 3$) of nine antipsychotic compounds in sediment porewater ($C_{\text{porewater}}$) and extracted by acetonitrile (C_s) at 0 days and 11 days.

Compound	Day 0		day 11	
	$C_{\text{porewater}}$ (μg L^{-1})	C_s (μg kg^{-1})	$C_{\text{porewater}}$ (μg L^{-1})	C_s (μg kg^{-1})
Amitriptyline	50.33 ± 6.14	365.09 ± 58.24	58.70 ± 8.93	375.90 ± 59.44
Bupropion	176.33 ± 25.52	330.65 ± 34.64	187.13 ± 28.21	341.40 ± 36.54
Carbamazepine	1160.32 ± 146	893.28 ± 113.77	1178.85 ± 127.56	907.23 ± 107.49
Citalopram	44.96 ± 5.48	301.62 ± 46.48	54.00 ± 7.57	309.76 ± 46.85
Clozapine	71.52 ± 7.84	601.19 ± 71.92	81.76 ± 11.88	613.61 ± 64.05
Duloxetine	39.16 ± 4.42	326.09 ± 44.66	47.24 ± 6.40	333.73 ± 34.44
Fluoxetine	31.34 ± 3.44	381.00 ± 39.00	38.35 ± 4.07	389.81 ± 46.30
Lamotrigine	595.15 ± 65.64	1063.83 ± 164.49	603.28 ± 71.46	1,083.21 ±148.19
Venlafaxine	39.71 ± 5.67	475.89 ± 65.82	45.96 ± 6.52	490.06 ± 65.86

No significant difference for $C_{\text{porewater}}$ and Cs at day 0 and day 11, respectively was found by Tukey's posthoc test.

Accumulated masses of antipsychotic compounds in DGT were directly proportional to the duration of deployment (**Figure 3.6**). The nonlinear regression obtained from curves of masses *vs*. duration (hyperbola equation) indicates that the solid phase could not entirely supply porewater concentrations to sustain mass accumulation by DGT devices. Masses in DGT devices after all durations exhibited the same order of chemical accumulation as observed in sediment porewater. The fully sustained case with a theoretical straight line is related to the labile pool size and the desorption rate to resupply the sediment porewater (Lehto et al., 2008).

The deviation of accumulated masses from the theoretical relationship can be explained by the use of the DIFS model described in section 3.3.3 below.
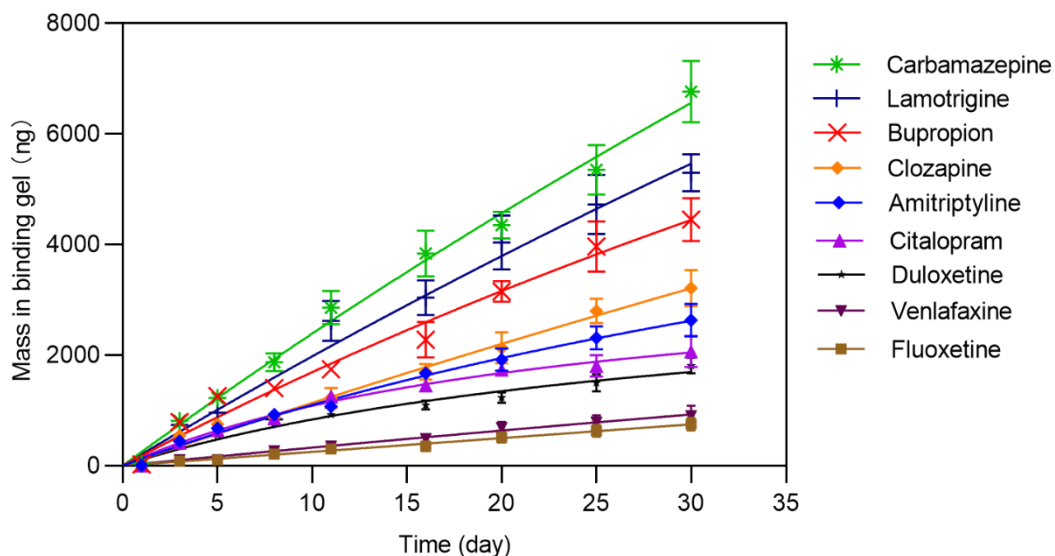
Figure 3.6 The accumulated masses (mean values of triplicate samples) of antipsychotics in the binding gel of DGT (0.75 mm diffusive gel) deployed in sediments with increasing deployment times.

Deployment of DGT devices of various thicknesses of diffusive gels can provide further information on resupply kinetics. A plot of 1/Δg vs. measured fluxes (**Figure 3.7**) indicated that concentrations of antipsychotic drugs were not fully replenished to sediment porewater through desorption from sediment particles. If the R ratio is equal to 1.0, there is no kinetic limitation in the rates of replenishment of the aqueous phase from the solid phase. In this case, the theoretical slope of the DC (D: diffusion coefficient; C: a constant concentration gradient is maintained in the diffusion layer of DGT devices, adapted from Eq. (2.4) is a straight line. However, concentrations of analytes could still not be efficiently resupplied from the solid phase since for all compounds, data fell below the $R = 1$ line. Duloxetine and fluoxetine exhibited < 5% difference among thicknesses of diffusion layers, which indicated that, compared to the other antipsychotics, despite all values being lower than the theoretical slope,

these two compounds had an extreme kinetic limitation of resupply from sediment particles. Fluxes to DGT devices with the smallest diffusion gel thicknesses were more limited through resupply from the solid phase. The largest values were observed for lamotrigine (0.42 pg cm^{-2} s^{-1}) and carbamazepine (0.83 pg cm^{-2} s^{-1}) for the 0.75 mm diffusive gel, which represented approximately 55% and 77% of the potential fluxes (based on C_d), respectively.
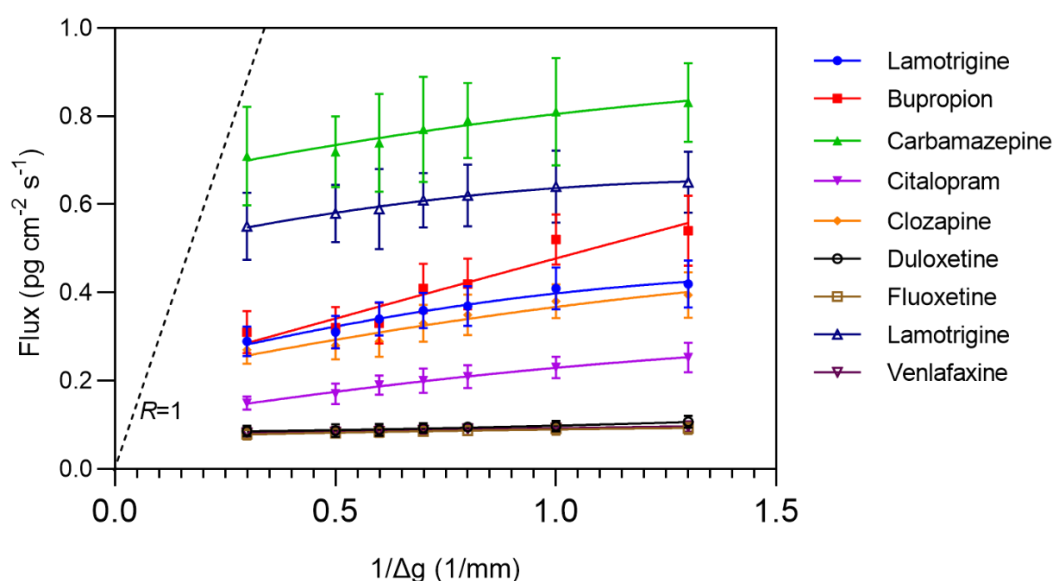
Figure 3.7 The plot of DGT-induced fluxes of nine antipsychotics against the reciprocal of the diffusive layer thickness in the submerged sandy sediment. The fluxes of each antipsychotic compound to the DGT device were calculated from the measured mass in the binding gel *via* a defined exposure area during the deployment time. The hypothesis that steady-state flux from porewater to meet the demand of the DGT devices was not satisfied. The dashed line indicates the theoretical line based on Eq. (3.1). Symbols represent mean values, error bars the standard deviation of measured triplicate data.

3.3.3 Resupply from spiked sediment

Kinetics of desorption of antipsychotics from solid phases of sediments to interstitial porewater can be obtained by fitting experimental data to the DIFS model. The ratio R, plotted against the duration of deployment, can provide information on rates of resupply of these compounds from sediment particles (**Figure 3.8**). For lamotrigine, carbamazepine, venlafaxine, citalopram,

bupropion, fluoxetine, and amitriptyline, there was an initially steep decrease in R, followed by either a less pronounced decrease. For clozapine and duloxetine, the ratio was constant. In theory, values of R increase during the initial phase of uptake while establishing a linear diffusion gradient within the diffusion layer. However, this process occurs very rapidly (< 1 day), so it was not visible for longer durations. Thus, this could have led to a constant R value after the first rapid increase if there was a rapid resupply from the solid phase with a constant labile concentration of antipsychotics. During our study, since these compounds diffused into and were adsorbed by the DGT more rapidly than they could be resupplied by the solid phase of the sediments, the gradual decline for all nine antipsychotics resulted from the decreasing concentration in the porewater at the DGT interface. The decreasing order of values observed for R was lamotrigine > carbamazepine > venlafaxine > clozapine > citalopram > fluoxetine > bupropion > duloxetine $\approx$ amitriptyline, which reflects the same order of chemicals to resupply antipsychotics from sediments to sustain initial concentrations. Apparent values of R for bupropion, duloxetine, and amitriptyline indicated that $C_{\text{porewater}}$ remained at a small concentration during the entire duration of the deployment. For clozapine, except for the first day, R values remained small, which indicated that the size of the labile pool of the compound was comparably small and not sufficient to resupply the soluble pool relative to the other antipsychotics.
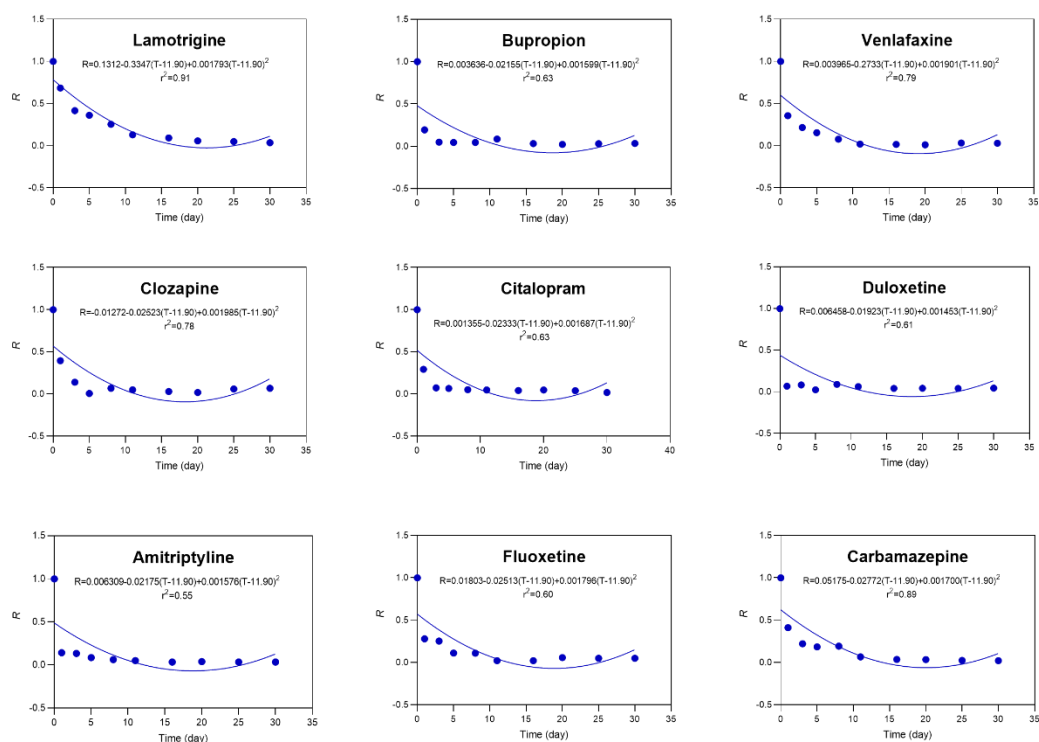
Figure 3.8 The dependence of experimentally measured *R* ratios for nine antipsychotics with increasing deployment time. The blue lines represent the best-fit lines of the 2D-DIFS model.

The best fit of *R* values, plotted against the duration of deployment for the 2D-DIFS model, was obtained by optimizing response times (T_c) and partition coefficients (K_{dl}) for each labile antipsychotic compound. Values of T_c and K_{dl} and derived parameters of dissociation and association rate constants are shown (**Table 3.2**). Comparisons of model simulations with empirical results were not ideal, with obvious deviations for all nine antipsychotics, especially when $T_c < 1$ day. Apart from potential experimental errors, this result indicated that the model does not accurately simulate all processes or compounds. Therefore, considering these limitations, parameters derived from the DIFS model should be used to estimate general kinetic information rather than detailed mechanisms, especially for various adsorption sites of various solid fractions.

Table 3.2 Parameters for nine antipsychotic compounds in sediment derived from the model fits using 2D-DIFS.

Compound	K_d^* (mL g^{-1})	K_{dl}^{**} (mL g^{-1})	T_c (s)	k_b (10^{-6} s^{-1})	k_f (10^{-5} s^{-1})
Amitriptyline	6.4	6.5	18,984	3.58	4.91
Bupropion	1.8	30	12,635	1.23	7.79
Carbamazepine	0.8	61	1,498	5.14	66
Citalopram	5.7	53	1,605	5.51	62
Clozapine	7.5	43	1,515	7.16	65
Duloxetine	7.1	7.7	17,184	3.38	5.48
Fluoxetine	10	44	9,581	1.11	10
Lamotrigine	1.8	76	1,844	3.38	54
Venlafaxine	11	49	2,458	3.89	40

[*] Values of K_d were calculated using acetonitrile extract (the values are present in Table 2.1).

[**] Values of K_{dl} were calculated from DGT labile concentrations.

T_c is sediment response time (s) during the exchange.

K_f and k_b are adsorption rate constant (s^{-1}) and desorption rate constant (s^{-1}), respectively.

3.3.4 Size of the labile pool and kinetics of exchange in spiked sediments

Generally, K_{dl} is proportional to the size of the labile pool, which determines the magnitude of R during long-term deployments, and T_c is related to the rate of resupply from materials adsorbed to the solid phase, which influences values of R during shorter durations of deployment and is related to initial steepness of decline (**Figure 3.5**) (Lehto et al., 2008). Values of K_{dl} were 4- to 42-fold greater than K_d ($p < 0.05$), except for duloxetine and amitriptyline, which exhibited comparable values. This implies that the two approaches access different solid phase pools. It appeared that during short durations of deployment, duloxetine and amitriptyline could not dissociate from the sandy sediment used for the present study. Other antipsychotics could be more quickly released initially, which is in agreement with the expected ionic interactions of antipsychotics, such as lamotrigine and carbamazepine (Zhang et al., 2010; Navon et al., 2011), with various sediment components (e.g., particles and minerals). Therefore, the labile fraction of antipsychotics cannot dissolve in acetonitrile, which also raises the issue that K_d of some compounds cannot be evaluated by extraction into acetonitrile. The fact that larger values of K_{dl} were observed for lamotrigine and carbamazepine implies that a large labile reservoir was available for resupplying these compounds to sediment porewater.

Values of T_c for these antipsychotics were in decreasing order: carbamazepine > clozapine > citalopram > lamotrigine > venlafaxine > fluoxetine > bupropion > duloxetine > amitriptyline. Carbamazepine, clozapine, citalopram, and lamotrigine could be supplied very quickly to sediment porewater (25−30 min). For lamotrigine and clozapine, the lesser values of T_c in the beginning resulted in an apparently greater resupply ®. However, increasing values of T_c

resulted in a 10-fold lesser R for bupropion and amitriptyline, suggesting that the supply of these compounds was initially limited kinetically. In general, the more hydrophobic antipsychotics (fluoxetine, bupropion, duloxetine, and amitriptyline) appeared to be more difficult to supply from solid phase to porewater during short periods. Given that our sediments had a comparably low organic carbon content, sediment mineral structure may be another factor that affects the release kinetics from the solid phase of these compounds. Kinetics of sorption of targeted antipsychotics have not previously been reported for sandy sediments. Values of k_f ranged from 7.79×10^{-5} to 66×10^{-5} s^{-1}, which is larger than k_b values (3.38×10^{-6} to 7.16×10^{-6}) in decreasing order of clozapine > citalopram > carbamazepine > venlafaxine > amitriptyline > duloxetine > lamotrigine > bupropion > fluoxetine, which indicated that adsorption, rather than desorption, dominated kinetics of sorption of all nine antipsychotics. The DIFS model can also be used to simulate the influence of kinetic factors on the transport of dissolved analytes (**Figure A6**). Depletion of $C_{porewater}$ for carbamazepine, lamotrigine, and venlafaxine reached 2 cm while citalopram, fluoxetine, bupropion, duloxetine, and amitriptyline never went beyond 1 cm. Clozapine and citalopram displacements of 1.31 cm and 1.05 cm were observed from the DGT-sediment interface, respectively. This movement corresponds well with the respective K_{dl} values. Larger pools of labile carbamazepine, lamotrigine, and venlafaxine could still maintain the resupply from sediments to the solution until the maximum concentration within 2 cm was reached. This demonstrates that releases of these compounds in the long term are controlled by K_{dl} values. In contrast, duloxetine and amitriptyline were dominated by initial replenishment, a conclusion that is supported by the values observed for T_c. However, the mechanism of

112

interaction between sediment properties and these compounds to explain DIFS-derived parameters requires further dedicated studies.

3.3.5 Availability and resupply in field sediments

DIFS modeling is able to provide helpful information concerning interactions between solid phases and solutions in sediments. Therefore, the application of DGT–DIFS can help further understand the in situ biogeochemical processes of antipsychotic drugs. The measured R for each antipsychotic compound was plotted against deployment time, showing an initial steep decline in R followed by a slower decrease, and finally reaching a stable value (**Figure 3.9**), which is the same trend as that in spiked sediments. Only venlafaxine showed a steeper decrease with longer deployment time (< 15 days). This indicates that all antipsychotics experienced the gradual decline in sediment porewater at the probe interface, meaning these compounds are adsorbed by DGT binding gel more rapidly than they were supplied by diffusion and released from the sediment solid phase. The order of R values was followed: carbamazepine > fluoxetine > bupropion > lamotrigine $\approx$ clozapine $\approx$ citalopram > amitriptyline > duloxetine > venlafaxine. This implies that the capability of the sediments in the field to remain initially the sediment porewater concentrations declined in the same order. However, this order is different from the results from spiked sediments. This may be due to the non-constant sustaining sources and dynamic sediment deposit rate to change the labile pool in the field.
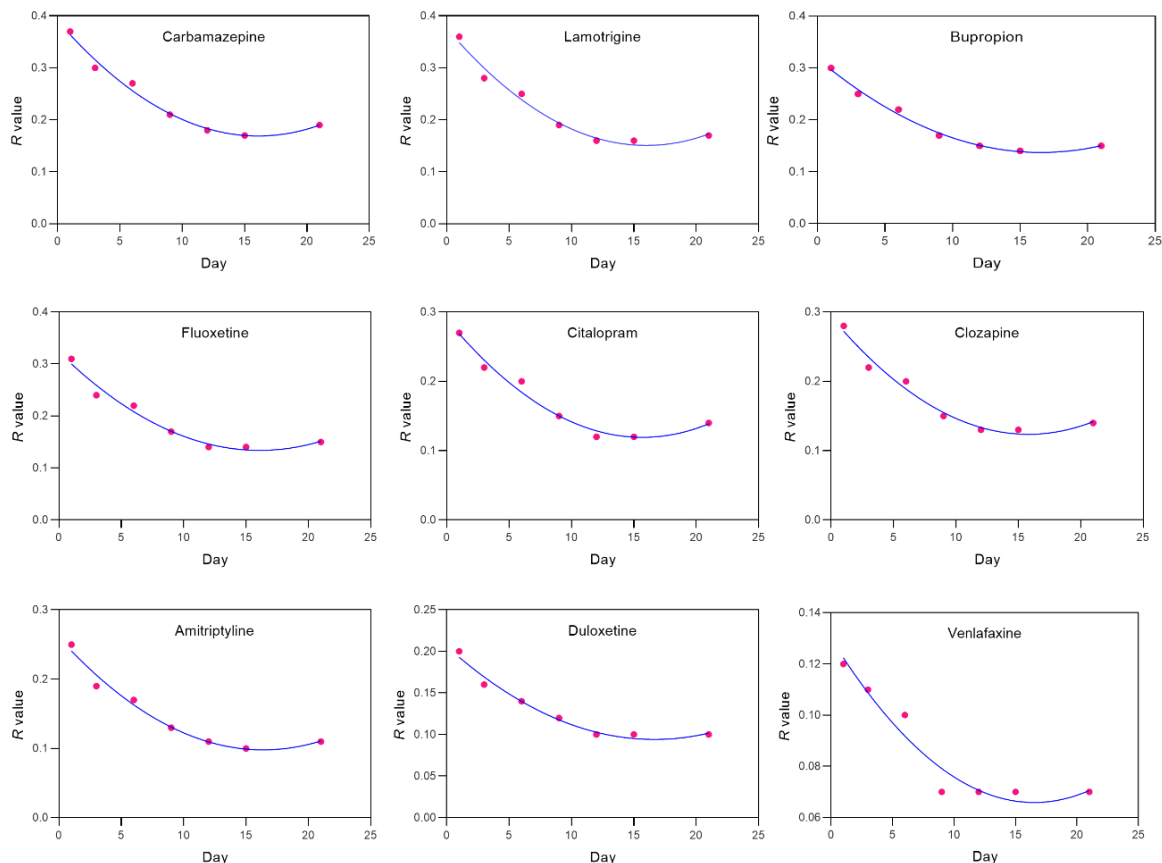
Figure 3.9 The dependence of experimentally measured R ratios for nine antipsychotics with increasing deployment time from the field. The blue lines represent the best-fit lines of the 2D-DIFS model.

The best fits of R versus deployment time for antipsychotics were derived from the DIFS model, showing that k_d and k_{dl} values of all antipsychotics were not close except for amitriptyline (**Table 3.3**). This implies that DGT and solvent extraction measurements access different solid phase pools, which is agreed to those obtained from spiked sediments (**Table 3.2**). T_c values for antipsychotics were in order of duloxetine > clozapine > citalopram > bupropion > amitriptyline > carbamazepine > lamotrigine > fluoxetine > venlafaxine. For venlafaxine, increasing T_c by an order of magnitude led to about a 25% decrease in R. The results of T_c showed that the supply of antipsychotics in the field is partly limited kinetically in field sediments with increasing deployment time. From k_b and k_f values, the adsorption process was still dominant in field sediments for most antipsychotics

whereas amitriptyline and duloxetine showed the predominant desorption process. This suggests

that amitriptyline and duloxetine could be constantly released to the environment from sediments,

which may be also ascribed to the small values observed for both k_d and k_{dl}.

Table 3.3 Parameters for nine antipsychotic compounds in the field sediment derived from the model fits using 2D-DIFS.

Compound	K_d (mL g^{-1})	K_{dl} (mL g^{-1})	T_c (s)	k_b (s^{-1})	k_f (s^{-1})
Amitriptyline	0.32	0.23	364,919	6.19E-07	2.04E-06
Bupropion	8.42	0.14	261,482	2.75E-06	8.45E-07
Carbamazepine	27.31	0.08	194,191	4.26E-06	8.13E-07
Citalopram	4.62	0.13	372,227	2.07E-06	6.51E-07
Clozapine	6.23	0.18	356,254	1.83E-06	8.43E-07
Duloxetine	0.24	0.43	710,013	9.20E-07	7.03E-07
Fluoxetine	10.24	0.06	332,839	2.77E-06	3.42E-07
Lamotrigine	18.75	0.07	196,907	2.45E-06	3.56E-07
Venlafaxine	0.03	0.009	145,000	7.25E-07	1.74E-08

The annotations are followed as Table 3.2.

3.4 Conclusion

The results of this study provide information related to the desorption kinetics of organic pollutants in sandy sediments with low organic matter content, which might be easily diffused and taken in by biota. Replenishment was most significant for lamotrigine and the least important for duloxetine and amitriptyline in spiked sediments, which could be explained by labile pool sizes for quick resupply over longer deployment times for lamotrigine and longer response time to supply the initial concentration in sediment porewater for duloxetine and amitriptyline. The difference in field sediments showed the most resupply from sediments to porewater was carbamazepine and lamotrigine, which is not highly dependent on the labile pool size derived from the DIFS model. The conventional experimental incubation DGT experiment may not represent the desorption process in natural sediments.

Although adsorption is still predominant in the study of both spiked and field sediments, the fluxes of DGT-induced gradient concentrations could be linked to their bioavailability. Fluxes measured by the use of DGTs have been indicated as an assessment/prediction tool for the potential bio-uptake of metals (Zhang et al., 2001; Degryse et al., 2006; Bade et al., 2012). The DIFS model opens up the possibilities of quantitative measurements of sorption-desorption kinetic processes. Subsequently, these parameters can be linked to the processes by which sediment biota can absorb these compounds, which could enhance our understanding of the bioavailability of these compounds as a potential tool for risk assessment.

CHAPTER 4: DGT technique and sequential extraction approach to investigate *in situ* desorption kinetics of emerging organic contaminants at the sediment−water interface

Overview

A version of this chapter has been published in *Water Research* with the following details:

Xiaowen Ji, Jonathan K. Challis, Jenna Cantin, Ana S. Cardenas Perez, Yufeng Gong, John P. Giesy, Markus Brinkmann. A novel passive sampling and sequential extraction approach to investigate desorption kinetics of emerging organic contaminants at the sediment−water interface. Water Research*, 2022, 217, 118455. Published: 15 June 2022. DOI: https://doi.org/10.1016/j.watres.2022.118455

Contributions

Xiaowen Ji: conducted the entire experiment and wrote the manuscript.

Jonathan K. Challis: set up the LC-MS methods for nine antipsychotics and revised the manuscript.

Jenna Cantin: participated in field sampling and DGT devices retrieval.

Ana S. Cardenas Perez: participated in field sampling and making DGT binding gels.

Yufeng Gong: supported laboratory consumables and revised the manuscript.

John P. Giesy: revised the manuscript.

Markus Brinkmann: designed the experiment, secured funding, and revised the manuscript.

Transition

Chapter 3 established the DGT devices that were adequate to deploy in the aquatic environment. Chapter 3 stated the difference in modeled results between laboratory-controlled conditions and natural rivers. To further assess the desorption mechanism of organic contaminants in the real environment, this chapter aimed to reveal *in-situ* desorption processes of organic contaminants at the sediment–water interface by using DGT samplers with the combination of fraction transfer model. Specifically, the sediment cores were synchronously sampled when DGT samplers were deployed and retrieved. According to different extraction methods, three fractions (i.e., fast-desorption, stable-desorption, and bound-residue) transfer model was developed to explain the desorption kinetics in sediments and fluxes of analytes across the interface of sediment and overlying water. This chapter was intended to fill the gap in resupply kinetics mechanism in sediments under natural conditions and its influence on the overlying water.

Abstract

Forms of organic contaminants are an important driver of bioavailable fraction and desorption kinetics of pollutants binding to sediments. To determine fluxes and resupply of nine environmentally relevant antipsychotic drugs, which are emerging pollutants that can have adverse effects on aquatic organisms, interface passive samplers of diffusive gradients in thin films (DGT) were deployed for 21 days, *in situ* at the sediment-water interface in submerged sandy riverbank sediments. At each deployment time, samples of sediment were collected and subjected to consecutive extraction of pore water, as well as rapidly-desorbing (labile), stable-desorbing, and bound residue fractions. Concentrations of antipsychotic drugs decreased with sediment depth with the greatest concentrations observed in the top 2 cm. Positive fluxes of antipsychotic drugs were observed from sediment to surface water. The dynamic fraction transfer model indicated that the labile fraction can be resupplied with a lag time (> 21 d). When results were further interpreted using the DGT-induced fluxes in soils and sediments (DIFS) model, partial resupply of antipsychotic drugs from sediment particles to porewater was demonstrated. Desorption occurred within the entirety of the observed 15 cm depth of sediment. The fastest rates of resupply were found for carbamazepine and lamotrigine. The size of the labile pool estimated by the DIFS model did not fully explain the observed resupply, while a first-order three-compartment kinetic model for the fast-desorbing fraction can be used to supplement DIFS predictions with estimations of labile pool size.

Keywords: DGT, DIFS model, desorption kinetics, antipsychotic drugs, sediment, adsorbing fractions

4.1 Introduction

In aquatic ecosystems, sediments can act as both sinks and sources of pollutants. Some micropollutants are transported in the water column and adsorbed to organic particles, which will ultimately be deposited during periods of lesser flow to bottom sediments (Megahan, 1999). Some organic pollutants sequestered in sediments are not prone to rapid biodegradation and can be accumulated into benthic organisms (Zhao et al., 2009).

The fates of organic compounds deposited in sediments depend on their net fluxes at the sediment–water interface. Fractions of organic compounds desorbed from sediment to water are largely controlled by processes of exchange between aqueous and solid phases within sediment (Bondarenko and Gan, 2004). An advective flux can be induced when concentrations of compounds in the solution phase are depleted and resupply to the solution phase occurs from the adsorbed fraction. This is based on the capacity of remobilization and the rate of desorption of chemicals from the solid phase. Generally, fluxes via molecular diffusion are driven by the concentration gradient between sediment porewater and overlying bulk water through a diffusion-limiting boundary layer, which is formed at the sediment-water interface (Eek et al., 2010). The flux can be estimated by use of passive sampling approaches that can pre-concentrate trace chemicals through non-disruptive *in situ* sampling (Alvarez et al., 2004).

A recently developed diffusive gradient in thin-films (DGT) technique is able to measure freely dissolved compounds (Fernandez et al., 2009) and has been used for investigating organic contaminants in sediments (Mechelke et al., 2019; Li et al., 2021b). DGT can be used as a dynamic tool for measuring labile concentrations, which are fractions of chemicals that can be

easily dissociated and resupplied to the porewater and its resupply capacity from the solid phase (Iuele et al., 2021). A numerical model, known as DGT-induced fluxes in soil and sediments (DIFS) which can be formulated in various dimensionalities (1D/2D/3D-DIFS) (Harper et al., 2000; Sochaczewski et al., 2007), was developed to simulate DGT adsorption and describe analyte resupply kinetics from solid phases. The DIFS model was first applied to quantify desorption kinetics and labile pools of pesticides in intact sediment cores in laboratory-controlled conditions (Li et al. (2021b). However, other influences, such as resuspension/desorption (Eek et al., 2010) and bioirrigation, by suction of overlaying water by benthic organisms through their burrows (Benoit et al., 2009) can affect the observed net fluxes.

Because sediment can be a heterogeneous matrix, organic pollutants can exist in various fractions, which can influence the kinetics of desorption. It has been reported that partitioning influences the distribution of organic pollutants in sediments (Demars et al., 1995; He et al., 2016). Although most studies considered the distribution of pollutants between solid fractions and interstitial water within sediments, the binding mechanisms and intensities established between particles and pollutants can be complex (Demars et al., 1995). Three fractions of organic pollutants in sediments have been widely recognized: (*i*) the fast–desorbing fraction is weakly and reversibly bound to sediments and can rapidly desorb into the interstitial water (Semple et al., 2004); (*ii*) the stable–desorbing fraction can be described as a reversibly bound but slow-desorbing fraction (Schwab and Brack, 2007); and (*iii*) the non-extractable phase, which is covalently bound to or sequestrated by organic matter in sediments (Schäffer et al., 2018) and has been defined as "bound residues" by the International Union of Pure and Applied Chemistry (Roberts, 1984).

When xenobiotics enter sediments, they can undergo transfer as well due to the wide range of structural units and functional groups present in organic macromolecules (Hayes and Swift, 1978). Therefore, organic pollutants can be stored as a bound-residue form in sediments where they might not appear to be hazardous in the short term, but might be released when a sudden alternation of environment occurs (**Figure A7**). This phenomenon has been defined as a 'chemical time bomb' (Doelman et al., 1991). This fraction of organic pollutants can be a potential source for re-supply to the aqueous phase. However, to date, there are no *in situ* studies of kinetics of desorption in sediments, that have considered these three fractions. The current DIFS model only considers the single labile pool size that is based on initial sediment solution concentration (Menezes-Blackburn et al., 2019). However, resupply to the labile pool needs to consider rates of transfer between various binding forms and the equilibrium of labile analytes reached by a kinetic model, which might provide additional information on kinetic processes in sediments and help describe the flux between sediment and water in aquatic systems.

To address these uncertainties and resolve gaps in data, the objectives of this study were to: (*i*) obtain time-resolved field measurements for nine selected antipsychotic pharmaceuticals; (*ii*) study the sorption phase for these compounds from water to sediments using DGT devices; (*iii*) investigate and model desorption rates from the fractions–transfer in sediments and compare measurements to values predicted by the DIFS model.

4.2 Materials and methods

4.2.1 Chemicals

Nine high purity (> 98%) antipsychotic drugs, amitriptyline, bupropion, carbamazepine,

citalopram, clozapine, duloxetine, fluoxetine, lamotrigine, and venlafaxine, and the corresponding nine stable isotope-labeled internal standards, i.e., amitriptyline-d_6, bupropion-d_9, carbamazepine-d_{10}, citalopram-d_6, clozapine-d_4, duloxetine-d_7, fluoxetine-d_5, lamotrigine-[^{13}C;^{15}N$_4$], and venlafaxine-d_6, were used (**Table A1** and **Appendix 1)**.

4.2.2 Assembly of DGT devices

Standard size of polytetrafluoroethylene (PTFE) DGT device with 0.75-mm Sepra^{TM}-ZT (surface modified styrene divinylbenzene, Phenomenex, Torrance, CA) binding gels (~25 mg per gel), 0.75-mm agarose diffusive gels, and a 0.45-μm pore size polyethersulfone (PES) filter membrane (Sartorius Stedim Biotech GmbH, Gottingen, Germany) were prepared as previously described (Challis et al., 2016). A DGT sediment probe (length: 170 mm and width: 40 mm, (**Figure A8**) was constructed from acrylonitrile butadiene styrene (ABS) polymer and contained the same three layers as the standard DGT device, with different dimensions of binding gel (~250 mg per gel), diffusive gel, and PES membrane (length: 150.3 mm and width: 20.4 mm). Results of adsorption tests with DGT molding, agarose gel, PES membrane, and binding gel are provided in **Appendix 2**.

4.2.3 Background of sampling site

The deployment and sampling site (52°19'10.8"N 106°27'34.3"W; Clarkboro Ferry, South Saskatchewan River, Saskatoon; **Figure A9a**) was selected because it is ~20 km downstream of the City of Saskatoon's wastewater treatment plant where targeted compounds have been detected previously and is situated in proximity of the laboratory so that DGT devices and samples can be obtained and transported quickly. The nine selected antipsychotic drugs were

found in water, sediments, and fish of this site during previous investigations (unpublished data).

The sampling site is in the prairie physiographic region, which is characterized by rich soil, thick glacial drift, and extensive aquifer systems. To avoid fluxes of chemicals from groundwater and significant runoff from the surrounding land surface, the deployment site (**Figure A9b**) was selected to be located in the riverbank (depth < 1m) with a stable deposited layer on 1st September 2021 (the physicochemical properties of sediment is shown in **Table A7**).

4.2.4 DGT field deployment and sediment sampling

In the field, one DGT probe was attached in the bottom, and three DGT samplers were attached above the DGT probe, on perforated stainless-steel profiles (thickness: 3.18 cm, width: 3.18 cm, length: 183 cm). Three separate profiles with attached samplers were slowly inserted into sediments, with 2 cm of the probe board exposed out of sediments (15 cm was put into the sediment), and were supported by three cement blocks (height: 19 cm, width: 27 cm) for protection (the setup is presented in **Figure 4.1**). DGT devices were deployed and replaced after 1, 3, 6, 9, 12, 15, and 21 d. Meanwhile, three sediment cores adjacent to the DGT probes were sampled using a PVC sampling tube (length: 15 cm, diameter: 2 cm).
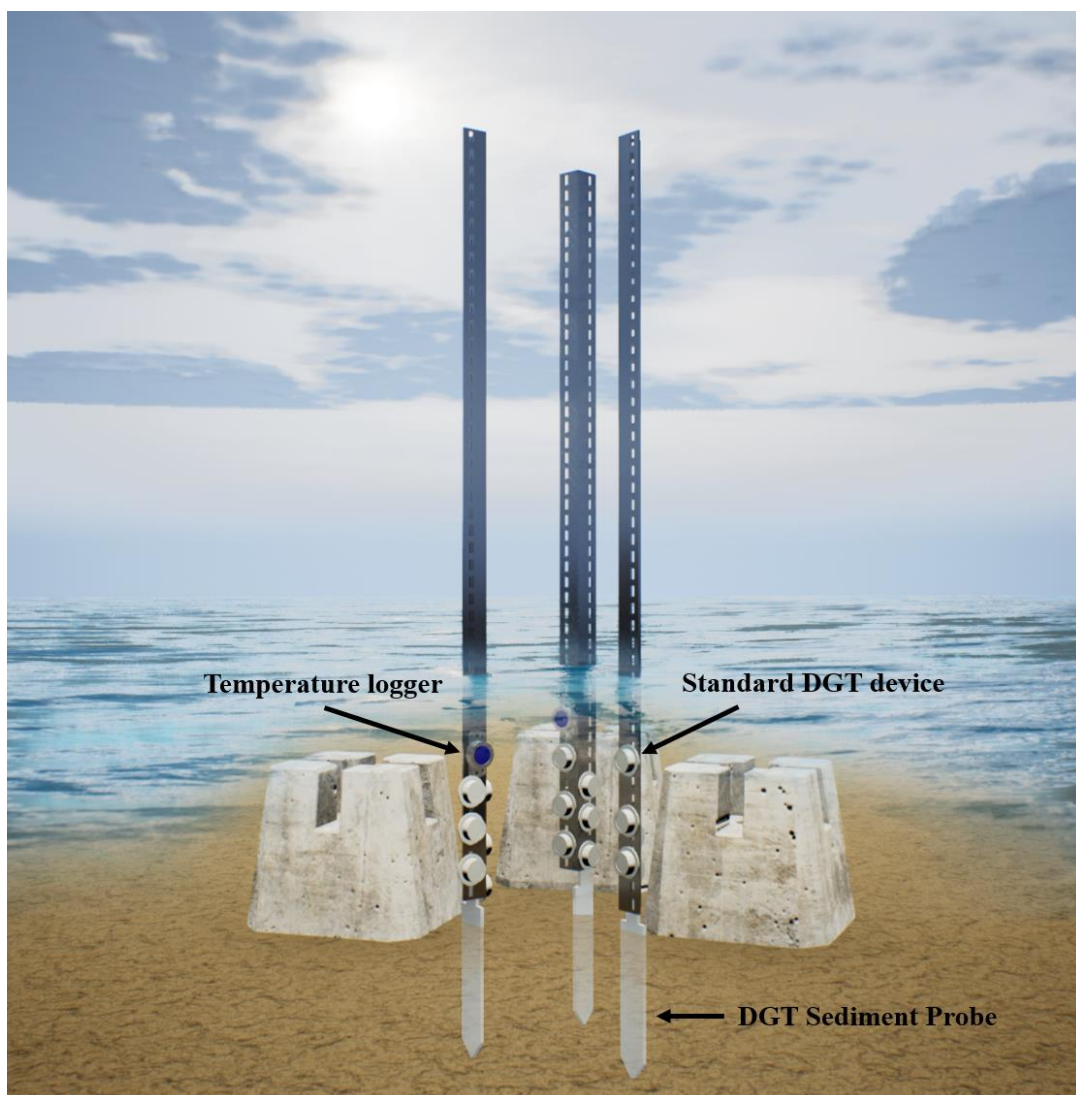
Figure 4.1 The three-dimensional simulation of the setup for fixation of DGT sediment probes and standard DGT samplers. The blue circular attachments are bluetooth-controlled temperature loggers.

Once the DGT devices were retrieved, the remaining sediment particles on probes and samplers were washed away using Milli-Q water, placed into sealed bags, and wrapped with aluminum foil. Sediment cores were stored in a cooler with ice bags. After the installation of new DGT devices, retrieved DGT devices and sampled sediments were immediately transported to the laboratory (Toxicology Centre, University of Saskatchewan), where the binding gels were carefully removed and placed into amber glass vials. Wet sediment cores were immediately drained for 2 h to determine the maximum water-holding capacity (Priha and

Smolander, 1999). Then, sediment cores were sliced into 2 cm-intervals, and each slice was centrifuged at $1,280 \times g$ for 40 min to obtain sediment porewater that was filtered through a 0.20-μm membrane filter (13 mm diameter, Millex-GN Nylon membrane, hydrophilic, MilliporeSigma, Oakville, ON) and then concentrated by solid-phase extraction (Strata-X SPE cartridge, details in **Appendix 3**). The binding gel was removed by use of a round spatula from the standard DGT device. The binding gel of the DGT sediment probe was sliced at 2 cm intervals using a razor blade (pre-rinsed by methanol). All binding gels were transferred to 30-mL amber glass vials.

4.2.5 Extraction

4.2.5.1 DGT binding gel

Fifty nanograms of internal standards were added to the binding gel. Five milliliters of methanol were added into the vial for ultrasonic extraction for 10 min, for a total of three times. Extracts were combined and concentrated to dryness with a gentle flow of nitrogen gas, reconstituted in 1 mL of methanol, and filtered through Target2™ 0.2 μm PTFE syringe filters (Thermo Scientific, Waltham, MA) into 2-mL LC vials.

4.2.5.2 Sediment

After collecting the porewater, sediments were transferred to a freezer (-20 °C) for 24 h and lyophilized (Dura-Dry MP FD2085, Stone Ridge, NY). The triplicates of a 5-g aliquot of sediment at different sampling times were transferred to Lysing matrix E 50 mL tubes (Fisher Scientific) for sequential extraction (**Figure 4.2**). The fast–desorbing fraction, stable–desorbing

fraction, and bound-residue fraction of antipsychotic drugs (Log K_{ow} = 0.99–4.95, **Table A1**)

were sequentially extracted using (1) methanol, (2) a mixture of methanol and dichloromethane

(1:1, *v:v*) with ultrasound, and (3) alkaline hydrolysis at 80 °C, respectively.

4.2.5.2.1 Fast-desorbing fraction

The fast-desorbing fraction is defined as consecutive desorption with time, which can be

represented by single-point extraction methods (Muijs and Jonker, 2011). A single-point

extraction by methanol was used in this study, and extraction time was determined by a

consecutive extraction using a first-order three-compartment kinetic model (details shown in

Appendix 4). In order to conduct consecutive extraction, 5 g of lyophilized sediment was

extracted using 5 mL methanol in a shaker (1500 rpm, Heidolph™ Multi Reax Vortex Mixer,

Fisher Scientific). Five milligrams of sodium azide were added for inhibition of microbial

activity (Skipper et al., 1996). At the time intervals of 0.2, 0.4, 0.6, 1, 3, 10, 24, 48, 96, and 250

h, the samples were centrifuged, and the methanol was sampled and refreshed. The sampled

methanol was passed through a 0.2-μm PTFE membrane filter after the addition of internal

standards and concentrated to 1 mL for instrumental analysis.
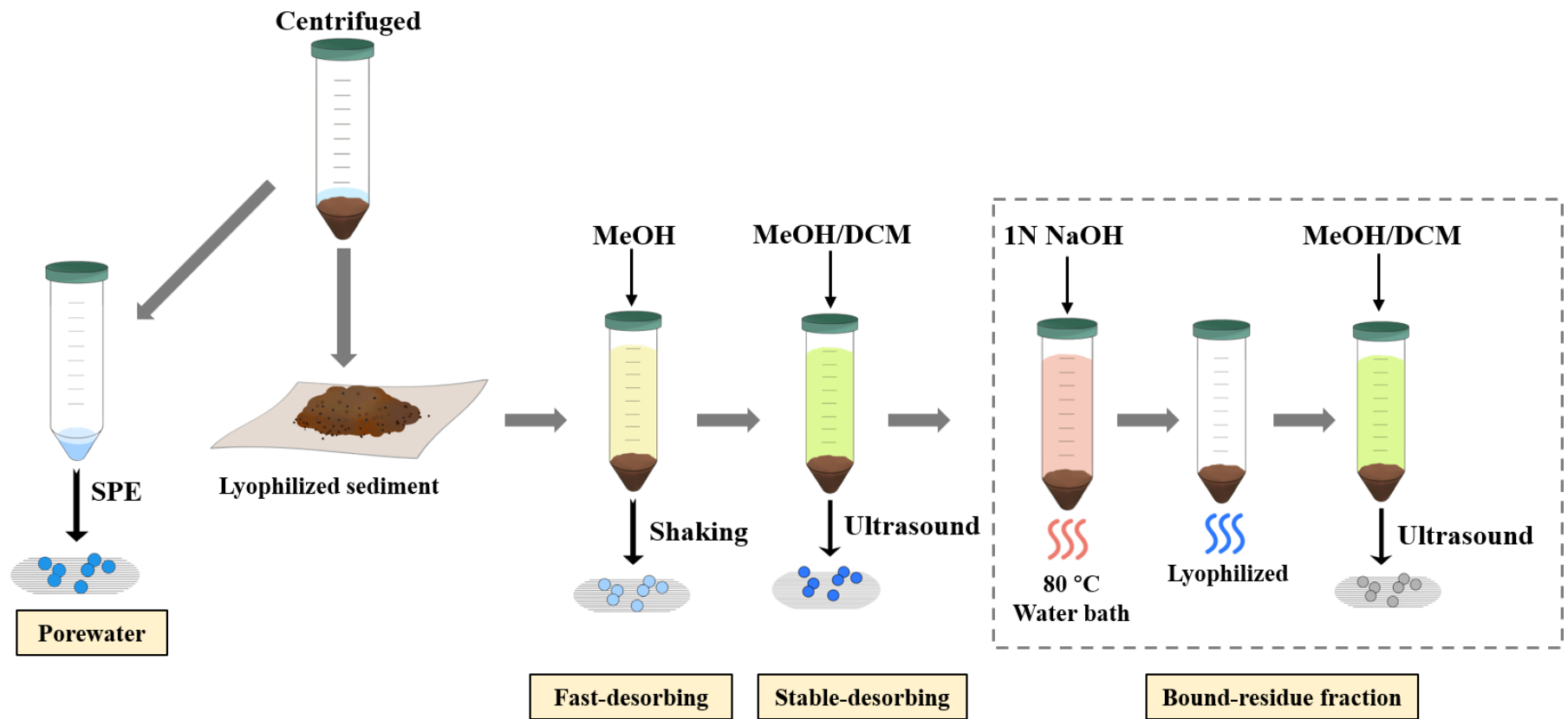
Figure 4.2 Process diagram of the sequential extraction procedure to obtain rapidly-desorbing, stable desorbing, and bound residue fractions of lyophilized sediments after separation of porewater.

4.2.5.2.2 Stable desorbing fraction

The stable desorbing fractions of antipsychotic drugs were extracted three times with 10 mL methanol: dichloromethane (1:1, v/v) with ultrasound (**Figure 4.2**). After centrifugation, the combined extracts were passed through a 0.2-μm PTFE membrane filter, followed by an SPE concentration procedure (**Appendix 3**) before instrumental analysis.

4.2.5.2.3 Bound-residue fraction

Alkaline hydrolysis has been widely used for the dissolution of organic matter, which in turn releases non-extractable organic pollutants, which are sequestrated or occluded with organic matter in soils and sediments. This method was adopted in the present study to extract the bound-residue fraction of antipsychotic drugs in sediments. Residual sediments from previous ultrasonic extractions were added to 5 mL of 1 M NaOH solution and then heated at 80 °C for 8 h. After cooling, the samples were lyophilized and extracted using the same procedure as the stable desorbing fraction. In order to test whether high temperature or hydrolysis would influence the analytes, the mixture of nine antipsychotic drugs was spiked in 10 mL of 1 M NaOH solutions to reach the concentration of 1, 10, and 100 μg L^{-1}, and heated at 80 °C for 8 h. After cooling, the solutions were processed following the previously described SPE procedure.

4.2.6 Determination of agarose diffusion coefficient

To determine the efficiency of deriving diffusion coefficients (D) for the nine analytes, two major methods were compared: the diffusion cell method (Westrin et al., 1994) and the slice stacking method (Rusina et al., 2010). Both methods were conducted in an environmental chamber at a

temperature of 25 °C. The diffusion coefficient of analytes in water (D_w) was further estimated by the Hayduk-Laudie equation (Hayduk and Laudie, 1974).

The diffusion cell method is based on the analytes passing through a membrane from one water cell to another (**Figure A10a**). Each cell (made of clear acrylic) held ca. 50 mL and had a 2.3 cm^2 circular connecting window. A diffusive gel was placed on the window (a spacer was made based on the gel thickness) between the two cells and gently sealed together with clamps. Each cell had a total volume of 40 mL. To each cell, 20 mL of 10 mM NaCl was added, followed by a spike of the 9-analyte stock mixture (1,000 μg L^{-1}) prepared in 5% methanol into the source cell at a target concentration of 500 μg L^{-1}. Meanwhile, 20 mL of 5% methanol spike was added to the receiving cell. Both cells were stirred gently on stir plates. Triplicate samples (200 μL) were taken from the receiving cell and source cell at ten different time points spread out over the experimental duration (5 to 140 min). Samples were pipetted directly into LC vials before instrumental analysis. External standardization was applied for these experiments due to no extraction processes.

The slice stacking method is based on analytes diffusing through several layers of gels (**Figure A10b**). Sixteen agarose gels were spiked by immersing them in 50 mL spiked at a concentration of 500 μg L^{-1} of the nine antipsychotic drugs for 24 h. Afterward, 10 spiked gels were removed and capped with 7 unspiked gels on a glass plate wrapped with aluminum foil. The remaining gels were taken as blank for measuring the initial analyte concentrations. The exposure time was selected as 60, 90, and 120 min. After exposure, the stacks were disassembled, and each gel was extracted with the same method of extraction used for binding gels (chapter 2.5.2.1). Calculations of D values for both methods and different temperatures are detailed in **Appendix 5**.

4.2.7 Calculation of DGT-derived parameters

Binding layers in DGT function as a sink for compounds in the sediment porewater/water, where an induced flux from the sediment/water passes through the diffusive layer and is bound in the binding layer. For sediments, the magnitude of this flux can be measured through interfacial concentration, which is determined by the desorption kinetics between the adsorption of solute induced by the DGT probe and the capability to resupply solute from the sediment solid phase to the probe interface. The time-averaged interfacial concentration of dissolved compounds at each deployment time ($C_{DGT,i}$) can be calculated (Eq. 4.1) (Zhang and Davison, 1995).

$$C_{DGT,i} = \frac{M_i \times \delta_{total}}{D_{m,i} \times A_e \times t_i} \quad (4.1)$$

where M_i is the accumulated mass of analyte in the binding gel at deployment time i (t_i), δ_{total} is the total thickness of the diffusive layer (it includes the 0.15-mm PES filter membrane and the 0.75-mm agarose diffusive gel), $D_{m,i}$ is the mean temperature-adapted diffusion coefficient of each analyte at each deployment time i, and A_e is the effective exposure window of DGT devices (3.14 cm^2 for standard device and 30.66 cm^2 for DGT probe). An index of the magnitude of depletion of sediment porewater concentration to the device interface, R, is the ratio between $C_{DGT,i}$, and the initial sediment porewater concentration ($C_{p,i}$) at each deployment time i (Eq. 4.2).

$$R = \frac{C_{DGT,i}}{C_{p,i}} \quad (4.2)$$

In most common cases in the real aquatic ecosystem, the R value meets the partial case ($0.1 < R < 0.95$), in which some resupply from the solid phase but is inadequate to maintain the initial $C_{p,i}$ (Harper et al., 1998). The calculation of diffusion between sediment and water is shown in **Appendix 6**.

4.2.8 Numerical modeling of DGT deployments using DIFS

The 2D/3D-DIFS model developed by Sochaczewski et al. (2007) simulates DGT-induced fluxes from soil or sediments in consideration of solute diffusion within two dimensions and incorporation of essential model calibrations. Although 2D-DIFS considers the domain as the partial cross-section along the axis perpendicular to the diffusive gel interface, of which the origin is situated at the center, the 2D model was shown to be a good approximation of the full 3D model (Sochaczewski et al., 2007). Therefore, in the study, the results of which are presented here, the 2D framework was employed.

The parameters describing the desorption kinetics of dissolved organic compounds between solid and solution phases were identical to other studies previously employed in soils or sediments (Chen et al., 2015; Ren et al., 2020; Li et al., 2021b). The DIFS model describes the dynamics of dissolved analytes (C_p) and the labile fraction associated with the solid phase (C_l), along with the deployment time to fit first-order exchange kinetics (Eq. 4.3),

$$C_p \xrightleftharpoons[k_{-1}]{k_1} C_l \quad (4.3)$$
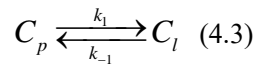
where the rate constants at which the two fractions' magnitudes change are defined as the rate constants of adsorption (k_1) and desorption (k_{-1}), governed by the labile concentration of compounds and the particle concentration of sediment ($P_c = m/V$, where m is the total mass of solid particles and V is the sediment porewater volume) (Eqs. 4.4 and 4.5).

$$\frac{\partial C_p}{\partial t} = -k_1 \times C_p + (k_{-1} \times P_c \times C_l) \quad (4.4)$$

$$\frac{\partial C_l}{\partial t} = \frac{k_1 \times C_p}{P_c} - (k_{-1} \times C_l) \quad (4.5)$$

Rate constants and particle concentrations in the sediment could be used together to fit the linear

sorption isotherm, K_{dl}, which defines the partitioning between the solution phase and labile solid phase that could exchange with the solution phase and represents the size of the labile pool in the solid phase. A response time to depletion associated with desorption processes from solid phase to porewater (K_{dl}) can be equilibrated, T_c, is calculated using Eqs. (4.6 and 4.7).

$$K_{dl} = \frac{C_l}{C_p} = \frac{1}{P_c} \times \frac{k_1}{k_{-1}} \quad (4.6)$$

$$T_c = \frac{1}{k_1 + k_{-1}} \quad (4.7)$$

When considering C_p was depleted to 0, T_c can reach $1 - (1/e)$, or 63% of the equilibrium solution-solid partitioning value (Honeyman and Santschi, 1988). Labile concentrations (C_l) of antipsychotic drugs were determined by the method of fast-desorbing fraction (section 4.2.5.2.1) at the time at which the equilibrium of the first-order three-compartment kinetic model was reached. The concentration of antipsychotic drugs in sediment porewater (C_p) at each deployment time was described in Chapter 3.2.4. The calculation of the labile phase pool is shown in **Appendix 7**.

4.2.9 Instrumental analysis

Quantifications of nine analytes from all reconstituted samples in methanol were conducted using a Vanquish UHPLC and Q-Exactive™ HF Quadrupole-Orbitrap™ hybrid mass spectrometer (Thermo-Fisher, Mississauga, ON). Analytical details are presented in section 4.2.9.

4.2.10 Data analysis

Statistical analyses were conducted in IBM SPSS Statistics 26. Data obtained from DGT devices and the consecutive extraction method were checked for normality and homogeneity

of variance using Levene's test. Since the data did not meet normality criteria and did not show homogeneous variances, non-parametric Kruskal–Wallis tests and Spearman's correlation (significant at $p < 0.05$) were used for comparison and correlation among samples. The desorbing fraction transfer was calculated using MATLAB R2019b.

4.3 Results and discussions

4.3.1 DGT performance

The nine target antipsychotic compounds were tested for adsorption to DGT materials, the adsorption capability of the binding gel, and the maximum exposure time for DGT sampling. Steady-state sorption concentrations of the nine antipsychotics were quickly reached (< 0.5 h) for DGT molding and diffusive gel. Concentrations remained consistent for 168 h with a negligible fraction (< 0.01% total mass of the standard solution) adsorbed to DGT moldings (both PTFE and ABS) and diffusive gels. Concentrations of all compounds on the PES filter membrane increased within an hour and reached steady state sorption within 2 h. Proportions of analytes sorbed were negligible (< 1% of the total mass of the standard solution) for all durations. Detailed data have been shown in Chapter 3.

Adsorption of the nine analytes to Sepra^{TM}-ZT binding gel was rapid, within four hours, and became slower as it reached a steady-state and the available surface binding sites became saturated (**Figure 3.2, Chapter 3**). To quantify the adsorption capacity of a Sepra^{TM}-ZT binding gel for the analytes from a given solution, amounts of each analyte adsorbed by Sepra^{TM}-ZT binding gel *vs.* the original concentration of each analyte in the solution were plotted (**Figure 3.3, Chapter 3**). An increasing trend of the adsorbed amount with solute concentration was

observed for all nine compounds, ranging from 200 to 2,000 μg L^{-1} without a significant deviation from linearity. At a solute concentration of 5,000 μg L^{-1}, the amounts adsorbed were not significantly different from that at 2,000 μg L^{-1}, which indicated that binding sites of the Sepra^{TM}-ZT adsorbents were saturated.

In order to guarantee the DGT device does not approach equilibrium and to estimate the maximum permissible exposure time for comprehensive sampling, the sorption isotherm of analytes between the measured concentration sorbed by Sepra^{TM}-ZT (C_{sorbed}) and that in water (C_{w}) can be described by the distribution constant, which can be calculated by fitting the measured concentrations to the linear sorption model ($C_{sorbed} = K_{Sepra-ZT} \cdot C_w$). The correlation coefficients in the linear sorption model are good for most compounds (**Table 4.1**), whereas the compounds with lesser correlation coefficients (r^2) require more complex sorption models (i.e., Freundlich and Langmuir) to better predict the measured data (Bäuerlein et al., 2012). Belles et al. (2017) recommended that it is appropriate to use an adapted linear model to evaluate the sampler's equilibrium. For comprehensive sampling, the DGT devices should be far from the equilibrium at all sampling times and hence the ratio C_{sorbed}/C_w should be less than the $K_{Sepra-ZT}$ values, which can be combined with Eq. (4.1) and shown as:

$$t_{\text{max}-measured} \ll t_{\text{max}-estimated} = \frac{K_{Sepra-ZT}\delta_{total}}{D \cdot A} \quad (4.8)$$

where $t_{\text{max-measured}}$ and $t_{\text{max-estimated}}$ are measured and estimated maximum exposure time to achieve $K_{\text{Sepra-ZT}}$ respectively. Our results showed the exposure time for each compound was more than 100 times less than the threshold, which indicates the device remained far from equilibrium conditions at all times.

Table 4.1 Agarose gel diffusion coefficient (D) determined by the diffusion cell method (D_{cell}) and the slice stacking method (D_{stack}) along with associated standard deviation (SD), and estimated diffusion coefficient in water (D_w). Sepra^{TM}-ZT-water distribution coefficient ($K_{Sepra-ZT}$), with correlation coefficient (R^2) of the linear sorption isotherm in brackets; measured maximum exposure time to achieve equilibrium of the binding gel (t_{max}); and estimated maximum exposure time to achieve $K_{Sepra-ZT}$ for DGT sampler (t'_{max}).

Compounds	D_{cell}	SD	D_{stack}	SD	D_w^a	Log $K_{Sepra-ZT}$	$t_{max-measured}$	$t_{max-estimated}$
	10^{-6} m^2 s^{-1}					L kg^{-1}	h	d
Carbamazepine	5.82	0.79	4.55	0.70	4.46	2.89 (0.83)	1.7	37
Bupropion	4.74	0.69	5.12	0.63	5.19	2.90 (0.74)	4	47
Lamotrigine	5.29	0.65	5.44	0.80	5.41	2.91 (0.92)	1.5	42
Amitriptyline	6.45	0.97	NA	-	4.46	2.89 (0.79)	4	33
Venlafaxine	3.63	0.47	NA	-	4.56	2.89 (0.95)	4	59
Duloxetine	3.80	0.39	NA	-	4.54	2.89 (0.61)	4	57
Fluoxetine	4.68	0.72	4.64	6.20	4.67	2.88 (0.67)	4	44
Citalopram	4.20	0.51	4.34	5.50	4.31	2.89 (0.76)	10	30
Clozapine	5.07	0.65	4.41	4.80	4.39	2.88 (0.84)	4	42

NA: We were unable to measure the D value using the slice stacking method.

[a] D values were estimated by the model established by Hayduk and Laudie (1974): $D_w = (13.26 \times 10^{-9})/(\eta^{1.4} V_m^{0.589})$ where η (cP) is the viscosity of water and V (cm^3 mol^{-1}) is the molar volume of the diffusing analyte at its normal boiling point, which is estimated by the Le Bas increment method (Le Bas, 1915).

4.3.2 Diffusion coefficient

Diffusion coefficients at 25 °C of the nine antipsychotic drugs determined using the diffusion cell method and the slice stacking method are shown (**Table 4.1**). D_{cell} and D_{stack} values were not significantly different ($p > 0.05$) for any of the compounds through comparison of triplicate measurements. For the diffusion cell method, the variables from Eq. (A5.1) were linearly correlated ($r^2 = 0.988–0.998$) with experimental time (**Figure A11**). Mean D_{cell} values for the studied antipsychotic drugs ranged from 3.63 to 7.20 × 10^{-6} cm^2 s^{-1}, while D_{stack} values ranged from 4.34 to 5.44 × 10^{-6} cm^2 s^{-1}. No statistically significant correlations between D and the molecular mass of compounds were observed, which might have resulted from the narrow

molecular mass range of these compounds (236.27–326.80 Da). This result is consistent with those of previous studies (Urík et al., 2020) for perfluoroalkyl compounds, pharmaceuticals, and personal care products with a range of molecular masses of 151 to 377 Da and polychlorinated biphenyls and polycyclic aromatic hydrocarbons with molecular masses in the range of 128.2 to 429.8 Da) (Rusina et al., 2010). The D_{cell} for carbamazepine (5.54×10^{-6} cm^2 s^{-1}), fluoxetine (4.72×10^{-6} cm^2 s^{-1}), and bupropion (4.48×10^{-6} cm^2 s^{-1}) determined during this study were similar to previously reported values in 1.5% agarose hydrogel, with D values of 5.01×10^{-6}, 4.38×10^{-6}, 5.21×10^{-6} cm^2 s^{-1} for carbamazepine, fluoxetine, and bupropion, respectively (Challis et al., 2016; Fang et al., 2019). The D_{stack} for carbamazepine (4.55×10^{-6} cm^2 s^{-1}) was comparably less than the value (5.33×10^{-6} cm^2 s^{-1}) reported by Urík et al. (2020). Three compounds, e.g., venlafaxine, duloxetine, and amitriptyline (Log K_{ow} =3.28, 4.68, and 4.95, respectively), failed to be measured by the slice stacking method.

Despite the different experimental designs of the two methods, the D value derived from the diffusion cell method is simply dependent on logarithmic linearization. However, the slice stacking method requires extraction and concentration procedures, causing more uncertainty in the analytical processes. The relative error values in our study for both methods were derived from the model regression fitting to the data. The previous example for estimating the rising uncertainty of D value for copper in the DGT sampler was negligible for these factors (e.g., pH and ionic strength) in comparison to the estimated diffusion area and analytical processes. Nevertheless, since slight differences between the two methods, the D values measured using the diffusion cell method were used for the calculation DGT-derived concentrations in this study.

4.3.3 DGT fluxes of antipsychotic drugs in sediment

When concentrations of antipsychotic drugs were averaged by day in water and sediment a declining trend of concentrations in the water column (8−2 cm) and a similar decreasing trend in the vertical scale of sediment porewater was observed, except for lamotrigine and bupropion, with the greatest concentrations at a depth of -2 to -4 cm (**Figure 4.3)**. This result is consistent with previous observations that increasing dissolved concentrations of organic compounds were found in closer proximity to the sediment (Grimalt et al., 2001; Fernandez et al., 2012). The difference between lamotrigine and bupropion might be related to historical input to sediments. However, for most compounds, except for lamotrigine and bupropion, concentrations in sediment porewater generally remained unchanged ($p > 0.05$) at depths below -2 cm. Concentrations between water and porewater remained within the same order of magnitude for lamotrigine, bupropion, and carbamazepine, while concentrations of other compounds in sediment porewater were approximately 10-fold less than those in the water column. The greatest concentration at 8 cm in water was for carbamazepine (15.73 ± 2.14 μg L^{-1}), which was greater than at 6 cm ($9.58 \pm 1.30 \mu$g L^{-1}) and 2 cm (0.54 ± 0.08 μg L^{-1}). The greatest mean concentrations among water matrix samples were observed for carbamazepine (8.61 μg L^{-1}), followed by duloxetine, amitriptyline, and citalopram ($4.30−8.16$ μg L^{-1}). Venlafaxine was observed at significantly lesser mean concentrations in both water (0.077 μg L^{-1}) and sediment (0.009 μg L^{-1}).

Because DGT devices are time-weighted, temporal variability of water concentrations diffusing laterally could not be measured. Therefore, constant concentrations close to the water-sediment interface were assumed for calculating diffusive fluxes. Nevertheless, fluxes were

normalized per day, which showed net positive fluxes towards water from sediment (**Figure 4.3**). Overall lesser fluxes (0.0012–0.089 ng cm^{-2} d^{-1}) were observed for lamotrigine, bupropion, venlafaxine, and duloxetine, while citalopram (0.10 ng cm^{-2} d^{-1}) and fluoxetine (0.14 ng cm^{-2} d^{-1}) had similar fluxes. The greatest flux was found for carbamazepine, indicating that sediment-borne carbamazepine has the potential resupply ability to porewater and is prone to partition back to water at the water-sediment interface.
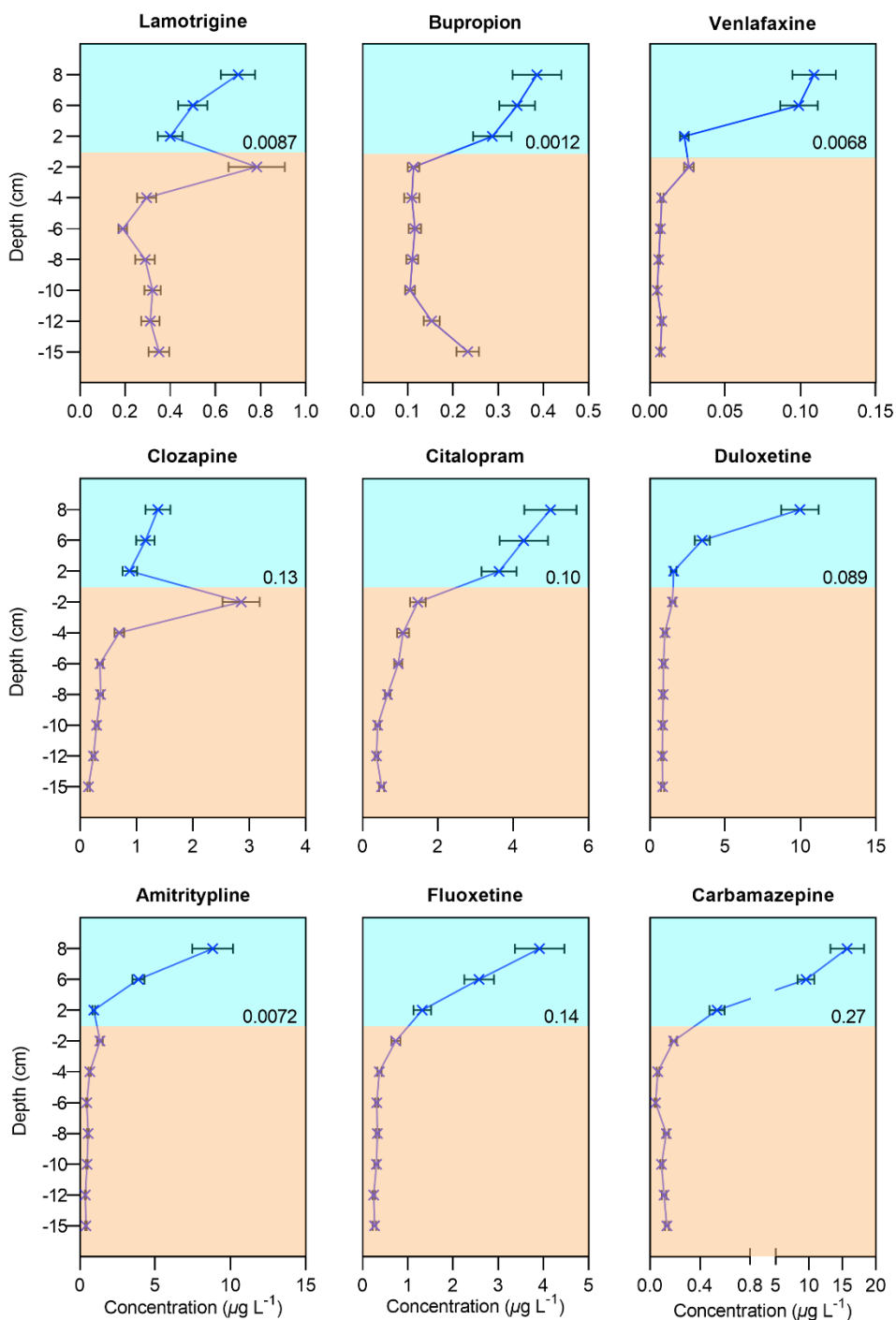
Figure 4.3 The plot of profiles of water column and sediment porewater average concentrations of nine antipsychotic drugs measured by DGT devices. The error bars were generated by the data obtained from three DGT devices. The numbers (ng cm^{-2} day^{-1}) in black were calculated flux from sediment porewater to the water environment. The blue color background represents the water column matrix and the light brown color background represents the sediment column matrix. The y-axis is the depth according to DGT field deployment and the x-axis scale is varied based on the better resolution of vertical distribution for each compound.

4.3.4 Three adsorbing fractions of antipsychotic drugs

4.3.4.1 Fast-desorbing fraction

The plot of S_t/S_0 versus extraction time for desorption of antipsychotic drugs in sediments sampled at day 1 and day 21 during the DGT deployment period is shown in **Figure 4.4**, where the solid line derived from exponential curve fitting by Eq. (A4.1) in **Appendix 4**. The kinetic parameters obtained from Eq. (A4.1) are shown in **Table A8**. Desorption of antipsychotic compounds decreased with increasing the deployment time. Mean desorptions of all compounds in sediment were approximately $21 \pm 2.3\%$ for day 1 and $10 \pm 1.2\%$ for day 21. The F_r values decreased from 0.249 to 0.184 for amitriptyline, 0.403 to 0.331 for bupropion, 0.409 to 0.355 for carbamazepine, 0.261 to 0.127 for citalopram, 0.298 to 0.236 for clozapine, 0.198 to 0.147 for duloxetine, 0.320 to 0.275 for fluoxetine, 0.411 to 0.329 for lamotrigine, and 0.120 to 0.098 for venlafaxine, which indicated that the labile fraction of these compounds decreased in sediments.
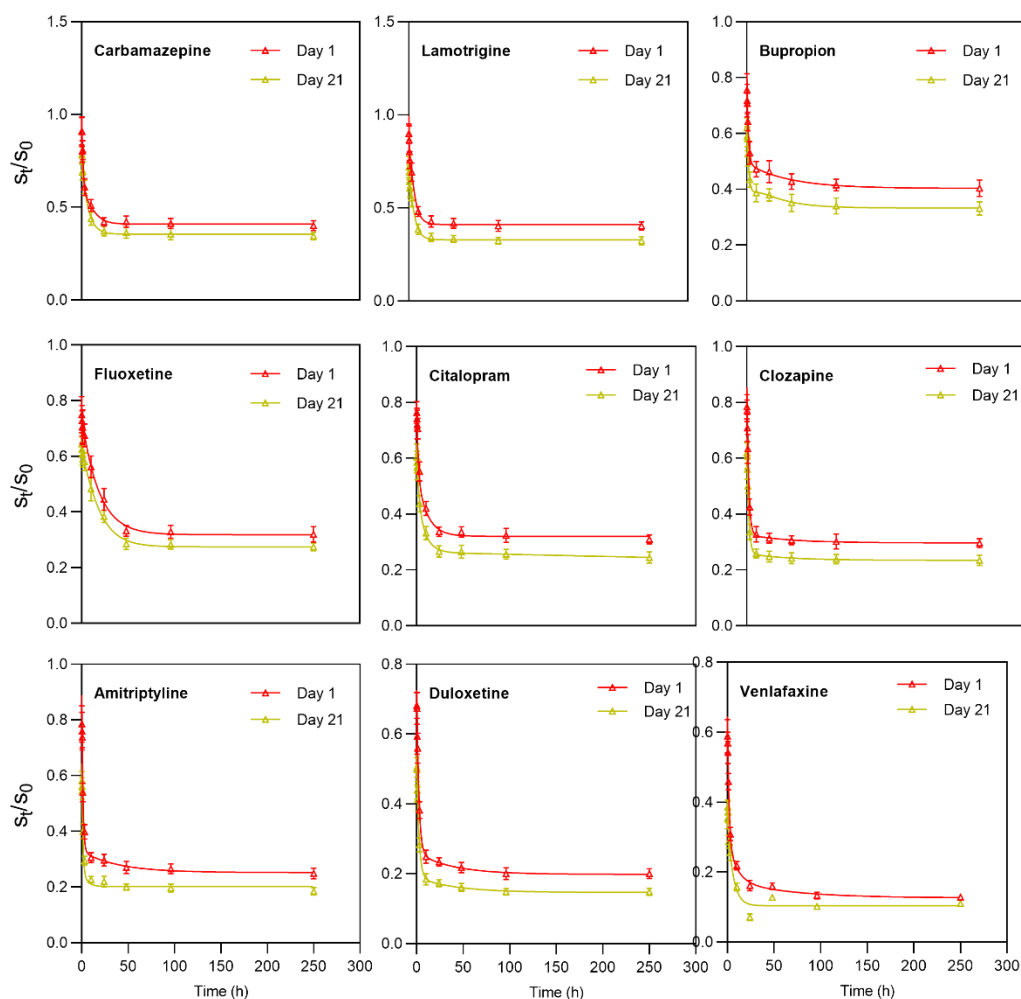
Figure 4.4 Desorption kinetics of nine antipsychotic drugs fitted by consecutive methanol extraction. S_t/S_0 was the compound depletion in the sediment at each extraction time (h). Day 1 and Day 21 represent the sediment sampling day in the field during DGT deployment.

Constants k_{rapid} and k_{slow} ranged from 10^{-1} to 10^{-2} h^{-1} and k_{sv} ranged from 10^{-5} to 10^{-6} h^{-1} (**Table A8**), which is comparable to the magnitude of these parameters from previous labile fraction kinetic studies (You et al., 2007; Trimble et al., 2008; Cheng et al., 2019). The greatest k_{rapid} values both at day 1 and day 21 were found for carbamazepine (0.517 and 0.367 h^{-1}) and lamotrigine (0.531 to 0.383 h^{-1}), while the least values (0.032 and 0.016 h^{-1}) were found for venlafaxine. This result suggests that carbamazepine and lamotrigine could be resupplied from other fractions in sediments while venlafaxine was prone to remain in sediment particles, which

might be associated with the ionic interactions of these compounds (e.g., lamotrigine and carbamazepine) (Zhang et al., 2010; Navon et al., 2011) and the potential pool size of compound in sediment. Despite the F_r values of all compounds being stable within a 24-hour extraction period, variations in nonlinear sorption might influence the magnitude (ten Hulscher et al., 1999). The ratios of F_{24h} to F_r in sediments on day 1 and day 21 showed that the ratio ranged from 77% to 93% (**Table A8**). This suggests that a single extraction by methanol for 24 h is sufficient to represent the rapidly-desorbing fraction of these drugs. These findings are similar to previous results in that the equilibrium of F_r could be reached in a short time (< 10 h) during laboratory simulation with a positive linear regression between F_r and F_{10h} (Cheng et al., 2019).

4.3.4.2 Stable desorbing fraction

The trend of the concentration in sediments extracted following that of the rapidly-desorbing fraction at each deployment time showed that a slightly decreasing concentration with deployment time was observed for most compounds, whereas duloxetine showed a slightly declining concentration at day 21 (**Figure A12** and **Table A9**). The most significant extent of concentration increase was found for bupropion from 2.21 to 6.32 μg kg^{-1} and for fluoxetine from 0.73 to 1.43 μg kg^{-1}. This result indicates the relatively stable state for fraction transfer from stable-desorbing fraction.

4.3.4.3 Bound residue fraction

Despite the hydrolysis method effectively releasing the bound-residue fraction of organic compounds from sediments (Northcott and Jones, 2000), the uncertainty remains whether the hydrolysis processes or high temperature would influence the analytes and lead to inaccurate

quantification. For the accuracy and reliability of analysis results, a single standard solution of each nine antipsychotic drugs was spiked in 10 mL of 1 M NaOH solution at the target concentrations of 10, 100, or 1000 μg L^{-1}, at 80 °C for 24 h to test whether the degradation occurred among nine antipsychotic drugs. Poor recoveries (< 30%) were observed for bupropion and duloxetine while recoveries for other compounds were greater than 80% at all three concentrations. This is consistent with previous observations that bupropion and duloxetine are not resistant to alkaline hydrolysis (Rao et al., 2010; Abbas et al., 2012). Therefore, bupropion and duloxetine are not included in the bound-residue fraction discussion. In comparison to the concentration of stable-desorbing fraction, except for citalopram, clozapine, and fluoxetine having no significant changes ($p > 0.05$), the concentrations of other compounds showed apparent increases (**Table A10**). Generally, bound-residue concentrations of antipsychotic drugs were increasing with sampling time.

4.3.5 Transfer of antipsychotic drugs in sediment

During 21 sampling days, the total measured portions of antipsychotic drugs, not considering bupropion and duloxetine, changed from 20% to 70% (**Table A11**), where total concentration was increased from 1.37 to 4.00 μg kg^{-1} for amitriptyline, 0.46 to 1.28 μg kg^{-1} for carbamazepine, 0.02 to 0.06 μg kg^{-1} for citalopram, 1.60 to 1.99 μg kg^{-1} for fluoxetine, 1.61 to 6.11 μg kg^{-1} for lamotrigine, and 2.13 to 5.51 μg kg^{-1} for venlafaxine, whereas an approximately 50% decrease was observed in clozapine, from 1.83 to 0.94 μg kg^{-1}. This suggests a continuous resupply of most selected compounds over time in the real environment while clozapine might experience a poor source pool and different mechanisms of degradation. Microbial degradation has been

observed for several antipsychotic drugs (carbamazepine, oxazepam, and codeine) followed by a lag period of about 1 day under laboratory simulation (Stein et al. (2008). Therefore, we could not interpret whether degradation was due to biological processes or photodegradation in real matrices. However, our results demonstrated that certain levels of antipsychotic drugs persist in surface sediments.

The labile, stable-adsorbing, and bound-residue fractions of antipsychotics in sediments are presented in **Figure 4.5**, calculated as the % of the total concentrations of three fractions. This can reflect the resupply ability of compounds to labile fraction. The percentage of labile fraction of all antipsychotic drugs declined with the sampling time, suggesting that the potential bioavailability of these drugs declined. This decline only reflected the static-state distribution of these compounds in sediments. However, while bound-residue or stable-desorbing fraction increased, indicating a risk for fraction transfer to further influence the desorption rate of compounds from sediments to aqueous phase. The relatively slow declines were observed within 6 days, which might be inferred that some competition in sorption sites for different compounds, and these compounds might be easier to diffuse to sediment porewater rather than sorption sites. With increasing sampling time, the gradual decrease of labile fraction could be caused by organic sequestration, clay sorption, and diffusion to sediment micropores. The stable-adsorbing fraction of antipsychotic drugs showed decreases over time for amitriptyline (8% to 5%), carbamazepine (29% to 15%), lamotrigine (27% to 14%), and venlafaxine (46% to 19%); increases for citalopram (43% to 50%), clozapine (17% to 50%), and fluoxetine (48% to 72%). This difference for different compounds might be due to the intensity of binding forces or sequestration through the transfer from stable-desorbing fraction to bound-reside fraction.
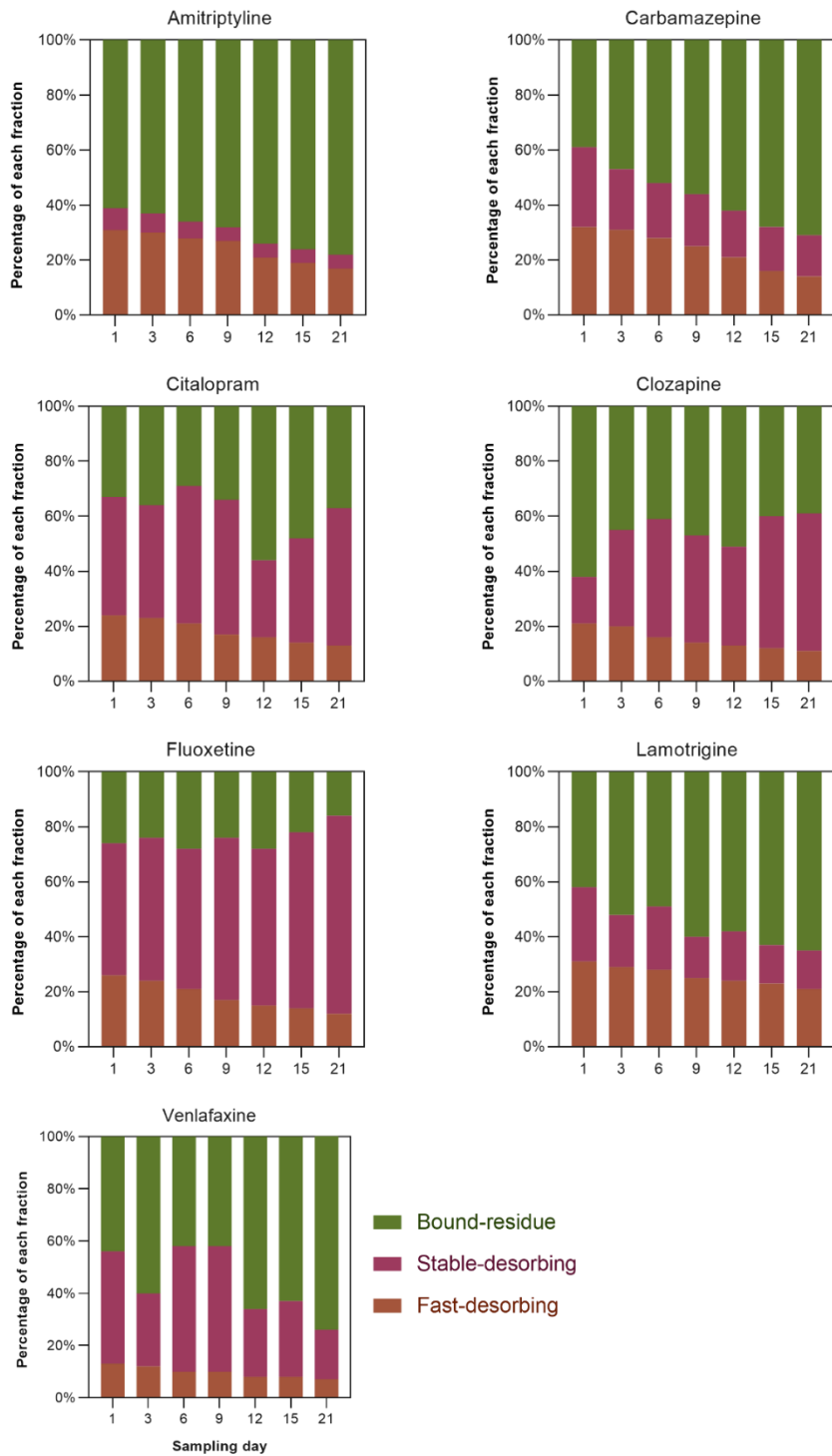
Figure 4.5 Rapidly-desorbing (labile), stable desorbing, and bound residue fractions of antipsychotic drugs in sediments from different sampling days during DGT deployment. Rapidly-desorbing fraction: consecutive extraction by methanol. Stable desorbing fraction: ultrasound extraction by 1:1 methanol: dichloromethane. Bound residue: extraction by alkaline hydrolysis.

The bound-residue fraction of antipsychotic drugs from 1 to 21 d ranged from 61% to 81% for amitriptyline, 39% to 71% for carbamazepine, 33% to 37% for citalopram, 42% to 65% for lamotrigine, 41% to 75% for venlafaxine, 62% to 39% for clozapine, and 26% to 16% for fluoxetine. Despite the bound-residue fraction is generally accompanied by the other two fractions, increasing the bound-residue fraction here for the majority of compounds was not directly to the increase of labile fraction, especially for 1 to 6 d. This observation is based on the solid sediment capacity of solutes (Weber and Huang, 1996; Cornelissen et al., 1997b), which is, the fraction for some compounds, clozapine, and fluoxetine, could not firmly adsorb onto sediment particle surface, and the occurrence of channels and nanopores for sandy texture led to slow diffusion into internal sediment matrix where organic compounds could be eventually retained. Generally, results reported here indicate that the bound-residue fraction of antipsychotic drugs can be an important resupply source for transfer to the labile fraction that is continuously increased with sampling days. A previously developed mathematical model (Cheng et al., 2019) was used to simulate the processes of three fractions' transfer over sampling time without considering degradation conditions (**Figure A13**) (Eqs. 3.9-3.11).

$$\frac{\mathrm{d}C_{labile}}{dt} = -k_{fs} - k_{fb} + k_{fs}C_{stable} + k_{bf}C_{bound} \quad (3.9)$$

$$\frac{\mathrm{d}C_{stable}}{dt} = -k_{sf} - k_{sb} + k_{fs}C_{labile} + k_{bs}C_{bound} \quad (3.10)$$

$$\frac{dC_{bound}}{dt} = -k_{bf}C_{bound} - k_{bs}C_{bound} + k_{fb} + k_{sb}C_{stable} \quad (3.11)$$

where C_{labile}, C_{stable}, and C_{bound} are the concentrations of labile (fast-desorbing), stable-desorbing, and bound-residue fractions, respectively (**Table A11**). k_{fs} and k_{sf} represent the rate coefficients of partitioning between labile and stable-adsorbing fractions for antipsychotic drugs; k_{fb} and k_{bf} represent the rate coefficients partitioning between labile and bound-residue fractions for

antipsychotic drugs; k_{sb} and k_{bs} represent the rate coefficients partitioning between stable and bound-residue fractions for antipsychotic drugs. The detailed computation processes of the model are shown in **Appendix 8**. A good correlation for model-fitting ($r^2 = 0.915–0.993$) for three different fractions was observed (**Figure 4.6**). The constant coefficients (k) were not constant during the sampling day and were significantly different (**Table 4.2**). Overall, k_{fs} is bigger than k_{sf} from the first to last sampling day for all compounds, implying these antipsychotic drugs were prone to retain in the sediment particle rather than sediment porewater. At 21 d, the increasing k_{fs} values suggested that more antipsychotic drugs escaped from the labile phase to the stable-desorbing fraction. k_{fb} and k_{bf} standing for the ability to sequester compounds in sediment particles and its antidromic release, respectively, were nearly 0 at day 1, indicating little labile fraction transferred to bound-residue fraction. This result suggested that antipsychotic drugs had a lag time to be sorbed onto sediments. At 21 d, k_{fb} increased for all drugs except for citalopram, clozapine, and fluoxetine, showing these three drugs had been completely adsorbed by the adsorption sites of sediment particles, and pool size for them might be limited as well. The small values of k_{fb} indicated that antipsychotic drugs were partitioned to organic matter and blocked to have a fraction transfer, which is taken as the final fate for organic contaminant (non-bioavailability). Although k_{fb} and k_{bf} were much lower than the other k values, the transfer between bound-reside and stable-desorbing fractions occurred before diffusion into sediment porewater. The increased k_{sb} and k_{bs} for amitriptyline, carbamazepine, lamotrigine, and venlafaxine could represent not irreversible processes, whereas slightly decreased k_{sb} was corresponding to the decreased values of k_{fb}. This could also reflect the dynamic processes in bound-residue fraction where fewer antipsychotic drugs could be

potentially released, to some extent, with accessibility to biota (Xing et al., 1996; Cheng et al., 2019).
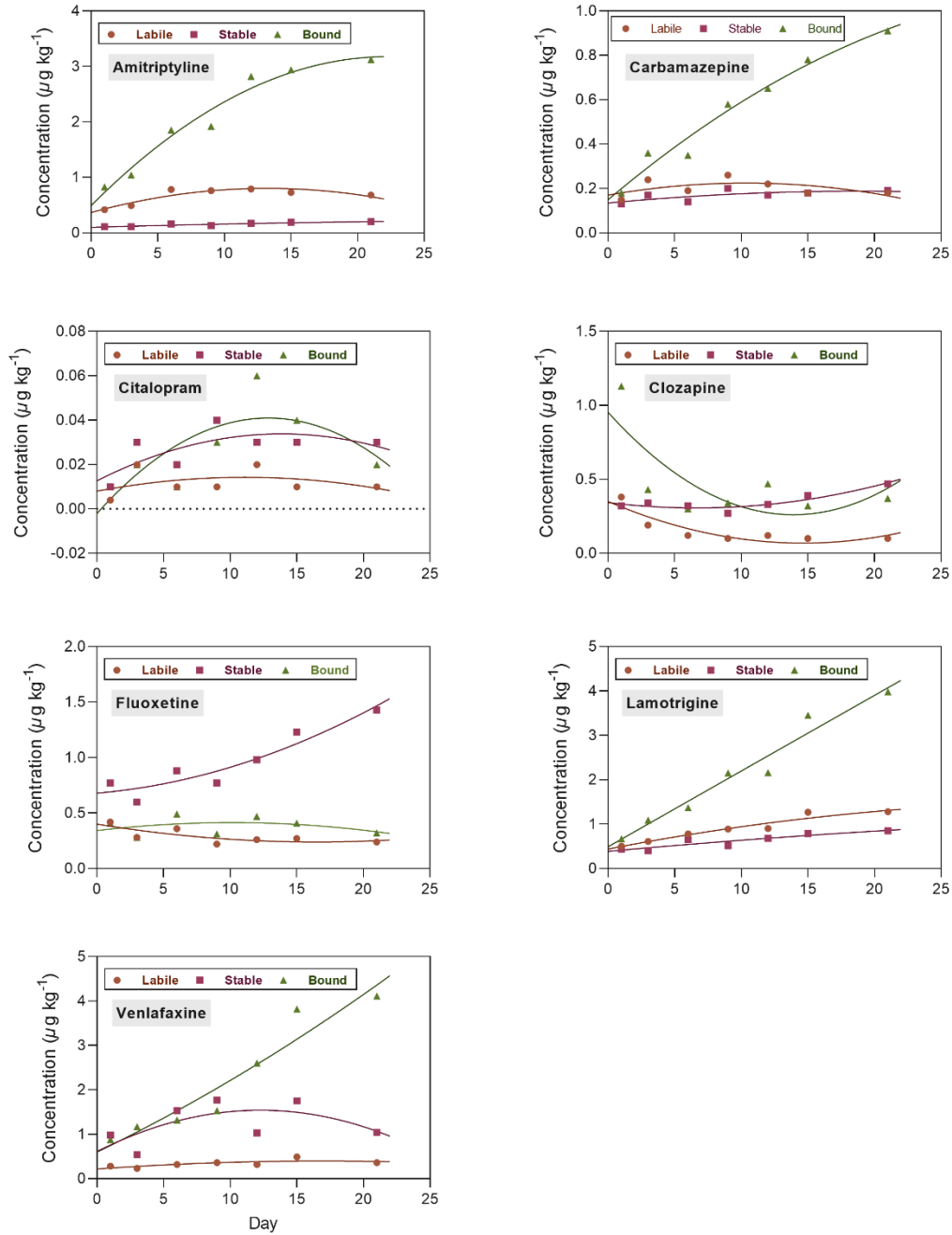
Figure 4.6 The experimental data and simulated data for labile, stable-adsorbed, and bound-residue fractions of antipsychotic drugs in sediments during sampling time. The shaped points are experimental results, and the lines are model-simulated results (Eqs. A8.1-8.4).

Table 4.2 Rate coefficients (k, d^{-1}) derived by fitting of the transfer model.

	Amitriptyline		Carbamazepine		Citalopram		Clozapine		Fluoxetine		Lamotrigine		Venlafaxine	
	1 d	21 d	1 d	21 d	1 d	21 d	1 d	21 d	1 d	21 d	1 d	21 d	1 d	21 d
k_{fs}	0.0023	0.0043	0.0650	0.0774	0.0032	0.0037	0.0034	0.0039	0.0019	0.0023	0.0022	0.0027	0.0007	0.0008
k_{sf}	0.0040	0.4500	0.0075	0.0087	0.0047	0.0056	0.0052	0.0062	0.0033	0.0038	0.0038	0.0044	0.0013	0.0016
k_{fb}	0.0003	0.0005	0.0009	0.0010	0.0007	0.0050	0.0047	0.0055	0.0002	0.0000	0.0003	0.0003	0.0001	0.0001
k_{bf}	0.0004	0.0004	0.0005	0.0006	0.0019	0.0022	0.0020	0.0024	0.0003	0.0004	0.0004	0.0005	0.0001	0.0001
k_{sb}	0.0065	0.0073	0.0087	0.0101	0.0004	0.0003	0.0003	0.0003	0.0055	0.0012	0.0062	0.0074	0.0018	0.0021
k_{bs}	0.0430	0.0540	0.0120	0.0138	0.0023	0.0027	0.0025	0.0029	0.0353	0.0409	0.0404	0.0465	0.0108	0.0129

The subscripts *f*, *s*, and *b* represent the fast-desorbing fraction, stable desorbing fraction, and bound residue fraction, respectively.

4.3.6 Resupply kinetics and labile size of antipsychotic drugs in sediment

The R-value represents the resupply of antipsychotic drugs from the sediment particles to porewater, which responds to the depletion by DGT devices. The R values in sediment depth of 2−15 cm ranged from 0.15 to 0.41 for carbamazepine, 0.14 to 0.39 for lamotrigine, 0.12 to 0.35 for bupropion, 0.13 to 0.34 for fluoxetine, 0.11 to 0.30 for citalopram, 0.11 to 0.29 for clozapine, 0.09 to 0.25 for amitriptyline, 0.08 to 0.22 for duloxetine, and 0.05 to 0.15 for venlafaxine. When there was no supply from sediment but only diffusion to supply, R_{diff} values derived from the DIFS model varied from 0.02 to 0.04 for all drugs. Therefore, the sediment for all antipsychotic drugs can supply the positive fluxes from the solid phase to the sediment solution. In general, R values decreased gradually with deployment time and also with depth (**Figure A14**), and the differences between 8 and 15 cm were not significant ($p > 0.05$) for all drugs, indicating the resupply ability decreased with the depth and resupply could not be quickly provided during the time interval of DGT deployment in real conditions. Additionally, the largest R values were found for carbamazepine and lamotrigine while venlafaxine showed the lowest value, which is similar to the values of k_{sf} and k_{bf}, indicating the low supply to sediment porewater for venlafaxine while carbamazepine and lamotrigine could be resupplied quicker.

The labile antipsychotic drugs in the solid phase could be released during DGT deployment to supply those depleted by DGT from sediment solution. The estimated pool size for antipsychotic drugs varied from 0.07 to 0.50 μg kg^{-1} (**Table 4.3**) using Eq. (A7.2). The distribution coefficient (K_d), calculated as the ratio of the concentration of labile antipsychotic drugs (the equilibrium-reached concentration using consecutive extraction for fast-desorbing

fraction at 10 h) to C_p can be used to indicate the labile pool size in sediments. Our K_d values (0.02–32.32 cm^3 g^{-1}) (**Table 4.3**) are within the ranges published (0.01–64 cm^3 g^{-1}) (Payá-Pérez et al., 1992; Ben-Hur et al., 2003; Ling et al., 2005; Li et al., 2021b). The order of average K_d values is as follows: carbamazepine > lamotrigine > fluoxetine > bupropion > clozapine > citalopram > amitriptyline > duloxetine > venlafaxine. Interestingly, our data showed K_d declined with depth for all drugs except values for fluoxetine were close to 0, and the difference between K_d and K_{dl} was one order of magnitude while no significant decrease with depth was found in K_{dl}. This difference could be due to the solvent extraction to get the maximum compounds from the labile fraction; and the loss for porewater taken over time (e.g., evaporation and redistribution out of field condition). However, it is important that K_d and R values can get the same results for resupply abilities. By calculating labile pool size indicating K_d can be a parameter to use for predicting the magnitude of resupply for organic compounds. Considering the alkaline drugs, the slightly decreasing pH and lower organic matter in our sediment had little influence on the adsorption. Additionally, the response time (T_c) and the desorption/adsorption rate constant (k_{-1}/k_1) at different depths (**Table 4.3**) showed that the greatest values were found at 2 cm, demonstrating the top layer has the fastest resupply. Ten-fold greater k_{-1} values than k_1 values for all drugs were found, indicating the desorption processes were dominant within 2–15 cm depth.

As the investigated sediment was in a neutral pH environment, the measured antipsychotic drugs remained in their neutral form with adsorption mainly through van der Waals forces or hydrogen bonding, which might be related to the dissolved organic matter for controlling the fraction transfer, resupply kinetic characteristics, and labile pool size.

Table 4.3 Parameters for analytes at various sediment depths derived from model fits using 2D-DIFS. K_d and K_{dl} (mL g^{-1}) is the distribution coefficient derived from methanol extraction and 2D-DIFS, respectively. T_c (s) is the response time. k_{-1} and k_1 (s^{-1}) are the rate constant of desorption and sorption, respectively. $C_{l\text{-estimated}}$ (μg L^{-1}) is an estimate of the labile concentration.

	Depth (cm)	K_d	K_{dl}	T_c	k_{-1}	k_1	$C_{l\text{-estimated}}$
Carbamazepine	1	32.32	0.05	1.72E+05	5.14E-06	6.62E-07	0.07
	4	26.33	0.07	1.97E+05	4.27E-06	8.03E-07	0.09
	8	18.74	0.11	2.20E+05	3.58E-06	9.65E-07	0.12
	15	13.29	0.16	2.46E+05	2.90E-06	1.17E-06	0.20
Lamotrigine	1	21.43	0.05	1.66E+05	5.39E-06	6.32E-07	0.06
	4	17.75	0.07	1.87E+05	4.56E-06	7.89E-07	0.08
	8	12.57	0.10	2.13E+05	3.70E-06	9.86E-07	0.12
	15	9.38	0.15	2.29E+05	3.17E-06	1.20E-06	0.19
Venlafaxine	1	0.04	0.01	1.11E+06	8.87E-07	1.36E-08	0.01
	4	0.03	0.01	1.35E+06	7.24E-07	1.64E-08	0.01
	8	0.03	0.01	1.63E+06	5.94E-07	2.06E-08	0.02
	15	0.02	0.02	1.92E+06	4.95E-07	2.48E-08	0.03
Clozapine	1	7.42	0.12	3.55E+05	2.16E-06	6.53E-07	0.14
	4	6.14	0.18	3.84E+05	1.79E-06	8.14E-07	0.25
	8	4.66	0.25	3.97E+05	1.53E-06	9.87E-07	0.30
	15	3.41	0.37	3.92E+05	1.31E-06	1.24E-06	0.50
Citalopram	1	5.87	0.08	3.28E+05	2.51E-06	5.37E-07	0.12
	4	4.71	0.12	3.68E+05	2.07E-06	6.49E-07	0.15
	8	3.49	0.18	3.88E+05	1.76E-06	8.16E-07	0.22
	15	2.47	0.26	4.05E+05	1.49E-06	9.79E-07	0.32
Fluoxetine	1	12.12	0.15	2.32E+05	3.11E-06	1.20E-06	0.18
	4	10.32	0.05	3.32E+05	2.66E-06	3.53E-07	0.07
	8	7.45	0.07	3.71E+05	2.27E-06	4.27E-07	0.09
	15	5.25	0.11	4.13E+05	1.89E-06	5.32E-07	0.13
Bupropion	1	10.56	0.08	2.39E+05	3.47E-06	7.24E-07	0.10
	4	8.45	0.12	2.64E+05	2.89E-06	8.92E-07	0.15
	8	6.05	0.18	2.86E+05	2.41E-06	1.08E-06	0.21
	15	4.50	0.16	2.10E+05	3.40E-06	1.36E-06	0.20
Duloxetine	1	0.28	0.20	6.08E+05	1.08E-06	5.65E-07	0.25
	4	0.22	0.30	6.19E+05	9.16E-07	7.00E-07	0.39
	8	0.16	0.43	6.16E+05	7.73E-07	8.51E-07	0.50
	15	0.11	0.62	5.92E+05	6.53E-07	1.04E-06	0.75
Amitriptyline	1	0.37	0.08	3.25E+05	2.58E-06	5.01E-07	0.10
	4	0.30	0.12	3.73E+05	2.06E-06	6.21E-07	0.15
	8	0.22	0.17	3.99E+05	1.76E-06	7.54E-07	0.23
	15	0.16	0.26	4.24E+05	1.42E-06	9.34E-07	0.31

4.4 Conclusion

This study used *in-situ* deployed DGT devices in water and sediment in the field for 21 days. Our results showed positive fluxes of nine antipsychotic drugs from sediment to water. Processes were controlled by the resupply capability from solid phase to sediment porewater. Although rapidly-desorbing (labile) fractions declined during 21 days, the constant coefficients of antipsychotic drugs could be supplied to the labile phase quickly from the stable desorbing and bound residue fractions with a lag time. The quickest transfer rate to labile fraction was found for amitriptyline and carbamazepine and the slowest for venlafaxine, which has been also verified by the R ratio, response time, and desorption rate constant obtained from the DIFS model. The estimated labile pool size from DIFS might not be the best way to reflect the real status, while the labile pool size calculated at equilibrium from a first-order three-compartment kinetic model could fit the changes of R values well. We propose that this could be an auxiliary parameter to understand DIFS output, which is helpful in understanding the dynamic processes of organic pollutants in sediments.

CHAPTER 5: Combining passive sampling with fraction transfer and toxicokinetic modeling to assess bioavailability of organic pollutants in a benthic invertebrate, *Lumbriculus variegatus*

Overview

Contributions

Xiaowen Ji: conducted the entire experiment and wrote the manuscript.

Jenna Cantin: ran LC-MS methods for nine antipsychotics of part of samples.

Ana S. Cardenas Perez: prepared diffusive gels and binding gels for DGT devices.

Yufeng Gong: assisted with running LC/MS.

John P. Giesy: revised the manuscript.

Markus Brinkmann: designed the experiment, secured funding, and revised the manuscript.

Transition

Chapter 4 used the well-established devices in the vertical profile of sediment and overlying water in the natural river for fluxes of analytes at the interface of sediment and water as well as the desorption kinetics of analytes. The kinetics-modelled data was explained by the fraction transfer model for their inherent transfer mechanisms. Although this chapter has quantitively revealed resupply processes in the aquatic system, the biological absorption of organic contaminants by aquatic biota residing in the interface of sediment and water was still unknown. To assess this part of the bioavailable fraction of contaminants, this chapter aimed to first assess the bio-uptake of analytes by passive transport without consideration of food and sediment organic particle consumptions. To achieve this, benthic invertebrates under laboratory-controlled conditions using established DGT samplers were conducted for passive bio-uptake model to predict the bioavailability of organic contaminants, DGT-derived desorption kinetic model, and the fraction transfer model. The results of this chapter explained the bioavailable portion of organic contaminants passively absorbed by benthic invertebrates and the mechanisms of the resupply processes of this bioaccessible fraction.

Abstract

This study investigated the passive adsorption of nine antipsychotic drugs by the benthic oligochaete, *Lumbriculus variegatus* from spiked freshwater sediments. Based on a combination of diffusive gradients in thin-films (DGT) passive sampling and modeling, specifically the DGT-induced fluxes in sediments (DIFS) model and fractions-transfer models, an uptake and diffusion-induced model was established for oligochaetes. Lamotrigine and bupropion showed positive fluxes from sediment to overlying water. Oligochaetes accumulated both lamotrigine and carbamazepine. The simulation model for transfer showed that after 30 days antipsychotic compounds in sediment were present predominantly in stable or bound fractions, rather than labile fractions. Dissolved organic carbon and degradation were important drivers of dissipation rates of antipsychotic compounds in sediments and labile pool size. Uptake by oligochaetes and diffusion-induced models matched measured concentrations well (R^2= 0.83–0.95 and R^2= 0.99–1.00, respectively). Processes of uptake by oligochaetes were comparable to DIFS results, where fast desorption to the labile pool in the short response time and adsorption processes, except carbamazepine and lamotrigine, in sediments dominated kinetics. It suggests a link between the bioavailability of organic pollutants for sediment-dwelling organisms and desorption kinetics involved with fractions transfer within sediments, which has important implications for the environmental risk assessment of these chemicals.

Keywords: benthic worm, sediment, antipsychotic compounds, passive uptake, DGT

5.1 Introduction

Due to recent improvements in surface water quality globally, sediments have shifted from being recognized as predominant sinks of pollution to being potential sources of hydrophilic and hydrophobic contaminants (Moermond et al., 2004). Its induced alterations in nutrient loading, e.g., decreases in eutrophication, structures of food webs, and growth and biomass of biota can likewise be influenced (Leip et al., 2015; Meunier et al., 2016), which can affect bioavailability and fates of contaminants. Organic contaminants in aged sediments can be bound in various forms, which might result in various mechanisms of release into aquatic ecosystems, especially for shallow areas, such as the hyporheic zone, in which the heterogeneous characteristics provide a variety of microhabitats, inhabited by microscopic and macroscopic organisms (Woessner, 2017). For benthic invertebrates in the hyporheic zone, ingestion of sediment is a major route of uptake of hydrophobic contaminants (Moermond et al., 2004; Ferguson et al., 2008; Casatta et al., 2016), despite differences among species (Wang and Kelly, 2018). Due to the ecological significance of hyporheic exchange and deposition of clays, fates of hydrophobic contaminants in sediments are controlled by adsorption to clay minerals that have sufficient hydrophobic active sites (Ugochukwu, 2019). Hydrophilic contaminants appear to be easily exchangeable with sediment porewater and biota. However, in sediments, most studies to date have focused on measuring the bioconcentration of more hydrophobic contaminants with Log K_{ow} (octanol/water partition coefficients) > 5 (Moermond et al., 2004; Bao et al., 2013; Cui et al., 2013) and hydrophilic to moderately hydrophobic contaminants have received lesser attention.

Despite the variability and complexity of sediment composition and potential sorptive interactions, Karickhoff (1981) reported that at low loading rates, sorption isotherms of neutral organic contaminants with solubilities in water of less than 10^{-3} M, appeared to be linear and reversible. This dynamic kinetic process might significantly influence the uptake of organic contaminants by sediment infauna. Dissipation of organic contaminants associated with uptake by biota from sediments has often been assessed by exhaustive extraction with organic solvents (Talley et al., 2002). However, structurally and/or chemically different constituents of sediment interact differently with organic contaminants and thus have different binding energies and relevant rates of adsorption and desorption.

Theoretically, organic contaminants are present in sediments as three major fractions: fast-desorbing (labile), stable-adsorbing, and bound-residues (Semple et al., 2004; Schwab and Brack, 2007; Schäffer et al., 2018). The labile fraction is usually considered as a freely dissolved concentration of organic compounds in sediment porewater that may be bioavailable to benthic organisms through diffusion and ingestion and able to enter the overlying water (Dueri et al., 2008; Li et al., 2013a). In sediments, the bioavailability of organic contaminants to sediment-inhabiting organisms can be limited by the fast-desorbing fraction (Lydy et al., 2015). In contrast, the stable-adsorbing fraction can also contribute to the bioavailable fraction, but generally over longer time scales. Due to aging phenomena characterized by the formation of a bound-residue fraction, bioavailability from sediments can decrease markedly (Palomo and Bhandari, 2006; Cheng et al., 2020). Therefore, it is important to properly characterize fractional changes of organic contaminants in sediments to understand bioavailability and contributions of uptake into benthic organisms and the formation of bound residues to

159

dissipation processes.

Diffusion is an important process to finally approach biota during the exchange for a labile fraction of organic compounds between biota interface and aquatic compartments through various time scales. The time scale for the diffusion of chemical transport over distance is typically within the range of 1 s to 100 s (100 μm to 1 mm) for uptake by organisms (van Leeuwen et al., 2005), such as benthic invertebrates in sediments. This time scale is similar to that of transport through diffusion layers in mildly stirred media or through membrane layers, such as those used in the diffusive gradients in thin film (DGT) technique (van Leeuwen et al., 2005). Application of DGT for organic pollutants is a relatively recent advance that can be used for measuring time-integrated concentrations and fluxes of labile organic compounds from sediment porewater and solid phases (Li et al., 2021b; Ji et al., 2022b). There is growing evidence that labile concentration or chemical activity measured by passive samplers can be an alternative to efficiently evaluate bioavailability (Joyce et al., 2016). When DGT samplers are inserted into sediments, dissolved compounds in porewaters will rapidly accumulate in the binding layer, generating a localized area of depletion in the porewater that contains the release of weakly bound compounds (labile) from the solid phase of sediments (Li et al., 2021b). To further explain the dynamic processes assessed by DGT in sediments, a numerical model, DGT-induced fluxes in soils and sediments (DIFS), was developed (Harper et al., 2000). It has been successfully deployed for interpreting the desorption kinetics of organic compounds in sediments (Li et al., 2021b; Ji et al., 2022b). However, other than a positive correlation between DGT-derived concentrations and whole-body concentrations that were observed in zebrafish exposed to methamphetamine (Yin et al., 2019), there are no studies focusing on the

bioavailability of organic contaminants to benthic invertebrates using DGT and the numerical

model to interpret the relationships between dissipation in sediments and uptake by benthic

invertebrates for organic contaminants. Results of a previous study found that the combination

of the three desorbing fractions transfer model for the fast-desorbing fraction and DIFS model

could better estimate dynamics of exchange of organic compounds in sediments (Ji et al.,

2022c). It seems that these two models can be further linked to include uptake by sediment

organisms.

As stated above, sediment–interstitial water–biota interactions play a key role in the

bioavailability and dissipation of organic contaminants in sediments. To date, there are still

deficiencies in quantitative modeling for the uptake of organic compounds by sediment

organisms. In this study, we chose nine environmentally relevant antipsychotic drugs (i.e.,

amitriptyline, bupropion, carbamazepine, citalopram, clozapine, duloxetine, fluoxetine,

lamotrigine, and venlafaxine) with Log K_{ow} values of 0.99–4.95 as model organic contaminants

that range from hydrophilic to moderately hydrophobic and were detected in river sediments in

our previous investigation (Ji et al., 2022b). The hypothesis of this study is that the passive

uptake of organic compounds through the direct integumental contact with sediment porewater

for a benthic worm (*Lumbriculus variegatus*) can be equivalent to the uptake by the passive

sampler (DGT) based on equilibrium partitioning. Specifically, the objectives of this study were

to: (1) determine the uptake of antipsychotic compounds and their dissipation for *L. variegatus*

in sediments; (2) develop a mathematical model based on the concentrations determined by

DGT to predict the uptake of antipsychotic compounds in worms; (3) investigate the potential

connection of the fraction transfer and desorption kinetics in sediments for the mechanism of

bioavailability of these compounds for the benthic worms.

5.2 Materials and methods

5.2.1 Bioaccumulation design

Glass tanks used for exposing worms and deploying DGT devices in spiked sediments are shown (**Figure 5.1a**). The glass tank was equally separated into six spaces (L: 9.6 cm, W: 6.1 cm H: 7.2 cm) by PVC plates. Three spaces were used for the worm uptake experiment and the other three were used for deployment of DGT devices. Accurately weighed aliquots of spiked sediments (200 g ± 0.05 g) were filled into each space and carefully flattened to a height of approx. 2 cm, given a particle density of 1.65 g cm^{-3}. Afterward, 1 L of moderately hard, reconstituted water for freshwater organisms from the Aquatic Toxicology Research Facility (ATRF), University of Saskatchewan, was slowly poured into each space. After reaching a steady state and no suspended particles were observed in the water layer anymore, air stones connected to an aerator pump were inserted. Then, fifty previously cultivated worms were transferred to each corresponding space. It took about 12 hours for the worms to accommodate the new habitat, and to present part of their bodies above the sediment−water interface. Meanwhile, three DGT devices were pressed firmly onto sediments in individual corresponding spaces.

Experiments with two spike concentrations (1 mg kg^{-1} and 10 mg kg^{-1}) in sediments and one laboratory control with the same number of worms in quartz sands were conducted in parallel. DGT devices were retrieved and deployed for 1, 3, 6, 9, 14, 18, 23, 28, and 30 days, in which three replicates of worms from each space were randomly sampled with a polyethylene Pasteur

pipette (**Figure 5.1b**). The water temperature during the experiment was stable at 21±0.5 °C. Water quality parameters, e.g., DO, temperature, pH, conductivity, and ammonia concentration, were monitored daily (**Table A12**). DO, pH, and conductivity were measured using an Orion Star™ A329 multiparameter sonde (Thermo-Scientific, Mississauga, ON). Ammonia was measured by Orion™ AQUAfast™ AQ4000 Colorimeter coupled with an AC20212 ammonia as nitrogen indophenol blue kit (Thermo-Scientific).
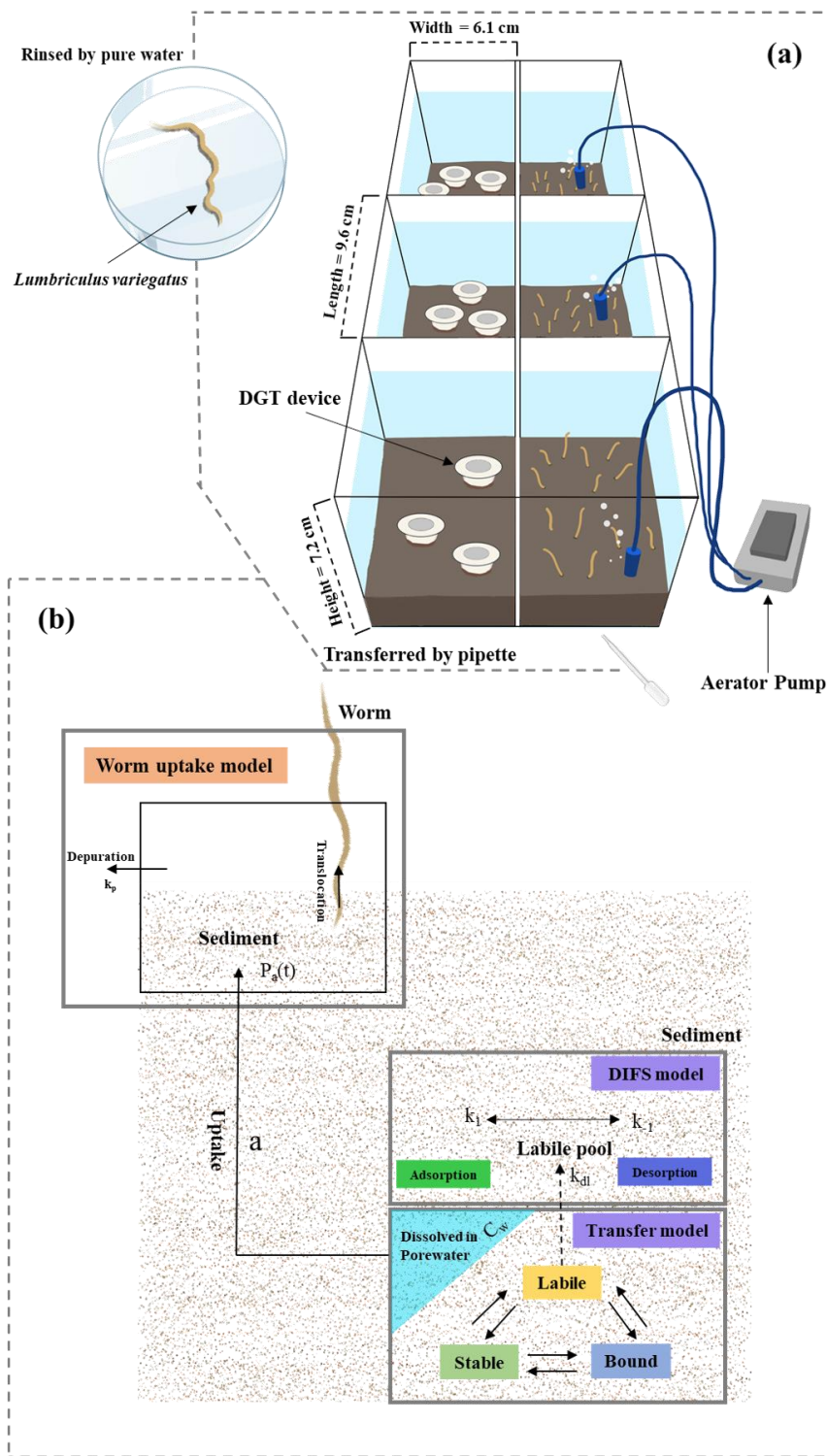
Figure 5.1 Bioaccumulation experiment of benthic worms (*Lumbriculus variegatus*) in spiked sediments: (**a**) deployment of DGT device and cultivation of worms in a glass tank; (**b**) conceptual model for uptake in worms, and fractions transfer and desorption kinetics for nine antipsychotic compounds in sediments.

5.2.2 Preparation of spiked sediments

Surface sediments (depth: ~5 cm) were obtained from a shallow hyporheic zone in the fluvial riverbank of the South Saskatchewan River in Saskatoon, Canada. These sediments did not contain detectable quantities of the studied analytes and the details of sediment sampling and analysis are shown in our previous investigation (Ji et al., 2022b). The sediment was comprised of 54% sand, 35% silt, 11% clay, and 1.5% organic matter, and had a pH-$CaCl_2$ of 6.7. To reach two spiked concentrations of nine antipsychotic compounds, i.e., 1 mg kg^{-1} and 10 mg kg^{-1}, for the purpose of providing adequate fluxes from sediment particles to porewater, the mixture of antipsychotic compounds was dissolved in a small amount of methanol and diluted by 50 mL deionized water. The mixture solution was gradually added to the sediments, and each spiked sediment was thoroughly stirred and homogenized. The experiment started after the evaporation of the solution in sediments.

5.2.3 Worm cultivation

L. variegatus was cultured at the Toxicology Center, University of Saskatchewan (SK, Canada) and cultured at 21±0.5 °C with a 16:8 light: dark illumination period in quartz sand according to the U.S Environmental Protection Agency (USEPA, 2000). The water was partially renewed, and the worms were fed with commercial fish feed weekly. Worms were sieved from quartz sands to select adult worms (> 3 cm) of relatively uniform size for studies of bioaccumulation. Worms were not fed during the experiment. For testing purging the guts of analytes by efficient time, three groups of 10 worms were isolated and placed into 500 mL breakers containing 1 mg kg^{-1} of 10 g same sediments as the same condition mentioned above

for 14 days. Three groups of worms were treated without the purging, with 6 h purging, and with 24 h purging in deionized water. The results (**Table A13**) showed that the concentration difference of antipsychotic was 3-5% between 6 h purging and 24 h purging and was 3-7% between 6 h purging and non-purging. Therefore, worms sampled during the experiment were individually placed in a petri dish filled with deionized water to purge their gut contents for 6 h. Then, the water was removed, and worms were immediately stored in a freezer at -20 °C.

5.2.4 Diffusive gradient in thin films

Standard-size DGT devices with an exposure area of 2.54 cm^2 were prepared following the procedure described previously (Ji et al., 2022b). The DGT device includes a 0.75 mm 2% agarose binding gel containing 35 mg Sepra^{TM}-ZT adsorbent (particle size: 30 μm, pore size: 85 Å, Phenomenex, Torrance, CA), a 0.75 mm thick 2% agarose diffusive gel, and a 0.45 μm pore-size, 0.1 mm polyethersulfone filter membrane. Preparation of gels and manipulation of DGT devices were conducted in a laminar flow hood. Before deployment, DGT devices were conditioned by soaking for 12 h in 0.1 M HNO$_3$ solution bubbled with nitrogen gas for 1 h and then maintained in HPLC water until deployment. At each retrieval and deployment time, extra triplicate DGT devices were placed in a glass breaker containing HPLC-grade water as a laboratory control.

The time-average interfacial concentration (C$_{DGT}$) of solutes accumulated on the binding gel can be calculated (Eq 5.1) (Lehto et al., 2008).

$$C_{DGT} = \frac{m\Delta g}{\varepsilon ADT} \quad\quad\quad (5.1)$$

where m (mg) is the mass of analyte in the binding gel, Δg is the thickness of the diffusive gel

(0.75 mm), ε is the porosity of the agarose diffusion gel (0.9805), A is the area of exposure surface (2.54 cm^2), D (cm^{-2} s^{-1}) is the diffusion coefficient of the individual analyte, and T (s) is deployment time. D values of nine antipsychotic compounds at 21 °C were measured by diffusion cell method in a previous study (Ji et al., 2022b): 5.97×10^{-6} cm^2 s^{-1} for amitriptyline, 4.03×10^{-6} cm^2 s^{-1} for bupropion, 4.98×10^{-6} cm^2 s^{-1} for carbamazepine, 6.02×10^{-6} cm^2 s^{-1} for citalopram, 4.66×10^{-6} cm^2 s^{-1} for clozapine, 3.27×10^{-6} cm^2 s^{-1} for duloxetine, 4.24×10^{-6} cm^2 s^{-1} for fluoxetine, 4.92×10^{-6} cm^2 s^{-1} for lamotrigine, and 3.17×10^{-6} cm^2 s^{-1} for venlafaxine.

5.2.5 Extraction and purification

5.2.5.1 DGT devices

Upon retrieval, DGT devices were thoroughly rinsed with deionized water and immediately disassembled to remove the binding gel that was placed into 25 mL amber glass vials. Then, 50 μL of a 1 mg L^{-1} internal standard solution was added to each vial, followed by the addition of 10 mL methanol, and the vials were ultrasonically extracted for 10 min and this procedure was repeated three times. Combined extracts were reduced to dryness under nitrogen gas, reconstituted in 1 mL of methanol, and filtered through 0.2 μm polytetrafluoroethylene (PTFE) syringe filters (Waltham, MA) into a 2 mL LC vial prior to instrumental analysis.

5.2.5.2 Worms

Frozen samples of worms were lyophilized, spiked with 50 ng internal standards, thoroughly ground with quartz sand, and then ultrasonically extracted with 10 mL of 50:50 (v: v) methanol: dichloromethane for 25 min ($\times$ 3). The extract was centrifuged at 1280 $\times g$ for 8 min and the

supernatant was pipetted to another glass tube. The collected extracts were eluted with 500 mL

HPLC-grade water. Strata-X SPE cartridges (30 mg, Phenomenex, CA) were preconditioned

with 5 mL methanol and 10 mL (methanol: dichloromethane, 50:50), followed with 10 mL

HPLC-grade water, after which the cartridge was loaded with the diluted solution (pH was

adjusted to ~7) under vacuum. After loading, 5 mL of HPLC-grade water was used to wash the

cartridge. Afterward, the thoroughly dried cartridge was eluted with 5 mL methanol three times,

followed by the concentration of nitrogen gas, and reconstituted in 1 mL methanol. Final

reconstituted solutions were filtered through 0.2 μm PTFE filters before instrumental analysis.

5.2.5.3 Water

Samples of water were collected twice a day with a time interval of approx. 12 h until the

last day of the experiment. A volume of 950 μL of water samples was pipetted from the upper

layer of each space, fortified with 50 μL of a 1 mg L^{-1} internal standard solution, and filtered

through a 0.2 μm PTFE filter before instrumental analysis.

5.2.5.4 Sediments

Before retrieval of DGT devices, a small fraction of sediment (~ 0.5-1 g, wet weight) adjacent

to DGT devices was sampled. The sampled sediments were drained for 2 h to reach maximum

water holding capacity (Priha and Smolander, 1999) and then immediately centrifuged at 1280

$\times g$ to obtain sediment porewater. Porewater, spiked with internal standards was diluted by

HPLC-water, concentrated through SPE cartridge, and finally reconstructed in 1 mL methanol

as described above. Afterward, wet sediments were extracted by shaking for 1 h with 2 M KCl

(sediment-to-solution ratio of 1:5) for dissolved organic carbon (DOC) (Jones and Willett,

2006). The solution samples were analyzed for DOC content by a TOC analyzer (Bureau Veritas Laboratory, Edmonton, AB). The remaining sediments were lyophilized and weighed, and sequential extraction was conducted as follows (*i*) methanol shaking for fast–desorbing fraction, (*ii*) 50:50 methanol: dichloromethane with ultrasound for stable–adsorbing fraction, and (*iii*) alkaline hydrolysis at 80 °C for bound-residues fraction. The details of the sequential extraction method are described in our previous study (Ji et al., 2022c).

5.2.6 Instrumental analysis and data processing

Nine antipsychotic compounds were analyzed in the reconstituted samples in methanol spiked with internal standards by a Vanquish UHPLC equipped with a reversed-phase Kinetex 1.7 μm XB-C18 LC column (100 × 2.1 mm) (Phenomenex, Torrance, CA) and Q-Exactive[TM] HF Quadrupole-Orbitrap[TM] hybrid mass spectrometer (Thermo-Scientific, MA, USA). The nine antipsychotic compounds and their isotope-labelled internal standards for analysis were described in detail during previous studies (Ji et al., 2022b, c). Analytical methods have been presented previously (Ji et al., 2022b, c).

Chromatographic peaks of analytes were automatically identified (mass tolerance 5 ppm, minimum data points to 6) and integrated by the ICIS algorithm of TraceFinder (version 4.1, Thermo-Fisher). Integrations of all peaks were manually checked. Quantification followed in the isotope dilution approach, where internal standards matched to each analyte were used. The linear calibration curves (1/x-weighted) were created using fitting analyte concentrations (x) against response ratios (y) of STD to IS peak area without constraining the fit through zero.

Worm uptake, diffusion-induced transport, and fraction transfer models were calculated from

triplicate samples using Matlab R2019b. A genetic algorithm was used for model calibration. The DIFS model was solved by an executable program previously developed by Harper et al. (2000). The nonparametric Kruskal-Wallis H test was conducted for statistical comparison between samples since the majority of data followed strongly skewed distributions.

5.2.7 Numerical model

In the present study, four numerical models were used to quantify the uptake of antipsychotic compounds by worms, diffusion-induced transport, fractions transfer, and the DIFS model for the labile pool size (**Figure 5.1b**).

5.2.7.1 Accumulation by worms

L. variegatus does not preferentially consume the organic compounds that are bound mostly to sediment clays and organic carbon because the worm has significant sediment avoidance (Keilty et al., 1988; White and Keilty, 1988; Kukkonen and Landrum, 1994) and the significant accumulation of organic compounds from sediment porewater (Kukkonen and Landrum, 1994). Therefore, the accumulation of antipsychotic compounds by worms can be assumed to be the result of mostly passive uptake of the dissolved fraction. Theoretically, the accumulation of antipsychotic compounds can be determined with the difference between the total uptake and depuration in worms, which can be expressed as Eq. (5.2).

$$\frac{dC}{dt} = \frac{p_a(t) \times V_S}{m(t)} - k_{pl} C \qquad (5.2)$$

where C is the concentration of antipsychotic compounds in worms (ng g^{-1}), $p_a(t)$ (ng cm^{-3} day^{-1}) is the mass of antipsychotic compounds removed per unit time in a unit sediment by DGT

devices, $m(t)$ is the total mass of triplicate worms from each space at time t (day), V_S (cm^3) is

the volume of sediment in each space of glass tank, and k_{pl} (day^{-1}) is the depuration rate constant

of antipsychotic compounds in worms. The details of the derivation procedure are presented in

Appendix 9.

5.2.7.2 Diffusion-induced transport

The dissolved fraction of organic contaminants is a vital driver of the bioavailability of

chemicals to organisms in sediment (Simpson et al., 2016). The component of this dissolved

fraction reaches the reversible equilibrium between the adsorbed fraction from the

porewater–sediment interface (C_{labile}), and the mobilization of organic compounds into

sediment porewater. The dissolved fraction of organic contaminants can be transported along

solubilization gradients, which result from sediment DOC (Yamamoto et al., 2003; Cheng et

al., 2020). Generally, the transport process of solutes in sediment porewater can be expressed

by an advection-dispersion equation. In this study, water flow caused by bioturbation was

considered negligible. Therefore, the transport of antipsychotic compounds in sediments can be

described by the diffusion equation (Eq 5.3).

$$ b_w \frac{\partial(\theta F_w)}{\partial t} = D_w f \frac{\partial^2(\theta F_w)}{\partial x^2} - \theta k_{\deg} F_w \qquad (5.3) $$

where b_w is sediment buffer power for antipsychotic compounds, which was obtained from the

sorption curve of antipsychotic compounds in sediments (**Figure A15**) obeying the Freundlich

adsorption isotherm (**Figure A16**), θ is water content, F_w is the concentration of dissolved

antipsychotic compounds in sediment porewater, f is the diffusion impedance factor for

sediments (Bhadoria et al., 1991), and k_{deg} is the first-order microbial degradation rate for

antipsychotic compounds in sediments (day^{-1}).

Changes of DOC in sediments can influence the solubility of antipsychotic compounds in sediment porewater and thus the influence of DOC on the solubility of antipsychotic compounds should be considered. The modified transport of antipsychotic compounds in sediments can be depicted as Eq. (5.4).

$$b_w \theta \frac{\partial (F_w - \lambda C_{DOC})}{\partial t} = D_w f \frac{\partial^2 (\theta F_w)}{\partial x^2} - \theta k_{\deg} F_w \qquad (5.4)$$

where λ is antipsychotic compounds–DOC interaction coefficient in the sediment, and C_{DOC} (mg L^{-1}) is the concentration of DOC in sediment porewater. Considering the decomposition of DOC in sediment porewater obeying first-order kinetics, the concentration of DOC can be described following a diffusion formula including a term of a first-order degradation (Eq 5.5):

$$b_{DOC} \frac{\partial (\theta C_{DOC})}{\partial t} = D_{DOC} f \frac{\partial^2 (\theta C_{DOC})}{\partial x^2} - \theta k_{DOC} C_{DOC} \qquad (5.5)$$

where b_{DOC} is sediment buffer power for DOC, D_{DOC} is the diffusion coefficient of DOC in sediment porewater, and k_{DOC} is the constant rate of DOC decomposition. The derivative processes (Eqs 5.3–5.5) (**Appendix 10**). The parameters and processes for calculating the solubilization of antipsychotic compounds by DOC are summarized in **Text A11** and **Figure SA17**.

5.2.7.3 Fractions transfer

Based on the fractions transfer modeling used before (Cheng et al., 2019; Ji et al., 2022c), the modified model with diffusion-induced fractionation can be described (Eqs 5.6–5.8):

$$\frac{dC_{labile}}{dt} = -k_{fs} C_{labile} - k_{sb} C_{labile} + k_{sf} C_{stable} + k_{bs} C_{bound} + b_w \theta \frac{\partial (F_w - \lambda C_{DOC})}{\partial t} \qquad (5.6)$$

$$\frac{dC_{stable}}{dt} = -k_{sf}C_{stable} - k_{sb}C_{stable} + k_{fs}C_{labile} + k_{bs}C_{bound} \qquad (5.7)$$

$$\frac{dC_{bound}}{dt} = -k_{bs}C_{bound} - k_{bs}C_{bound} + k_{sb}C_{labile} + k_{sb}C_{stable} \qquad (5.8)$$

where C_{labile}, C_{stable}, and C_{bound} (μg kg^{-1}) are the concentrations of labile (fast-desorbing) faction,

stable-adsorbing fraction, and bound-residues fraction of antipsychotic compounds in

sediments, respectively, k (day^{-1}) is the rate constant of compound transfer between different

fractions, and subscript f, s, and b represent fraction of fast-desorbing, stable-adsorbing, and

bound-residues, respectively.

5.2.7.4 DIFS model

An indicator for the degree of sediment porewater concentrations depleted at the DGT

interface, R, can be described as the ratio of C_{DGT} to the initial sediment porewater ($C_{porewater}$),

which depends on deployment time (Eq 5.9) and is an important parameter in the DIFS model.

The DIFS model can quantify the dependence of R on the resupply of analytes from the solid

phase to porewater combined with a supply from diffusion in the sediment to the interface,

which also passes through the diffusion layer to the ultimate sink in the binding layer, and is

modeled by Fick's second law (Ernstberger et al., 2005; Sochaczewski et al., 2007). The

adsorption-desorption kinetics can be determined by the equilibrium distribution coefficient,

K_{dl} (Eq 5.10), and the response time, T_c, (Eq 5.11) to simulate labile pool size and constant rate

of adsorption (k_1) and desorption (k_{-1}). K_{dl} is the distribution coefficient of the labile analyte that

can be exchanged with the sediment porewater and represents the labile pool size in the solid

phase. T_c represents the response time to depletion and is associated with resupply processes of

desorption kinetics.

$$R(t) = \frac{C_{DGT}(t)}{C_{porewater}} \quad (5.9)$$

$$K_{dl} = (\frac{C_{labile}}{C_{porewater}})_{eq} = \frac{k_1}{P_c k_{-1}} \quad (5.10)$$

$$T_c = \frac{1}{k_{-1} + k_1} = \frac{1}{k_{-1}(1 + K_{dl}P_c)} \quad (5.11)$$

Based on the model of operation, T_c and k_{-1} can be estimated by fitting R versus time. P_c is the particle concentration of the sediment ($P_c = m/V$, where m is the total mass of solid sediment and V is porewater volume in the total volume of sediment). C_{labile} was equal to the equilibrium concentration of fast-desorbing fraction using a first-order three-compartment kinetic model (Ji et al., 2022c). The key parameters used in the DIFS model are presented (**Table A2**).

5.2.7.5 Benthic boundary layer model

Fluxes at the interface of sediment and water were obtained by the benthic boundary layer model (Higashino et al., 2008; Mustajärvi et al., 2017). The transport of antipsychotic drugs in the boundary layer (between overlying water and sediment) contained diffusion exchange of dissolved fraction between surface water and sediment porewater, DOC-induced diffusion transport, and bioturbation (i.e., biodiffusion caused by worms). The flux can be determined (Eq 5.12):

$$F = k_w \cdot (C_{pw} - C_w) \quad (5.12)$$

where F (ng cm^2 day^{-1}) represents the flux, C_{pw} represents the concentration of antipsychotic compounds measured in the DOC adsorbed in sediment porewater, k_w represents the overall mass transport coefficient (m s^{-1}), and C_w represents the concentration of antipsychotic compounds in the water. C_{pw} was corrected by water–DOC fractional distribution constant ($a_w =$

$(1+K_{DOC}C_{DOC}))$ derived from D_{OW} (the ratio of the summed concentration of chemical species in octanol to the summed concentration of chemical species in water) to estimate k_{DOC} (L kg^{-1}). k_{DOC} was estimated by DOC−water distribution constant (k_{DOC}=0.4 D_{OW}).

The overall sediment−water mass transport coefficient can be characterized by Eq. (5.13).

$$\frac{1}{k_w} = \frac{1}{k_{LW} + k_{LDOC}k_{DOC} \cdot C_{DOC}} + \frac{1}{k_{LBio}} \quad (5.13)$$

where k_{LW}, k_{LDOC}, and k_{LBio} are the mass transport coefficients of each antipsychotic compound dissolved in water, DOC-associated, and bioturbation, respectively. Mass transport coefficients were estimated as $k_{LDOC} = 0.02\ k_w$, and $k_{LBio} = C_{sediment}/C_{pw}\lambda_{bio}$, (ter Laak et al., 2009; Kupryianchyk et al., 2013). $\lambda_{bio} = h/D_b k_d \rho_b$ where h (m) is the mean bioturbation depth in the sediment, D_b (m^2 d^{-1}) is a biodiffusion coefficient, k_d (L kg^{-1}) is the sediment-to-water partition coefficient, and ρ_b is the dry density of the particles (Thibodeaux et al., 2001). The value of λ_{bio} was taken as 9.57×10^8 s L kg^{-1} m^{-1} (Foster and Leahigh, 2021).

5.2.7.6 Quality assurance and quality control

All organic solvents were HPLC grade, and all glassware was pre-ashed at 550 °C for 5 h before use. After spiking sediment, 5 g of triplicate samples were randomly chosen from each space and followed the extraction and purification processes for stable-adsorbing fraction (section 2.5.4), showing that the variation coefficient was lower than 15% for both 1 and 10 mg kg^{-1} spiked sediments (**Table A15**).

The standard solution of antipsychotic compounds at 50 μg L^{-1} was run in the middle of the sample sequences for each run, and the RSD was lower by 20%. The limit of detection (LOD) for nine antipsychotic compounds, determined by 3 times the S/N ratio, ranged from 0.12 to

1.38 μg L^{-1} (**Table A15**). The method detection limit (MDL) for the measurement of DGT, worm, sediment, and water samples, and limits of quantitation (LOQ) are shown in **Table A16**. The recovery of nine antipsychotic compounds during the procedure from DGT extraction, worm tissue extraction, and SPE enrichment to final reconstitution was all acceptable (**Table A17**). During the instrumental analysis, each sequence created in Xcalibur 4.3 (Thermo-Scientific) includes solvent blanks, matrix blanks, matrix spikes (50 μg L^{-1}), and two solvent blanks were inserted every five samples. The detection of analytes in solvent blanks and matrix blanks were below LODs, and the results of matrix spikes were within reasonable range (**Table A18**).

5.3 Results

5.3.1 Fluxes of antipsychotic compounds at the sediment-water interface

During the incubation period of 30 days, the differences in fluxes for all antipsychotic compounds between the two spiked concentrations were < 5% (**Figure A18**). Lamotrigine and bupropion showed positive fluxes from sediment porewater to surface water during all experiments, whereas negative fluxes were observed for other compounds after 9 days. The fluxes of lamotrigine and carbamazepine increased first and declined until day 30. Lower fluxes (0.22–0.44 ng cm^{-2} day^{-1}) on day 1 were observed for bupropion, clozapine, duloxetine, citalopram, and venlafaxine, which reached an equilibrium between water and sediments with fluxes of ~ -0.01 to -0.08 without significant differences ($p > 0.05$) after 3 days.

5.3.2 Uptake of antipsychotic compounds by worms

Concentrations of antipsychotic compounds in sediment porewater and worms at 1 mg kg^{-1} and 10 mg kg^{-1} spike levels at each sampling time followed the same pattern (**Figure A19**). For 1 mg kg^{-1} spiked sediments, mean concentrations (ng mg^{-1}) of antipsychotic compounds accumulated by worms during the 30-day experiment ranged from 1.30 ± 0.17 (lamotrigine) to 6.27 ± 0.84 (amitriptyline). Higher mean concentrations (ng mg^{-1}) were detected in worms exposed to 10 mg kg^{-1} spiked sediments, ranging from 26.77 ± 3.53 (lamotrigine) to 68.51 ± 4.13 (duloxetine).

Generally, greater accumulation of most antipsychotic compounds by worms was found for both spiked sediments, followed by a stable level, except for citalopram, fluoxetine, amitriptyline, and venlafaxine, and a decline was found at day 3 followed by the stable trend for amitriptyline and venlafaxine.

5.3.3 Diffusion-induced fraction transfer

The transfer of labile, stable-adsorbing, and bound-residues fractions of antipsychotic compounds in sediments during incubation is presented in **Figure 5.2**, shown as the percentages of the remaining concentrations of antipsychotic in sediments. Due to their low tolerance for the hydrolysis process using 1 M NaOH solution, bupropion and duloxetine were not included in the fraction transfer model (Ji et al., 2022c). The residual concentrations of antipsychotic compounds and DOC concentrations on day 30 were plotted together in **Figure A20a**, including the positive correlation between labile concentrations of citalopram, amitriptyline, and venlafaxine, and DOC concentrations (**Figure A20b**).
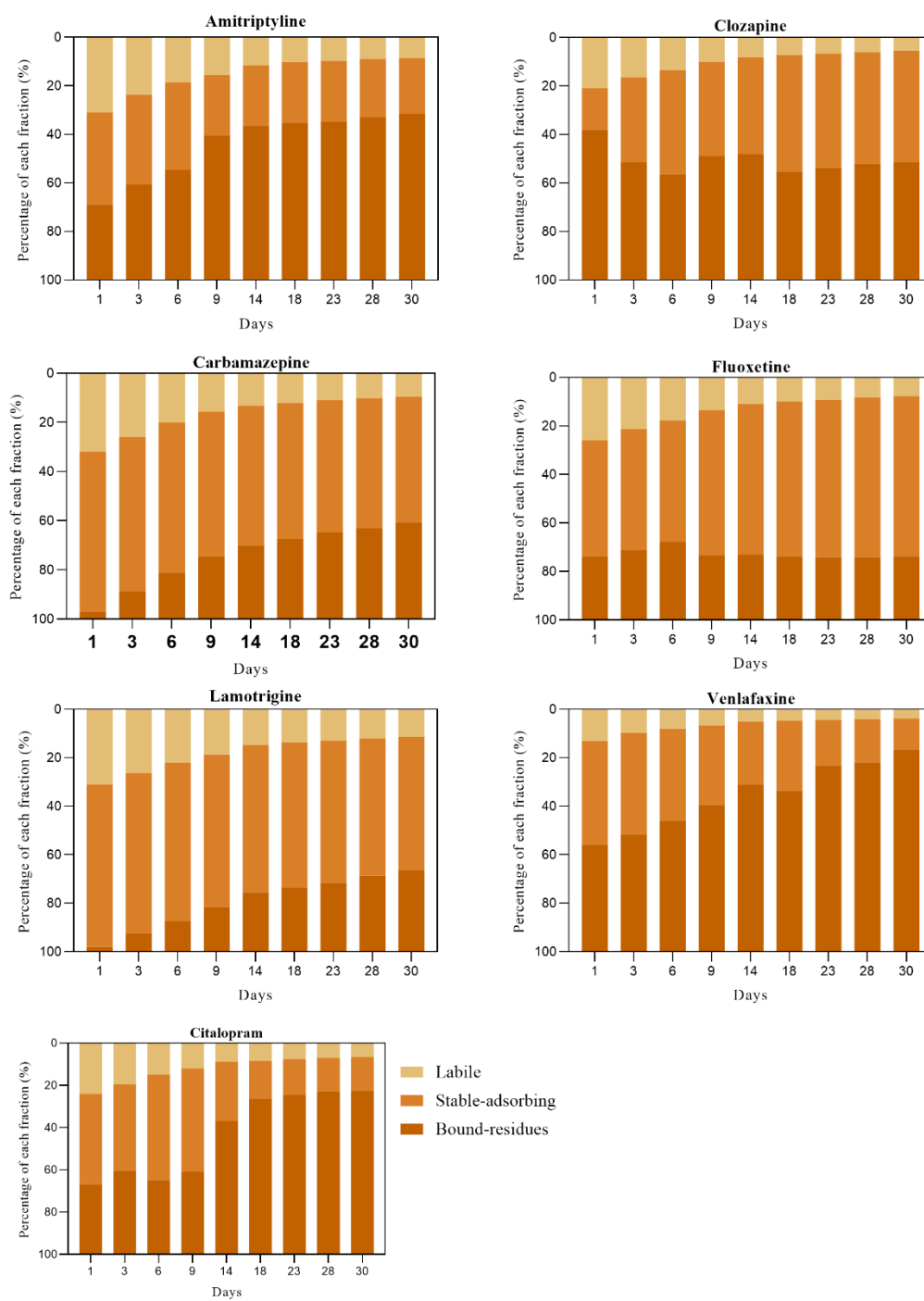
Figure 5.2 The dynamic labile, stable-adsorbing, bound-residues fractions of antipsychotic during the whole incubation experiment. The error for these percentages was less than 5%.

5.3.3.1 Labile fraction

In spiked sediments, the labile fraction of antipsychotic compounds decreased gradually within 30 days: amitriptyline (31% to 9.8%), carbamazepine (32% to 9.4%), citalopram (24% to 5.6%), clozapine (21% to 5.8%), fluoxetine (26% to 7.2%), lamotrigine (31% to 8.3%), and venlafaxine (13% to 3.3%). Correspondingly, labile concentrations (μg kg^{-1}) also decreased for these compounds.

5.3.3.2 Stable–adsorbing fraction

The stable-adsorbing fraction of most antipsychotic compounds decreased during the incubation time, whereas clozapine and fluoxetine showed an increasing trend. The order of decease for stable-adsorbing fraction during 30 days showed venlafaxine (43% to 13%) > citalopram (43% to 27%) > amitriptyline (38% to 23%) > lamotrigine (67% to 55%) > carbamazepine (65% to 54%). The stable-adsorbing fraction of clozapine and fluoxetine increased from 17% to 46% and 48% to 66%, respectively.

5.3.3.3 Bound–residues fraction

Formation of bound-residues fraction increased for from for amitriptyline (31%−66%), carbamazepine (3%−37%), citalopram (33%−77%), lamotrigine (2%−36%), and venlafaxine (43%−83%). Specifically, fluoxetine was increasingly transferred to bound-residues fraction from 26 to 33% on day 6, followed by a decrease to 26% on day 23, which was similar to the initial fraction in sediments. Moreover, the bound-residues fraction of clozapine showed a rapid increase from day 1 to day 23 (17% to 47%).

5.3.4 Modeling fitting

Measured concentrations of antipsychotic compounds passively adsorbed by DGT devices were fitted to the worm uptake model for the total accumulated antipsychotic compounds in worms (R^2 = 0.83–0.95, **Figure 5.3a**). Depuration rate constants of antipsychotic compounds in worms (k_{pl}) after 30 days of incubation were estimated at 0.007 day^{-1} (lamotrigine) – 0.035 day^{-1} (amitriptyline). The total mass of chemicals accumulated by worms was estimated to be 70 ng (lamotrigine) to 320 ng (amitriptyline), representing 0.45% to 0.60% removal of antipsychotic compounds from the spiked sediments.

Diffusion-induced transport of antipsychotics fitted well against the observed concentrations (R^2 = 0.99 to 0.96) (**Figure 5.3b**). The rate of degradation (k_{deg}) after 30 days was calculated to be 0.14 day^{-1} (fluoxetine) to 0.26 day^{-1} (bupropion).
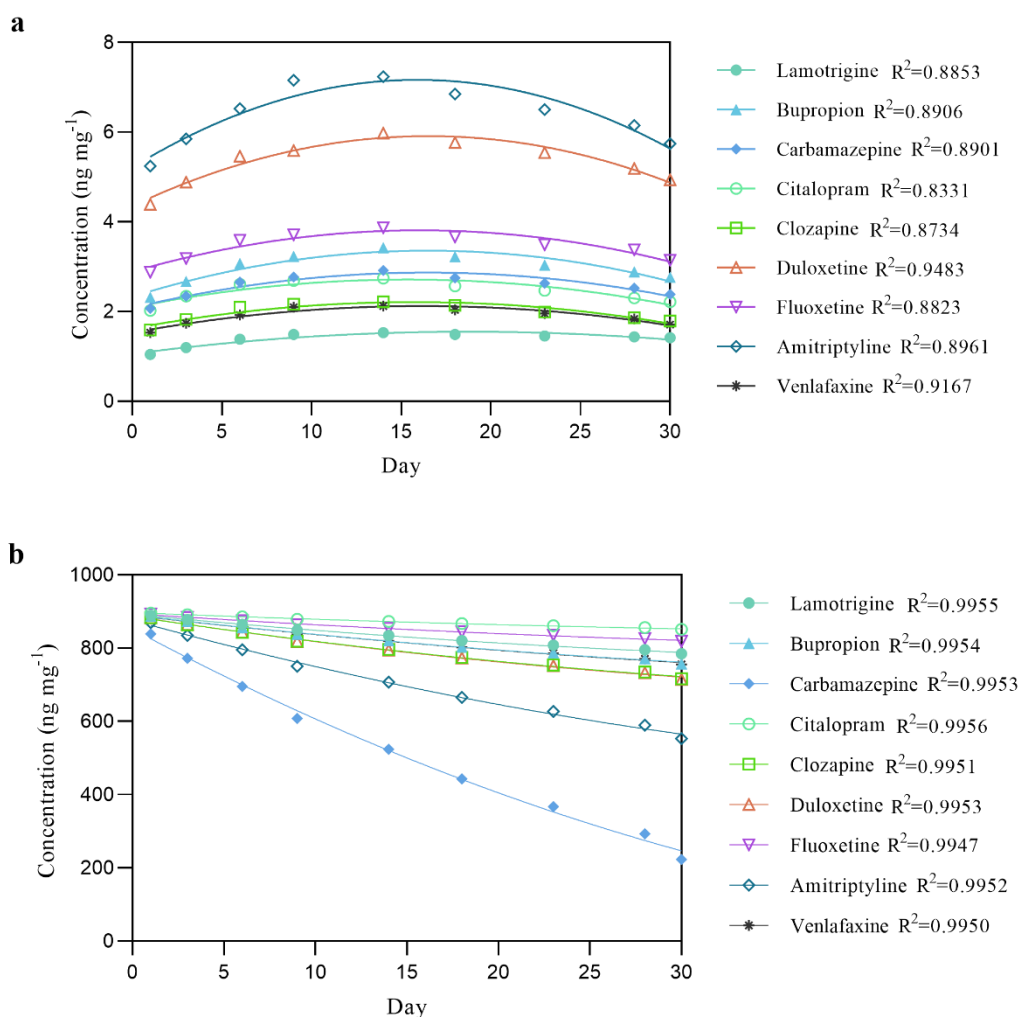
Figure 5.3 Simulation results of (a) the worm uptake of antipsychotic compounds, and (b) residual concentrations of antipsychotic compounds. Discrete circles represent experiment data, and lines represent model simulations.

The fraction transfer model fitted reasonably well according to R^2 values ranging from 0.79 to 0.98 (**Figure 5.4**). Relatively poor fits were observed for the stable-adsorbing fraction and bound-residues fraction of citalopram ($R^2 = 0.53$ and 0.59, respectively), and bound-residues fraction of amitriptyline ($R^2 = 0.57$). The modeled transfer rate coefficients (k) on day 14 are presented in **Table 5.1**. The estimated k_{sf} and k_{bf} (day^{-1}) values during 14−30 days were statistically distinguishable ($p < 0.05$) for all antipsychotic compounds. A significant increase in k_{sf} value from 0.00085 to 0.041 was observed for amitriptyline during 14−30 days. Generally,

transfer to the labile fraction (k_{sf} and k_{bf}) became greater on day 30, which was similar for transfers to the stable-adsorbing fraction and bound-residues fraction (**Figure 5.5a**). For example, the stable-adsorbing fraction of carbamazepine transferred 17% to the labile fraction, while the labile fraction transferred 25% of that to bound-residues. Other antipsychotic compounds showed labile fraction transferred 10%–41% and 4%–41% to stable-adsorbing fraction and bound-resides fraction, respectively.
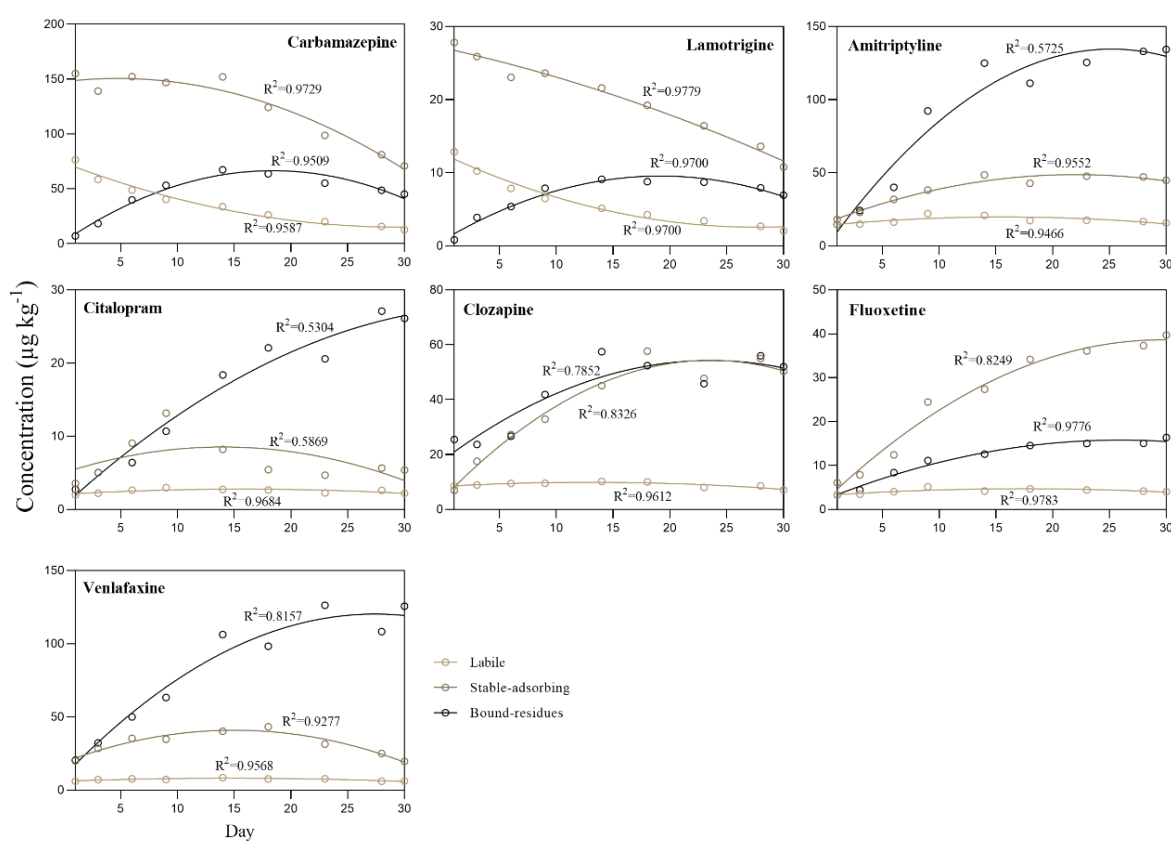
Figure 5.4 Comparison of simulated and experimental data for the labile, stable-adsorbing, and bound-residues fractions of antipsychotic compounds in sediments during incubation experiment. Discrete circles represent experimental data, and lines represent model simulations.

Table 5.1 Rate constant (day^{-1}) of fractions transfer for antipsychotic compounds on the 14th and the 30th day of incubation experiment.

	Amitriptyline		Carbamazepine		Citalopram		Clozapine		Fluoxetine		Lamotrigine		Venlafaxine	
	14 days	30 days	14 days	30 days	14 days	30 days	14 days	30 days	14 days	30 days	14 days	30 days	14 days	30 days
k_{fs}	4.25E-04	3.93E-03	1.27E-02	7.14E-02	7.13E-04	3.43E-03	6.57E-04	3.76E-03	3.28E-04	2.20E-03	4.02E-04	2.56E-03	1.21E-04	7.39E-04
k_{sf}	8.47E-04	4.14E-02	1.34E-03	7.88E-03	8.58E-04	5.25E-03	7.94E-04	5.87E-03	5.36E-04	3.63E-03	6.32E-04	4.05E-03	2.31E-04	1.49E-03
k_{fb}	7.42E-05	4.68E-04	1.82E-04	9.57E-04	1.11E-04	4.68E-03	7.92E-04	5.14E-03	3.73E-05	9.16E-03	7.08E-05	3.09E-04	1.96E-05	1.15E-04
k_{bf}	8.46E-05	3.81E-04	8.84E-05	5.35E-04	4.34E-04	2.00E-03	3.42E-04	2.19E-03	8.25E-05	3.60E-04	7.14E-05	4.28E-04	2.59E-05	1.30E-04
k_{sb}	1.38E-03	6.90E-03	1.61E-03	9.37E-03	9.76E-05	2.82E-04	4.35E-05	3.08E-04	1.25E-03	1.12E-03	1.30E-03	6.72E-03	2.90E-04	1.97E-03
k_{bs}	8.39E-03	4.96E-02	2.34E-03	1.32E-02	5.31E-04	2.52E-03	3.79E-04	2.71E-03	6.93E-03	3.77E-02	9.71E-03	4.23E-02	1.63E-03	1.17E-02
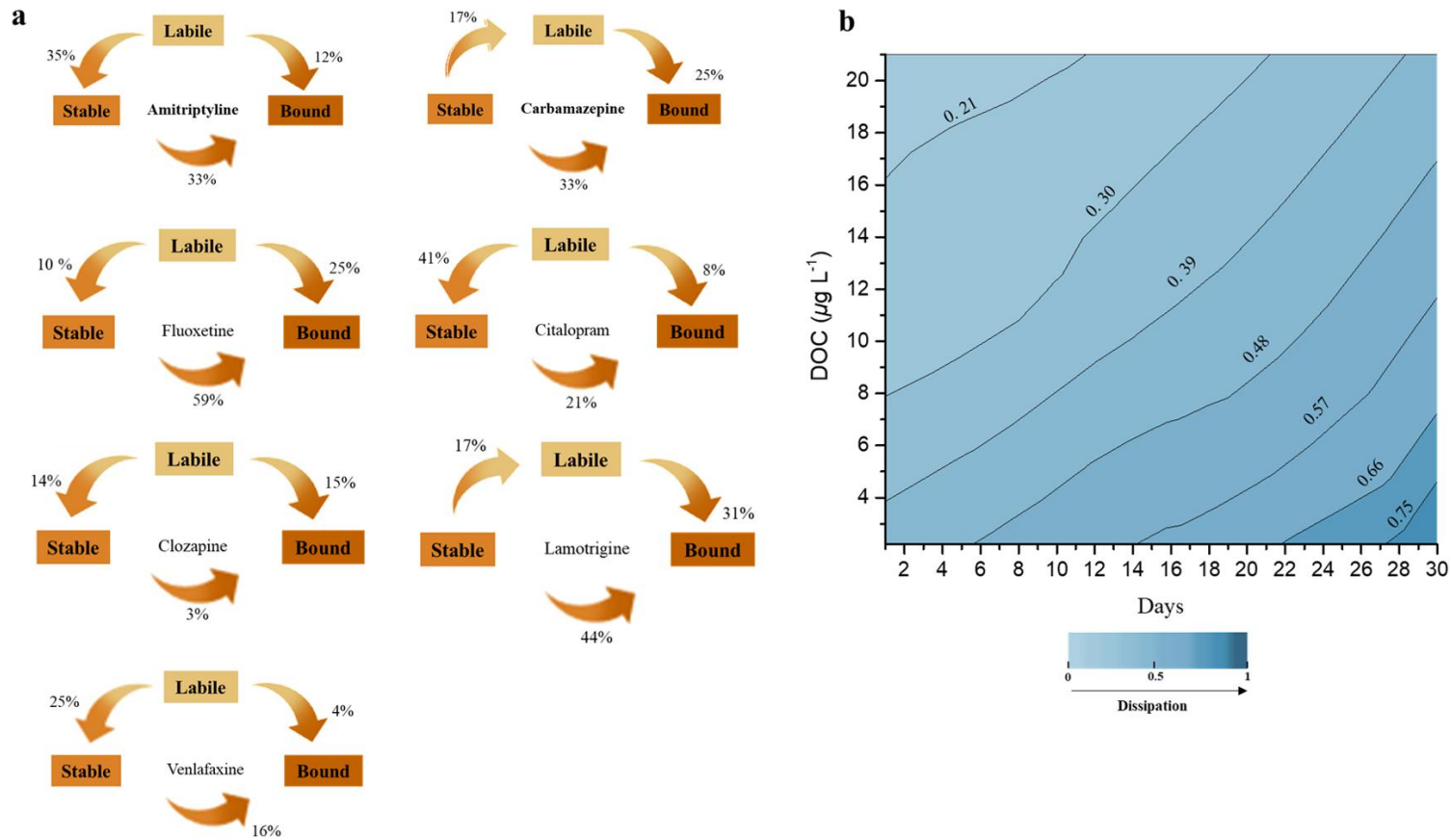
Figure 5.5 Simulation results of (**a**) transfer direction of antipsychotic compounds fractions in sediments and (**b**) dissipation rate of total antipsychotic compounds in sediments shown as a contour map where the values represent dissipation rate (from diffusion, degradation, and uptake by worms).

5.3.5 DIFS modeling results

To obtain the dynamic kinetics of resupply from the sediment particles to porewater of these antipsychotic compounds, experimental data were fitted by the DIFS model, and measured R (the ratio of C_{DGT} to the sediment porewater concentration) was plotted against each sampling time for individual antipsychotic compounds (**Figure 5.6**). Two parameters, the response time (T_c) and the partition coefficient (K_{dl}), were derived from the best fit of R against deployment time through the DIFS model (**Table A2**).

Generally, all compounds followed an initial steep decrease of R values followed by a slower decline to reach a relatively constant value. The largest R values were found for carbamazepine (0.33) followed by lamotrigine (0.32). The least changes in R values at the end of deployment time were observed for amitriptyline and venlafaxine, with a decline of 25% and 37%, respectively.

An estimate of K_d was obtained from the ratio of labile concentration (the equilibrium-reached concentration using consecutive extraction for the labile fraction) to sediment porewater concentrations. Apparently, the K_{dl} values were greater, by a factor of 4 to 511 ($p < 0.05$) than the K_d values for carbamazepine, lamotrigine, clozapine, citalopram, fluoxetine, bupropion, and amitriptyline, whereas K_{dl} values of venlafaxine and duloxetine were close to those values of K_d ($p > 0.05$). The T_c value (s) of venlafaxine (1.33×10^6) was one magnitude higher than that of other antipsychotic compounds ($2.03 \times 10^5 - 7.17 \times 10^5$). The other two DIFS-model derived values of adsorption (k_1) and desorption (k_{-1}) rate constants (s^{-1}) showed that k_1 values ($1.11 \times 10^{-8} - 6.10 \times 10^{-7}$) were greater than k_{-1} values ($7.43 \times 10^{-7} - 2.97 \times 10^{-6}$) for most

185

compounds except slightly greater k_{-1} values than k_1 values for carbamazepine and lamotrigine

(**Table 5.2**).

Table 5.2 Output parameters of antipsychotic compounds in sediments from DIFS-model fits.

	K_d (cm^3 g^{-1})	K_{dl} (cm^3 g^{-1})	T_c (s)	k_{-1} (s^{-1})	k_1 (s^{-1})
Carbamazepine	26.26	0.51	1.03×10^6	5.53×10^{-7}	4.21×10^{-7}
Lamotrigine	17.57	0.47	1.03×10^6	5.28×10^{-7}	4.39×10^{-7}
Venlafaxine	0.03	0.01	1.33×10^6	1.11×10^{-8}	7.43×10^{-7}
Clozapine	5.98	0.12	4.14×10^5	5.61×10^{-7}	1.85×10^{-6}
Citalopram	4.83	0.08	3.97×10^5	4.38×10^{-7}	2.08×10^{-6}
Fluoxetine	10.22	0.02	3.62×10^5	1.03×10^{-7}	2.66×10^{-6}
Bupropion	8.67	0.08	2.79×10^5	6.10×10^{-7}	2.97×10^{-6}
Duloxetine	0.23	0.21	7.17×10^5	4.81×10^{-7}	9.14×10^{-7}
Amitriptyline	0.30	0.07	3.95×10^5	4.05×10^{-7}	2.13×10^{-6}

K_d values were obtained from concentration of labile antipsychotic compounds determined by the equilibrium-reached concentration using consecutive extraction for fast-desorbing fraction.
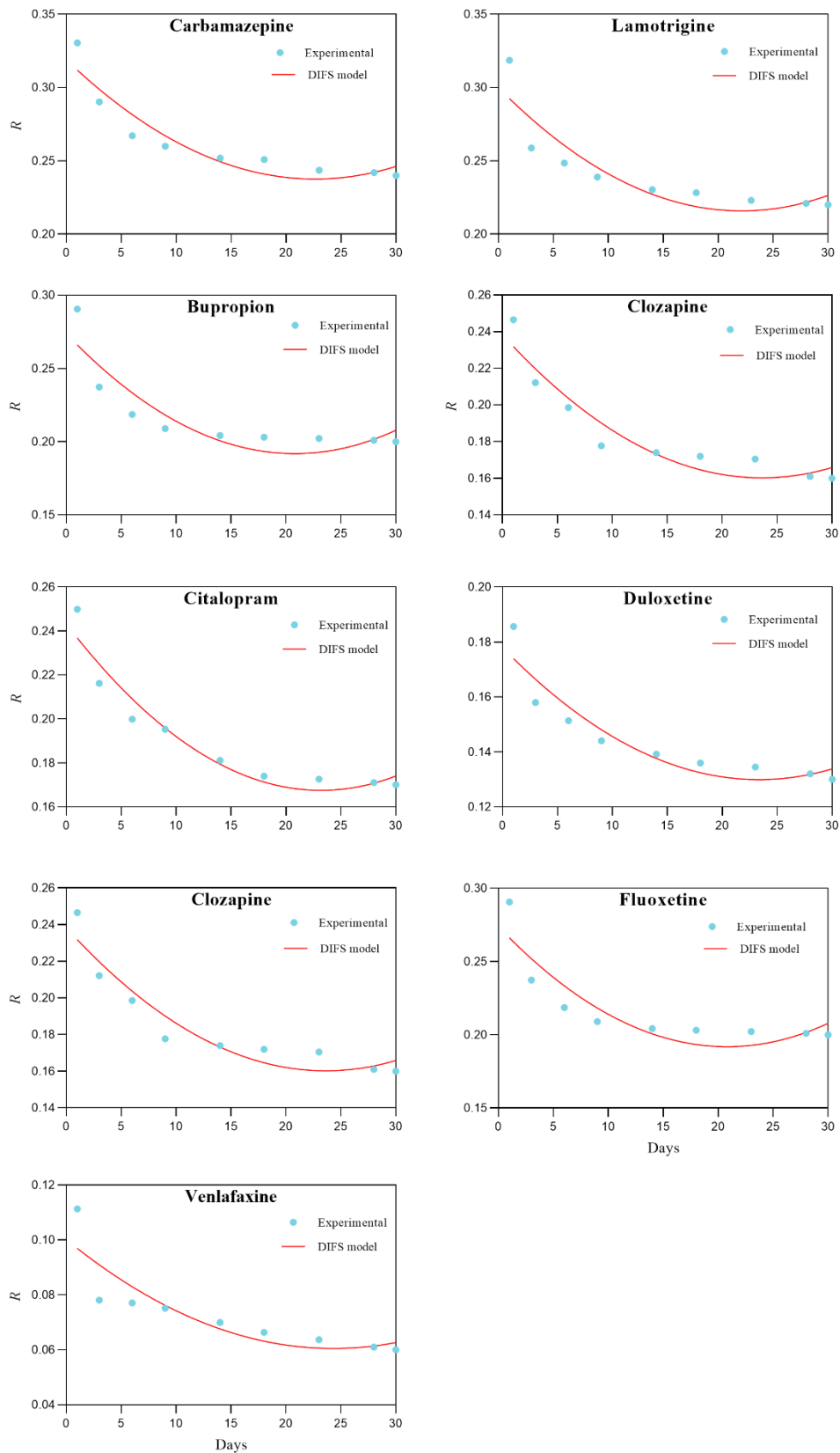
Figure 5.6 Dependence of measured values of R for antipsychotic compounds in sediments with the deployment time. The lines represent the best fits using the DIFS model.

5.4 Discussion

5.4.1 Vertical transport of antipsychotic compounds

All antipsychotic compounds could rapidly escape from sediments during the first day (**Figure A18**), which is consistent with the highest concentration in sediment porewater from the initial time (**Figure A19**). The two more hydrophilic compounds, i.e., lamotrigine and carbamazepine, revealed significantly greater positive fluxes compared to the other compounds ($p < 0.05$), indicating the ability to supply these compounds from porewater to surface water was adequate. Interestingly, a similar magnitude of fluxes was observed for all compounds during 30 days of incubation ($p > 0.05$), indicating that the saturation of compounds in sediment porewater was not only determined by the concentrations of compounds in sediments, especially for ionizable compounds that are expected to interact extensively with sediments. Foster and Leahigh (2021) found that both positive and negative fluxes at the sediment−water interface were observed at different sites of natural rivers for bupropion and venlafaxine, and only negative fluxes were observed for carbamazepine and fluoxetine (only detected in one site). This may be due to the instantaneous condition at the sampling sites, whereas our study experienced a transition from an initially unstable status to a stable environment between water and sediments. However, the sorption of organic compounds to solid phases in sediments is a complex process driven by several potential mechanisms, especially for the positively charged antipsychotic compounds at environmental pH (Martínez-Hernández et al., 2014). Mineral sorption may be an important controlling factor for ionizable chemicals in sediments (Delle Site, 2001). Among the antipsychotic compounds, eight (except for amitriptyline) have more

than one proton donor/ acceptor site which may be prone to multiprotic cationic speciation in a neutral pH environment. Although our data showed that most compounds were bound more tightly to sediments with increasing incubation time, the clay content (11%) was not high in the sediments used in our study. Our results were similar to a previous study where the sorption of hydrophobic compounds was high due to hydrophobic and electrostatic interactions (Karlsson et al., 2016). Meanwhile, hydrological conditions (e.g., water velocity) may play a role in some real environments for the sediment turnover, which may need further investigations.

Bioturbation can also greatly influence the magnitude of fluxes for organic compounds (Kupryianchyk et al., 2013; Sun et al., 2018). When comparing fluxes between spaces with worms and without worms, only a small difference (< 2%) was observed. The mass transfer coefficients between sediment porewater and overlying water through a stagnant thin film at the interface can be estimated through $k_{LW} = D_w/\delta_w$ with the method reported by Schwarzenbach et al. (2017). The thickness of a boundary diffusion layer (δ_w) of 700 μm was used in the flux calculation, which was estimated by Eek et al. (2010) through alabaster plate diffusion *in situ* experiments in harbor sediments. The value was similar to the determined values of 642 μm by using gypsum dissolution in sediment cores for N and P fluxes from a natural lake (Anthony and Lewis, 2012). The errors derived from our estimated fluxes by using Sobol Global Sensitivity Analysis (Sarrazin et al., 2016) for K_w value varied from 8% to 25%. Therefore, the fluxes estimated in **Figure A18** can be considered to have an equivalent maximum error of ±25%.

The values of k_w can be used to determine the sorptive tendencies of compounds to sediments (Kupryianchyk et al., 2013; Foster and Leahigh, 2021) and it appeared that the hydrophilic

compounds (lamotrigine and carbamazepine) showed the least sorption to the sediments. However, k_{LDOC} and k_{LBio} were negligible in comparison to k_w and did not contribute significantly to k_w for all selected antipsychotic compounds. Therefore, fluxes at the sediment–water interface were dependent on the magnitudes of diffusion of each compound from sediment particles to porewater, and exchanges between porewater and overlying water.

5.4.2 Worm uptake

The good correlation ($R^2 = 0.89$–0.92, $p < 0.05$) between porewater concentrations and worm concentrations for all compounds showed that uptake of organic compounds by worms might be highly associated with the labile phase of compounds in sediments. A previous uptake experiment of fluoxetine for *L. variegatus* showed a stable concentration in the water phase during 48 h without the parent and any transformation products to *L. variegatus* (Karlsson et al., 2016). In our study, fluoxetine, citalopram, amitriptyline, and venlafaxine also showed no obvious fluctuations of accumulation into *L. variegatus* during all incubation times (**Figure A19**). This observation may be due to the rapid equilibrium of fluoxetine and citalopram reached between the surface and porewater–sediment. Additionally, little degradation (e.g., fluoxetine) ensured stable levels of compounds in porewater (Kwon and Armbrust, 2006) that could be passively absorbed by worms. Passive uptake of organic compounds is believed to be dominated by uptake through the integument (Karlsson et al., 2016). This may account for the initial increasing concentration of lamotrigine, bupropion, carbamazepine, clozapine, and duloxetine.

The increasing order of accumulated concentrations in worms and porewater followed the

Log K_{ow} values for the respective compounds, which is supported by the previous observation that the magnitude of hydrophobicity takes a significant role in playing the uptake of pharmaceuticals into aquatic organisms (Ashauer et al., 2010). Hendriks et al. (2001) used the prediction model based on *Gammarus pulex* and found negligible dietary uptake (less than 2% of total uptake) for 14 organic micropollutants. Although the relationships were not clear among the hydrophobicity of organic compounds, their partitioning in water and sediment materials, and the contribution of dietary uptake, our results showed the capability to adsorb organic pollutants by passive bioaccumulation for sediment-dwelling worms without feeding and with very limited ingestion of organic particles. In 1 mg kg^{-1} spiked sediments, the worm uptake for all compounds was similar (1.30–6.55 ng mg^{-1}) whereas greater worm uptake (9.31–40.46 ng mg^{-1}) was observed in 10 mg kg^{-1} spiked sediments. This may result from the weak base (environment pH $\approx$ 7) of our compounds which are soft electrophiles reacting with cysteine groups in protein, which in turn would hinder the elimination of metabolites when the concentration of these compounds was high enough. Despite our study showed the uptake rate is associated with the hydrophobicity of a chemical, not all compounds with Log $K_{ow} > 3$ showed obviously higher bioconcentration (e.g., fluoxetine and venlafaxine), which is more relevant to the diffusion mechanism from the aqueous phase in sediment to worms for different compounds.

5.4.3 Bioavailability of antipsychotic compounds during fractions transfer

The decreasing labile fraction of all compounds in the first 9 days (**Figure 5.2**) indicates less bioavailability of these compounds in the sediments, corresponding well with the accumulated

concentrations in worms. Good correlations ($R^2 = 0.74$–0.91) between labile concentrations and worm uptake concentrations of antipsychotic compounds were observed, while no correlations were found for other fractions or the residual concentrations in sediments. This implies that the labile fraction in sediments is a better indicator of the bioavailability of organic pollutants for sediment-dwelling invertebrates than total concentrations (Brinkmann et al., 2015; Brinkmann et al., 2021; Müller et al., 2021). The Log K_{ow} values seemed to not be the only factor to influence the labile fraction in sediments, albeit some hydrophilic compounds (e.g., carbamazepine and lamotrigine) had a relatively higher fraction of the labile phase in the initial time. This is also supported by the hydrophobic partitioning of compounds (e.g., citalopram and fluoxetine) may not be the primary mechanism of sediment binding in some cases (Schultz et al., 2010).

The decreased labile fraction can be explained by the variability of the stable-desorbing fraction. The increase of stable-adsorbing fraction for clozapine, carbamazepine, fluoxetine, and lamotrigine may be due to mixed influences of transfer to the labile fraction and consolidation into sediment organic matter as the bound-residues fraction (Li et al., 2013b). As an interim fraction in sediments, the decreasing stable-adsorbing fraction of amitriptyline, venlafaxine, and citalopram might indicate the access of these compounds for worms in sediments was more dependent on transfer between labile and bound-residue fractions. This could be also seen through the lack of obvious increases in uptake by worms for amitriptyline, venlafaxine, and citalopram in both spiked sediments (**Figure A19**). Considering the stable-adsorbing fraction is regarded as a reversible adsorption to sediment particles, amitriptyline, venlafaxine, and citalopram may transition to more persistent bound phases during aging, while

clozapine, carbamazepine, fluoxetine, and lamotrigine may easily form a loosely adsorbed fraction from the labile fraction. Additionally, stable-desorbing fraction was negatively correlated (R^2= 0.88 to 0.93, $p < 0.05$) with the bound-residues fraction for amitriptyline, venlafaxine, and citalopram over 30 days of incubation. This implies that the molecules of amitriptyline, venlafaxine, and citalopram could be sequestrated by the active adsorption sites (Voice and Weber, 1983). Other antipsychotic compounds could be formed as dissolution in porewater to have molecular diffusion in sediment water.

The bound-residues fraction of amitriptyline, citalopram, and venlafaxine were dominant at the end of the experiment. This process can be seen as a net sink for these compounds. However, there was no obvious decrease in the uptake of these compounds by worms. Obviously, the formation of bound-resides for clozapine, carbamazepine, fluoxetine, and lamotrigine was restrained since these compounds seemed to not be strongly sorptive to sediment particles. Generally, the major mechanisms for bound-residues formation of organic compounds entails physical binding in micropores of sediment aggregates, and partitioning and slow diffusion to sediment organic matter (Li et al., 2011). Antipsychotic compounds partitioned into organic matter could be released to the sediment porewater under mineralization, where decomposition of organic matter could occur by microbial activities (Wang et al., 2018). DOC concentrations dropped from 21.00 to 2.21 mg L^{-1} (**Figure A20a**), indicating that amitriptyline, citalopram, and venlafaxine released to porewater with decreasing DOC concentrations due to more hydrophobic compounds bound with organic carbon (**Figure A20b**). The exception of fluoxetine showed a different bonding form rather than only bonding with sediment organic matter. Therefore, it is suggested that enhanced dissipation of different antipsychotic

compounds in sediment is not just an excitation of organic matter decomposition to transfer bound residues to labile fraction for uptake by worms, but also reversible sorption onto sediments as an intermediate phase.

5.4.4 Potential connections between the models

Even though rates of accumulation of the tested compounds by *L. variegatus* are unknown, this experiment was designed for non-feeding exposure to achieve bioconcentration mainly through passive uptake. The k_{pl} values showed the depuration by worms was more efficient in relatively hydrophilic compounds (k_{pl} = 0.022–0.031 day^{-1}), e.g., carbamazepine, lamotrigine, venlafaxine, and clozapine. This result was similar to the previous observation that the bioavailability dissipation of hydrophobic organic contaminants in sediments was less (Cui et al., 2013). However, the greater estimated degradation rate (k_{deg}= 0.368–0.417 day^{-1}) of all antipsychotic compounds indicated that bacterial degradation in sediments was more dominant than dissipation through worm uptake. In the model, carbamazepine did not show the primary transfer to labile fraction with 25% of labile fraction to bound-resides fraction and 17% of stable-adsorbing fraction to labile fraction (**Figure 5.5a**). The labile fraction for other compounds appeared to be transferred to other fractions at the end of the experiment. However, the rate of transfer to labile fraction from stable-adsorbing fraction (k_{sf}) and bound-residues fraction (k_{bf}) showed that labile fractions of these compounds were prone to remain in more stable forms in sediments. Similar to k_{pl} values, k_{sf} and k_{bf} of carbamazepine showed the highest transfer rate at 7.88×10^{-3} day^{-1} and 5.35×10^{-3} day^{-1}, respectively. This indicates that the depuration of antipsychotic compounds became limited due to a decreasing labile pool in

sediments. Although the tested compounds were structurally quite dissimilar, most of them finally transferred to bound-residues fraction (45% to 84%) with the exception of citalopram and venlafaxine (mostly transferred to the stable-adsorbing fraction), possibly because citalopram and venlafaxine were not tightly incorporated with current sediments.

This study attributed the dissipation of total antipsychotic compounds, e.g., desorption, degradation, and worm uptake, which was facilitated by (*i*) direct dissolution in sediment porewater to be bioavailable, and (*ii*) solubilization together with DOC to sediment porewater (**Figure 5.5b**). This dissolved fraction can influence the transfer of antipsychotic compounds fraction and further influence the availability of bioaccumulation by worms.

The DIFS model could further describe the processes of desorption kinetics for the availability of antipsychotic compounds available for exposure to the worms. The declined *R* values represented the gradual decrease in the concentration of antipsychotic compounds in the porewater because these were removed by DGT devices more rapidly than they could be resupplied by diffusion and desorption from the sediment particles. The largest *R* values for carbamazepine (0.33) and lamotrigine (0.31) (**Figure 5.6**) reflect that they can be quickly resupplied by the solid phase of sediments. This can be consistent with higher concentrations accumulated in worms for these compounds. The estimated K_d values were higher than K_{dl}, which shows that the first-order kinetic model for labile fraction by methanol extraction could show a bigger labile pool when it comes to the ionic interactions between antipsychotic compounds and sediment components such as clay minerals. Despite the differences between K_d and K_{dl}, the relative ranking of the labile pool in sediments remained the same. K_{dl} finally regulates the magnitude of resupply of these compounds to the concentration in sediment

porewater from the sediment solid phase (Harper et al., 1998). The values of T_c for carbamazepine and lamotrigine revealed the quickest resupply to the sediment porewater. For example, lowering the T_c of carbamazepine by an order of magnitude can lead to a ~14% increase in R values. The rapid response time might explain the initial increase of passive uptake by worms (**Figure 5.3a**). However, the same order of decline of T_c values for citalopram, amitriptyline, and venlafaxine would only increase about 5% in R, which suggests that the supply of these compounds was partially limited kinetically during the short experiment time, and it was limited by diffusion and potential dissipation by the sediment solid phase for longer time. This would further account for the decrease in worm uptake after the first incubation day.

Generally, apart from greater desorption rates (k_{-1}) (**Table 5.2**) for carbamazepine and lamotrigine, the other antipsychotic compounds still continued to adsorb to sediments after 30 days incubation, which is consistent with previous studies on sorption kinetics for similar organic pollutants in soils and sediments (Stein et al., 2008; Chen et al., 2014; Ren et al., 2020; Li et al., 2021b). This could also be proved by the increased values of k_{sb} and k_{fb} during 30 days for most compounds. Although all these model results showed that a limited diffusion of labile antipsychotic compounds with increasing time, they could become accessible to worms dwelling in sediments.

5.5 Conclusion, limitation, and environmental relevance

This study presents a combined investigation of nine environmentally relevant antipsychotic compounds (from hydrophilicity to moderate hydrophobicity) for the relationship between dissipation of worm passive uptake, fractions transfer, and DIFS model using *L. variegatus* in

spiked sediments with limited ingestion of organic particles. Hydrophilic compounds (lamotrigine and carbamazepine) accumulated mostly in the worms with higher depuration rates. The porewater concentrations and DOC concentrations are two important factors to influence the labile fractions that can be bioavailable. Although labile fraction can be quickly resupplied in the response time, labile fraction of antipsychotic compounds was prone to remain in more stable forms in sediments. The contribution of worm passive uptake was quite small (< 1% for all compounds), and the worm uptake model and diffusion-induced model fitted the measured concentrations well. These models can further be calibrated for different exposure or uptake pathways.

The models used for the current study were different from these for bioconcentration factors, in that they are process-based models that frame and characterize the dissipation pathways and quantify the portion by worm depuration and accumulation in sediments. During the increasing experiment time, microbial activities and DOC contents may be significant factors contributing to bioavailability through the release of compounds from the labile pool. The attention of dominant bound-residue formation for organic contaminants should be raised due to the turnover of sediment organic matter with the change in conditions. The processes of distribution of antipsychotic compounds that we have characterized here can provide a deeper understanding of the uptake of sediment-dwelling invertebrates and the transport processes of these compounds within sediments and the interface between sediment and overlying water.

The models of diffusion and accumulation by worms were based on the first-order model for passive transport in sediments. The potential food sources and active absorption in real environments were not considered, which needs to be further examined. Future work needs to

fit DIFS and fractions-transfer modeled output parameters to sediment invertebrate uptake model for a better prediction. Considering invertebrates, sediment porewater is in direct integumental contact with xenobiotic chemicals except for contaminated sediments for benthic invertebrates (Leppänen and Kukkonen, 2000), DGT passive sampler can be used directly as a surrogate for the initial screening of pollutants before bioassays for risk assessment for chemical burden in sediment-dwelling organisms.

CHAPTER 6: Predicting kinetics of resupply of organic pollutants from sediments, using diffusive gradients in thin films (DGT) samplers and their bioavailability to aquatic invertebrates

Overview

A version of this chapter has been accepted in *Environmental Toxicology and Chemistry* with the following details:

Xiaowen Ji, Catherine Estefany Davila Arenas, Ana Sharelys Cardenas Perez, John P. Giesy, Markus Brinkmann. Predicting kinetics of resupply of organic pollutants from sediments, using diffusive gradients in thin films (DGT) samplers and their bioavailability to aquatic invertebrates. Environmental Toxicology and Chemistry, 2023, 42, 1696-1708. Published: 7 June 2023. DOI: https://doi.org/10.1002/etc.5681

Contributions

Xiaowen Ji: designed and conducted the experiment, and wrote the manuscript.

Catherine Estefany Davila Arenas: conducted crayfish and DGT sampling and measured crayfish length.

Ana Sharelys Cardenas Perez: conducted DGT deployment and retrieval.

John P. Giesy: revised the manuscript.

Markus Brinkmann: conducted crayfish sampling, provided research funding, and revised the manuscript.

Transition

Chapter 5 has demonstrated the passive uptake of organic contaminants by benthic invertebrates and this passive-induced fraction could be simulated well by DGT samplers. Another gap was the bio-uptake of contaminants by benthic invertebrates in a real complex environment and whether DGT-derived concentrations can predict this bioavailable fraction. To achieve this, chapter 6 aimed to fill this gap by establishing a predictive model by DGT samplers for the bioavailable concentrations of analytes in crayfish sampled from a contaminated site. This chapter revealed the correlation among the concentrations in water, sediment, and crayfish. Besides, a chemical uptake model based on the mass balance of organic chemicals between crayfish and the aquatic environment was established and tested. The resupply kinetics used in the previous chapters were also conducted to explain the dynamic accessible fraction of organic contaminants by crayfish.

Abstract

The current study used diffusive gradients in thin films (DGT) samplers deployed *in-situ* at a wastewater-impacted site (Clarkboro Ferry, Warman, SK) for 20 days to develop a predictive model between time-weighted mean concentrations of seven, selected antipsychotic compounds in water and those in resident benthic invertebrates, specifically crayfish (*Faxonius virilis*). The model was further combined with a model of desorption of antipsychotic compounds to predict kinetics at the sediment-water interface. Antipsychotic compounds were mostly detected in adult crayfish and internal concentrations were similar among targeted compounds, with the exception of lesser concentrations of duloxetine. The model, based on the mass balance of organic chemicals, to predict uptake by organisms, exhibited good agreement with measured values ($R^2 = 0.53$–0.88), except for venlafaxine ($R^2 = 0.35$). At the sediment-water interface, positive fluxes were observed for antipsychotic compounds, and the results from DGT-induced fluxes in sediments (DIFS) coupled with equilibrium hydroxyl-β-cyclodextrin extraction further indicated partial resupply of antipsychotic compounds from sediments to the aqueous phase, despite the labile pool being relatively limited. The results of this study affirm that the DGT technique can be used as a predictive tool for contamination in benthic invertebrates and can estimate the ability of contaminant resupply from sediments.

Keywords: organic pollutants; drugs, pharmaceuticals, crayfish; prediction; DGT; desorption kinetics

6.1 Introduction

Effects of contaminants on local environments are often of concern at sites downstream of point sources, such as wastewater treatment plants. Water, sediment, and aquatic biota are traditionally used to monitor for contamination using chemical analytical methods (Porte and Albaigés, 1994). Among these samples, contextualizing the importance of sediment concentrations is not always straightforward because contaminants (especially organic compounds) can bind with substrata by adsorption and become less bioavailable for direct uptake by aquatic organisms (Schilderman et al., 1999). Furthermore, varied concentrations measured in sediments often only reveal variations in sediment binding properties instead of changes in actual concentrations of contaminants (Muncaster et al., 1990). Similarly, direct analysis of hydrophobic contaminants in water is often challenging, since concentrations on bulk water samples are often less than limits of detection (LOD), but still in a range that could cause biological effects (Muncaster et al., 1990). For example, 5.5 ng L^{-1} of 17α-ethynylestradiol in water can affect the reproductive system in juvenile rainbow trout (*Oncorhynchus mykiss*) (Rehberger et al., 2020). In such circumstances, studies using living organisms that have been exposed through their entire life-cycle, accumulating lipophilic chemicals into their lipid tissues from the contaminated sites, can be useful since amounts of residues measured in these organisms can provide an integrative measure of contamination at the site (Muncaster et al., 1990; Schilderman et al., 1999; He et al., 2021). Also, in some cases, such as fishes, collecting and measuring tissue levels of contaminants can also be aimed at protecting consumers. Although measurement of contaminants in living organisms has its

advantages, sampling the appropriate organisms to evaluate contamination levels requires specific knowledge concerning the organism and the local ecosystem, and is often logistically difficult, time-consuming, and costly. Significant sampling operations can also adversely affect ecosystems. Moreover, other aspects concerning home ranges, ease of collection, as well as spatiotemporal variations in contamination should be considered when interpreting in-situ trends of chemical concentrations in organisms (Forsberg et al., 2014; Paulik et al., 2016). Therefore, developing a method to predict concentrations of contaminants in aquatic organisms would be useful to avoid collecting a large number of organisms.

The most frequent method to assess the accumulation of contaminants by aquatic organisms from abiotic environments is the use of bioaccumulation factors (BAFs), usually described as the ratio of a chemical's concentration in organisms on a lipid-normalized basis to its concentration in bulk water samples (Bierman, 1990). BAF assessment hypothesizes that collected organisms are at or near a steady state with abiotic media, such as surrounding water and or sediments. However, since organisms are mobile, reliable predictions of bioaccumulation account for spatial and temporal variability, leading to variable exposure concentrations through water and diet (Jon and Frank, 2006). This could cause variability by orders of magnitude when applying published BAFs for a given chemical to predict concentrations in aquatic organisms at specific sites (Booij et al., 2006). Besides, when the aqueous concentration is close to the analytical detection limit, the assessment of BAFs can be uncertain (Jon and Frank, 2006).

To partly solve this latter issue, due to the advantages of *in-situ* accumulation of contaminants, measurement of time-weighted average concentration of freely dissolved concentration, their

low cost, and ease of deployment, passive samplers have received much attention (Kot-Wasik et al., 2007). Passive samplers have been considered to be a complementary tool for evaluating environmental contamination by the EU Water Framework Directive (EU, 2012) and the U.S. Environmental Protection Agency Superfund program (Burgess, 2012). Among these, some studies have attempted to use passive samplers, such as semipermeable membrane devices and low-density polyethylene, to predict concentrations of organic contaminants in wild or laboratory-exposed aquatic organisms (Hofelt and Shea, 1997; Axelman et al., 1999; Boehm et al., 2005), from concentrations in passive samplers, by use of multivariate, linear regression methods (Forsberg et al., 2014; Paulik et al., 2016).

Recently developed methods based on diffusive gradients in thin films (DGT) for organic residues have been used to predict the flux and concentrations of trace organic contaminants between water and sediments (Chen et al., 2012; Li et al., 2021b; Ji et al., 2022c). Compared to other passive samplers, accumulations of organic chemicals by DGT samplers are typically less affected by water flow velocity or temperature due to the presence of a hydrogel that is used as the diffusive layer, that constrains chemical mass diffusion within this well-defined thickness layer (Bondarenko et al., 2011; Challis et al., 2016). Furthermore, DGT has also been developed as a dynamic technique that can account for dynamic processes driving changes in chemical concentrations in sediment pore water and its resupply from the solid phase in soils or sediments (Li et al., 2021b). A numerical model, known as the DGT-induced fluxes in soils and sediments (DIFS), can simulate chemical desorption kinetics in two dimensions for soils or sediments (Sochaczewski et al., 2007). The DIFS model has been applied to organic contaminants samples by DGT in sediments under laboratory-controlled conditions (Li et al., 2021b) and in the field

(Ji et al., 2022c).

DGT samplers deployed in water or sediment have been used to simulate the biological uptake of metals in aquatic organisms, such as fish (Pelcová et al., 2017; Pelcová et al., 2018), clams (Clarisse et al., 2012), and snails (Yin et al., 2014) in the field or under controlled laboratory conditions. However, examples of predicting the bioaccumulation of organic contaminants in aquatic organisms are quite limited. To date, one study has tried to predict *in vivo* bioaccumulation of methamphetamine and its metabolite in exposed zebrafish by deploying DGT (Yin et al., 2019). Another study used DGT to mimic the passive uptake of benthic worms from sediments spiked with antipsychotics, with the interpretation of resupply processes by the DIFS model (Ji et al., 2023). However, current studies assessing the bioavailability of organic contaminants to aquatic organisms using passive samplers have focused on hydrophobic persistent organic pollutants (Baussant et al., 2001; Ke et al., 2007; Forsberg et al., 2014; Paulik et al., 2016) and mass balances of moderately hydrophobic organic contaminants (log K_{ow}, octanol-water partition coefficient: 4−5) have not been conducted.

In this study, concentrations of antipsychotic drugs in crayfish (*Faxonius virilis*) collected from a location downstream from a wastewater treatment facility were related to freely dissolved moderately hydrophobic contaminants collected by DGT samplers. Three antipsychotic compounds, i.e., duloxetine (log K_{ow}=4.68), amitriptyline (log K_{ow}=4.95), fluoxetine (log K_{ow}=4.65), bupropion (log K_{ow}=3.85), citalopram (log K_{ow}=3.74), clozapine (log K_{ow}=3.35), and venlafaxine (log K_{ow}=3.28), were chosen as target chemicals. Crayfish were chosen due to the relatively limited biotransformation (James and Boyle, 1998) smaller excretion rates of chemicals compared to other benthic invertebrates (Jewell et al., 1997), small

home range (Merkle, 1969), and possibly direct route of exposure to accumulated contaminants through human consumption (Jorhem et al., 1994). Furthermore, based on equilibrium-based and dynamic partitioning of organic chemicals between solid and aqueous phases in sediments (Sijm et al., 2000), this study introduced the chemical bioaccessible capacity−that is when a compound is released from the solid phase into the aqueous phase, it can be instantaneously captured by cyclodextrin (a group of cyclic oligosaccharides containing polar exterior and a nonpolar cavity) (Hartnik et al., 2008) – into the DIFS model., where often used single organic extractants (Chen et al., 2014; Ren et al., 2020; Li et al., 2021b) cannot represent bioaccessible fractions accurately, to explain the mechanism of uptake processes by aquatic invertebrates.

6.2 Materials and methods

6.2.1 Study site, sample collection, and preparation

The study site (52°19'05.2"N; 106°27'39.6" W) was located at Clarkboro Ferry approximately 20 km northeast of Saskatoon (SK, Canada). The surrounding landscape is profoundly shaped by fluvial processes, aeolian deposits, and anthropogenic farmlands. The Saskatoon municipal wastewater treatment plant is located about 30 km upstream from the study site, where the targeted antipsychotic compounds were previously detected (Ji et al., 2022c). Deployment and sampling of DGTs were performed during the summer of 2022.

Three DGT standard devices and a temperature logger were attached to a stainless-steel profile, of which one DGT sediment probe (L: 170 mm; W: 40 mm) was attached to the bottom (**Figure 6.1**). Three individual profiles were slowly inserted into sediments with an exposure area of approximately 150.3 × 20.4 mm completely buried in the sediments. The DGT sampler

was comprised of a 0.45 μm polyethersulfone filter membrane (Sartorius Stedim Biotech GmbH, Germany), a 0.75 mm 1.5% agarose diffusive gel, and a 0.75 mm β-cyclodextrin-based polymer binding gel (40 mg per gel for DGT device and 400 mg per gel for DGT probe). The preparation of gels has been described previously (Ji et al., 2022b) and the synthesis process and laboratory test of β-cyclodextrin-based polymer are described in **Appendix 12**. After deployment, DGT samplers were retrieved and replaced at 1, 3, 5, 10, 15, and 20 d. The filter surface of retrieved DGT samplers was jet washed with ultrapure water and samplers were transported to the laboratory, where the binding gels were disassembled, spiked with isotope-labeled surrogates, and placed into 50 mL glass vials. Then, 10 mL methanol was added to the tube for 10 min ultrasonic extraction, and the process was repeated three times. Extracts were reconstituted in 1 mL of methanol after drying with a gentle stream of nitrogen gas and passed through a 0.2 μm syringe filter (PTFE, Thermo, MA) before chemical analysis. For DGT probes, the gels were first cut from the window area in 2 cm sections using a razor blade, followed by the same extraction processes.
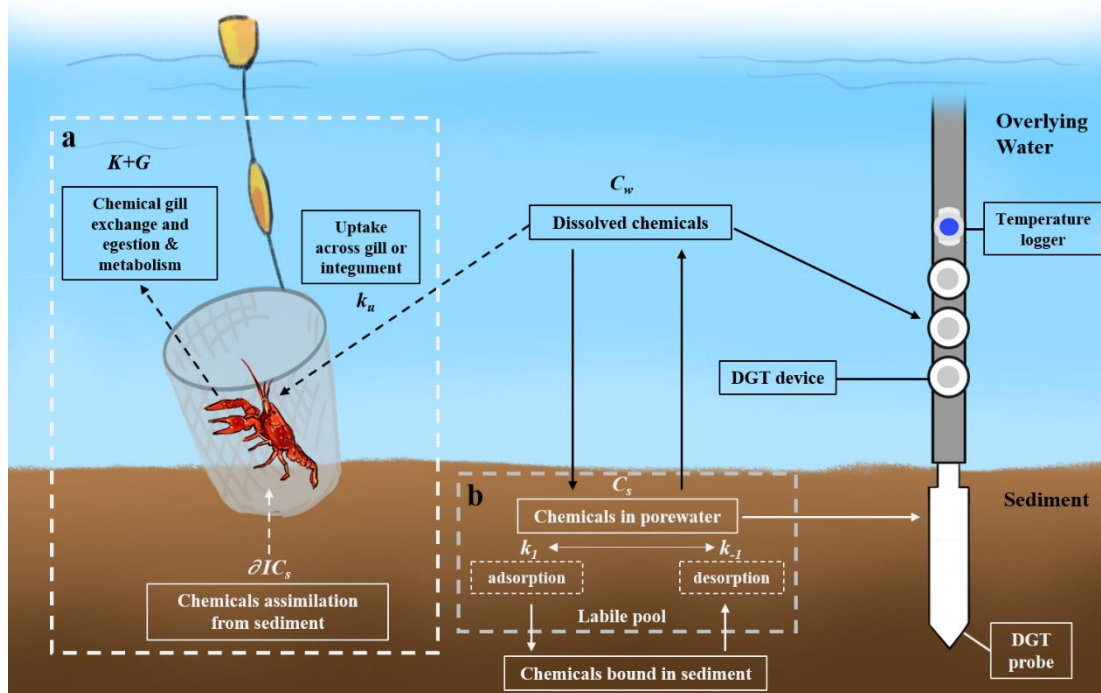
Figure 6.1 Conceptual diagram of **(a)** uptake and elimination routes of organic contaminants for crayfish, where C_s is the concentration of the dissolved compounds in sediments, k_u is the uptake rate constant through the gill, $K+G$ is the chemical gill exchange rate + organism growth rate, and αI is the chemical assimilation and metabolism rate, and the schematic diagram of DGT probe and standard DGT devices in sediment and water respectively, where processes induced by DGT samplers as highlighted. C_s is progressively depleted. During the desorption from the sediment solid phase, **(b)** the concentrations of compounds are instantaneous at the interface between DGT and sediment, where k_1 and k_{-1} is the adsorption rate constant and desorption rate constant, respectively. C_w is the concentration of the dissolved compound in water.

Crayfish (*F. virilis*) were collected from the surroundings of the DGT deployment site at each DGT retrieval. *F. virilis* generally migrate within a limited home range depending on water temperature and reproduction (Momot and Gowing, 1972; Wetzel, 2002). A total of 50 crayfish were manually caught using dip nets. Crayfish were stored in a cooler box filled with ambient water and transported to the laboratory. Then, external crayfish surfaces were cleaned using ultrapure water and anesthetized on ice for 30 mins, euthanized by severance of the supra-esophageal ganglion, after which each crayfish was measured (carapace length and full body

length), weighed, sexed, and dissected to remove the exoskeleton. Composite samples of tissues were lyophilized and homogenized to fine powders by a granite mortar and pestle. Homogenized tissue samples were spiked with isotope-labeled surrogates and subsequently Soxhlet extracted with 300 mL dichloromethane (40ºC) for 24 h, after which the extracts were dried by rotary evaporation and reconstituted in 5 mL methanol, which was further diluted by 100 mL HPLC-grade water for clean-up by solid phase extraction (SPE) (details in **Appendix 3**). The eluates were concentrated using nitrogen gas to a volume of 1 mL in methanol.

Before deployment and when DGTs were retrieved, three sediment cores (15 cm depth) and three surficial (~ 5 cm) sediment samples were collected at the site of DGT deployment following the previous method (Ji et al., 2022c) (**Table A19**). Wet sediment samples were drained for 2 h to obtain maximum water holding capacity (Priha and Smolander, 1999). Sediment cores were sliced into 2 cm sections. Each section was centrifuged at 3,000 rpm for 20 min to obtain porewater. The supernatants were spiked with isotope-labeled surrogates, filtered, preconcentrated by SPE, and reconstituted to 1 mL methanol.

For hydroxyl-β-cyclodextrin extraction, different amounts of hydroxyl-β-cyclodextrin was added to 1 g of lyophilized sediment to achieve cyclodextrin-to-sediment ratios from 1:1 to 1:7 (by mass). A 20 mL aliquot of a 5 mM NaN_3 solution was added to cyclodextrin-sediment mixtures in 50 mL glass centrifuge tubes (polypropylene screw cap with PTFE liner), which were shaken (1,500 rpm, Heidolph™, Fisher Scientific) for 1, 3, 10, 24, 48, and 72 h. The supernatants were spiked with isotope-labeled surrogate standards, filtered, and preconcentrated by SPE as mentioned above.

6.2.2 Chemical analysis

All final reconstituted samples were analyzed for amitriptyline, duloxetine, and fluoxetine with the corresponding isotope-labeled internal standards (i.e., amitriptyline-d_6, duloxetine-d_7, fluoxetine-d_5, bupropion-d_9, citalopram-d_6, clozapine-d_4, and venlafaxine-d_6) using a Vanquish UHPLC containing a 100 × 2.1 mm Kinetex 1.7 μm XB-C18 LC column (Phenomenex, CA) and Q Exactive™ Plus Hybrid Quadrupole-Orbitrap™ Mass Spectrometer (Thermo-Scientific, MA). The details of the analytical method and chemicals have been described in detail previously (Ji et al., 2022b) and in the previous chapters respectively.

Chromatographic peaks of targeted antipsychotics were manually confirmed by precursor ions and product ions (**Table A3**) using Freestyle software (version 1.6, Thermo-Fisher Scientific) and integrated by the ICIS algorithm of Quan Browser (version 4.3, Thermo-Fisher Scientific). The concentrations of individual analytes were calculated using the stable isotope dilution method based on the internal standard (IS) to analyte response ratio. The calibration curve of each analyte was established (1/x as the weighting factor) between analyte concentrations (x) and instrument response (y, peak ratio of analyte peak to IS peak).

The recovery of seven antipsychotic compounds during the procedure from DGT extraction, and SPE enrichment to final reconstitution was 75%–93%. During the instrumental analysis, each sequence created in Xcalibur 4.3 includes solvent blanks, matrix blanks, and matrix spikes (50 μg L^{-1}), and two solvent blanks were inserted every five samples. The standard solution of antipsychotic compounds at 50 μg L^{-1} was run in the middle of the sample sequences for each run, and the RSD was lower by 20%. All organic solvents were HPLC grade and all glassware was pre-ashed at 550 °C for at least 5 h before use.

6.2.3 DGT-derived concentration calculation

According to Fick's first law of diffusion, the time-averaged concentration measured by DGT (C_{DGT}) can be calculated from the mass of analyte accumulated by the binding gel of DGT (M) (Equation 6.1) (Davison and Zhang, 1994):

$$C_{DGT} = \frac{M \Delta g}{D A t} \quad (6.1)$$

Where: Δg is the thickness of the diffusive layer, A is the exposed area of the diffusion layer, t is deployment time, and D is each analyte's diffusion coefficient through the diffusive layer. D values (10^{-6} m^2 s^{-1}) of seven antipsychotics at 25ºC were measured by the diffusion cell method in a previous study (Ji et al., 2022c): 6.45 for amitriptyline, 3.80 for duloxetine, 4.68 for fluoxetine, 4.47 for bupropion, 3.63 for venlafaxine, 4.20 for citalopram, and 5.07 for clozapine. An empirical relationship between D at 25 ºC and temperature allows for the calculation of D at the temperature of the study site.

6.2.4 Model framework

6.2.4.1 Organism uptake model

The predictive, simulation model was based on a steady state and follows a previously established framework for modeling organic chemical accumulation in sediment macroinvertebrates (**Figure 6.1a**) (Thomann et al., 1992). The benthic macroinvertebrate compartment was hypothesized to be a deposit consumer that ventilates porewater and feeds on sediment. The mass balance of organic chemicals between crayfish and the aquatic environment is associated with (*i*) chemical sediment/water partitioning, (*ii*) the bioenergetics (e.g., growth rate), and (*iii*) chemical-related parameters (e.g., chemical assimilation efficiency), which can

be described mathematically (Equation 6.2).

$$\frac{dC_i}{dt} = k_u C_w(t) + \partial I C_s(t) - (K + K_m + G)C_i \qquad (6.2)$$

Where: C_i is chemical concentration in crayfish (μg kg[lipid]$^{-1}$), C_w is dissolved chemical in overlying water (μg L^{-1}), C_s is dissolved chemical in sediment porewater (μg L^{-1}), k_u is chemical uptake from water (L kg[lipid]$^{-1}$ d^{-1}), ∂ is chemical assimilation efficiency, I is sediment ingestion rate (kg[organic C] kg [lipid]$^{-1}$ d^{-1}), K is chemical gill exchange and egestion rate (d^{-1}), K_m is chemical metabolism rate (d^{-1}), and G is organism metabolism rate (d^{-1}). ∂, I, and G were 0.8 d^{-1}, 0.062 d^{-1}, and 0.063 d^{-1}, respectively, taken from previously published bioenergetics literature for crayfish (Thomann and Komlos, 1999). k_u can be described as the chemical across gills or integument (Thomann, 1989) (Equation 6.3).

$$k_u = \frac{\beta \rho}{C_o} \qquad (6.3)$$

where β is the ratio of chemical transfer efficiency to oxygen transfer efficiency, ρ is the respiration rate (mg O$_2$ kg[lipid]$^{-1}$ d^{-1}), taken as 0.015 for crayfish (Thomann and Komlos, 1999), and C_o is the oxygen concentration, measured as 8.7 mg L^{-1}. β can be estimated empirically for benthic invertebrates and crayfish (Equation 6.4).

$$\log \beta = 2.048 - 0.3 \log K_{ow} \qquad (6.4)$$

6.2.4.2 Three-phase equilibrium model

The applicability of hydroxyl-β-cyclodextrin as a good biomimetic extraction is based on the theory of a three-phase equilibrium model (i.e., sediment, water, and cyclodextrin) (Hartnik et al., 2008) (Equation 6.5).

$$\frac{M_{i,\text{water}}}{V_{water}} = \frac{M_{i,\text{CD}}}{M_{\text{CD}}K_{i,\text{CD}}} = \frac{M_{i,\text{sediment}}}{M_{\text{sediment}}K_{i,\text{OC}}f_{OC}} \qquad (6.5)$$

where: $M_{i,\text{water}}$, $M_{i,\text{CD}}$, and $M_{i,\text{sediment}}$ represent the mass of a chemical i in water, hydroxyl-β-cyclodextrin, and sediment (obtained by methanol ultrasonic-extraction), respectively and V_{water}, M_{CD}, and $M_{sediment}$ represent the volume of the water and the masses of cyclodextrin and sediment used for extraction. $K_{i,\text{CD}}$, and $K_{i,\text{OC}}$ represent the partitioning coefficients for water–cyclodextrin and water–organic carbon, respectively, and f_{OC} represents the fraction of organic carbon in sediment.

$K_{i,\text{CD}}$ can be determined (Equation 6.6).

$$\frac{C_{i,free}}{C_{i,total}} = \frac{1}{1 + K_{i,CD}C_{CD}} \qquad (6.6)$$

where $C_{i,\text{total}}$ represents the concentration of a dissolved and encapsulated compound in water and C_{CD} represents the concentration of cyclodextrin in water. The partition coefficient is better based on the extraction capacity than the stability constant for cyclodextrin complexes.

Adsorption capacity (AC) and cyclodextrin-extraction capacity (EC) can be described mathematically (Equations 6.7 and 6.8).

$$AC = M_{\text{sediment}} f_{OC} K_{i,\text{OC}} \qquad (6.7)$$

$$EC = M_{CD} K_{i,\text{CD}} \qquad (6.8)$$

When the chemicals were initially dissolved in water and released from sediment, the total mass of a chemical ($M_{i,\text{total}}$) can be theoretically calculated (Equation 6.9).

$$M_{i,\text{total}} = M_{i,\text{sediment}} + M_{i,\text{CD}} + M_{i,\text{water}} = AC(C_{i,\text{water}}) + EC(C_{i,\text{water}}) + M_{i,\text{water}} \qquad (6.9)$$

in which, $C_{i,\text{water}}$ is the concentration of a dissolved chemical in water. Assuming the moderately hydrophobic analytes were mostly adsorbed by cyclodextrin when the system reaches

equilibrium, $M_{i,\text{water}}$ can be negligible. Maximum extractable fraction (MEF) of a chemical from sediment can be obtained through the transformation (Equation 6.10).

$$MEF = \frac{AC}{AC + EC} \tag{6.10}$$

6.2.4.3 DIFS model

The DIFS model can be used to quantify the kinetic processes of chemicals in the labile phase in sediments (**Figure 6.1b**) (Harper et al., 2000; Sochaczewski et al., 2007). It is based on an indicator (R) for the magnitude of depletion of sediment porewater concentrations at the DGT interface, which can be described as the ratio of C_{DGT} to the initial sediment porewater concentration (C_p) (Equation 6.11). In the real environment, chemicals can be only partially resupplied from the aqueous phase in sediment ($0.1 < R < 0.95$). Two model parameters, K_{dl} (Equation 6.11) and T_c (Equation 6.12) describe labile pool size and rate constant of adsorption (k_1) and desorption (k_{-1}), respectively. K_{dl} is the distribution coefficient of labile chemicals in the solid phase that can be exchanged with porewater and accounts for the labile pool size. T_c is the response time of the (de)sorption process where the partitioning components between the solid phase and porewater reach 63% of their equilibrium assuming the initial aqueous concentration is zero (Honeyman and Santschi, 1988).

$$R(t) = \frac{C_{DGT}(t)}{C_p} \tag{6.11}$$

$$K_{dl} = (\frac{C_l}{C_p})_{eq} = \frac{k_1}{P_c k_{-1}} \tag{6.12}$$

$$T_c = \frac{1}{k_1 + k_{-1}} = \frac{1}{k_{-1}(1 + K_{dl} P_c)} \tag{6.13}$$

Concentrations of labile chemicals (C_l) were determined by extraction into hydroxyl-β-

cyclodextrin as $C_{i,CD}$ based on a three-phase equilibrium model. This model can quantify the relationship among R, K_{dl}, and T_c. T_c can be derived from the model when $R(t)$ and K_{dl} are input parameters and k_{-1} can be obtained from eq 6.11. P_c (g cm^{-3}) is related to the sorbed concentration (mol g^{-1}) to a porewater concentration (mol cm^{-3}) (Equation 6.14).

$$P_c = \frac{m}{V} \qquad (6.14)$$

where m is the total mass of the entire sediment solid phase (g) and V is the porewater volume (cm^{-3}) in a given total volume of sediment.

6.2.5 Statistical methods

All measured concentrations were checked for normality using Shapiro-Wilks tests. Comparisons between samples were performed using Kruskal-Wallis' H Test. Differences were considered statistically significant at $p \leq 0.05$. Antipsychotic concentrations in crayfish were expressed on a dry tissue weight basis. All statistical analyses were performed using SPSS Statistics (version 26, IBM, NY).

6.3 Results and discussion

6.3.1 Crayfish morphometrics

A total number of 50 crayfish were caught in the Saskatchewan River, comprising 34 males and 16 females (**Table A20**). Patterns of accumulation of organic residues in crayfish can be strongly related to body size and age (Balzani et al., 2022). In the present study, no such relationships were observed for concentrations of the seven, targeted antipsychotic drugs and carapace length, whole-body length, and body mass among the crayfish caught at different

sampling times (One-way ANOVA on ranks, $p > 0.2$ for all tests), which might be due to different habitats. Age of crayfish was generally equal to or greater than 2 years through the comparison between previous studies for *F. virilis* (3.6−6.2 cm at age 2) (Momot, 1967; Hazlett and Rittschof, 1985) and current data (3.5−5.6 cm, mean of 4.3 ± 0.6 cm). Therefore, crayfish sampled within the current study are suitable sentinels to reveal contamination patterns at this specific study site.

6.3.2 Chemical concentrations in crayfish and dissolved phase

The range of measured antipsychotic compounds in crayfish and calculated fluxes (calculation details in **Appendix 6**) at the interface of water and sediments (**Figure 6.2a** and **6.2b**; the concentration profile from sediment to water measured by DGT samplers is shown in **Figure A21)**. Despite some samples being less than the limit of detection for duloxetine, amitriptyline, and fluoxetine, all seven antipsychotic compounds were generally observed in tissues of crayfish, Amitriptyline showed the greatest median concentration (11.1 ng g^{-1} ww), followed by venlafaxine (6.28 ng g^{-1} ww) and clozapine (6.24 ng g^{-1} ww). Concentrations of antipsychotic compounds in crayfish were 10- to 100-fold less than those for hydrophobic compounds (e.g., PAHs and PCBs) typically reported for other locations (Rao et al., 1996; Forsberg et al., 2014; Paulik et al., 2016). This is likely due to greater bioaccumulation of hydrophobic contaminants among neutral lipid classes (Geisler et al., 2012). Besides, the targeted compounds (*p*Ka: 7.5−10.09) are ionizable so that the interaction with sediments may cause sorption with sediment particles, resulting in reduced bioaccessibility by benthic invertebrates.
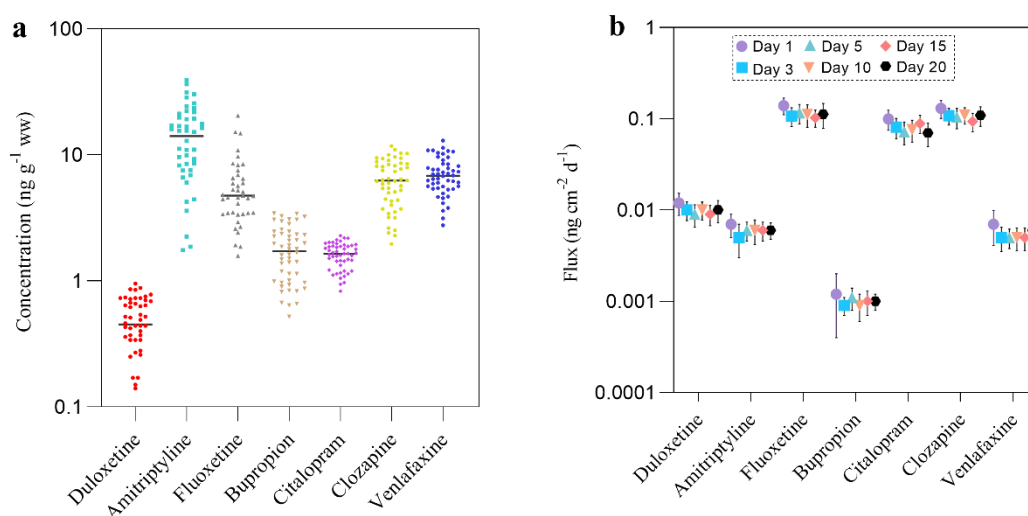
Figure 6.2 Concentrations of targeted antipsychotic compounds in resident crayfish (**a**) and (**b**) calculated flux (mean and standard deviation) at the interface of sediment and water following the sampling days using the measured data from the standard DGT devices and sediment probes in the co-located sampling/deployment site.

Concentrations of antipsychotic compounds normalized by whole deployment days showed a slightly decreasing trend from the water column, except for citalopram which might be due to instantaneously higher concentrations in water (**Figure A21**). The antipsychotic compounds in sediment porewater at a depth of 2 cm generally exhibited lesser concentrations than those observed in the overlying water. This is consistent with the results of previous studies in which concentrations of dissolved organic pollutants were greater at the interface between water and sediment (Fernandez et al., 2009; Ji et al., 2022c). However, concentrations of only duloxetine were greater than the LOD in sediments below 2 cm. Among the seven analytes, concentrations between sediment porewater and bulk water were within the same order of magnitude without being statistically different ($p > 0.05$) for five compounds, while concentrations of bupropion and venlafaxine were 10-fold less than those of other compounds. From the calculated vertical diffusive fluxes at the water-sediment interface, net positive fluxes were observed for all

antipsychotic compounds from day 1 to day 20 (**Figure 6.2b**). Fluxes of fluoxetine, citalopram, and clozapine ranged within the same order of magnitude (> 0.1 ng cm^{-2} d^{-1}), whereas fluxes of duloxetine, amitriptyline, bupropion, and venlafaxine were one or two orders of magnitude lower. This indicates that fluoxetine, citalopram, and clozapine could be released to bulk water from the aqueous phase in sediments. A previous study showed that high-molecular-weight compounds are likely to sorb to dissolved and particulate-bound organic carbon, which results in their limited solubility (Axelman et al., 1999; Forsberg et al., 2014). However, this was not observed in the study, the results of which are presented here. This result could be due to different adsorption mechanisms for positively charged antipsychotic compounds under the environmental conditions (pH $\approx$ 8 for the current study site) and a relatively narrow range of molecular masses (297.4–309.3 Da). Considering the small content of carbon of sediments in this study ($< 1\%$), mineral sorption might be the factor controlling concentrations near the water-sediment interface, especially for more than one proton donor/ acceptor site of the current analytes (except for amitriptyline). This conclusion is consistent with previous observations that hydrophobic and electrostatic interaction both account for the sorption of chemicals to sediments (Karlsson et al., 2016).

Positive fluxes of antipsychotic compounds at the sediment–water interface might indicate the bioavailability of chemicals to benthic crayfish, whereas the concentration in crayfish was not directly correlated with magnitudes of these fluxes. For example, the greatest median concentration in crayfish was observed for amitriptyline, while the fluxes of amitriptyline were < 0.01 ng cm^{-2} d^{-1}. This difference could be the result of the dynamic equilibrium of the compounds between water and sediment, and the complex sorption to the sediment. Since the

uptake of antipsychotic compounds by crayfish occurred from both water and sediment assimilation simultaneously, bioavailable concentrations of antipsychotic compounds in water and sediment were the main drivers for the uptake process. Nevertheless, constant resupply from sediment to surface water provided an extra exposure route for the residing crayfish.

6.3.3 Prediction by chemical uptake model

To evaluate the effect of deployment time on organism uptake, Sobol Global Sensitivity Analysis (SGSA) was used (Sobol, 2001) (**Appendix 13**). The parameter of uncertainty (S_t) was used to estimate the sensitivity of model output to exposure time to select the best-fit number for the chemical uptake model (**Figure A22**). Based on the 2–5 years life span of the crayfish, exposure times were estimated in that range with a time interval of 1 d. The results showed that the chemical concentration in crayfish was the most sensitive parameter influenced by exposure time, where more variable values may be obtained from the model within 755 d. For the dissolved chemical concentration in water, the sensitivity influenced by exposure time was very limited, indicating relatively stable concentrations measured by DGT devices. Moreover, the sensitivity of chemical concentration in sediment porewater was higher than that in water, while S_t values were relatively higher, with no further differences observed ($p > 0.05$) after 932 days at each deployment time. It was observed that chemicals in sediment contributed a comparably larger proportion to the uptake processes by crayfish.

Based on the steady state of a constant relationship between the water column and sediment, the organism uptake model linked the concentrations of antipsychotic compounds in the overlying water measured by DGT devices to predict concentrations in crayfish. (**Figure 6.3**).

Plots of calculated versus field-measured concentrations were produced to evaluate the predicted deviations, where values consistent with the fitted regression line represented better prediction (**Figure 6.3**). Generally, differences between measured and predicted values were variable among the seven antipsychotic compounds, where predicted values for most compounds were 20-80% less than measured values. Higher predicted values (23-48% than measured values) were only observed for bupropion. R^2 values of all compounds ranged from 0.35 to 0.88. Values of venlafaxine did not follow a linear relationship. This is caused by significant differences in rate (1%-88%) between predicted and measured values for venlafaxine, indicating the uptake processes and fluctuation levels of venlafaxine were not reflected by DGT measurements. This is consistent with previous observations that the accumulation of residues by aquatic organisms was not related to passive samplers in a strict one-to-one fashion (Booij et al., 2006). Except for bupropion with a relatively good R^2 value, a lower correlation between predicted and measured values was observed for the other compounds (**Figure 6.2a**). The wider confidence interval also suggests that the average response was not modeled very well (**Figure 6.3**). Considering the high partitioning between water and sediment (> 0.1), the origin of available ionizable antipsychotic compounds for crayfish might be associated with increased desorption to dissolved pools in sediments.
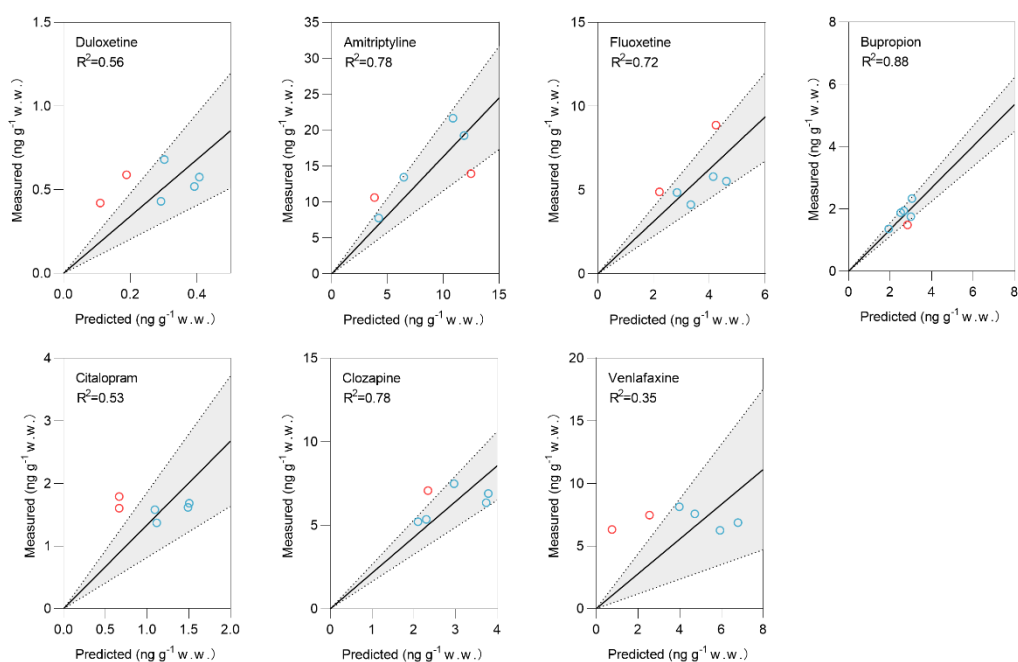
Figure 6.3 Measured and model-calculated concentration of antipsychotic compounds in crayfish using DGT measured average concentration in overlying water (at 2 cm depth) and surficial sediments (at -2 cm depth) at each deployment time. The measured concentrations below the method detection limits were excluded. The solid line represents the plotted simple linear regression by forcing the intercept of a regression model to equal zero. The red circle and blue circle represent the values beyond or within the 95% confidence interval (grey area), respectively.

Some studies have used linear regression models through inputting the transformed units of concentrations of contaminants, measured by a passive sampler in water and measured in crayfish to predict the contaminant concentrations in crayfish by the regression slope from the equation of the line of best fit (Thomann and Komlos, 1999; Forsberg et al., 2014; Paulik et al., 2016). Although R^2 values of the best fit of these studies were similar to our results, the similar issues that predicted values were more variable and differed rather substantially from the measured ones still remained. It has been reported a partial least-square calibration model using MDLs substitution to improve the predicted concentrations in crayfish tissue for higher molecular-weight polycyclic aromatic hydrocarbons compared to equilibrium partitioning-

based crayfish-sediment accumulation factors (Forsberg et al., 2014). In our study, all predicted values were above the MDLs and therefore, differences were less than a factor of 10 among predicted values except only one predicted value for venlafaxine was about 80fold less than the measured value. Previous studies also showed that uptake across the gill may also occur through not just simple passive diffusion of the ionic compounds and thereby carrier-mediated transport might affect the ionic species (Sugano et al., 2010; Kell and Oliver, 2014). Since the simulation model applied in this study was based on a steady-state value for chemical mass balance in the relatively homogenous polluted site (non-point pollution sources), the sensitivity of multiple variables was dependent on the individual compound level and resupply ability in the aqueous phase of both water and sediment.

6.3.4 Determination of labile chemicals in sediment

To better estimate the labile pool of antipsychotic compounds in sediments, hydroxyl-β-cyclodextrin extraction was conducted with increasing extraction time, showing that hydroxyl-β-cyclodextrin extractability increased and reached the maximum concentrations after 24 h (**Figure 6.4a**). There was no significant difference ($p > 0.05$) for extracted concentrations of all compounds after 24 h. Furthermore, increased concentrations resulted from the increased amount of hydroxyl-β-cyclodextrin (**Figure 6.4b**), while the curve leveled off at a hydroxyl-β-cyclodextrin-to-sediment ratio of 1:3.5 and less than 2% increase of extracted concentrations at the ratio of 1:7, which is consistent with previous study for hydrophobic compounds (Hartnik et al., 2008).
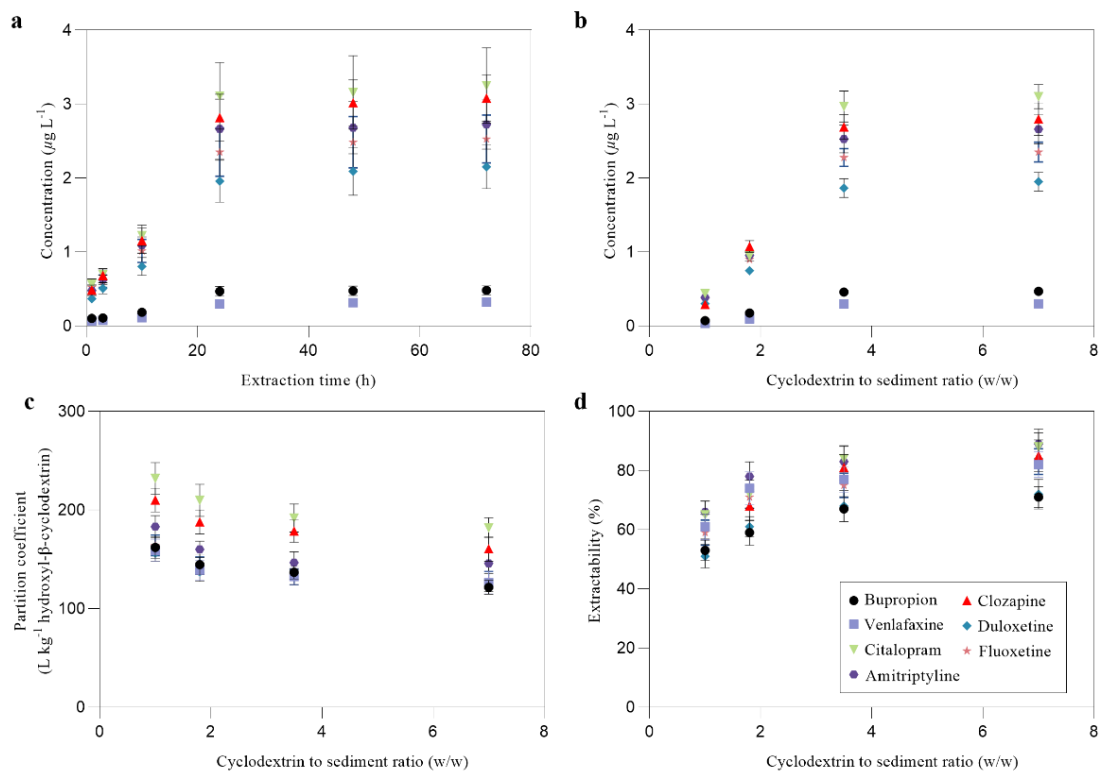
Figure 6.4 Influence of extraction time by a hydroxyl-*β*-cyclodextrin to sediment ratio of 3.5 (**a**), concentration extracted by hydroxyl-*β*-cyclodextrin using 24 h (**b**), partition coefficient of individual chemical between hydroxyl-*β*-cyclodextrin and water (**c**), and maximum extractable fractions for seven antipsychotic compounds (**d**). Error bars in the figures represent standard deviations of triplicates.

When it comes to explaining the extraction capability with increased extraction time, this is highly dependent on whether the system is in a steady state since two scenarios, equilibrium between hydroxyl-*β*-cyclodextrin and sediment, and slow desorption kinetics, may occur. Our results showed that the hydroxyl-*β*-cyclodextrin-to-sediment ratio of 1:3.5 was adequate to constantly deplete the aqueous phase until 24 h because the extraction concentrations did not significantly increase at the higher ratio for antipsychotic compounds.

When sediment was extracted with increasing amounts of hydroxyl-*β*-cyclodextrin, the freely dissolved concentrations of all antipsychotic compounds exhibited an inverse

relationship. Partition coefficients between bound and freely dissolved compound (K_{CD}) ranged from 156 ± 8 to 210 ± 14 L kg^{-1} of hydroxyl-β-cyclodextrin at a ratio of 1:1 (**Figure 6.4c**), while K_{CD} only decreased about 20% at the ratio of 1:7. This indicates that each antipsychotic compound formed a roundly 1:1 inclusion complex with hydroxyl-β-cyclodextrin. The differences in extraction capacity can be revealed in the MEF (the maximum fraction of a chemical in sediment) according to eq 9. Generally, the hydroxyl-β-cyclodextrin-to-sediment ratio of 1:7 did not lead to a higher extraction efficiency (only 24−28%, **Figure 6.4d**), and this difference between the ratio of 1:3.5 and 1:7 was < 10%. Since these sediments were not spiked, an accessible fraction of the total fraction among these compounds could not be measured. However, our results clearly indicate that dissolved antipsychotic concentrations reached an equilibrium between sediment−water−hydroxyl-β-cyclodextrin when the hydroxyl-β-cyclodextrin-to-sediment ratio was 1:3.5, which was selected in our extraction method for the concentration of a labile chemical in DIFS model.

6.3.5 Chemical resupply kinetics and labile pool

The resupply ability of antipsychotic compounds from the solid phase to the sediment solution can be reflected by R values that correspond to the depletion at the interface of sediment and DGT probes. The R values of antipsychotic compounds generally declined with the increasing deployment time, but R values remained stable after 5 h, except venlafaxine, which had comparable R values (0.11−0.15) at all deployment times. This indicates that these compounds in sediment porewater could be quickly resupplied from the solid phase whereas the resupply decreased and reached the equilibrium (**Figure 6.5**), which is also supported by

the positive fluxes from sediment to overlying water (**Figure 6.2b**). T_c value is associated with the rate of supply from the solid phase to sediment porewater, which reflects the R changes in the short durations as the initial steepness of decline in our results (**Figure 6.5**). The greatest value of T_c was observed for venlafaxine (1.38×10^6 s) whereas other compounds had the same order of magnitude for T_c values (2.63×10^5–4.10×10^5 s), indicating that venlafaxine had less resupply ability in the initial time as shown by the lowest R values for venlafaxine on day 1. Although the initial supply process was sufficient for most antipsychotic compounds, the supply process was limited kinetically with increasing time. This may be partially related to the interaction of ionizable antipsychotic compounds with mineral materials of the sandy sediments investigated here.
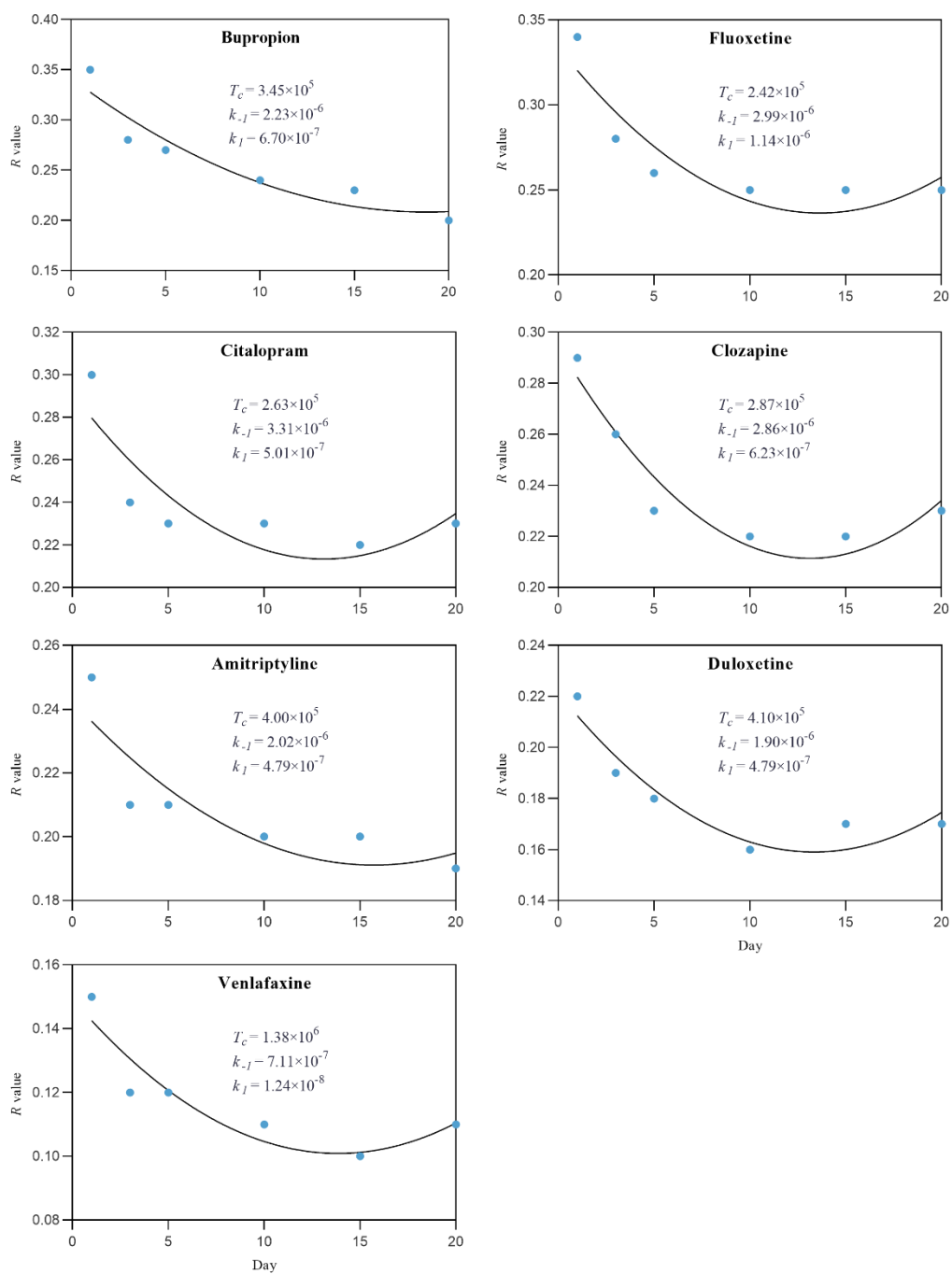
Figure 6.5 The dependence of experimentally measured R ratios for antipsychotic compounds from the filed deployment time. The black line represents the best-fit line of the DIFS model. T_c is the response time (s). k_{-1} and k_1 are the rate constant of desorption and adsorption, respectively.

The Kinetics of resupply is usually important when there is a sufficient labile reservoir in the solid phase. Generally, previous studies(Chen et al., 2014; Li et al., 2021b) used K_d (determined by the extraction of the organic solvent) to reflect the small size of the labile pool when the labile phase will be rapidly depleted so that T_c has little influence on the uptake of analytes by DGT devices. However, results of previous studies (Ji et al., 2022b, c) demonstrated that the differences between K_d and K_{dl} could be 4- to 42-folder, which indicated that the two approaches access different labile pools in the solid phase. Current K_d values obtained by 24 h extraction by a ratio hydroxyl-β-cyclodextrin-to-sediment of 1:3.5 were comparable to K_{dl} derived from the DIFS model (**Table A21**), showing the dissolved phase of antipsychotics is mainly related to the aqueous phase in sediment that can be sufficiently diffused to DGT devices when the water-sediment system reaches equilibrium. The K_{dl} for antipsychotic compounds ranged from 0.01 to 0.15, showing the labile phase was not generally large, which corresponded to R values < 0.5 at the initial time. However, despite the limited labile phase, k_{-1} values were higher for all compounds (**Figure 6.5**), showing the desorption process was dominant in current surficial sediment, which can be accessible by crayfish.

6.5 Conclusion

Prediction of concentrations of organic contaminants in benthic biota and desorption kinetics of contaminants at the interface between water and sediment are meaningful for human health. Combining DGT passive sampling techniques with the steady-state uptake model and DIFS model in the current study provided a close prediction compared to the measured values, except for bupropion and venlafaxine. Desorption processes for seven ionizable moderately

hydrophobic antipsychotics from sediments were accurately modeled. Although the sampling sites had historical detections for the analytes and showed positive fluxes from sediment to overlying water, current equilibrium assumptions for uptake and egestion processes mostly underestimated mean, measured concentration. This is likely because of the individual differences of residues for crayfish and the heterogeneous distribution of contaminants in sediments. The antipsychotic compounds showed the constant ability to resupply compounds to solution, resulting in concentrations greater than MDLs for most captured crayfish, indicating continuous exposure. In different pH environments, ionizable organic compounds may be neutral or ionized, resulting in different binding mechanisms, which will further impact the characteristics of desorption.

CHAPTER 7: General discussion

7.1 Scientific gaps filled in this thesis

Sediment is an important source and sink of various hydrophilic to hydrophobic contaminants, e.g., herbicides, pesticides, antibiotics, and pharmaceuticals, which are present as either dissolved or sorbed to suspended matter and sediment particles based on their physicochemical properties. In anaerobic conditions of sediments, contaminants are less biodegradable, and therefore, stored contaminants in sediments can become a long-lasting potential source, where contaminants may accumulate, recycle, or transform, and interact with the overlying water and the biota that inhabit the space in and above the sediment. This thesis provides a low-cost and effective passive sampler with a series of numerical models to better describe this complex dynamic system in aquatic systems. The scientific gaps that have been filled by this thesis are given below:

● Current DGT passive samplers with a small load (~25 mg) of adsorbent that is commercially accessible have been tested under laboratory-controlled and natural conditions. The DGT samplers could be easily deployed and retrieved in natural aquatic environments. Current DGT samplers could accurately measure the time-weighted average concentration in water with a short deployment period (< 3 weeks).

● Most studies focused on very hydrophobic and neutral organic contaminants in sediments with higher carbon content. This thesis tried to fill this gap by providing measurements of moderately hydrophobic and ionizable organic contaminants in sandy sediments with low

organic matter (~1%). The current numerical model based on DGT samplers (DIFS model) could quantitatively describe that these organic pollutants in the aqueous phase of sediment could be constantly replenished from the sediment solid phase. Furthermore, the magnitude of their desorption rates could be determined by the modeled labile pool size of these chemicals in sediments.

- To our best knowledge, this is the first study to conduct *in-situ* DGT deployment in water and sediment in the natural river for modeling the sorption-desorption kinetic processes of organic contaminants. This is the first time to find that, despite the observation of positive fluxes of detected organic contaminants from sediment to overlying water, the labile pool size derived from the DIFS model cannot reflect the real circumstances for the desorption of organic contaminants. Herein, a supplementary three-compartment kinetic model based on different extraction methods was introduced for the first time and was successfully used to explain the desorption processes within the sediment solid phase.

- To fill the gap of benthic biota bioaccumulation during an exchange of organic contaminants between biological interface and water–sediment compartments by a passive diffusion process, a first-order model for passive transport based on DGT-derived concentrations under a laboratory-controlled experiment was developed and successfully predicted the sediment invertebrate uptake of antipsychotic compounds. This model elucidated that the uptake of organic contaminants by sediment-dwelling invertebrates was highly associated with desorption processes, although the contribution of passive uptake was quite small (<1 %).

- Considering that complex and dynamic sediment–water systems are affected by

hydrodynamic factors, microbial transformations, and physicochemical processes, a mathematical model based on the mass balance of organic chemicals between the aquatic environment and crayfish was developed using the data obtained from DGT samplers deployed in the field and captured crayfish. Although current results based on DGT data underestimated the mean measured concentration in crayfish for some organic contaminants, this model still had the ability to predict the bioconcentration in crayfish. Therefore, the DGT sampler can be proposed as a useful predictive tool for bioaccumulation in benthic invertebrates, and can also provide information on contaminants' resupply from sediments.

7.2 Practical application in aquatic system

Generally, passive sampling strategies such as DGT samplers can be a great supplement for chemical monitoring in the aquatic environment to assess compliance with water quality thresholds and temporal and geographical trends that are used for emission control and source identification, respectively. Passive sampling can be a good option for monitoring micropollutants in a large volume of daily total effluent discharge from wastewater treatment plants (WWTPs) (Challis et al., 2016). Furthermore, ambient water monitoring is also suitable for passive sampling techniques since diluted pollutant concentrations and different pollution sources require continuous monitoring using chemical, toxicological, and biological data.

The development of DGT has been used to investigate the small-scale distribution, resupply kinetics, bioavailability, and speciation of metals and elements in the aquatic system (van Leeuwen et al., 2005; Eismann et al., 2020). Although the DGT sampler had been developed

and tested for ~142 different organic compounds in laboratory-controlled water, WWTPs, and natural water (Ji et al., 2022a), only this present thesis conducted *in situ* DGT deployment in natural water bodies to study the physical processes of organic chemical distribution in sediments. Therefore, the current DGT setup has a wide range of future applications in organic (bio)chemistry and ecotoxicology in the aquatic environment. Furthermore, the combination of DGT-DIFS and biouptake models can also be applied to controlled experiments to better understand the mobility/retention of organic chemicals at the interface of water–sediment and within sediments, as well as bioavailability and associated microbial processes, and persistence of these contaminants. The application of current models with DGT *in situ* deployment can quantitatively provide labile pool size and kinetic resupply, which is very helpful for bioremediation and risk assessment of trace organic contaminants.

Despite the current DGT-associated predictive model for sediment invertebrates not providing a good fit for all organics, the DGT passive sampling strategy still could be used as a tool to measure the labile (desorbing) fraction of organic contaminants for their bioaccessibility and chemical activity. This application can avoid extensive sampling of all relevant matrices (e.g., water, sediment, and prey animals). Moreover, the dissolved concentrations determined by this method allow a direct assessment of whether sediment serves as a sink or a diffusive source due to the fixed transfer process from high to low chemical concentrations. Finally, low cost, easy use, and reutilization after retrieval of this device fit environmental sustainability well. Therefore, the application of the DGT passive sampling technique presented in this thesis can provide more integrated information on contamination and the potential release of these contaminants in the aquatic system for scientists, policy-

makers, and environmental managers.

7.3 Limitations of the current study and future works

In the current DGT configuration, there were no issues of retention of the analytes in the PES filter membrane. However, our review found that the PES filter membrane may not be suitable for all organic compounds, in which a lag time was caused by this filter membrane. Therefore, further developments in DGT configuration are needed. For example, using a new material for the diffusive gel directly as the outer membrane that is more robust with a larger pore size (higher sampling rate).

The DGT sediment probe deployed in sediment cores in this thesis could only provide low-resolution information (~2 cm), which could not accurately provide a finer spatial scale for processes at the interface of water and sediment. Therefore, finer spatial scales of the DGT sediment probe will need to be conducted in the future in order to clarify the dynamic processes of microlayer in the interface of water and sediment and to explain the role of anoxic or oxic environments in regulating retention of organic contaminants in sediments or supply to the overlying water. To date, there is no DGT setup to study trace organic contaminants in three dimensions at the fine scale (mm). This will be beneficial for improvements of detection limits and systems to better understand the biological and (geo)chemical processes of trace organics.

Although the current study observed that the DGT-DIFS model and the first-order three-compartment kinetic model could fit the resupply of organic compounds in sediment porewater well, the mechanism of desorption kinetics may be quite different according to the texture of sediments and physicochemical properties of organics. Therefore, sandy sediments and

ionizable antipsychotic compounds in this thesis provided a limited calibration space for different groups of chemicals and sediments. It should also be noted that porewater collection in this study was conducted in the laboratory with the method of maximum water holding capacity in sediment rather than *in-situ* sediment porewater collection, which may not represent all pressure fluctuations in the water environment due to current and advective flows of dissolved organic matter and particulate. However, there is no standard way to *in-situ* collect sediment porewater in aquatic environments. Thus, the *in-situ* techniques to collect sediment porewater with minimal perturbation of natural porewater inside of the sediment column are urgently needed to develop in the future.

The current diffusion model for bioaccumulation in this thesis was based on non-feeding exposure through passive uptake. However, the food sources and active absorption for sediment-dwelling invertebrates are quite complex. Thus, the uptake model only predicted the small chemical portion in organisms. Besides, the predictive simulation model was based on the chemical mass balance between the organism's depuration/uptake and the aquatic environment under steady-state conditions. Current predicted values could not fit all tested analytes. This uncertainty in the model was highly dependent on the bioenergetics and chemical-related parameters, which need future work considering natural environmental conditions to improve the model-predicted results by calibrating these parameters for different species and organic compounds. Despite bioavailability models for organics first established by DGT-derived concentrations, bioassays to test adverse effects on these aquatic organisms were not included in this thesis. Therefore, future works should combine the modeled bioavailable concentrations and appropriate bioassays to test the toxicity of aquatic organisms.

APPENDICES

Appendix Texts

Appendix 1: Standards, reagents, and chemicals

Nine high purity (> 98%) antipsychotics (amitriptyline[a], bupropion[b], carbamazepine[b], citalopram[a], clozapine[b], duloxetine[a], fluoxetine[c], lamotrigine[a], and venlafaxine[a]) and the corresponding nine mas-labelled internal standards (amitriptyline-d$_6$[b], bupropion-d$_9$[b], carbamazepine-d$_{10}$[b], citalopram-d$_6$[b], clozapine-d$_4$[b], duloxetine-d$_7$[b], fluoxetine-d$_5$[b], lamotrigine-[^{13}C;^{15}N$_4$][a], and venlafaxine-d$_6$[a]) were used. The standard compounds were purchased from: [a] Sigma-Aldrich (Oakville, ON), [b] Toronto Research Chemicals Inc. (North York, ON), and [c] Tokyo Chemical Industry Co., Ltd (Tokyo, Japan).

Antipsychotic stock solutions at 1 mg L^{-1} and internal standard (IS) mixture at 50 µg L^{-1} were dissolved in pure methanol. HPLC grade methanol, dichloromethane, and water purchased from Fisher Scientific (Ottawa, ON) were used for LC solvents, sample extraction, and chemical standards. Optima LC/MS grade formic acid was used as an additive of the LC mobile phase (Fisher Scientific). Agarose and potassium nitrate from Fisher Scientific were used for making gels and adjusting ionic strength, respectively. Milli-Q ultrapure water (EMD Milli-Pore Synergy® system, Etobicoke, ON) reaching resistivity of 18.2 MΩ.cm at 25 °C and total organic carbon (TOC) less than 5 ug/L (ppb) was used for making gels. All glassware was ashed at 450 °C for longer than 4 h and prewashed with methanol before use.

Appendix 2: Sorption experiments of DGT materials

For testing of the potential adsorption of analytes in DGT, it is assumed that all DGT materials (molding, diffusive gel, and PES filter membrane) except for the binding gel do not have a significant affinity to adsorb analytes. A standard solution of the nine antipsychotic compounds at 250 μg L^{-1} was prepared in 1 mM KNO$_3$, and DGT materials were separately exposed to this solution as follows: All DGT materials were separately immersed in 50 mL of the standard solution that was placed in a 100 mL pre-ashed (450 °C in muffle furnace) glass beakers. A magnetic stir bar was added for agitation (4 rpm) at a water temperature of 21$\pm$ 0.5 °C. In order to control for potential changes compared to initial concentrations, analytes in solution were quantified at various durations of 0.5, 1, 2, 48, 60, 72, 96, or 168 h. Samples of 190 μL were taken from the solution, transferred to LC vials, spiked with 10 μL of 1000 μg L^{-1} internal standards, and analyzed by LC-MS. DGT moldings, diffusive gels, and PES filter membrane were spiked with 50 ng internal standards, eluted with 5 mL of methanol, and sonicated three times for 10 min. Eluents were evaporated to near dryness by gentle nitrogen gas, reconstituted in 1 mL methanol, then filtered through a 0.2 μm polytetrafluoroethylene syringe filter into LC vials before quantification by use of LC-MS.

Adsorption experiment by binding gel

Efficient contact times were determined by placing a binding gel (25 mg Sepra^{TM} ZT sorbent) into a 50 mL glass beaker. Thirty milliliters of the standard solution (500 μg L^{-1}) were added to the beaker and magnetically stirred at a constant speed of 4 rpm at 21$\pm$0.5 °C for 24 h. Triplicate samples of water were taken at 11-time intervals (0.5, 0.7, 0.8, 1, 1.5, 1.7, 4, 10, 12, 21 or 24 h), spiked with internal standards and then filtered through a 0.2 μm polytetrafluoroethylene

syringe filter into LC vials before LC-MS analysis.

Capacities of Sepra^{TM} ZT binding gel to adsorb nine (9) antipsychotic compounds were conducted, using the same procedure as the determination for efficient contact time, but at different concentrations (200, 400, 500, 600, 800, 1000, 2000, and 5000 μg L^{-1}) at pH of 7 and 21 ± 0.5 °C. Amounts of analytes adsorbed (Q_e) were calculated according to the initial concentrations (C_0) and the steady state concentrations (C_e) as shown in Eq. (A2.1),

$$Q_e = \frac{(C_0 - C_e) \times V}{1000m} \qquad (A2.1)$$

where V and m represent the volume of the standard solution (mL) and the mass of adsorbent in the binding gel (mg), respectively.

Appendix 3: Procedure of solid-phase extraction (SPE)

The sediment porewater or sediment extract was eluted using 250 mL HPLC-grade water (Fisher Scientific, Ottawa, ON) with the addition of 50 ng internal standards. Strata-X SPE cartridge (Polymeric Reversed Phase, 30mg/1mL, Phenomenex, CA) was initially preconditioned with 5 mL methanol and 10 mL (methanol: dichloromethane, 50:50), followed by 10 mL HPLC-grade water, after which the cartridge was loaded with the diluted sediment porewater/extracts (pH was adjusted to 7) by a vacuum manifold assisted to suck samples. After the suction of the samples, 5 mL of HPLC water was added to wash off the remaining traces of samples. Afterward, the thoroughly-dried cartridge was eluted using 5 mL methanol two times and followed by the concentration by gentle pure N$_2$ flow at a temperature of 15 °C. When the eluents were nearly dry, 1 mL methanol was added to reconstitute. Separated triplicate samples were added of 50 ng internal standards before reconstitution of 1 mL for calculating the

recovery rate. The recovery rate was 77% for amitriptyline-d_6, 75% for bupropion-d_9, 104% for carbamazepine-d_{10}, 82% for citalopram-d_6, 86% for clozapine-d_4, 73% for duloxetine-d_7, 74% for fluoxetine-d_5, 92% for lamotrigine-$[^{13}C;^{15}N_4]$, and 75% for venlafaxine-d_6.

Appendix 4: The first-order three-compartment kinetic model for fast-desorbing fraction

The measure concentrations from the consecutive desorption extraction were fitted with the first-order three-compartment kinetic model, which has been used in soils and sediments (Pignatello, 1990; Cornelissen et al., 1997a):

$$\frac{S_t}{S_0} = F_{rap}e^{-k_{rap}t} + F_{slow}e^{-k_{slow}t} + F_{vs}e^{-k_{vs}t} \quad (A4.1)$$

Where:

$$\frac{dF_{rap}}{dt} = -k_{des}^{rap}F_{rap} \quad (A4.2)$$

$$\frac{dF_{slow}}{dt} = -k_{des}^{slow}F_{slow} \quad (A4.3)$$

$$\frac{dF_{vs}}{dt} = -k_{des}^{vs}F_{vs} \quad (A4.4)$$

Where S_0 and S_t are the mass of psychotic drugs at the beginning (t=0) and interval time during the consecutive extraction period. Because this was not a spiking experiment, S_0 used the total mass of the fast-desorbing fraction, stable-desorbing fraction, and bound-residue fraction. S_t/S_0 is the remaining fraction of analytes in the sediment at each time interval. F_{rap}, $F_{slow,}$ and F_{vs} are the fractions of rapid desorption, slow desorption, and very slow desorption, respectively. k_{rapid}, k_{slow}, and k_{vs} (h^{-1}) are the first-order rate constants of rapid desorption, slow desorption, and very slow desorption, respectively.

When the desorption initially occurs in sediments (t=0), three compartments can be summed

as:

$$F_{rap}^{initial} + F_{slow}^{initial} + F_{vs}^{initial} = 1 \ (A4.5)$$

At each time, all compartments reach balance as:

$$F_{rapid} + F_{slow} + F_{vs} + F_{cum} = 1 \ (A4.6)$$

Where F_{cum} represents the compartment of cumulative desorption.

Appendix 5: Calculation of agarose diffusion coefficient (*D*)

The diffusion cell method

A value for D_{cell} can be calculated by eq. (A5.1) (Cussler, 2009) when the hydrogel-water

distribution coefficient = 1 due to negligible adsorption to the agarose gel.

$$D_{cell} = \frac{1}{\beta t} \ln(\frac{C_S^i - C_R^i}{C_S(t)C_R(t)}) \ \ (A5.1)$$

in which,

$$\beta = \frac{A}{\delta}(\frac{1}{V_S} - \frac{1}{V_R}) \ \ (A5.2)$$

C^i and $C(t)$ represent the initial concentration of the analyte and the concentration at time (t)

respectively. The subscripts S and R represent the source and receiving cell, respectively. A is

the superficial area of the agarose gel, δ is the thickness of the agarose gel, and V is the volume

of solution in each cell. The term $\ln(\frac{C_S^i - C_R^i}{C_S(t)C_R(t)})$ in eq. (A5.1) was plotted against

experimental time, which was fitted using linear regression. Then, the value of D_{cell} was

obtained from the slope of the regression.

The slice-stacking method

The D_{stack} value was calculated for each individual exposure time by fitting data to the model

in Eq. (A5.3) derived from Crank (1979).

$$C = C_i \left(\frac{h}{l} + \frac{2}{\pi} \sum_{n=1}^{\infty} \frac{1}{n} \sin\left(\frac{n\pi h}{l}\right) \exp\left(-\frac{D_{stack} n^2 \pi^2 t}{l^2}\right) \cos\left(\frac{n\pi x}{l}\right) \right) \quad (A5.3)$$

where C and C_i (ng g^{-1}) represent the analyte concentration at the distance of the top of the stack (cm) and the measured initial concentration of the spiked gels, respectively. h and l (cm) represent the thickness of the stack and the thickness of the spiked gels respectively. t (s) is the exposure time and n is the summation index. The measured D_{stack} values were averaged across all exposure times experiments, in which the ultimate concentrations of spiked gels range from 40 to 75% of initial concentrations in consideration of an obvious concentration gradient. For a minimum of the uncertainty, the data out of this range was abandoned.

Appendix 6: Diffusion between sediment and water

The flux of dissolved antipsychotic drugs by diffusion between sediment and water (F_{SW}, ng m^{-2} d^{-1}) can be calculated using Eq. (A6.1).

$$F_{sw} = -k_{sw}\left(C_{DGT-w} - \frac{C_{DGT-s}}{K_s}\right) \quad (A6.1)$$

where C_{DGT-s} is the concentration of analytes in sediments measured using the DGT probe (ng kg^{-1}), and K_s is the sediment-water partitioning coefficient (cm^3 kg^{-1}) based on Schwarzenbach et al. (2017) using f_{oc}=0.014 in the studied sediment, and k_{sw} is the diffusion coefficient (cm d^{-1}) between water and sediment, which can be calculated using Eq. (A6.2). The term C_{DGT-s}/K_s indicates the dissolved concentration in sediment porewater.

$$k_{sw} = \frac{D_w}{\delta_{bl}} \quad (A6.2)$$

where δ_{bl} is the thickness of the boundary layer (m). In this study, the small scale of turbulent

flows was considered only for vertical transport induced by cascading turbulent eddies due to the limited transverse transport distance. The vertical turbulent eddies are defined as the distance from the sediment surface where overturning turbulent motion is governed by molecular viscosity. In this study, δ_{bl} could not be directly characterized using the linear concentration gradient where the transport is dominant by molecular diffusion. δ_{bl} of 0.2 mm was used for all analytes through the calculation based on a kinematic viscosity of 0.013 cm^2 s^{-1} and a fraction velocity of 0.5 cm s^{-1} (Wang et al., 2001; Sherwood et al., 2002).

Appendix 7: Estimation of the labile phase pool

In this study, $C_{DGT, i=21\ d}$ derived from the last day of DGT deployment (21 d) was used to calculate the effective concentration by Eq. (A7.1) to define the available antipsychotic drugs in sediment porewater and the labile pool from the solid phase (Zhang et al., 2006). The effective concentration ($C_{e,\ i=21\ d}$) expresses the concentration ranges of C_{DGT} in the sediment pools for antipsychotic drugs, which describes the desorption behavior of antipsychotic drugs from the solid phase during the DGT deployment (Eq. A7.1).

$$C_{e,i} = \frac{C_{DGT,i=21d}}{R_{diff,i=21d}} \quad (A7.1)$$

where R_{diff} is the ratio of C_{DGT} to C_p in the hypothetical case that the depleted antipsychotic drugs are only supplied from diffusion in porewater without supplies from the solid phase. R_{diff} was calculated by the 2D-DIFS model, which requires sediment porosity (ϕ), particle concentration (P_c), and diffusion layer thickness (δ_{total}) according to the simulation parameter requirements (Harper et al., 1998).

The best-fitted K_{dl} was used to estimate the labile concentration ($C_{l\text{-estimated}}$) of antipsychotic

drugs, expressed as Eq. (A7.2).

$$C_{l-estimated} = C_p \times K_{dl} \quad (A7.2)$$

The $C_{l\text{-estimated}}$ was compared to the concentrations at the beginning and interval time during the consecutive extraction period.

Appendix 8: The computation processes of fraction transfer modeling.

The first-order difference method was used to differentiate the model:

$$\frac{C_{labile}^{i+1} - C_{labile}^{i}}{\tau} = -k_{fs}C_{labile}^{i} - k_{fb}C_{labile}^{i} + k_{sf}C_{stable}^{i} + k_{bf}C_{bound}^{i} \quad (A8.1)$$

$$\frac{C_{stable}^{i+1} - C_{stable}^{i}}{\tau} = -k_{sf}C_{stable}^{i} - k_{sb}C_{stable}^{i} + k_{fs}C_{labile}^{i} + k_{bs}C_{bound}^{i} \quad (A8.2)$$

$$\frac{C_{bound}^{i+1} - C_{bound}^{i}}{\tau} = -k_{bf}C_{bound}^{i} - k_{bs}C_{bound}^{i} + k_{fb}C_{labile}^{i} + k_{sb}C_{stable}^{i} \quad (A8.3)$$

Rate coefficient k was estimated by Genetic algorithm using the results from **Table 3.2**. The minimizations of the residual errors between modeled and measured psychotic drug concentrations were set as the fitness function:

$$\min fit(\gamma) = \sum_{i}(C_{cal}(t_i,\gamma) - C_{obs}(t_i,\hat{\gamma}))^2 \quad (A8.4)$$

$C_{cal}(t_i,\gamma)$ and $C_{obs}(t_i,\hat{\gamma})$: the modeled and measured concentrations. γ: the parameters need to be estimated. τ was set as 0.2 days to run the model.

Appendix 9: The Derivation process for the worm uptake model.

Worms accumulate organic compounds through the passive uptake of dissolved fractions in sediment porewater, which could be regarded as the flow of organic compounds exposed to the

worms as a water resource. The extent of potential water uptake is defined as S_w, corresponding

to the potential depletion rate, T_d, which is affected by several variables, such as DOC,

temperature, microbial activities, and chemical degradation. When the uptake rate of potential

water was distributed equally over a two-dimensional rectangle space, S_w can be expressed as:

$$S_w(t) = \beta(t)\gamma T_d(t) \quad \text{(A9.1)}$$

where S_w (day^{-1}) is the potential water uptake at time t, T_d (cm day^{-1}) is the potential depletion

rate, $\beta(t)$ (cm^{-2}) is the normalized function of water uptake distribution, γ is the water stress

response function, which is a dimensionless function of sediment porewater and osmotic

pressure heads stated in previous reports (Hoffman and Van Genuchten, 1983; Hao et al., 2005).

$\beta(t)$ is the function of time and space, enabling the uptake diffusion to the worm, and can be

further integrated to unity over the diffusion domain as:

$$\int_{\Omega S} \beta(t) dR = 1 \quad \text{(A9.2)}$$

$$\beta(t) = \frac{\rho}{\int_{\Omega S} \rho dz} \quad \text{(A9.3)}$$

where ΩS (cm^3) is the sediment zone for worm habitation, ρ is the particle density. We consider

that worm distribution is uniform during the whole incubation and thus the equation can be

simplified as:

$$\beta(t) = \frac{\rho}{\int_{\Omega S} \rho dz} = \frac{\rho}{\rho \times S_S(t)} = \frac{1}{S_S(t)} \quad \text{(A9.4)}$$

where $S_S(t)$ (cm^2) is the area of the zone where worms inhabit statically. Due to no stress

response in our stably controlled glass tank, γ is equal to 1. The potential loss rate, $T_l(t)$ (ng day^{-1}) can be described as:

$$T_l(t) = T_e \cdot \frac{m_w(t)}{M_w} \quad \text{(A9.5)}$$

243

where T_e is the maximum potential loss rate of worms ($\approx$ 0.2 ng day^{-1}) on the 30th day. $m_w(t)$ (ng) is the total mass of worms on t days, and M_w (ng) is the maximum total mass of worms on the 30th day and they were wet weights by the minusing in this study. The dissolved fraction of analytes in sediment porewater could be approachable to the worms following the water flow within the sediments. Thus, passive analyte uptake by multiplying worms with the dissolved concentrations can be simulated as:

$$P_a(t) = S_w(t) \cdot F_w(t) \quad \text{(A9.6)}$$

Where P (ng cm^{-3} day^{-1}) is the mass of antipsychotic compounds removed per unit time from a unit volume of sediments caused by the passive uptake by worms (simulated by passive samplers–DGT devices), F_w (ng cm^{-3}) is the dissolved concentration of antipsychotic compounds in sediment porewater that can be taken by worms during passive transport. The uptake rate of antipsychotic compounds by worms a can be determined as:

$$a = \frac{S_w(t)}{\theta} \quad \text{(A9.7)}$$

in which, θ is the maximum water content in sediments due to the sediments being submerged by water. Eventually, the accumulated antipsychotic compounds in worms can be described as:

$$\frac{dC}{dt} = \frac{p_a(t) \times V_S}{m(t)} - k_{pl}C \quad \text{(A9.8)}$$

where C represents the concentration of antipsychotic compounds in worms (ng g^{-1}), $p_a(t)$ (ng cm^{-3} day^{-1}) is the mass of antipsychotic compounds removed per unit time in a unit sediment by worm uptake, $m(t)$ is the total mass of triplicate worms from each space at time t (day), V_S (cm^3) is the volume of sediment in each space of glass tank, and k_{pl} (day^{-1}) is the depuration rate constant of antipsychotic compounds in worms. The model was fitted well with R^2=0.826–0.934, and the k_{pl} was calibrated (**Appendix Table A14**).

Appendix 10: Diffusion-induced transport.

The dissolved fraction of analytes is an important part of the labile fraction that dissolves and transports in sediment porewater (F_w) and reversibly gets equilibrium that the fast–desorbing fraction exchange with the fraction adsorbed in sediments (F_s). F_w can transfer the fraction in sediment porewater and F_s is involved in the transfer process, which can be described as:

$$C_{total} = C_{labile} + C_{stable} + C_{bound} \quad \text{(A10.1)}$$

$$C_{labile} = F_w + F_s \quad \text{(A10.2)}$$

$$F_{solid} = F_s + C_{stable} + C_{bound} \quad \text{(A10.3)}$$

$$F_{total} = F_w + F_{solid} \quad \text{(A10.4)}$$

Where C_{labile}, C_{stable}, and C_{bound} are the concentration of the labile (fast-desorbing), stable-adsorbing, and bound-residues fractions of antipsychotic compounds in sediment, respectively. F_w, F_s, and F_{solid} are the concentration of dissolved fraction in sediment porewater, labile fraction associated between the particle sediment and porewater, and total adsorbed on sediment solid phrases, respectively. Thus, the diffusion of antipsychotic compounds in sediments can be simulated as:

$$\frac{\partial F_{total}}{\partial t} = \frac{\partial(\theta F_w)}{\partial t} + \frac{\partial(\rho F_{solid})}{\partial t} = \frac{D_w \theta f \partial^2 F_w}{\partial x^2} - \theta k_{pl} \cdot F_w \quad \text{(A10.5)}$$

Where D_w represents the diffusion coefficient of antipsychotic in sediment porewater, which is taken from our previous study (Ji et al., 2022c), f represents the diffusion impedance factor, and k_{pl} represents the first-order degradation rate constant of dissolved antipsychotic compounds in sediment.

Derivation by chain rule:

$$\frac{\partial F_{solid}}{\partial t} = \frac{\partial F_{solid}\partial F_w}{\partial F_w \partial_t} \quad (A10.6)$$

and

$$\frac{\partial C_{labile}}{\partial t} = (1 + \frac{\rho \partial F_s}{\theta \partial F_w})\frac{\partial (\theta F_w)}{\partial t} \quad (A10.7)$$

The buffering factor was considered (Nelson and Sommers, 1996):

$$b_w = 1 + \frac{\rho \partial F_s}{\theta \partial F_w} \quad (A10.8)$$

The final equation can be given as:

$$b_w \frac{\partial (\theta F_w)}{\partial t} = D_w f \frac{\partial^2 (\theta F_w)}{\partial x^2} - \theta k_{pl} F_w \quad (A10.9)$$

Appendix 11: Modeled solubilization of antipsychotic compounds by DOC

The solubility of compounds in sediment porewater can be associated with diffusion-induced DOC changes. Thus, the solubilization of antipsychotic compounds by DOC during transport can be also influenced. According to the diffusion of two interacting solutes in soil (Nye, 1983), the transport of antipsychotic compounds in the sediments can be described by the diffusion equation as shown below:

$$b_w \theta \frac{F_w - \lambda M}{\partial t} = D_w \theta f \frac{\partial^2 F_w}{\partial^2 x} - \theta k_{deg} F_w \quad (A11.1)$$

where λ is an interaction coefficient between each antipsychotic compound and DOC in the sediments. The relationship between difference of concentrations in porewater with sediment particles can be described by the following equation (Barrow, 2008):

$$\left(-\frac{\Delta C}{\Delta M}\right)_{[F_w]} = \frac{\lambda b_w}{b_M} \quad \text{(A11.2)}$$

The value of b_w can be obtained from the sorption curve of each compound (**Figure A15**), obeying the Freundlich adsorption isotherm (**Figure A16**). The value $\left(-\Delta C / \Delta M\right)_{[F_w]}$ can be obtained from the plot of the depletion of each compound's concentration and DOC (**Figure A17**). The model was fitted well with R^2=0.9960-0.9968. Other parameters can be found in **Table A14**.

Appendix 12: Synthesis process and laboratory test of *β*-cyclodextrin-based polymer

First, tetrafluoroterephthalonitrile (TFTPN) (0.81 g, 4.05 mmol) was dissolved in epichlorohydrin (EPI, 15.00 mL) in a 90 °C water bath and stirred. Next, β-CD (6.12 g, 5.39 mmol) that was previously dissolved in aqueous NaOH (3 mol/L, 10.00 mL) was added dropwise to the solution. Then, the mixture was further stirred for 3 h at 90 °C and then cooled and filtered. The residue was fully washed with water and methanol, and the sequence was carried out three times to obtain a light-yellow solid. After lyophilization for 12 h, EPI–TETPN-crosslinked β-cyclodextrin polymer (T–E–CDP, 3.05 g, 31.7% yield) was finally obtained as a pale-yellow powder (**Figure A23**).

In the adsorption experiments at different concentrations, the adsorbed T–E–CDP agarose gel was extracted with methanol to get a mixture of different compounds and then concentrated to a suitable volume for HPLC-MS analysis.

Adsorption kinetic studies were performed using a 100 mL beaker equipped with magnetic stir bars. All studies were conducted at 25 °C and a stirring rate of 200 rpm. In each study, the

binding gel (adsorbent=50 mg) was added to a specific pollutant stock solution (50 mL) and stirred. At given intervals, about 1 mL of the sample was filtered by a 0.22 μm PTFE membrane filter. The efficiency of compound removal (%) was calculated (Equation A12.1).

$$\text{Removal efficiency} = \frac{C_0 - C_t}{C_0} \times 100 \qquad (A12.1)$$

where C_0 (mmol L^{-1}) is the initial concentration of the compounds in the stock solution, and C_t (mmol L^{-1}) is the residual concentration at time t of the pollutant in the taken sample. The adsorption capacity at contact time t (min) can be calculated by Equation A12.2:

$$q_t = \frac{(C_0 - C_t)V}{m} \qquad (A12.2)$$

where q_t (mmol g^{-1}) is the amount of pollutant adsorbed per gram of adsorbent at time t, m (g) is the mass of the adsorbent, and V (L) is the volume of the aqueous pollutant solution.

The kinetic data were fitted separately with Ho and McKay's pseudo-second-order adsorption model and the Elovich model, using the original equations represented by Equations A12.3 and A12.4, respectively:

$$q_t = \frac{k_2 q_e^2 t}{1 + k_2 q_e t} \qquad (A12.3)$$

$$q_t = \frac{1}{\beta} \ln(\alpha \beta t + 1) \qquad (A12.4)$$

where q_e is the adsorbate uptake (millimole of adsorbate per gram of polymer) at equilibrium, k_2 is the pseudo-second-order rate constant (g mmol^{-1} min^{-1}), α (mmol g^{-1} min^{-1}) is the initial adsorption rate, and β (g mmol^{-1}) is the desorption constant related to the surface coverage.

Our results showed the rapid removal of seven antipsychotic compounds in water (**Figure A24**). The adsorption efficiency for the T-E-CDP binding gel can be more than 90% within 30

min, which reflects the adsorption equilibrium within 30 min. The kinetics data fitted very well with the pseudo-second-order model and Elovich model with a good regression coefficient ($R^2 >$ 0.9) (**Figure A25**). Generally, the pseudo-second-order model assumes that the sorption rate is controlled by chemical sorption, and the sorption capacity is proportional to the number of active sites on the sorbent (Ho and McKay, 1999). The Elovich model indicates that sorption is controlled by multiple mechanisms (Yao et al., 2014). The adsorption mechanisms may include the formation of inclusion complexes between antipsychotic compounds and CD cavities in the polymer, and the formation of hydrogen bonds between hydroxyl groups of the polymer and ionizable antipsychotic compounds. Overall, T-E-CDP as an adsorbent in binding gel can have a good adsorption performance on these study compounds.

Appendix 13: Analysis details for Sobol Global Sensitivity Analysis (SGSA)

Sobol Global Sensitivity Analysis is a global sensitivity analysis for complex mathematical models. Based on Quasi-Monte Carlo methods, the estimation of SGSA can be more efficient for the low-discrepancy sequences. The computation steps are as follows:

1. Using a Quasi-Monte Carlo method to generate an $N*2d$ sample matrix, where N is the number of samples and d is the number of variables of the model. In the current computation, N was set as 50,000, and d was set as 3 for the three variables (C_i, C_w, and C_s) in the organism uptake model.

2. Take the first d columns from the matrix as matrix A, and the left d columns as matrix B.

3. Establish d further $N*d$ matrices AB^i, as $i = 1, 2, \ldots, d$. for AB^i, the ith column of AB^i = the ith column of B, and the left columns are from A.

4. Use A, B, and the d AB^i matrices as the input for the model and obtain the corresponding model output values as $f(A)$, $f(B)$, and $f(AB^i)$ (Equations A13.1–A13.5).

$$S_i = \frac{Var_{Xi}(E_{xi}(Y \mid Xi))}{Var(Y)} \qquad \text{(A13.1)}$$

$$STi = \frac{E_{xi}(Var_{xi}(Y \mid Xi))}{Var(Y)} \qquad \text{(A13.2)}$$

In which,

$$Var_{Xi}(E_{xi}(Y \mid Xi)) \approx \frac{1}{N}\sum_{j=1}^{N} f(B)_j \bullet (f(AB^i)_j - f(A)_j) \qquad \text{(A13.3)}$$
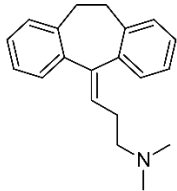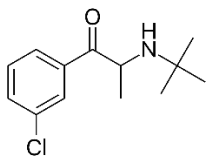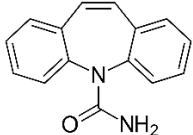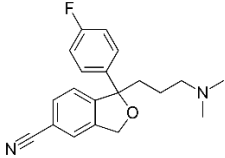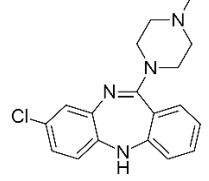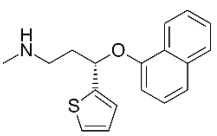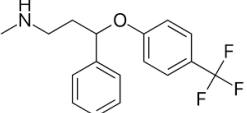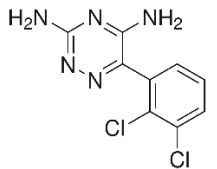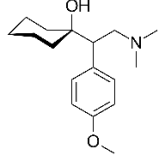
$$E_{xi}(Var_{Xi}(Y \mid Xi)) \approx \frac{1}{2N}\sum_{j=1}^{N}(f(A)_j - f(AB^i)_j)^2 \qquad \text{(A13.4)}$$

$$Var(Y) = Var(A + B) \qquad \text{(A13.5)}$$

From the parameters of uncertainty used in our computation of SGSA as S_i and S_t, the values of St represented the sensitivity to the model output.

Appendix Tables

Table A1 Physical-chemical properties of targeted antipsychotic compounds.

Compound	Structure	CAS	MW	S_W (mg/L)	$pK_{a1,2}$	$LogK_{ow}$
Amitriptyline		50-48-6	277.4	0.8239	9.4	4.95
Bupropion		34911-55-2	239.74	140.2	8.22	3.85
Carbamazepine		298-46-4	236.27	17.66	13.9	2.25
Citalopram		59729-33-8	324.4	31.09	9.78	3.74
Clozapine		5786-21-0	326.8	11.84	7.5	3.35
Duloxetine		116539-59-4	297.4	10.00	9.7	4.68
Fluoxetine		54910-89-3	309.33	38.35	9.8	4.65
Lamotrigine		84057-84-1	256.09	3127	8.53	0.99
Venlafaxine		93413-69-5	277.4	266.7	10.09	3.28

Water solubilities (S_W) and *n*-octanol-water partitioning coefficients ($LogK_{ow}$) were predicted

using US Environmental Protection Agency's EPISuite™.

Table A2 Key parameters and values of DGT induced fluxes in sediments (DIFS) model.

Parameter	Description	Units	Default values
C	Dissolved concentration	mol cm^{-3}	Auto
C_s	Sorbed concentration (solid phase)	mol g^{-1}	Auto
D_s	Diffusion coefficient in sediment	cm^2 s^{-1}	Auto
D_d	Diffusion coefficient in diffusion layer	cm^2 s^{-1}	Input
T_c	Response time	s	Input/output
K_d	Distribution rate	cm^3 g^{-1}	Input/output
k_f	Adsorption rate	s^{-1}	Output
k_b	Desorption rate	s^{-1}	Output
Δg	Thickness of diffusion layer	mm	Input
m	Mass accumulated by unit area of resin	mol cm^{-2}	1
F	Flux from sediment solution to	mol cm^{-2} s^{-1}	1
R	Ratio of DGT estimated to solution concentration	Dimensionless	Input
t	Deployment time	h	Input
P_c	Particle concentration	g cm^{-3}	2.1
Φ_s	Porosity of sediment	Dimensionless	0.56
Φ_d	Porosity of diffusion gel	Dimensionless	0.98

Table A3 Precursor and product ions ([M+H]$^+$), collision energy (HCD), and retention time of analytes using the full-scan parallel reaction monitoring (PRM) Orbitrap^{TM} mass spectrometer method.

Compound	Precursor ion	Product ion	HCD	Retention time (min)
Amitriptyline	278.190	233.132	35	7.57
Amitriptyline-D$_6$	284.228	233.132	35	7.57
Bupropion	240.115	184.052	25	5.45
Bupropion-D$_9$	249.171	185.059	25	5.43
Carbamazepine	237.102	194.097	35	8.08
Carbamazepine-D$_{10}$	247.165	204.159	35	8.04
Citalopram	325.171	109.045	40	6.59
Citalopram-D$_6$	331.209	109.045	40	6.59
Clozapine	327.137	270.079	35	6.29
Clozapine-D$_4$	331.162	272.092	35	6.24
Duloxetine	298.126	183.081	30	7.53
Duloxetine-D$_7$	305.170	189.118	30	7.50
Fluoxetine	310.141	148.112	25	7.70
Fluoxetine-D5	315.173	153.144	25	7.70
Lamotrigine	256.015	210.983	70	4.57
Lamotrigine-[^{13}C;^{15}N$_4$]	261.007	213.980	70	4.57
Venlafaxine	278.211	260.201	25	6.10
Venlafaxine-D$_6$	284.249	266.239	25	6.09

Table A4 Calibration curves (ranged from 0.01 to 950 μg L^{-1}) of the 9 antipsychotic compounds and R^2 ranges during the all samples run.

Compound	*Calibration curve	*R^2	R^2 ranges
Venlafaxine	Y = -0.00293663+0.0283401 X	0.9973	0.9964–0.9974
Fluoxetine	Y = -0.00472171+0.0295973 X	0.9986	0.9986–0.9994
Clozapine	Y = -0.00252042+0.0224591 X	0.9912	0.9908–0.9915
Citalopram	Y = -0.047859+0.208303 X	0.9944	0.9940–0.9949
Duloxetine	Y = -0.00679154+0.0288166 X	0.9911	0.9905–0.9920
Amitriptyline	Y = -0.0593065+0.377414 X	0.9970	0.9965–0.9978
Bupropion	Y = -0.000962958+0.0205702 X	0.9917	0.9912–0.9918
Carbamazepine	Y = 5.21523e-006+0.0256232 X	0.9930	0.9926–0.9939
Lamotrigine	Y = -0.00576197+0.0252794 X	0.9928	0.9924–0.9934

*It should be noted that the calibration curves and R^2 values were taken from the test of standard curve solutions.

Table A5 LOD, LOQ, and MDL (μg L^{-1}) for all nine antipsychotic compounds.

Compound	LOD	LOQ	MDL
Venlafaxine	0.23	0.77	0.033
Fluoxetine	1.46	4.87	0.024
Clozapine	0.38	1.28	0.035
Citalopram	2.14	7.13	0.016
Duloxetine	0.21	0.69	0.124
Amitriptyline	1.81	6.03	0.059
Bupropion	0.35	1.17	0.030
Carbamazepine	1.25	4.17	0.016
Lamotrigine	0.20	0.67	0.025

Table A6 Diffusion coefficients (cm^2 s^{-1}) of nine antipsychotic compounds (average ± standard deviation) in different thicknesses of agarose diffusive gel measured by the two-compartment diffusion cell at 21 °C.

Compound	0.75 mm	1 mm	2 mm	1.5 mm	1.8 mm	2 mm	3 mm
Carbamazepine	$4.98\times10^{-6}\pm6.25\times10^{-7}$	$4.88\times10^{-6}\pm6.66\times10^{-7}$	$4.95\times10^{-6}\pm1.17\times10^{-6}$	$4.90\times10^{-6}\pm7.13\times10^{-7}$	$4.96\times10^{-6}\pm1.23\times10^{-6}$	$4.79\times10^{-6}\pm9.06\times10^{-7}$	$4.72\times10^{-6}\pm7.47\times10^{-7}$
Bupropion	$4.03\times10^{-6}\pm4.61\times10^{-7}$	$3.95\times10^{-6}\pm1.01\times10^{-6}$	$3.98\times10^{-6}\pm5.5\times10^{-7}$	$4.02\times10^{-6}\pm9.19\times10^{-7}$	$4.01\times10^{-6}\pm5.68\times10^{-7}$	$3.87\times10^{-6}\pm8.58\times10^{-7}$	$3.85\times10^{-6}\pm4.98\times10^{-7}$
Lamotrigine	$4.92\times10^{-6}\pm2.83\times10^{-7}$	$4.99\times10^{-6}\pm3.4\times10^{-7}$	$4.98\times10^{-6}\pm2.91\times10^{-7}$	$5.00\times10^{-6}\pm3.13\times10^{-7}$	$5.01\times10^{-6}\pm3.48\times10^{-7}$	$4.94\times10^{-6}\pm3.50\times10^{-7}$	$4.97\times10^{-6}\pm4.36\times10^{-7}$
Amitriptyline	$5.97\times10^{-6}\pm1.24\times10^{-6}$	$5.86\times10^{-6}\pm8.44\times10^{-7}$	$5.86\times10^{-6}\pm6.92\times10^{-7}$	$5.96\times10^{-6}\pm6.37\times10^{-7}$	$5.88\times10^{-6}\pm1.03\times10^{-6}$	$5.78\times10^{-6}\pm1.03\times10^{-6}$	$5.66\times10^{-6}\pm7.91\times10^{-7}$
Venlafaxine	$3.17\times10^{-6}\pm5.09\times10^{-7}$	$3.12\times10^{-6}\pm7.16\times10^{-7}$	$3.12\times10^{-6}\pm7.22\times10^{-7}$	$3.14\times10^{-6}\pm5.62\times10^{-7}$	$3.13\times10^{-6}\pm3.66\times10^{-7}$	$3.07\times10^{-6}\pm7.93\times10^{-7}$	$2.98\times10^{-6}\pm3.09\times10^{-7}$
Duloxetine	$3.27\times10^{-6}\pm7.57\times10^{-7}$	$3.26\times10^{-6}\pm8.38\times10^{-7}$	$3.25\times10^{-6}\pm7.79\times10^{-7}$	$3.25\times10^{-6}\pm4.59\times10^{-7}$	$3.23\times10^{-6}\pm3.77\times10^{-7}$	$3.15\times10^{-6}\pm5.95\times10^{-7}$	$3.08\times10^{-6}\pm4.65\times10^{-7}$
Fluoxetine	$4.24\times10^{-6}\pm5.47\times10^{-7}$	$4.19\times10^{-6}\pm7.16\times10^{-7}$	$4.23\times10^{-6}\pm4.60\times10^{-7}$	$4.19\times10^{-6}\pm5.25\times10^{-7}$	$4.20\times10^{-6}\pm8.45\times10^{-7}$	$4.10\times10^{-6}\pm9.41\times10^{-7}$	$4.06\times10^{-6}\pm6.53\times10^{-7}$
Citalopram	$6.02\times10^{-6}\pm8.37\times10^{-7}$	$5.94\times10^{-6}\pm1.41\times10^{-6}$	$5.94\times10^{-6}\pm1.37\times10^{-6}$	$5.91\times10^{-6}\pm1.07\times10^{-6}$	$5.93\times10^{-6}\pm1.29\times10^{-6}$	$5.81\times10^{-6}\pm1.04\times10^{-6}$	$5.74\times10^{-6}\pm5.81\times10^{-7}$
Clozapine	$4.66\times10^{-6}\pm7.69\times10^{-7}$	$4.62\times10^{-6}\pm5.22\times10^{-7}$	$4.61\times10^{-6}\pm5.45\times10^{-7}$	$4.57\times10^{-6}\pm6.95\times10^{-7}$	$4.58\times10^{-6}\pm5.13\times10^{-7}$	$4.49\times10^{-6}\pm1.03\times10^{-6}$	$4.44\times10^{-6}\pm6.36\times10^{-7}$

Table A7 The physicochemical properties of sediment.

Depth (cm)	pH	Particle size distribution (%)			Total C (%)	Dissolved organic C (mg L^{-1})
		Sand	Silt	Clay		
0-2	7.65	49	36	15	1.4	630
4-6	7.43	48	37	15	1.9	634
6-8	7.12	45	34	21	1.2	658
8-10	6.93	43	32	25	1.5	692
10-12	6.82	42	36	22	1.2	623
12-15	6.97	39	38	23	1.1	631

pH was measured using a ratio of 1:2.5 dry sediment/1 M KCl. Total C was determined by combustion LECO method. Dissolved organic C in soil was extracted by 0.5 M K_2SO_4. Particle size distribution was measured by hydrometer method. All the measurements were conducted in Bureau Veritas Laboratory (Edmonton, AB).

Table A8 The fractions and rate constants for the rapid, slow, and very slow of nine psychotic drugs in sediment at DGT deployment day 1 and 2 predicted by the consecutive methanol extraction.

Compound	Day	F_{rapid}	k_{rapid}	F_{slow}	k_{slow}	F_{vs}	k_{vs}	r^2
Amitriptyline	1	0.249	0.174	0.322	0.021	0.417	0.000002	0.985
	21	0.184	0.083	0.303	0.015	0.500	0.000001	0.988
Bupropion*	1	0.403	0.466	0.429	0.145	0.155	0.000013	0.998
	21	0.331	0.415	0.343	0.103	0.314	0.000009	0.998
Carbamazepine	1	0.409	0.517	0.516	0.342	0.063	0.000031	0.991
	21	0.355	0.367	0.323	0.316	0.310	0.000029	0.992
Citalopram	1	0.261	0.143	0.378	0.121	0.349	0.000011	0.998
	21	0.127	0.042	0.353	0.025	0.508	0.000002	0.998
Clozapine	1	0.298	0.152	0.387	0.013	0.303	0.000001	0.998
	21	0.236	0.120	0.343	0.014	0.410	0.000001	0.995
Duloxetine*	1	0.198	0.150	0.350	0.024	0.440	0.000002	0.997
	21	0.147	0.113	0.311	0.018	0.531	0.000002	0.996
Fluoxetine	1	0.320	0.263	0.417	0.129	0.251	0.000012	0.998
	21	0.275	0.242	0.338	0.102	0.375	0.000009	0.998
Lamotrigine	1	0.411	0.531	0.406	0.256	0.172	0.000023	0.993
	21	0.329	0.383	0.398	0.213	0.261	0.000019	0.992
Venlafaxine	1	0.120	0.032	0.224	0.0407	0.644	0.000004	0.997
	21	0.098	0.016	0.218	0.0108	0.672	0.000001	0.996

*It should be noted that bupropion and duloxetine did not consider bound-residue fraction data to calculate the total concentration due to the significant loss during the alkaline hydrolysis.

Table A9 The concentration (μg kg^{-1}) of nine psychotic drugs with standard deviation from triplicate samples in sediment extracted for stable-desorbing fraction after the consecutive extraction for fast-desorbing fraction at each DGT deployment time.

Compound	D1	D3	D6	D9	D12	D15	D21
Amitriptyline	0.11±0.02	0.11±0.01	0.16±0.03	0.13±0.03	0.17±0.03	0.19±0.04	0.20±0.03
Bupropion	2.12±0.44	4.71±0.48	2.88±0.51	2.46±0.47	4.03±0.42	5.23±0.88	6.32±0.73
Carbamazepine	0.13±0.02	0.17±0.03	0.14±0.03	0.20±0.04	0.17±0.03	0.18±0.02	0.19±0.03
Citalopram	0.01±0.001	0.03±0.01	0.02±0.004	0.04±0.01	0.03±0.004	0.03±0.01	0.03±0.01
Clozapine	0.32±0.04	0.34±0.05	0.32±0.04	0.27±0.03	0.33±0.04	0.39±0.06	0.47±0.06
Duloxetine	0.03±0.01	0.02±0.002	0.03±0.01	0.01±0.001	0.02±0.002	0.02±0.003	0.01±0.001
Fluoxetine	0.77±0.08	0.60±0.08	0.88±0.16	0.77±0.09	0.98±0.21	1.23±0.14	1.43±0.28
Lamotrigine	0.44±0.05	0.40±0.05	0.65±0.13	0.52±0.06	0.68±0.12	0.79±0.10	0.85±0.16
Venlafaxine	0.98±0.13	0.54±0.07	1.53±0.24	1.77±0.34	1.03±0.15	1.75±0.26	1.04±0.15

Table A10 The concentration (μg kg^{-1}) of non-degraded psychotic drugs with standard deviation from triplicate samples in hydrolyzed sediment for bound-residue fraction at each DGT deployment time.

Compound	D1	D3	D6	D9	D12	D15	D21
Amitriptyline	0.83±0.09	1.04±0.13	1.85±0.26	1.92±0.25	2.82±2.82	2.94±0.34	3.12±0.43
Carbamazepine	0.18±0.02	0.36±0.05	0.35±0.05	0.58±0.07	0.65±0.09	0.78±0.08	0.91±0.14
Citalopram	0.01±0.001	0.02±0.003	0.01±0.002	0.03±0.003	0.06±0.01	0.04±0.01	0.02±0.003
Clozapine	1.13±0.13	0.43±0.06	0.30±0.03	0.34±0.05	0.47±0.07	0.32±0.04	0.37±0.04
Fluoxetine	0.41±0.06	0.28±0.03	0.49±0.07	0.31±0.03	0.46±0.07	0.41±0.05	0.32±0.04
Lamotrigine	0.67±0.10	1.09±0.16	1.37±0.22	2.15±0.31	2.16±0.28	3.45±0.44	3.98±0.57
Venlafaxine	0.98±0.14	1.17±0.17	1.32±0.17	1.58±0.16	2.60±0.41	3.82±0.49	4.11±0.47

Table A11 The concentration (μg kg^{-1}) of psychotic drugs in the three fractions in sampled sediments at individual time.

Compound	Fraction	1 d	3 d	6 d	9 d	12 d	15 d	21 d
Amitriptyline	Stable	0.11	0.11	0.16	0.13	0.17	0.19	0.20
	Bound	0.83	1.04	1.85	1.92	2.82	2.94	3.12
	Labile	0.42	0.49	0.78	0.76	0.79	0.73	0.68
	Total	1.37	1.64	2.80	2.82	3.78	3.86	4.00
Bupropion	Stable	2.12	4.71	2.88	2.46	4.03	5.23	6.32
	Bound	NA	NA	NA	NA	NA	NA	NA
	Labile	0.78	1.65	0.91	0.58	0.71	0.85	0.94
	Total	2.91	6.36	3.79	3.04	4.74	6.08	7.27
Carbamazepine	Stable	0.13	0.17	0.14	0.20	0.17	0.18	0.19
	Bound	0.18	0.36	0.35	0.58	0.65	0.78	0.91
	Labile	0.15	0.24	0.19	0.26	0.22	0.18	0.18
	Total	0.46	0.76	0.68	1.05	1.04	1.15	1.28
Citalopram	Stable	0.01	0.03	0.02	0.04	0.03	0.03	0.03
	Bound	0.01	0.02	0.01	0.03	0.06	0.04	0.02
	Labile	0.004	0.02	0.01	0.01	0.02	0.01	0.01
	Total	0.02	0.07	0.04	0.08	0.11	0.09	0.06
Clozapine	Stable	0.32	0.34	0.32	0.27	0.33	0.39	0.47
	Bound	1.13	0.43	0.30	0.34	0.47	0.32	0.37
	Labile	0.38	0.19	0.12	0.10	0.12	0.10	0.10
	Total	1.83	0.97	0.75	0.71	0.92	0.80	0.94
Duloxetine	Stable	0.03	0.02	0.03	0.01	0.02	0.02	0.01
	Bound	NA	NA	NA	NA	NA	NA	NA
	Labile	0.006	0.002	0.003	0.001	0.001	0.001	0.0004
	Total	0.04	0.02	0.03	0.01	0.02	0.02	0.01
Fluoxetine	Stable	0.77	0.60	0.88	0.77	0.98	1.23	1.43
	Bound	0.41	0.28	0.49	0.31	0.47	0.41	0.32
	Labile	0.42	0.28	0.36	0.22	0.26	0.27	0.24
	Total	1.60	1.16	1.73	1.29	1.72	1.91	1.99
Lamotrigine	Stable	0.44	0.40	0.65	0.52	0.68	0.79	0.85
	Bound	0.67	1.09	1.37	2.15	2.16	3.45	3.98
	Labile	0.50	0.61	0.78	0.89	0.90	1.27	1.28
	Total	1.61	2.09	2.80	3.56	3.73	5.50	6.11
Venlafaxine	Stable	0.98	0.54	1.53	1.77	1.03	1.75	1.04
	Bound	0.88	1.17	1.32	1.53	2.60	3.82	4.11
	Labile	0.28	0.23	0.32	0.36	0.32	0.49	0.36
	Total	2.13	1.94	3.17	3.65	3.95	6.07	5.51

Table A12 Daily monitored water quality parameters from surface water in the glass tanks (1 mg kg⁻¹ and 10 mg kg⁻¹ spiked).

Day	DO (mg/L)	Temperature (°C)	pH	Conductivity (µm/cm)	Ammonia (mg/L)
			1 mg kg⁻¹ spiked		
1	8.3±0.9	21.7	8.28±1.3	710±112	0.33±0.05
2	8.8±1.0	21.8	8.58±1.1	717±101	0.36±0.05
3	8.1±1.1	20.2	8.50±1.3	719±100	0.39±0.06
4	8.5±1.2	21.5	8.68±1.3	738±75	0.34±0.04
5	8.5±0.9	20.4	8.79±0.9	745±113	0.39±0.05
6	8.3±1.1	21.4	8.83±1.0	716±112	0.34±0.05
7	8.4±1.3	20.1	8.80±1.0	704±107	0.35±0.04
8	9.6±1.2	20.3	8.02±1.2	750±108	0.41±0.05
9	8.1±1.1	21.5	8.72±1.3	712±95	0.35±0.05
10	8.0±0.8	21.2	8.46±0.9	707±84	0.31±0.04
11	9.2±1.0	21.8	8.99±1.1	742±104	0.34±0.05
12	9.0±0.9	21.4	8.42±1.3	714±82	0.39±0.05
13	9.7±1.3	21.4	8.80±1.2	705±98	0.31±0.04
14	8.4±0.9	21.9	8.18±1.3	745±88	0.33±0.04
15	8.3±0.8	21.3	8.57±1.2	750±103	0.39±0.04
16	8.8±1.2	21.1	8.81±1.0	733±87	0.32±0.04
17	8.6±0.9	20.5	8.39±0.9	721±95	0.30±0.03
18	8.7±1.3	21.6	8.38±1.2	710±86	0.35±0.05
19	8.4±0.9	21.7	8.27±1.0	727±93	0.36±0.04
20	9.1±1.0	21.6	8.77±1.1	750±84	0.33±0.05
21	8.5±1.1	20.3	8.30±1.1	733±76	0.36±0.05
22	9.7±1.5	21.2	8.33±0.9	703±74	0.40±0.05
23	9.4±1.2	21.6	8.20±1.2	706±96	0.34±0.04
24	9.5±1.0	20.7	8.65±0.9	702±94	0.32±0.05
25	8.8±1.1	21.3	8.00±1.0	702±80	0.33±0.04
26	8.1±1.2	21.2	8.30±1.0	729±93	0.34±0.04
27	9.4±1.1	20.4	8.23±0.9	705±106	0.30±0.05
28	9.5±1.2	20.7	8.72±1.2	701±89	0.32±0.04
29	9.3±1.1	21.0	8.09±1.0	716±107	0.34±0.05
30	9.5±1.1	20.3	8.94±1.3	719±72	0.37±0.05
			10 mg kg⁻¹ spiked		
1	8.3±0.9	20.5	8.22±1.27	665±79	0.24±0.03
2	8.8±1.1	21.3	8.32±0.86	695±80	0.35±0.06
3	9.3±0.9	21.8	8.56±1.21	657±73	0.27±0.03
4	9.2±1.1	20.0	8.26±1.19	691±71	0.30±0.05
5	9.8±1.2	21.1	8.12±0.87	699±73	0.26±0.03
6	9.7±1.5	21.8	8.89±1.03	659±70	0.21±0.03
7	8.6±1.3	21.2	8.09±1.27	668±87	0.33±0.04

8	9.4±1.1	21.3	8.97±1.22	686±86	0.34±0.06
9	9.7±1.6	21.3	8.37±0.96	707±95	0.32±0.05
10	10.0±1.3	21.6	8.70±1.08	665±71	0.29±0.05
11	8.2±1.3	21.6	8.51±1.24	675±84	0.35±0.05
12	9.6±1.5	21.3	8.26±1.17	662±100	0.33±0.04
13	10.0±1.3	20.2	8.58±1.15	704±105	0.25±0.03
14	8.3±1.2	21.5	8.32±1.01	693±99	0.26±0.04
15	8.2±1.2	21.5	8.38±1.29	690±95	0.28±0.04
16	8.5±1.1	21.5	8.44±0.88	683±85	0.27±0.04
17	9.2±1.2	21.3	8.06±1.02	660±76	0.32±0.03
18	8.5±1.4	20.9	8.07±1.04	694±89	0.23±0.03
19	9.7±1.1	21.0	8.43±1.22	663±103	0.36±0.04
20	8.7±0.9	21.4	8.89±1.09	704±102	0.31±0.05
21	8.5±0.9	22.0	8.16±1.19	674±80	0.28±0.03
22	8.7±1.0	21.3	8.09±1.20	678±107	0.31±0.05
23	8.7±1.3	20.5	8.10±1.25	686±79	0.32±0.05
24	8.1±0.9	20.4	8.95±1.15	701±84	0.21±0.03
25	8.2±1.3	20.2	8.17±0.85	676±100	0.36±0.04
26	8.2±1.0	21.7	8.69±1.16	700±101	0.26±0.03
27	9.3±1.4	20.9	8.80±0.94	659±95	0.36±0.04
28	9.6±1.1	21.2	8.05±1.08	659±85	0.22±0.03
29	8.2±1.2	20.6	8.66±1.10	705±97	0.24±0.03
30	8.8±1.3	21.4	8.37±0.88	692±107	0.33±0.04

Table A13 The concentrations (ng mg^{-1}) of antipsychotic compounds in the tissue of *Lumbriculus variegatus* exposed to 1 mg kg^{-1} spiked sediment for 14 days without the gut purging, with 6 h purging, and with 24 h purging.

	Non-purging	6 h purging	24 purging
Lamotrigine	1.17±0.18	1.12±0.12	1.07±0.14
Bupropion	2.82±0.35	2.69±0.34	2.61±0.28
Carbamazepine	2.32±0.34	2.24±0.34	2.18±0.27
Citalopram	2.45±0.36	2.35±0.29	2.31±0.28
Clozapine	1.92±0.22	1.84±0.26	1.79±0.22
Duloxetine	4.99±0.64	4.81±0.57	4.57±0.69
Fluoxetine	3.18±0.40	3.00±0.43	2.87±0.32
Amitriptyline	6.59±0.79	6.14±0.66	5.83±0.77
Venlafaxine	1.75±0.19	1.69±0.20	1.61±0.19

Table A14 The parameters for the models.

	Carbamazepine	Lamotrigine	Venlafaxine	Clozapine	Citalopram	Fluoxetine	Bupropion	Duloxetine	Amitriptyline
Worm uptake									
γ^*					1				
T_e^*					0.2				
$k_{pl}^{\#}$	0.023	0.031	0.025	0.020	0.016	0.014	0.012	0.010	0.008
Diffusion-induced transport									
ρ^*					1.65				
θ^*					0.46				
λ^*	2.81×10^{-6}	3.76×10^{-6}	3.04×10^{-6}	2.90×10^{-6}	2.77×10^{-6}	2.86×10^{-6}	3.20×10^{-6}	2.92×10^{-6}	2.90×10^{-6}
$F_w^{\#}$	189	209	200	198	193	184	185	193	195
b_{DOC}^*					5.8				
$D_w^{\#}$	4.46×10^{-6}	5.41×10^{-6}	4.56×10^{-6}	4.39×10^{-6}	4.31×10^{-6}	4.67×10^{-6}	5.19×10^{-6}	4.54×10^{-6}	4.46×10^{-6}
$D_{DOC}^{\#}$					0.0043				
$k_{deg}^{\#}$	0.378	0.417	0.400	0.396	0.386	0.368	0.370	0.386	0.390
$k_{DOC}^{\#}$					0.001				
Fractions transfer									
$k_{fs}^{\#}$	7.14×10^{-2}	2.56×10^{-3}	7.39×10^{-4}	3.76×10^{-3}	3.43×10^{-3}	2.20×10^{-3}	/	/	3.93×10^{-3}
$k_{sf}^{\#}$	7.88×10^{-2}	4.05×10^{-3}	1.49×10^{-3}	5.87×10^{-3}	5.25×10^{-3}	3.63×10^{-3}	/	/	4.14×10^{-2}
$k_{fb}^{\#}$	9.57×10^{-4}	3.09×10^{-4}	1.15×10^{-4}	5.14×10^{-3}	4.68×10^{-3}	9.16×10^{-3}	/	/	4.68×10^{-4}
$k_{bf}^{\#}$	5.35×10^{-4}	4.28×10^{-4}	1.30×10^{-4}	2.19×10^{-3}	2.00×10^{-3}	3.60×10^{-4}	/	/	3.81×10^{-4}
$k_{sb}^{\#}$	9.37×10^{-3}	6.72×10^{-3}	1.97×10^{-3}	3.08×10^{-4}	2.82×10^{-4}	1.12×10^{-3}	/	/	6.90×10^{-3}
$k_{bs}^{\#}$	1.32×10^{-2}	4.23×10^{-2}	1.17×10^{-2}	2.71×10^{-3}	2.52×10^{-3}	3.77×10^{-2}	/	/	4.96×10^{-2}

[*] The parameter was measured by experiments.

[**] The parameter was used from the empirical value.

[#] The parameter was obtained by model calibration.

Table A15 The concentration (mg kg⁻¹) of antipsychotic compounds from triplicate samples of spiked sediments (1 and 10 mg kg⁻¹ respectively) in each space.

	Lamotrigine	Bupropion	Venlafaxine	Clozapine	Citalopram	Duloxetine	Amitriptyline	Fluoxetine	Carbamazepine
1 mg kg⁻¹ spiked sediments									
Space 1	0.11 ± 0.01	0.32 ± 0.05	0.15 ± 0.02	0.21 ± 0.02	0.12 ± 0.02	0.11 ± 0.01	0.32 ± 0.05	0.18 ± 0.02	0.38 ± 0.05
Space 2	0.10 ± 0.01	0.31 ± 0.03	0.13 ± 0.02	0.20 ± 0.03	0.12 ± 0.01	0.13 ± 0.02	0.29 ± 0.04	0.17 ± 0.02	0.36 ± 0.04
Space 3	0.10 ± 0.01	0.27 ± 0.03	0.11 ± 0.01	0.17 ± 0.02	0.12 ± 0.01	0.10 ± 0.01	0.25 ± 0.04	0.17 ± 0.02	0.35 ± 0.04
Space 4	0.09 ± 0.01	0.28 ± 0.04	0.13 ± 0.02	0.19 ± 0.03	0.13 ± 0.02	0.09 ± 0.01	0.29 ± 0.04	0.18 ± 0.02	0.31 ± 0.04
Space 5	0.09 ± 0.01	0.25 ± 0.03	0.10 ± 0.01	0.15 ± 0.02	0.12 ± 0.01	0.09 ± 0.01	0.24 ± 0.03	0.16 ± 0.02	0.30 ± 0.03
Space 6	0.12 ± 0.01	0.35 ± 0.05	0.12 ± 0.01	0.18 ± 0.03	0.12 ± 0.02	0.09 ± 0.01	0.31 ± 0.05	0.18 ± 0.03	0.36 ± 0.06
Average	0.10 ± 0.01	0.30 ± 0.03	0.12 ± 0.02	0.18 ± 0.03	0.12 ± 0.02	0.10 ± 0.02	0.28 ± 0.04	0.18 ± 0.02	0.34 ± 0.05
CV	12%	12%	13%	12%	1%	14%	10%	4%	8%
10 mg kg⁻¹ spiked sediments									
Space 1	1.02 ± 0.14	2.91 ± 0.45	1.28 ± 0.20	1.97 ± 0.24	1.30 ± 0.14	1.08 ± 0.12	2.94 ± 0.34	1.84 ± 0.24	3.42 ± 0.37
Space 2	0.94 ± 0.11	3.03 ± 0.45	1.17 ± 0.13	1.95 ± 0.30	1.34 ± 0.16	1.04 ± 0.14	2.96 ± 0.38	1.77 ± 0.20	3.58 ± 0.48
Space 3	1.00 ± 0.14	3.05 ± 0.32	1.25 ± 0.13	1.88 ± 0.23	1.26 ± 0.20	1.05 ± 0.12	2.93 ± 0.45	1.82 ± 0.27	3.47 ± 0.53
Space 4	1.00 ± 0.13	3.08 ± 0.43	1.17 ± 0.17	1.98 ± 0.25	1.32 ± 0.14	1.01 ± 0.15	2.85 ± 0.43	1.77 ± 0.22	3.49 ± 0.55
Space 5	0.94 ± 0.14	2.96 ± 0.30	1.28 ± 0.14	1.87 ± 0.29	1.36 ± 0.20	1.15 ± 0.14	2.85 ± 0.42	1.74 ± 0.28	3.48 ± 0.46
Space 6	0.95 ± 0.14	3.05 ± 0.47	1.19 ± 0.14	1.93 ± 0.30	1.35 ± 0.15	1.12 ± 0.14	2.81 ± 0.37	1.86 ± 0.27	3.47 ± 0.51
Average	0.98 ± 0.14	2.91 ± 0.41	1.22 ± 0.14	1.93 ± 0.27	1.32 ± 0.18	1.08 ± 0.14	2.89 ± 0.34	1.80 ± 0.25	3.48 ± 0.42
CV	4%	1%	4%	2%	3%	5%	2%	2%	1%

Table A16 LOD[1], LOQ[2], and MDL[3] (μg L^{-1}) for all nine antipsychotic compounds.

Compound	LOD	LOQ	MDL			
			DGT	Worm	Sediment	Water
Venlafaxine	0.23	0.77	0.045	0.050	0.057	0.054
Fluoxetine	1.46	4.87	0.012	0.014	0.015	0.014
Clozapine	0.38	1.28	0.026	0.030	0.034	0.030
Citalopram	2.14	7.13	0.021	0.024	0.026	0.024
Duloxetine	0.21	0.69	0.253	0.290	0.326	0.307
Amitriptyline	1.81	6.03	0.060	0.068	0.076	0.072
Bupropion	0.35	1.17	0.040	0.046	0.052	0.048
Carbamazepine	1.25	4.17	0.019	0.022	0.024	0.023
Lamotrigine	0.20	0.67	0.024	0.027	0.030	0.028

[1] Limits of quantitation (LOQ): the low concentration of analyte with a measured signal/noise (S/N) of 3 (LOD = $3\sigma_{blank}$/slope). Slope was obtained from the calibration curve.

[2] limits of detection (LOD): the low concentration of analyte with a measured signal/noise (S/N) of 3 (LOQ = $10\sigma_{blank}$/slope)

[3] Method detection limit (MDL): for DGT measurement, calculated by the average concentration of blank DGT devices, blank worms, blank sediments, and blank water samples from the laboratory control in each DGT retrieval/worm, sediment, and water sampling time plus three times the standard deviation (3σ).

Table A17 The average recovery (%)[*] of all nine antipsychotic compounds for DGT extraction, worm tissue extraction, and SPE enrichment.

Compound	DGT extraction[1]	Worm extraction[2]	SPE enrichment[3]
Venlafaxine	78 ± 8%	74 ± 6%	83 ± 12%
Fluoxetine	74 ± 12%	79 ± 7%	80 ± 9%
Clozapine	83 ± 9%	76 ± 9%	92 ± 7%
Citalopram	72 ± 3%	75 ± 9%	79 ± 6%
Duloxetine	87 ± 10%	82 ± 11%	94 ± 10%
Amitriptyline	76 ± 7%	72 ± 12%	81 ± 6%
Bupropion	81 ± 13%	77 ± 6%	85 ± 13%
Carbamazepine	92 ± 8%	87 ± 14%	98 ± 10%
Lamotrigine	73 ± 5%	78 ± 6%	80 ± 12%

[1] DGT extraction: three unused binding gels were directly spiked with 50 μL of 1 ng mL^{-1} mixed nine internal standards and followed the extraction procedure in chapter 2.5.1 and reconstituted to 1 mL methanol.

[2] Worm extraction: three worms were taken from laboratory control tank, lyophilized, and spiked with 50 μg L^{-1} standard solution of mixed nine internal standards, followed by the extraction and purification processes shown in chapter 2.5.2, and finally reconstituted to 1 mL methanol.

[3] SPE extraction: 500 mL HPLC-grade water spiked with 50 μg L^{-1} standard solution of mixed nine internal standards was dealt with same procedure of SPE enrichment to final reconstitution in 1 mL methanol.

[*] The obtained peak area of each analyte was divided by that from standard solution for calculating the recovery. The standard deviation presented in the table was calculated from the triplicate.

Table A18 The concentrations (μg L^{-1}) of matrix spikes[*] for blank DGT, worm, sediment, and water during the batches of sample run.

Compound	DGT	Worm	Sediment	Water
Venlafaxine	43.60±5.46	44.78±7.07	43.73±5.21	44.33±5.15
Fluoxetine	43.49±5.57	42.33±4.70	44.08±6.61	47.03±7.13
Clozapine	44.02±6.52	43.53±5.57	44.11±5.37	45.42±4.95
Citalopram	43.88±6.03	44.22±4.46	43.22±6.21	46.68±6.61
Duloxetine	44.19±6.25	43.41±4.65	42.43±5.10	41.45±6.42
Amitriptyline	43.98±6.80	43.95±6.97	43.30±6.87	44.41±5.29
Bupropion	42.62±4.93	42.52±4.97	43.74±6.55	40.81±5.90
Carbamazepine	44.25±4.56	44.41±5.74	44.90±4.52	45.03±5.58
Lamotrigine	43.93±5.06	42.49±5.65	42.61±6.00	43.89±5.50

[*] The matrix spikes: during each sampling time, triplicate samples of clean DGT devices, worm from the control experiment, clean sediment, and water from the control experiment were spiked with 50 ng mixed internal standards and followed the same extraction and concentration procedures. In the table, the average concentration and standard deviation were calculated from all data from all run sequences.

Table A19 The physicochemical properties of sediment.

Depth (cm)	pH	Particle size distribution (%)			Total C (%)	Dissolved organic C (mg L^{-1})
		Sand	Silt	Clay		
0-2	7.34	49	36	15	1.4	630
4-6	7.65	48	37	15	1.9	634
6-8	7.43	45	34	21	1.2	658
8-10	7.13	43	32	25	1.5	692
10-12	6.92	42	36	22	1.2	623
12-15	6.89	39	38	23	1.1	631

pH was measured using a ratio of 1:2.5 dry sediment/1 M KCl. Total C was determined by combustion LECO method. Dissolved organic C in soil was extracted by 0.5 M K_2SO_4. Particle size distribution was measured by hydrometer method. All the measurements (except pH) were conducted in Bureau Veritas Laboratory (Edmonton, AB).

Table A20 The morphological characteristics of crayfish (*Faxonius virilis*) collected from the field.

Crayfish number	Body length (cm)	Carapace length (cm)	Wet weight (g)
1	9.97	4.36	25.6
2	8.54	4.71	20.9
3	8.24	3.96	25.7
4	9.90	5.24	24.3
5	9.74	3.39	20.3
6	9.73	5.15	21.0
7	10.1	5.57	24.1
8	9.44	5.44	20.9
9	9.93	3.50	23.1
10	10.9	5.58	23.9
11	10.9	3.55	20.3
12	8.54	5.30	21.6
13	9.27	5.33	23.0
14	10.4	5.35	23.2
15	9.09	3.95	22.9
16	8.38	5.30	25.7
17	10.8	4.05	23.8
18	9.15	4.75	22.2
19	10.2	4.51	23.6
20	9.53	5.45	25.4
21	8.48	3.03	22.6
22	10.6	3.15	20.4
23	9.26	3.80	20.2
24	9.50	3.74	25.5
25	8.07	4.58	24.7
26	8.58	5.60	25.0
27	10.4	5.59	20.2
28	10.7	5.52	24.5
29	8.02	5.07	20.3
30	10.0	3.60	24.9
31	9.38	3.07	25.3
32	10.6	5.34	24.8
33	10.2	4.29	23.7
34	9.76	4.33	25.1
35	8.17	4.33	25.6
36	8.79	5.54	24.8
37	8.47	5.43	25.2
38	9.17	4.75	21.2
39	9.12	4.58	25.8
40	9.50	4.09	21.1
41	8.40	3.84	23.5

42	10.2	5.24	23.9
43	8.99	4.95	24.4
44	8.15	3.71	23.1
45	9.95	5.37	25.5
46	10.8	4.04	24.4
47	8.83	4.81	21.7
48	8.35	3.75	25.2
49	10.6	5.55	24.4
50	8.48	4.23	21.2

Table A21 The distribution coefficient (mL g^{-1}) derived from hydroxyl-β-cyclodextrin extraction (K_d) and DIFS model (K_{dl}).

	K_d	K_{dl}
Venlafaxine	0.007	0.007
Clozapine	0.085	0.079
Citalopram	0.059	0.060
Fluoxetine	0.149	0.148
Bupropion	0.118	0.128
Duloxetine	0.110	0.120
Amitriptyline	0.093	0.076

Appendix Figures
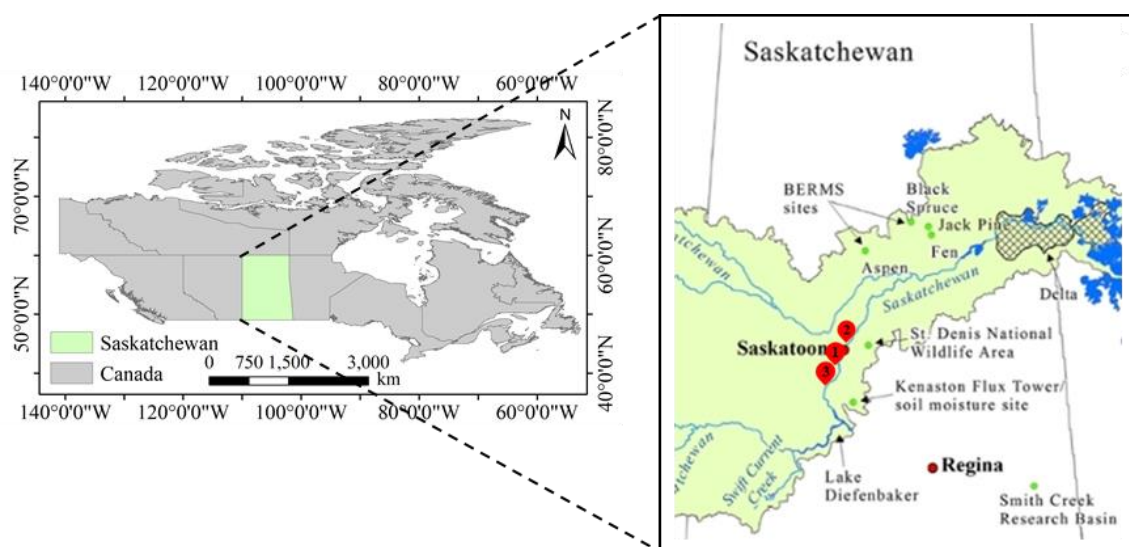
Figure A1 Sampling site of sediment and site of DGT deployment in South Saskatchewan River, Saskatoon, Saskatchewan, Canada. The number in map represents (1) Wastewater treatment plant, (2) the sampling site of sediment for spiking experiment, upstream of wastewater treatment plant, (3) in situ DGT deployment site in Fred heal Canoe Launch, downstream of wastewater treatment plant. The right graph is courtesy of the Global Institute for Water Security.

Figure A2 The setup for fixation of DGT sediment probes in the field.
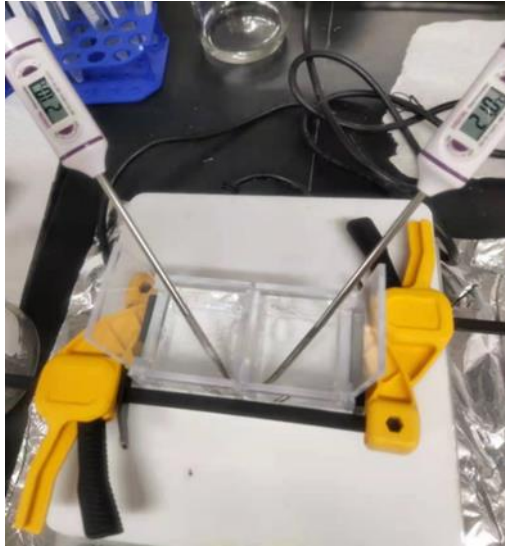
Figure A3 The setup of the diffusion cell.
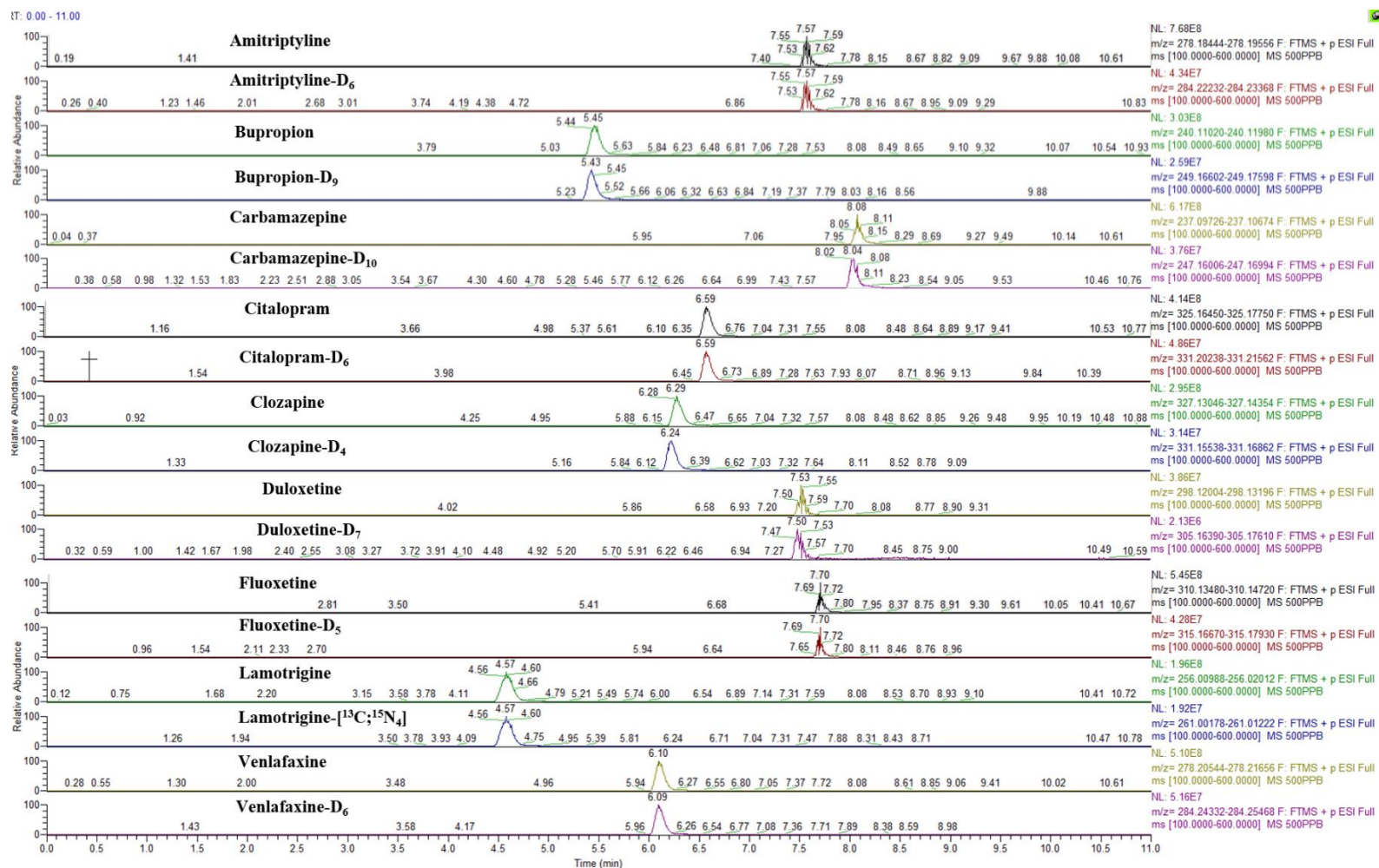
Figure A4 Example chromatograms of nine antipsychotic compounds and their internal standards with scan filter of precursor ion (*m/z*) for a 500 ng mL^{-1} standard solution.
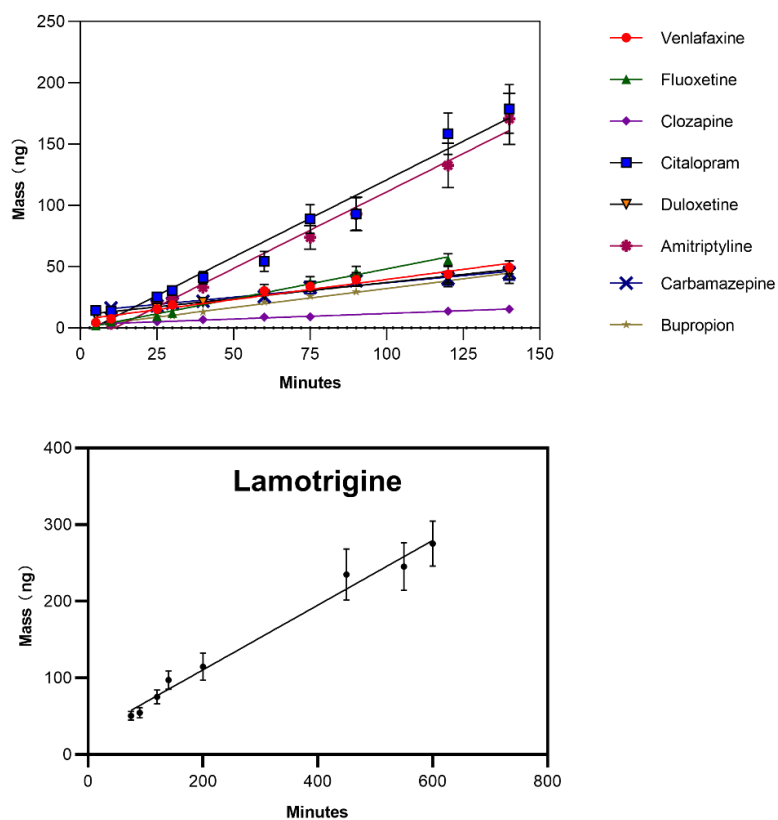
Figure A5 Diffused masses of bupropion, lamotrigine, amitriptyline, venlafaxine, duloxetine, fluoxetine, citalopram, and clozapine in the receiving cell through 0.75 mm agarose gel at different times in a diffusion cell with 500 μg L^{-1} standard compounds in the source cell at an initial time. The temperature was constant at 21 ± 0.5 °C, and ionic strength was 1 mM KNO_3. It should be noted that lamotrigine did not show a positive linear relationship with negligible mass detected before 75 mins. The symbols and errors bars represent the mean value calculated from mean values from three samples each time in triplicate parallel experiments.
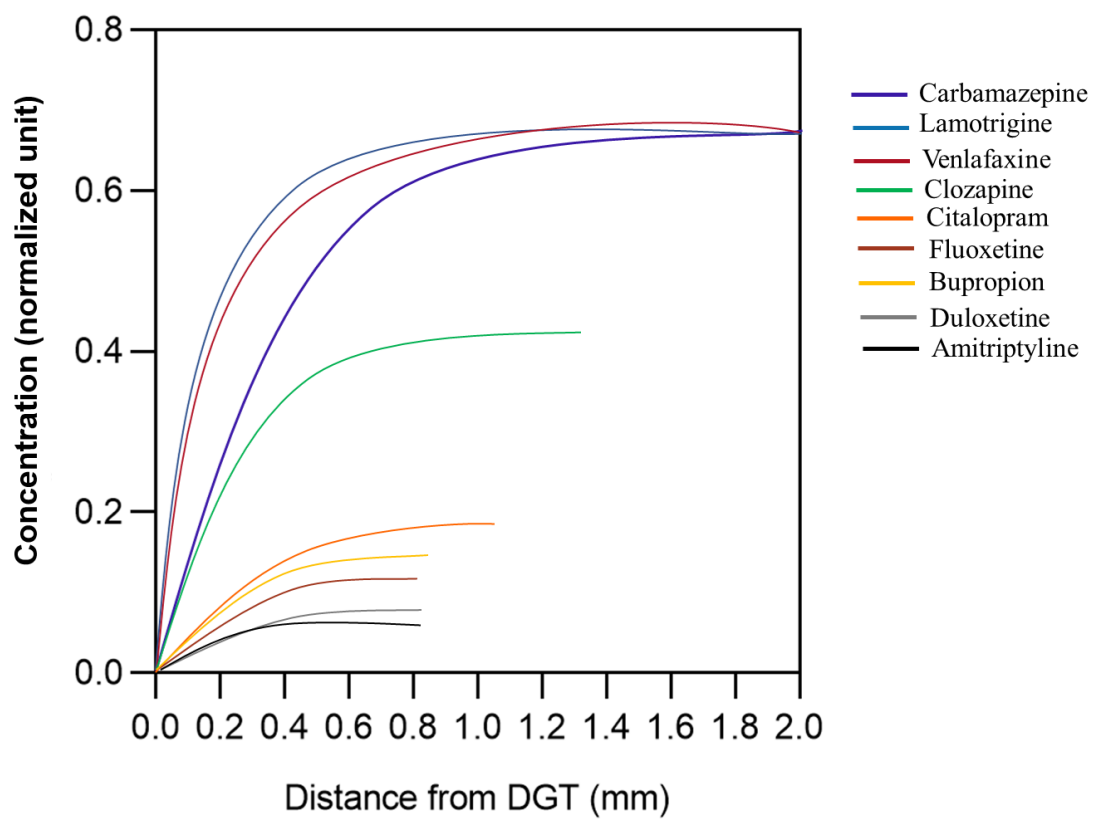
Figure A6 DIFS model (1D) output for nine antipsychotics in the sandy sediment simulating concentration in porewater on the distance of DGT interface at 30 days.
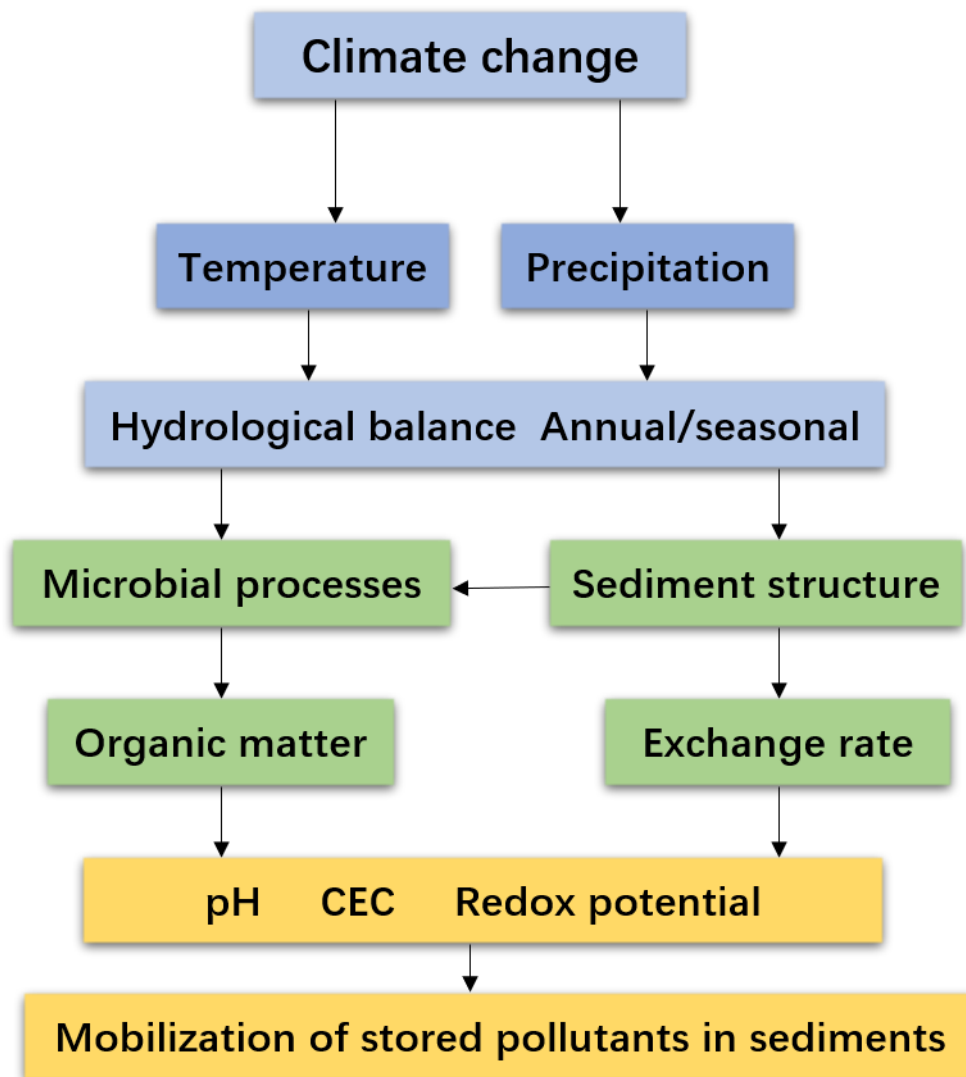
Figure A7 The linkage between the mobility of pollutants stored in sediments and climate change.
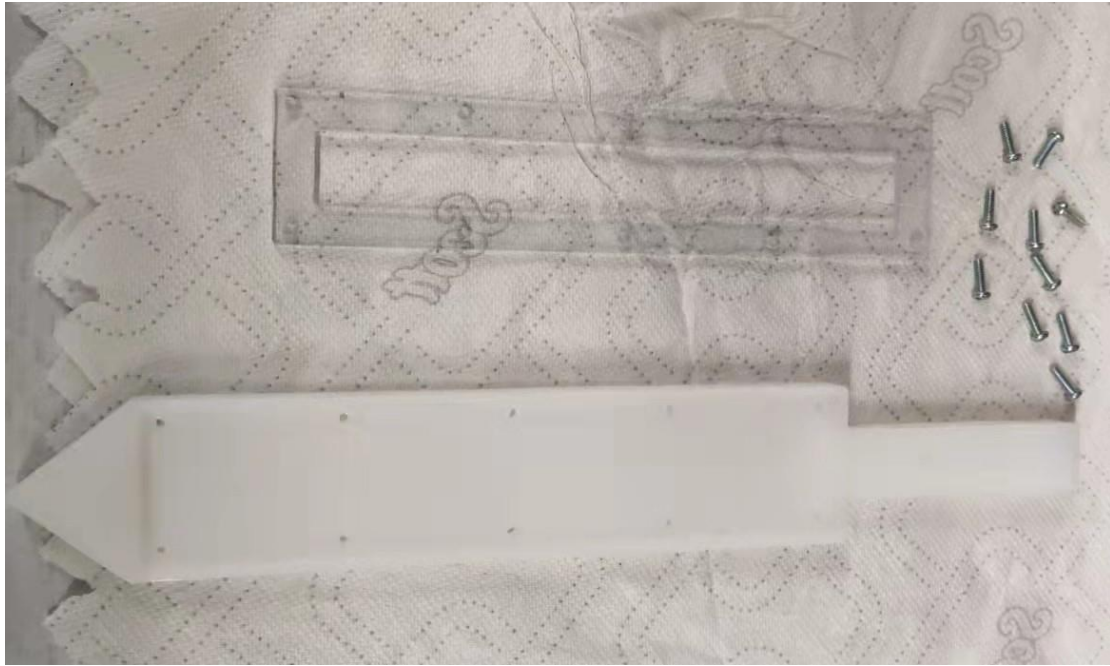
Figure A8 ABS DGT sediment probe with a PC cap.

a

b

DGT Deployment and Sampling Site
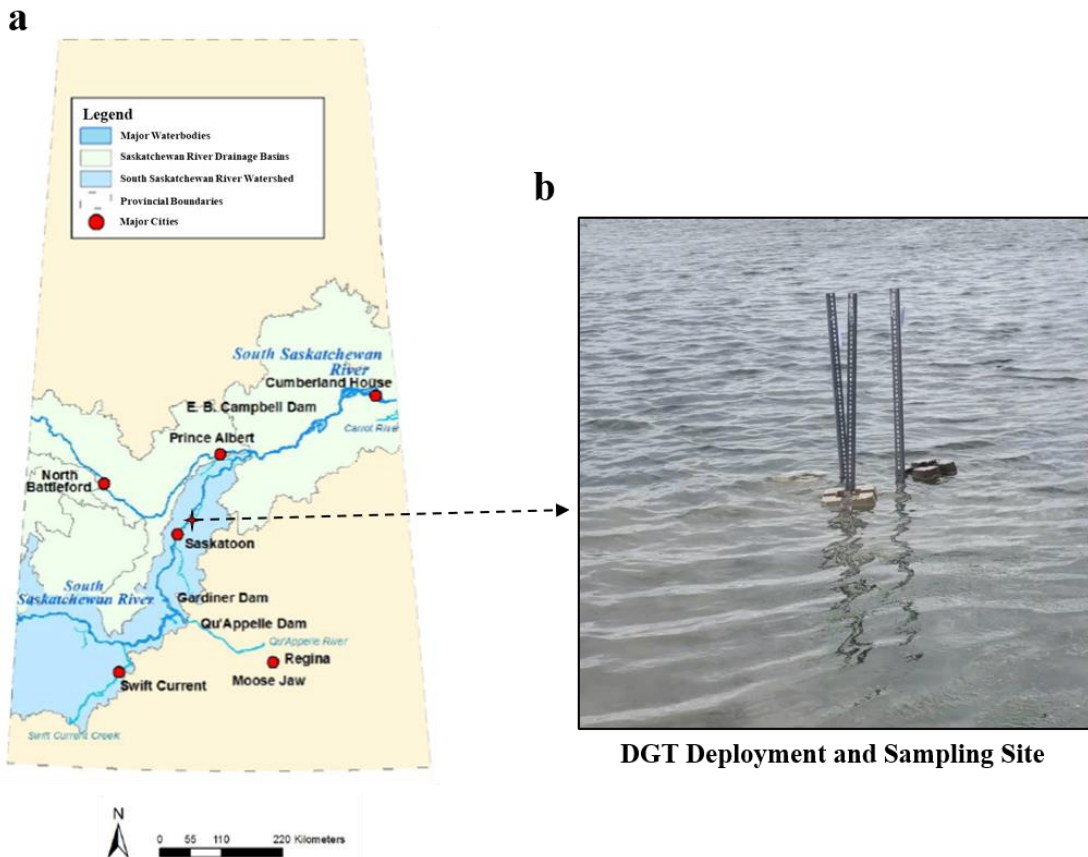
Figure A9 The site map for DGT deployment and sampling (a), modified from Page 6, Chapter 1−Introduction to the South Saskatchewan River Basin, Water Quality Assessment, South Saskatchewan River Watershed Stewards (https://southsaskriverstewards.ca/projects/water-quality-assessment/), and the field setup picture (b).
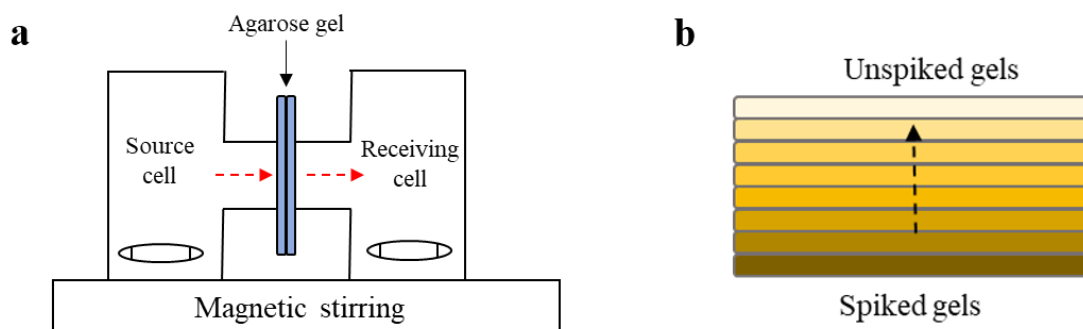
Figure A10 Schematic diagrams of diffusion cell method (a) and slice stacking method (b).
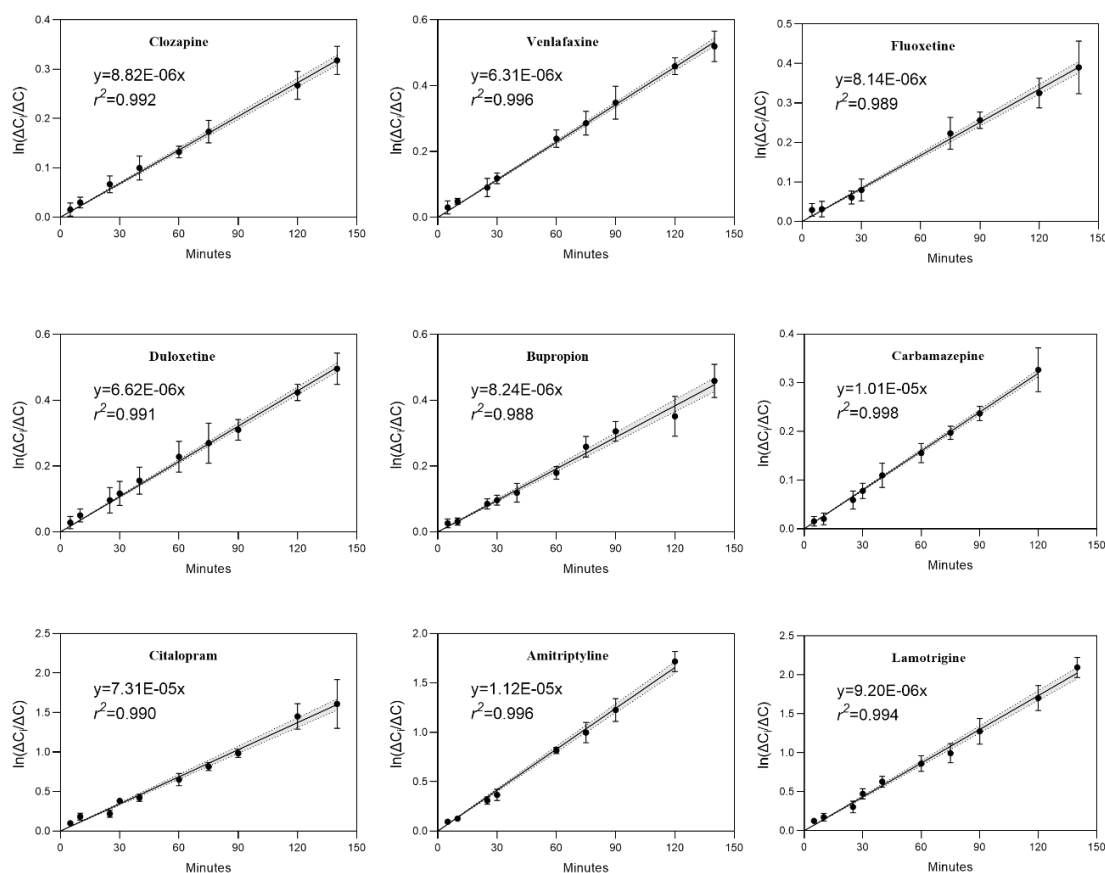
Figure A11 Natural logarithm of ratio of differences between concentration in source and receiving cell at the initial time (ΔC_i) and time t (ΔC) of the diffusion cell method for nine psychotic drugs. Slope of the linear regression is used for calculation of the diffusion coefficient (Eq. 1 and 2 in main text). The error bar represents the triplicate date used to calculate the ratio from the experiments. The grey area composed by dotted line represents the ratio ranged in 95% confidence interval.
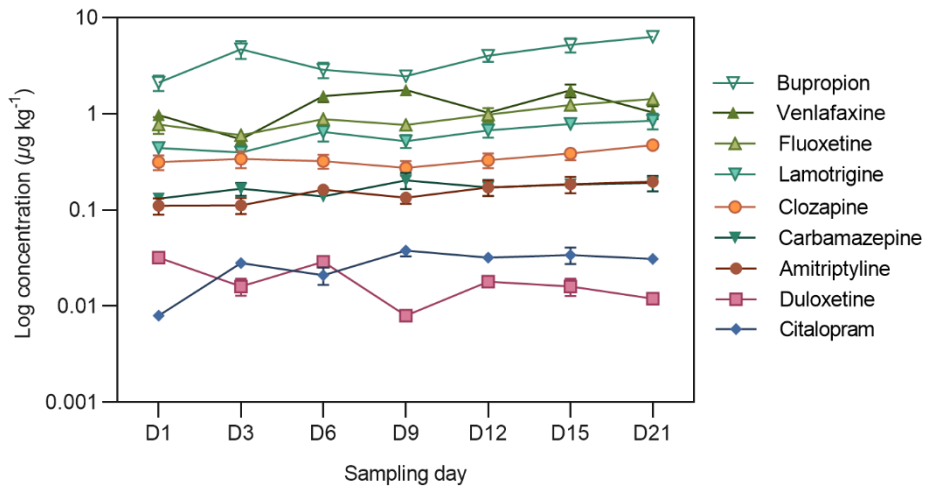
Figure A12 Logarithm-transformed concentration of nine psychotic drugs in sediment extracted for stable-desorbing fraction after the consecutive extraction for fats-desorbing fraction at each DGT deployment time. The concentration data is shown in Table A10.
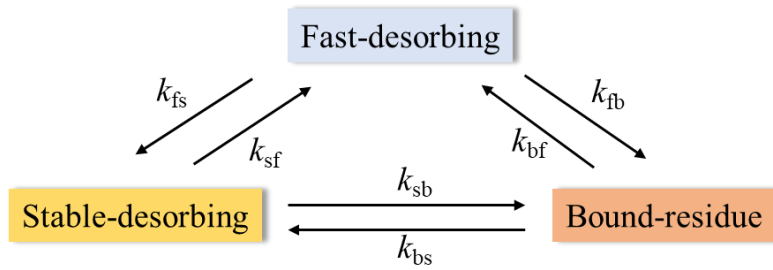
Figure A13 Illustration of transfer model of antipsychotic drug fractions in sediment.
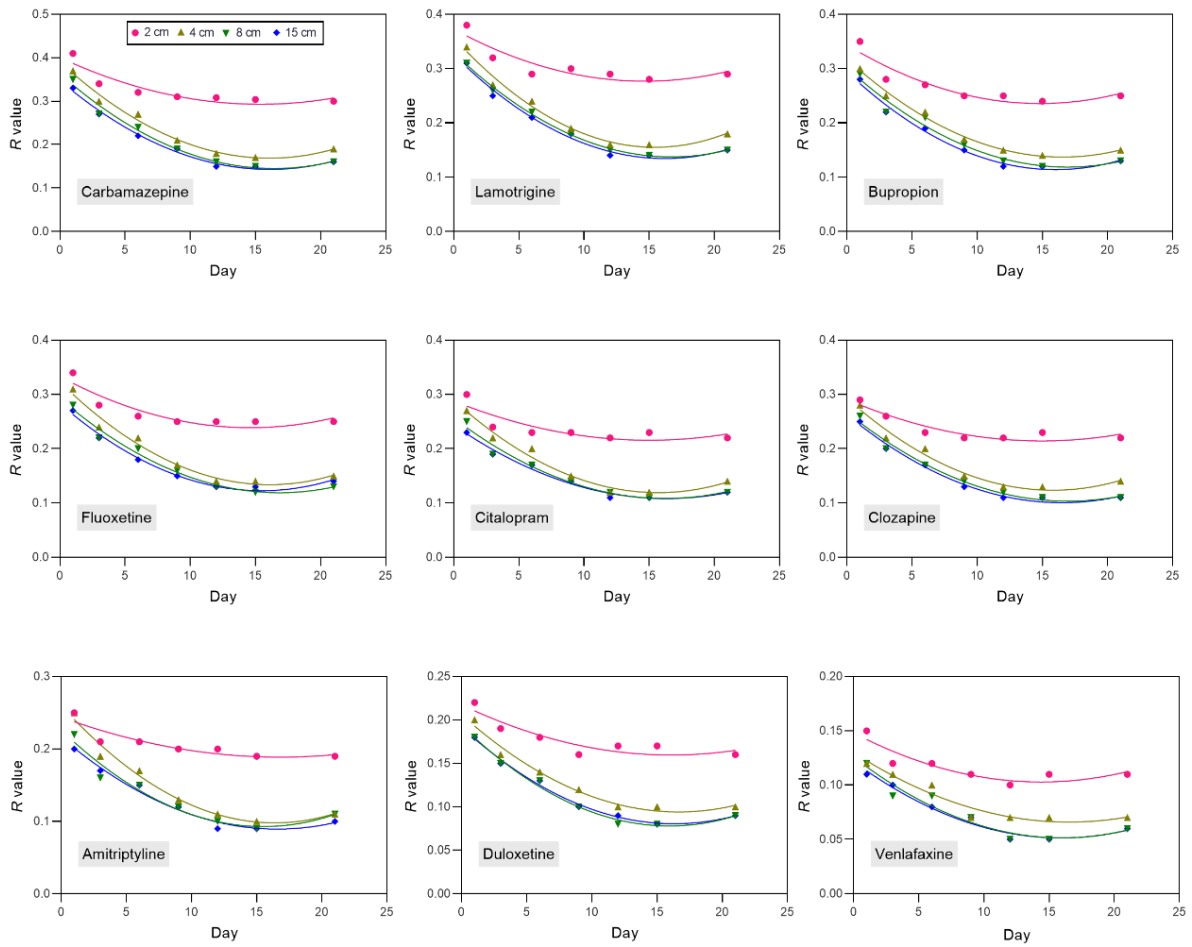
Figure A14 *R* values calculated from different depths in sediments plotted with sampling time.
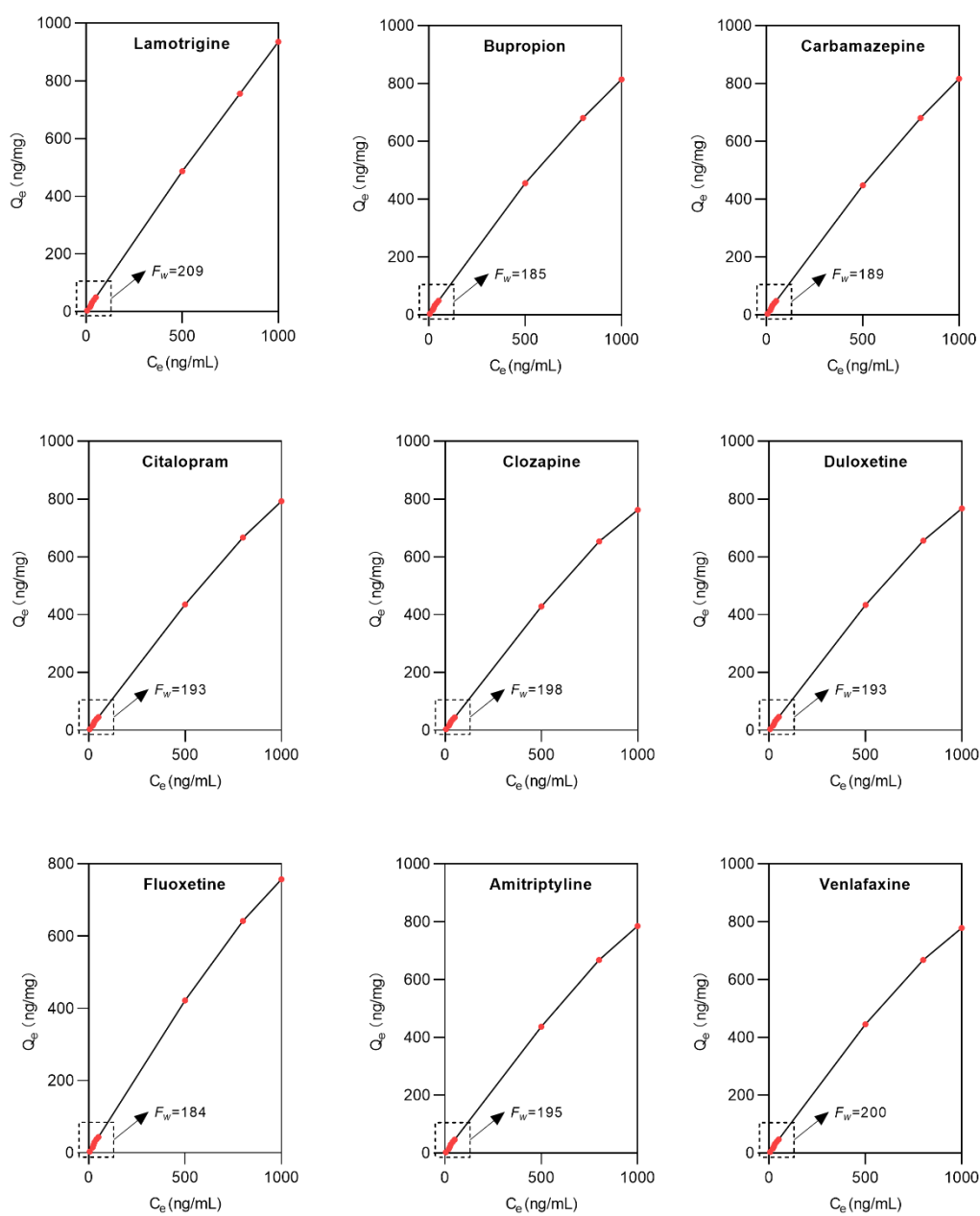
Figure A15 The sorption curve of antipsychotic compounds on sediments. Q_e (ng mg^{-1}) represents the compounds adsorbed on sediments and C_e (ng mL^{-1}) represent the compound concentration in solution.
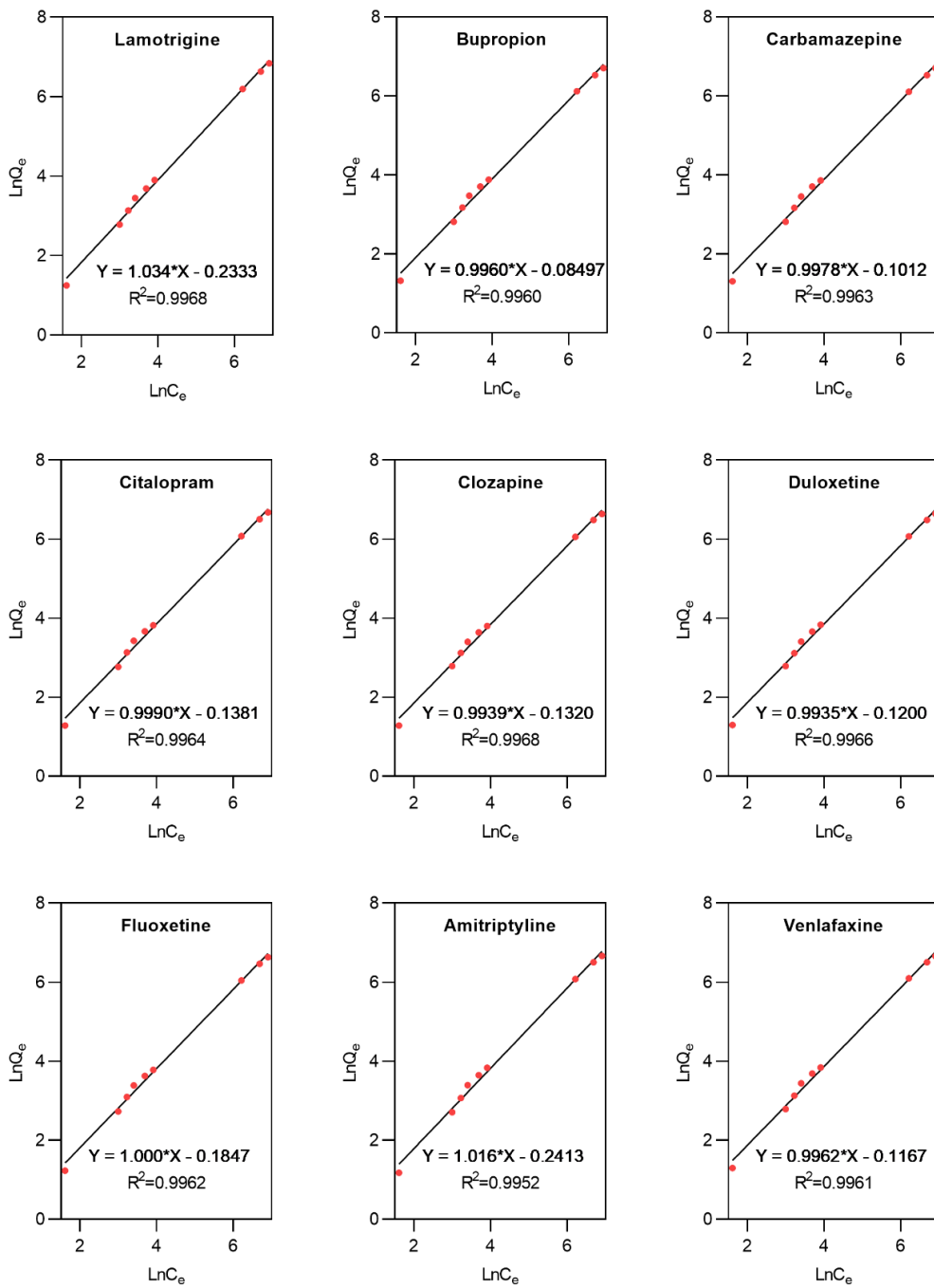
Figure A16 The Freundlich adsorption isotherm of antipsychotic compounds in the sediments.
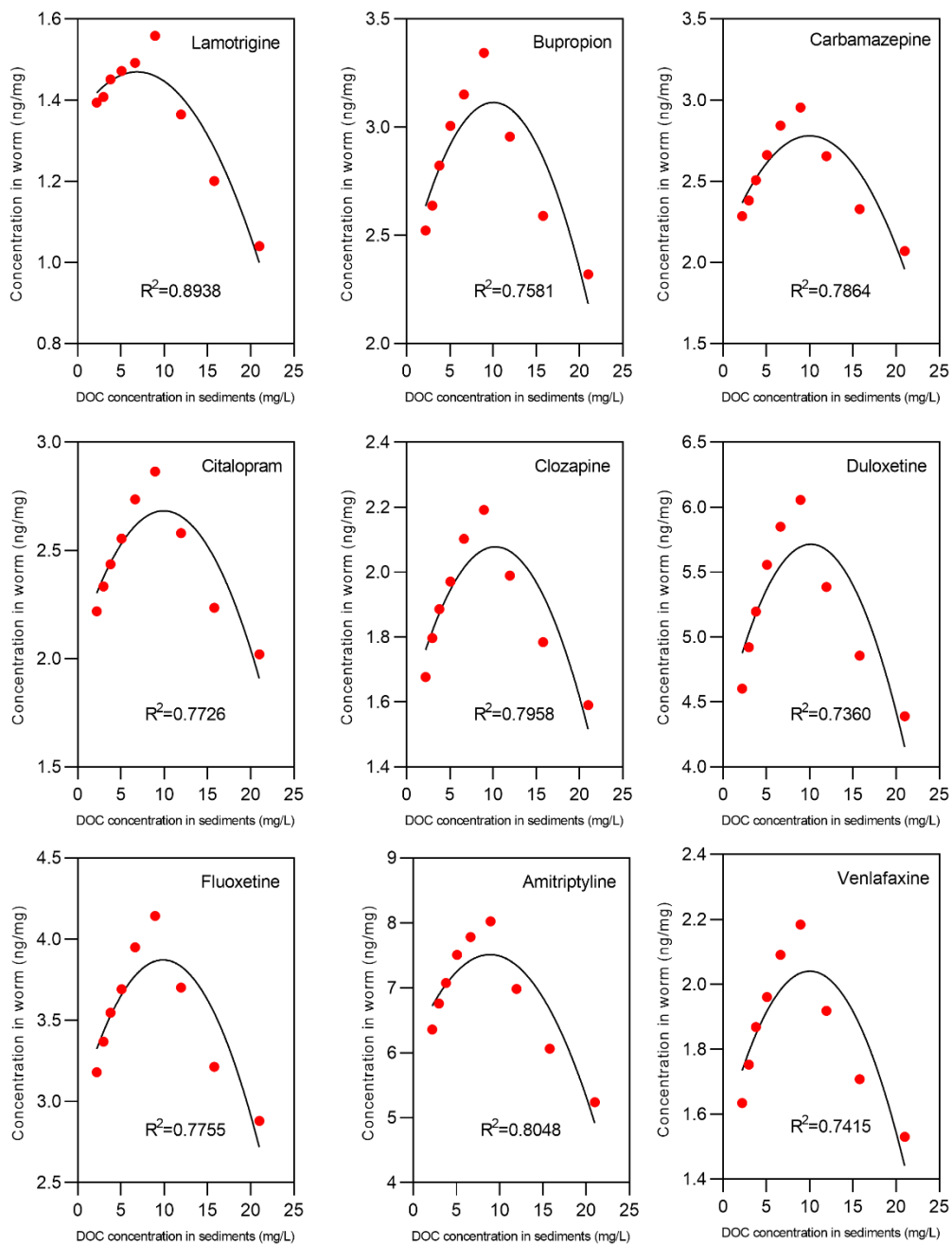
Figure A17 The estimated coefficient of $-\dfrac{\Delta C}{\Delta M}_{F_w}$ in the model.
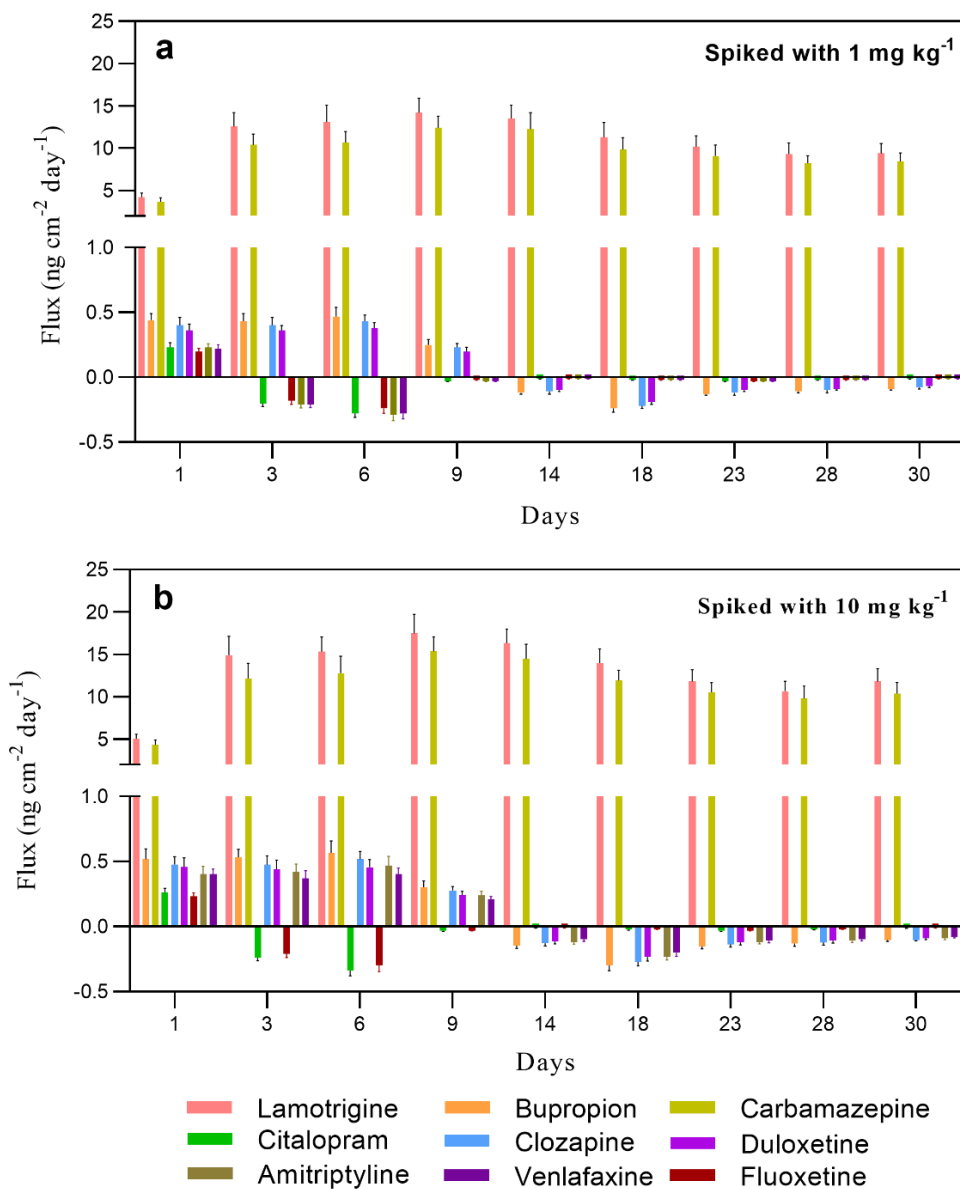
Figure A18 Sediment–water fluxes for individual antipsychotic compound in (a) 1 mg kg^{-1} spiked and (b) 10 mg kg^{-1} spiked sediments, respectively. The positive and negative value represent sediment porewater to surface water and surface water to sediment porewater, respectively.
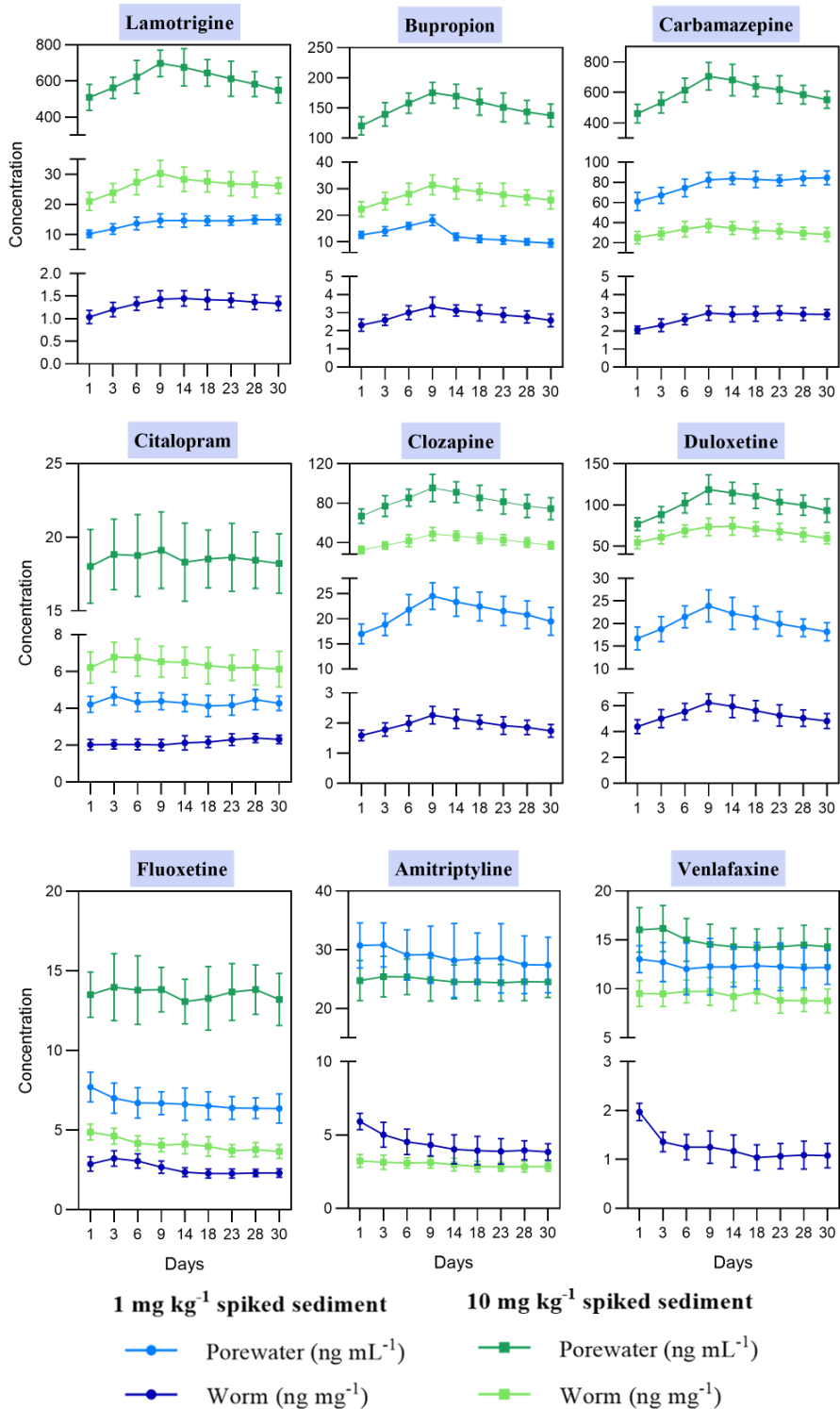
Figure A19 Concentration trend of antipsychotic compounds during incubation time for sediment porewater and worms in 1 mg kg^{-1} spiked sediments and 10 mg kg^{-1} spiked sediments, respectively.
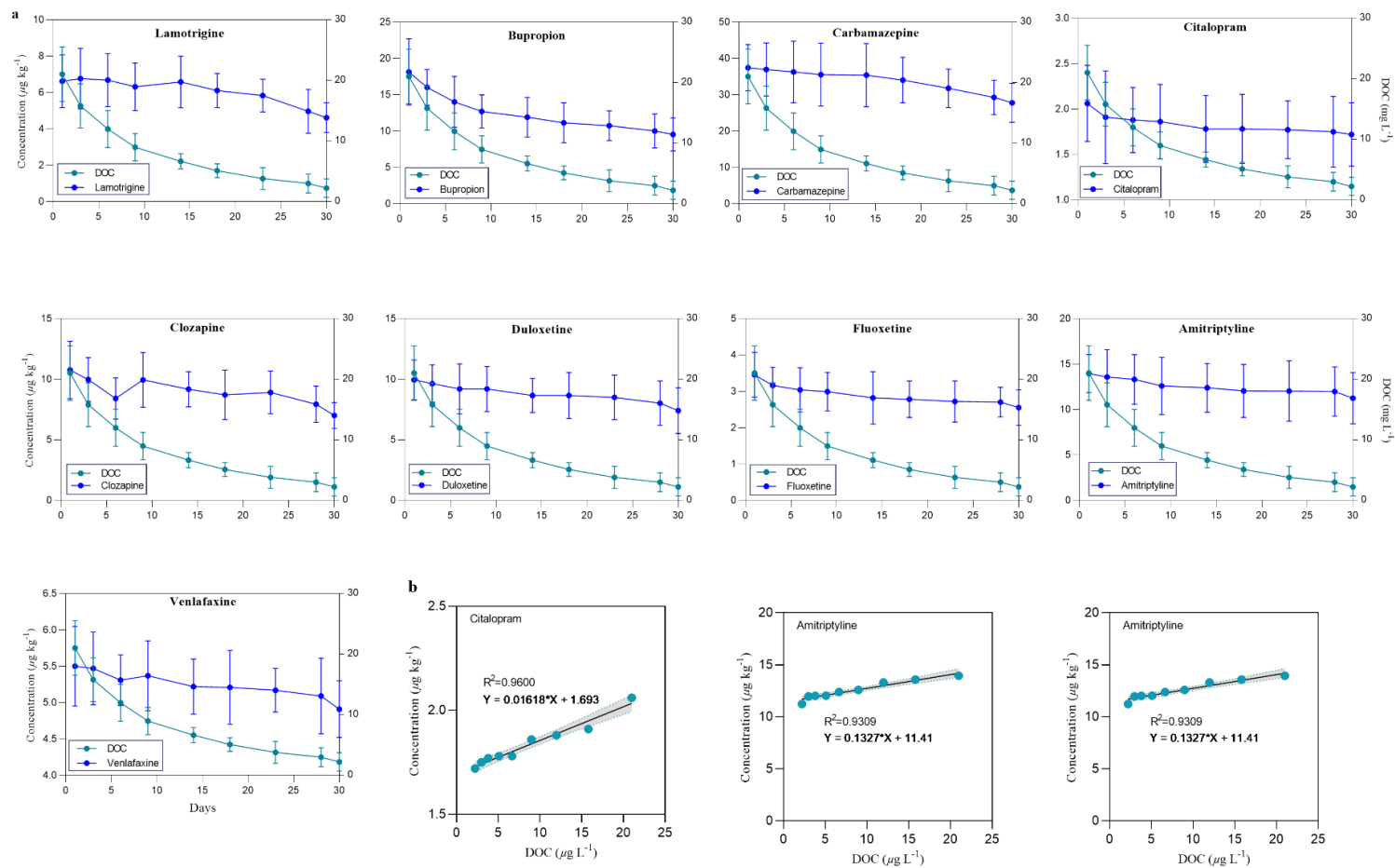
Figure A20 (a) Residual antipsychotic compounds and dissolved organic carbon (DOC) concentrations at the 30th day in 1 mg kg^{-1} spiked sediments. (b) Positive correlation between labile concentrations of antipsychotic compounds and DOC concentrations in 1 mg kg^{-1} spiked sediments.
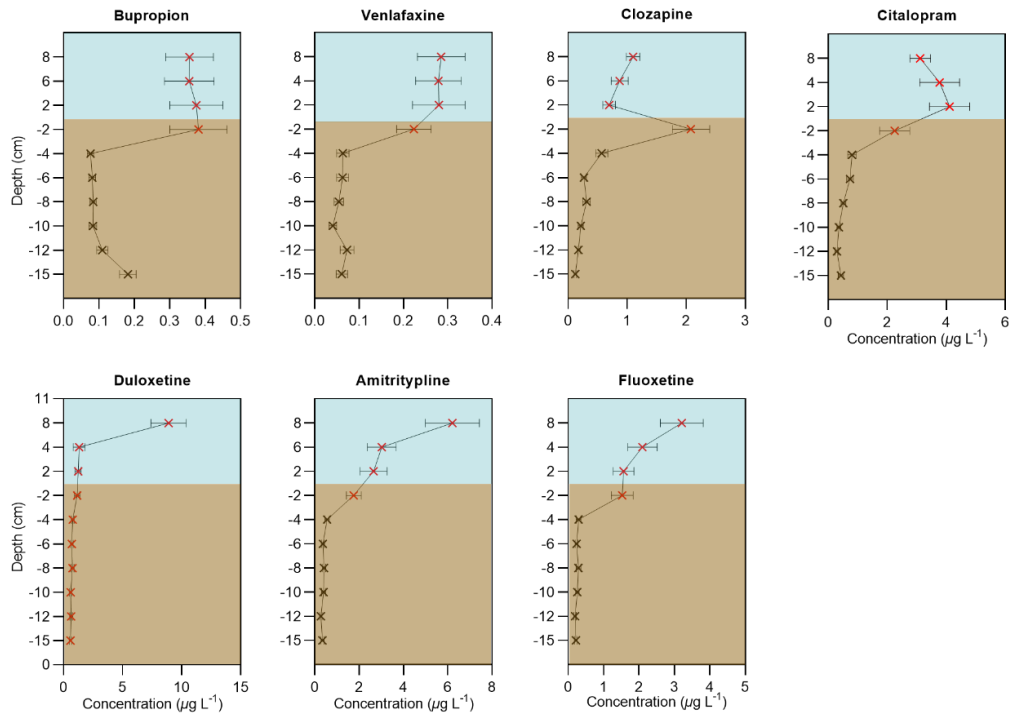
Figure A21 The vertical profiles of water and sediment solution concentrations (mean ± standard deviation) of antipsychotic compounds measured by DGT samplers. Black cross represents the concentration below the detection limit. Blue and brown color backgrounds represent the water and sediment matrix, respectively. The depth in y-axis is based on the DGT filed deployment.
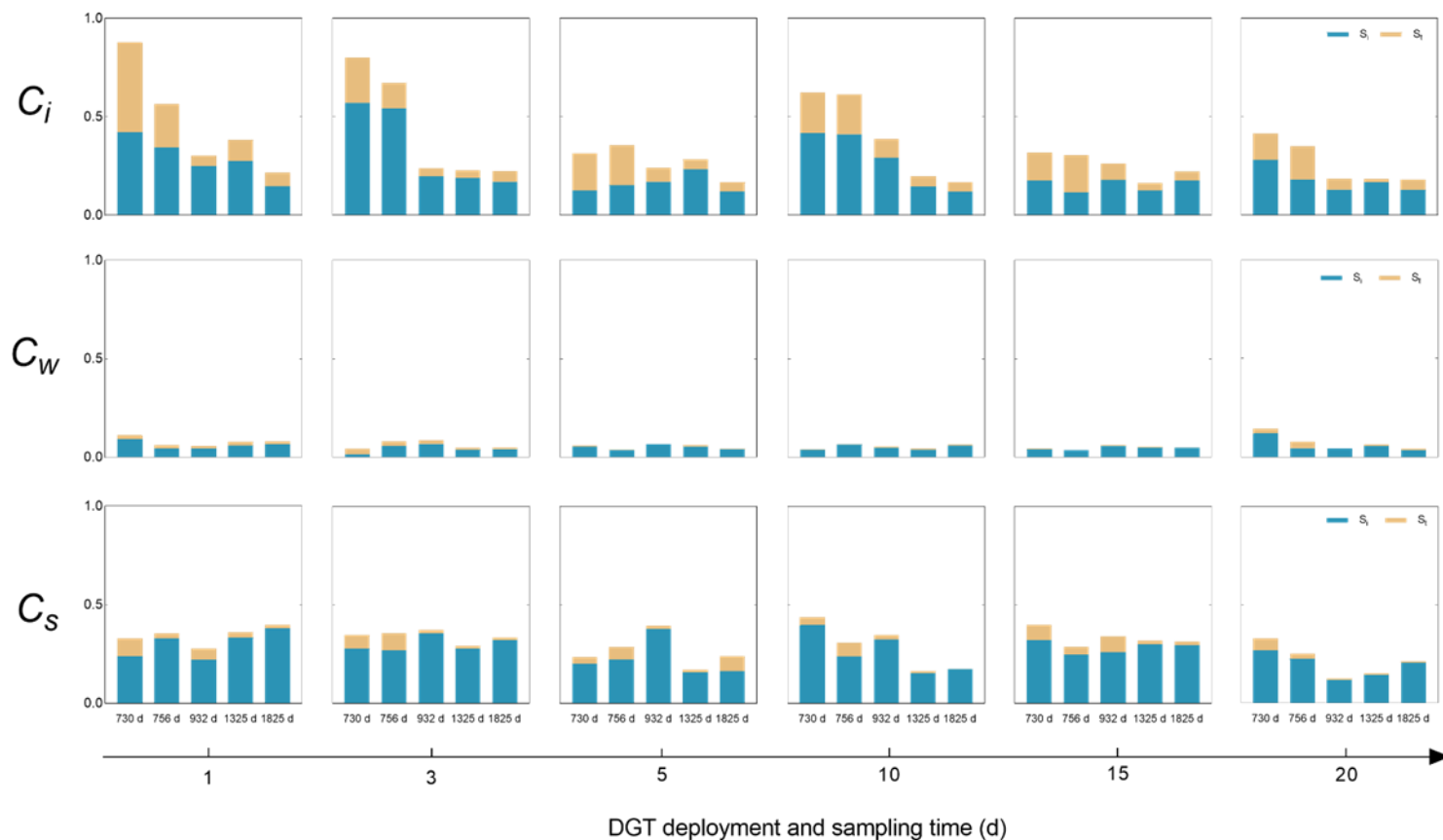
Figure A22 The sensitivity indexes of parameters in the organism uptake model. The x-axis is the assumed exposure time from 730 to 1825 day, shown as the most sensitivity results from the output values. S_t values determine the contribution to the model output. C_i, C_w, and C_s represent the chemical concentration in crayfish, overlying water, and sediment porewater respectively as the input parameters of the organism uptake model.
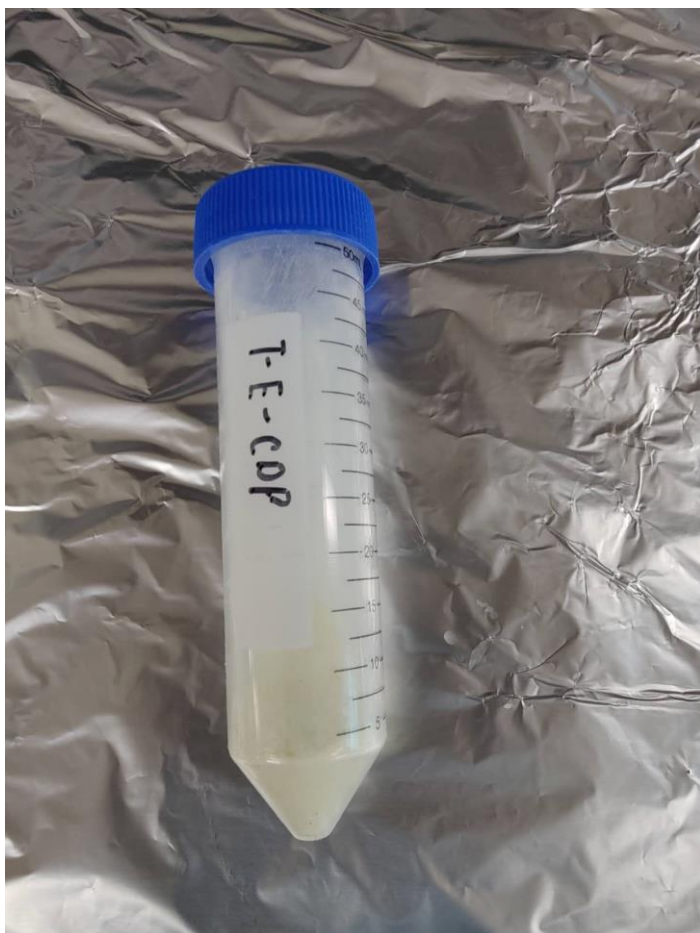
Figure A23 The facile synthesis of T–E–CDP.
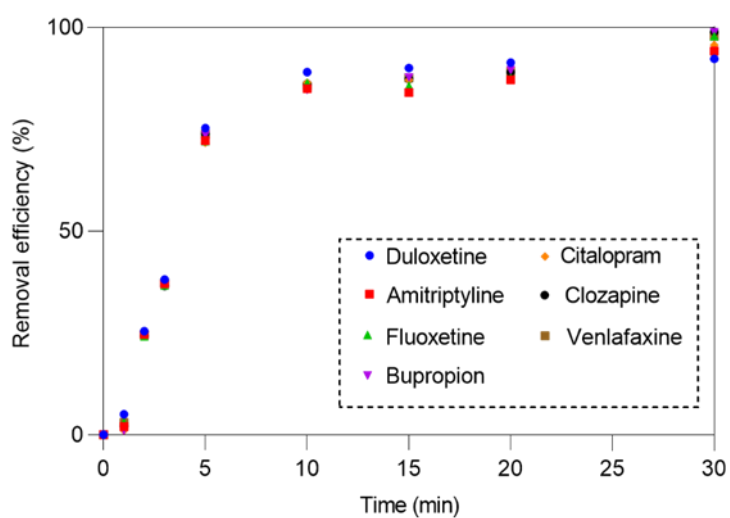
Figure A24 Time-dependent adsorption of antipsychotic compounds (0.1 mmol L^{-1}) by T–E–CDP binding gel (40 mg) under 25 °C.
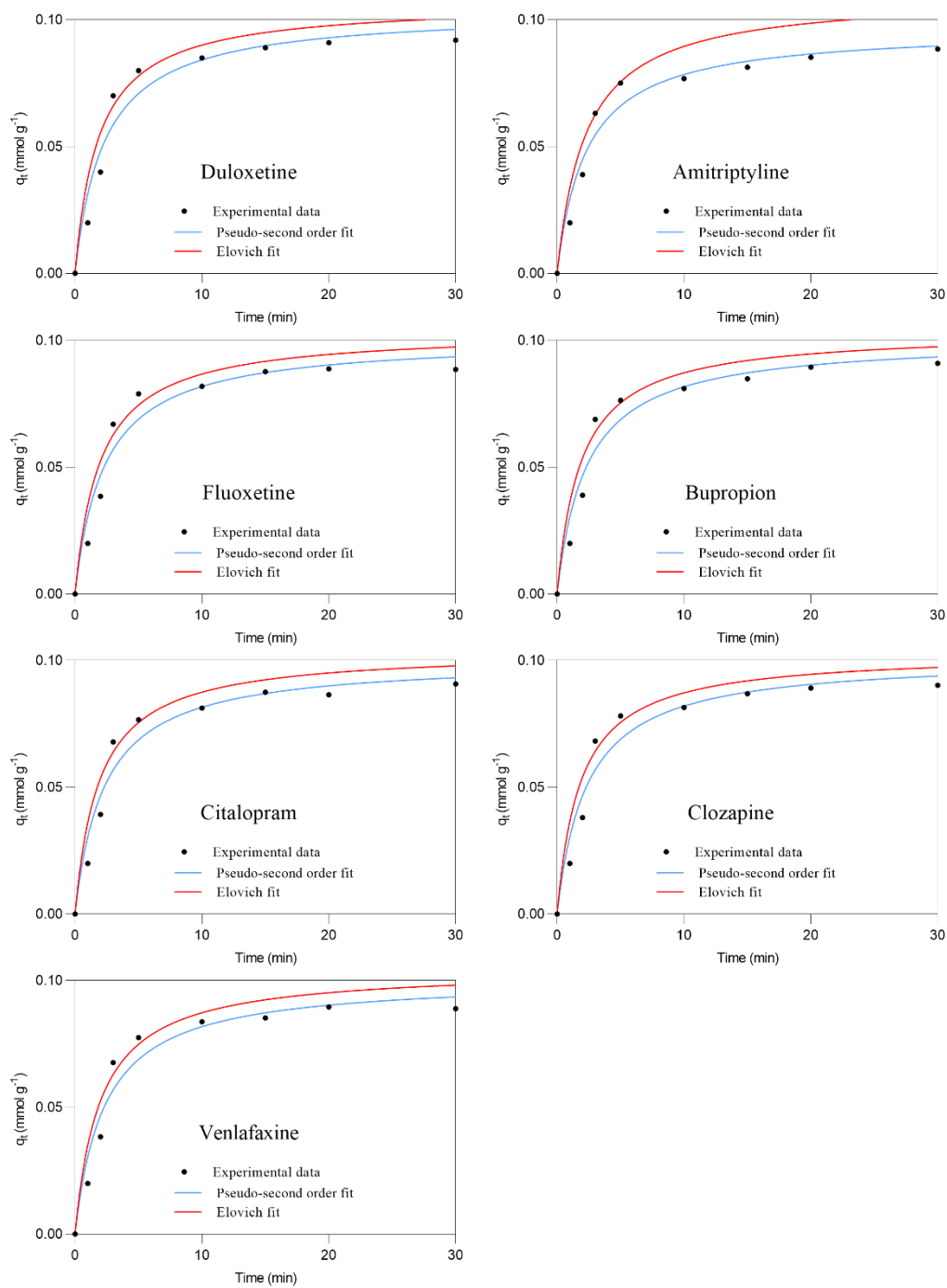
Figure A25 Adsorption kinetics data and modeling by Pseudo-second order and Elovich models for antipsychotic compounds onto T–E–CDP binding gel.

REFERENCES

Abbas, S.S., Elghobashy, M.R., Shokry, R.F., Bebawy, L.I., 2012. Stability indicating HPLC and spectrophotometric methods for the determination of bupropion hydrochloride in the presence of its alkaline degradates and related impurity. Bulletin of Faculty of Pharmacy, Cairo University 50, 49-59.

Addeck, A., Croes, K., Van Langenhove, K., Denison, M.S., Afify, A.S., Gao, Y., Elskens, M., Baeyens, W., 2014. Time-integrated monitoring of dioxin-like polychlorinated biphenyls (dl-PCBs) in aquatic environments using the ceramic toximeter and the CALUX bioassay. Talanta 120, 413-418.

Alvarez, D.A., Petty, J.D., Huckins, J.N., Jones-Lepp, T.L., Getting, D.T., Goddard, J.P., Manahan, S.E., 2004. Development of a passive, in situ, integrative sampler for hydrophilic organic contaminants in aquatic environments. Environmental Toxicology and Chemistry 23, 1640-1648.

Alygizakis, N.A., Gago-Ferrero, P., Borova, V.L., Pavlidou, A., Hatzianestis, I., Thomaidis, N.S., 2016. Occurrence and spatial distribution of 158 pharmaceuticals, drugs of abuse and related metabolites in offshore seawater. Science of The Total Environment 541, 1097-1105.

Amoozegar, A., Heitman, J.L., Kranz, C.N., 2023. Comparison of soil particle density determined by a gas pycnometer using helium, nitrogen, and air. Soil Science Society of America Journal 87, 1-12.

Anthony, J.L., Lewis, W.M., 2012. Low boundary layer response and temperature dependence

of nitrogen and phosphorus releases from oxic sediments of an oligotrophic lake. Aquatic Sciences 74, 611-617.

Armenta, S., Esteve-Turrillas, F.A., Garrigues, S., Guardia, M.d.l., 2017. Chapter One - Green Analytical Chemistry: The Role of Green Extraction Techniques. in: Ibáñez, E., Cifuentes, A. (Eds.). Comprehensive Analytical Chemistry. Elsevier, pp. 1-25.

Armstrong, D.E., Chesters, G., Harris, R.F., 1967. Atrazine Hydrolysis in Soil. Soil Science Society of America Journal 31, 61-66.

Ashauer, R., Caravatti, I., Hintermeister, A., Escher, B.I., 2010. Bioaccumulation kinetics of organic xenobiotic pollutants in the freshwater invertebrate Gammarus pulex modeled with prediction intervals. Environmental Toxicology and Chemistry 29, 1625-1636.

Axelman, J., Næs, K., Näf, C., Broman, D., 1999. Accumulation of polycyclic aromatic hydrocarbons in semipermeable membrane devices and caged mussels (Mytilus edulis L.) in relation to water column phase distribution. Environmental Toxicology and Chemistry 18, 2454-2461.

Azuma, T., 2018. Distribution of Anticancer Drugs in River Waters and Sediments of the Yodo River Basin, Japan. Applied Sciences 8, 2043.

Bade, R., Oh, S., Shin, W.S., 2012. Diffusive gradients in thin films (DGT) for the prediction of bioavailability of heavy metals in contaminated soils to earthworm (Eisenia foetida) and oral bioavailable concentrations. Science of The Total Environment 416, 127-136.

Balzani, P., Kouba, A., Tricarico, E., Kourantidou, M., Haubrock, P.J., 2022. Metal accumulation in relation to size and body condition in an all-alien species community. Environmental Science and Pollution Research 29, 25848-25857.

Bao, L.-J., Jia, F., Crago, J., Zeng, E.Y., Schlenk, D., Gan, J., 2013. Assessing bioavailability of DDT and metabolites in marine sediments using solid-phase microextraction with performance reference compounds. Environmental toxicology and chemistry 32, 1946-1953.

Barbosa, M.O., Moreira, N.F.F., Ribeiro, A.R., Pereira, M.F.R., Silva, A.M.T., 2016. Occurrence and removal of organic micropollutants: An overview of the watch list of EU Decision 2015/495. Water Research 94, 257-279.

Barceló, D., Alpendurada, M.E., 1996. A review of sample storage and preservation of polar pesticides in water samples. Chromatographia 42, 704-712.

Barrow, N.J., 2008. The description of sorption curves. European journal of soil science 59, 900-910.

Bashir, I., Lone, F.A., Bhat, R.A., Mir, S.A., Dar, Z.A., Dar, S.A., 2020. Concerns and Threats of Contamination on Aquatic Ecosystems. in: Hakeem, K.R., Bhat, R.A., Qadri, H. (Eds.). Bioremediation and Biotechnology: Sustainable Approaches to Pollution Degradation. Springer International Publishing, Cham, pp. 1-26.

Bäuerlein, P.S., Mansell, J.E., ter Laak, T.L., de Voogt, P., 2012. Sorption Behavior of Charged and Neutral Polar Organic Compounds on Solid Phase Extraction Materials: Which Functional Group Governs Sorption? Environmental Science & Technology 46, 954-961.

Baussant, T., Sanni, S., Jonsson, G., Skadsheim, A., Børseth, J.F., 2001. Bioaccumulation of polycyclic aromatic compounds: 1. Bioconcentration in two marine species and in semipermeable membrane devices during chronic exposure to dispersed crude oil.

Environmental Toxicology and Chemistry 20, 1175-1184.

Beiras, R., 2018. Marine pollution: sources, fate and effects of pollutants in coastal ecosystems. Elsevier Science.

Belles, A., Alary, C., Aminot, Y., Readman, J.W., Franke, C., 2017. Calibration and response of an agarose gel based passive sampler to record short pulses of aquatic organic pollutants. Talanta 165, 1-9.

Ben-Hur, M., Letey, J., Farmer, W.J., Williams, C.F., Nelson, S.D., 2003. Soluble and Solid Organic Matter Effects on Atrazine Adsorption in Cultivated Soils. Soil Science Society of America Journal 67, 1140-1146.

Benoit, J.M., Shull, D.H., Harvey, R.M., Beal, S.A., 2009. Effect of Bioirrigation on Sediment−Water Exchange of Methylmercury in Boston Harbor, Massachusetts. Environmental Science & Technology 43, 3669-3674.

Benotti, M.J., Trenholm, R.A., Vanderford, B.J., Holady, J.C., Stanford, B.D., Snyder, S.A., 2009. Pharmaceuticals and Endocrine Disrupting Compounds in U.S. Drinking Water. Environmental Science & Technology 43, 597-603.

Bhadoria, P.B.S., Kaselowsky, J., Claassen, N., Jungk, A., 1991. Impedance Factor for Chloride Diffusion in Soil as Affected by Bulk Density and Water Content. Zeitschrift für Pflanzenernährung und Bodenkunde 154, 69-72.

Białk-Bielińska, A., Maszkowska, J., Mrozik, W., Bielawska, A., Kołodziejska, M., Palavinskas, R., Stepnowski, P., Kumirska, J., 2012. Sulfadimethoxine and sulfaguanidine: Their sorption potential on natural soils. Chemosphere 86, 1059-1065.

Bierman, V.J., 1990. Equilibrium partitioning and biomagnification of organic chemicals in

benthic animals. Environmental Science & Technology 24, 1407-1412.

Björklund Blom, L., Morrison, G.M., Segura Roux, M., Mills, G., Greenwood, R., 2003. Metal diffusion properties of a Nafion-coated porous membrane in an aquatic passive sampler system. Journal of Environmental Monitoring 5, 404-409.

Boehm, P.D., Page, D.S., Brown, J.S., Neff, J.M., Edward Bence, A., 2005. Comparison of mussels and semi-permeable membrane devices as intertidal monitors of polycyclic aromatic hydrocarbons at oil spill sites. Marine Pollution Bulletin 50, 740-750.

Bollmann, A.F., Seitz, W., Prasse, C., Lucke, T., Schulz, W., Ternes, T., 2016. Occurrence and fate of amisulpride, sulpiride, and lamotrigine in municipal wastewater treatment plants with biological treatment and ozonation. Journal of Hazardous Materials 320, 204-215.

Bondarenko, A., Sani, D., Ruello, M.L., 2011. Design and Calibration of an Organic Diffusive Probe to Extend the Diffusion Gradient Technique to Organic Pollutants. International Journal of Environmental Research and Public Health 8, 3318–3332.

Bondarenko, S., Gan, J., 2004. Degradation and sorption of selected organophosphate and carbamate insecticides in urban stream sediments. Environmental Toxicology and Chemistry 23, 1809-1814.

Bonifacio, R.G., Nam, G.-U., Eom, I.-Y., Hong, Y.-S., 2017. Development of Solid Ceramic Dosimeters for the Time-Integrative Passive Sampling of Volatile Organic Compounds in Waters. Environmental Science & Technology 51, 12557-12565.

Booij, K., Robinson, C.D., Burgess, R.M., Mayer, P., Roberts, C.A., Ahrens, L., Allan, I.J., Brant, J., Jones, L., Kraus, U.R., Larsen, M.M., Lepom, P., Petersen, J., Pröfrock, D., Roose, P., Schäfer, S., Smedes, F., Tixier, C., Vorkamp, K., Whitehouse, P., 2016.

Passive Sampling in Regulatory Chemical Monitoring of Nonpolar Organic Compounds in the Aquatic Environment. Environmental Science & Technology 50, 3-17.

Booij, K., Smedes, F., Van Weerlee, E.M., Honkoop, P.J.C., 2006. Environmental Monitoring of Hydrophobic Organic Contaminants: The Case of Mussels versus Semipermeable Membrane Devices. Environmental Science & Technology 40, 3893-3900.

Boreen, A.L., Arnold, W.A., McNeill, K., 2003. Photodegradation of pharmaceuticals in the aquatic environment: A review. Aquatic Sciences 65, 320-341.

Brinkmann, M., Eichbaum, K., Reininghaus, M., Koglin, S., Kammann, U., Baumann, L., Segner, H., Zennegg, M., Buchinger, S., Reifferscheid, G., Hollert, H., 2015. Towards science-based sediment quality standards—Effects of field-collected sediments in rainbow trout (Oncorhynchus mykiss). Aquatic Toxicology 166, 50-62.

Brinkmann, M., Ouellet, J.D., Zennegg, M., Buchinger, S., Reifferscheid, G., Hollert, H., 2021. Combined sediment desorption and bioconcentration model to predict levels of dioxin-like chemicals in fish. Science of The Total Environment 758, 143891.

Bucheli, T.D., Grüebler, F.C., Müller, S.R., Schwarzenbach, R.P., 1997. Simultaneous Determination of Neutral and Acidic Pesticides in Natural Waters at the Low Nanogram per Liter Level. Analytical Chemistry 69, 1569-1576.

Budzinski, H., Dévier, M.-H., 2013. POCIS Passive Samplers in Combination with Bioassay-Directed Chemical Analyses. in: Férard, J.-F., Blaise, C. (Eds.). Encyclopedia of Aquatic Ecotoxicology. Springer Netherlands, Dordrecht, pp. 873-882.

Burgess, R., 2012. Guidelines for using passive samplers to monitor organic contaminants at

superfund sediment sites. US Environmental Protection Agency, Available at: https://cfpub.epa.gov/si/si_public_record_report.cfm?Lab=NHEERL&dirEntryId=23 8596.

Buzier, R., Guibal, R., Lissalde, S., Guibaud, G., 2019. Limitation of flow effect on passive sampling accuracy using POCIS with the PRC approach or o-DGT: A pilot-scale evaluation for pharmaceutical compounds. Chemosphere 222, 628-636.

Buzier, R., Tusseau-Vuillemin, M.-H., Mouchel, J.-M., 2006. Evaluation of DGT as a metal speciation tool in wastewater. Science of The Total Environment 358, 277-285.

Caldas, S.S., Rombaldi, C., de Oliveira Arias, J.L., Marube, L.C., Primel, E.G., 2016. Multi-residue method for determination of 58 pesticides, pharmaceuticals and personal care products in water using solvent demulsification dispersive liquid–liquid microextraction combined with liquid chromatography-tandem mass spectrometry. Talanta 146, 676-688.

Carman, P.C., 1937. Fluid Flow through Granular Beds. Trans. Inst. Chem. Eng. 15, 150-166.

Casatta, N., Stefani, F., Pozzoni, F., Guzzella, L., Marziali, L., Mascolo, G., Viganò, L., 2016. Endocrine-disrupting chemicals in coastal lagoons of the Po River delta: sediment contamination, bioaccumulation and effects on Manila clams. Environmental Science and Pollution Research 23, 10477-10493.

Challis, J.K., Almirall, X.O., Helm, P.A., Wong, C.S., 2020. Performance of the organic-diffusive gradients in thin-films passive sampler for measurement of target and suspect wastewater contaminants. Environmental Pollution 261, 114092.

Challis, J.K., Hanson, M.L., Wong, C.S., 2016. Development and Calibration of an Organic-

Diffusive Gradients in Thin Films Aquatic Passive Sampler for a Diverse Suite of Polar Organic Contaminants. Analytical Chemistry 88, 10583-10591.

Challis, J.K., Hanson, M.L., Wong, C.S., 2018a. Pharmaceuticals and pesticides archived on polar passive sampling devices can be stable for up to 6 years. Environmental Toxicology and Chemistry 37, 762-767.

Challis, J.K., Stroski, K.M., Luong, K.H., Hanson, M.L., Wong, C.S., 2018b. Field Evaluation and in Situ Stress Testing of the Organic-Diffusive Gradients in Thin-Films Passive Sampler. Environmental Science & Technology 52, 12573-12582.

Charriau, A., Lissalde, S., Poulier, G., Mazzella, N., Buzier, R., Guibaud, G., 2016. Overview of the Chemcatcher® for the passive sampling of various pollutants in aquatic environments Part A: Principles, calibration, preparation and analysis of the sampler. Talanta 148, 556-571.

Chen, B., Yuan, M., Liu, H., 2011. Removal of polycyclic aromatic hydrocarbons from aqueous solution using plant residue materials as a biosorbent. Journal of Hazardous Materials 188, 436-442.

Chen, C.-E., Chen, W., Ying, G.-G., Jones, K.C., Zhang, H., 2015. In situ measurement of solution concentrations and fluxes of sulfonamides and trimethoprim antibiotics in soils using o-DGT. Talanta 132, 902-908.

Chen, C.-E., Jones, K.C., Ying, G.-G., Zhang, H., 2014. Desorption Kinetics of Sulfonamide and Trimethoprim Antibiotics in Soils Assessed with Diffusive Gradients in Thin-Films. Environmental Science & Technology 48, 5530-5536.

Chen, C.-E., Zhang, H., Jones, K.C., 2012. A novel passive water sampler for in situ sampling

of antibiotics. Journal of Environmental Monitoring 14, 1523-1530.

Chen, C.-E., Zhang, H., Ying, G.-G., Jones, K.C., 2013. Evidence and Recommendations to Support the Use of a Novel Passive Water Sampler to Quantify Antibiotics in Wastewaters. Environmental Science & Technology 47, 13587-13593.

Chen, W., Li, Y., Chen, C.-E., Sweetman, A.J., Zhang, H., Jones, K.C., 2017. DGT Passive Sampling for Quantitative in Situ Measurements of Compounds from Household and Personal Care Products in Waters. Environmental Science & Technology 51, 13274-13281.

Chen, W., Pan, S., Cheng, H., Sweetman, A.J., Zhang, H., Jones, K.C., 2018. Diffusive gradients in thin-films (DGT) for in situ sampling of selected endocrine disrupting chemicals (EDCs) in waters. Water Research 137, 211-219.

Cheng, Y., Ding, J., Liang, X., Ji, X., Xu, L., Xie, X., Zhang, Y.-K., 2020. Fractions Transformation and Dissipation Mechanism of Dechlorane Plus in the Rhizosphere of the Soil–Plant System. Environmental Science & Technology 54, 6610-6620.

Cheng, Y., Ding, J., Xie, X., Ji, X., Zhang, Y., 2019. Validation and Application of a 3-Step Sequential Extraction Method to Investigate the Fraction Transformation of Organic Pollutants in Aging Soils: A Case Study of Dechlorane Plus. Environmental Science & Technology 53, 1325-1333.

Chlot, S., Widerlund, A., Öhlander, B., 2013. Interaction between nitrogen and phosphorus cycles in mining-affected aquatic systems—experiences from field and laboratory measurements. Environmental Science and Pollution Research 20, 5722-5736.

Ciffroy, P., Nia, Y., Garnier, J.M., 2011. Probabilistic Multicompartmental Model for

Interpreting DGT Kinetics in Sediments. Environmental Science & Technology 45, 9558-9565.

Clarisse, O., Lotufo, G.R., Hintelmann, H., Best, E.P.H., 2012. Biomonitoring and assessment of monomethylmercury exposure in aqueous systems using the DGT technique. Science of The Total Environment 416, 449-454.

Collins, C.D., Mosquera-Vazquez, M., Gomez-Eyles, J.L., Mayer, P., Gouliarmou, V., Blum, F., 2013. Is there sufficient 'sink' in current bioaccessibility determinations of organic pollutants in soils? Environmental Pollution 181, 128-132.

Cornelissen, G., Noort, P.C.M.v., Govers, H.A.J., 1997a. Desorption kinetics of chlorobenzenes, polycyclic aromatic hydrocarbons, and polychlorinated biphenyls: Sediment extraction with Tenax® and effects of contact time and solute hydrophobicity. Environmental Toxicology and Chemistry 16, 1351-1357.

Cornelissen, G., van Noort, P.C.M., Parsons, J.R., Govers, H.A.J., 1997b. Temperature Dependence of Slow Adsorption and Desorption Kinetics of Organic Compounds in Sediments. Environmental Science & Technology 31, 454-460.

Crank, J., 1979. The mathematics of diffusion. Oxford university press.

Cristale, J., Katsoyiannis, A., Chen, C.e., Jones, K.C., Lacorte, S., 2013. Assessment of flame retardants in river water using a ceramic dosimeter passive sampler. Environmental Pollution 172, 163-169.

Cui, X., Mayer, P., Gan, J., 2013. Methods to assess bioavailability of hydrophobic organic contaminants: Principles, operations, and limitations. Environmental pollution (1987) 172, 223-234.

Cussler, E.L., 2009. Diffusion: mass transfer in fluid systems. Cambridge university press.

D'Angelo, E., Starnes, D., 2016. Desorption kinetics of ciprofloxacin in municipal biosolids determined by diffusion gradient in thin films. Chemosphere 164, 215-224.

D'Angelo, E., Martin, A., 2018. Tetracycline desorption kinetics in municipal biosolids and poultry litter amendments determined by diffusive gradients in thin films (DGT). Chemosphere 209, 232-239.

Davison, W., 2016. Diffusive gradients in thin-films for environmental measurements. Cambridge University Press, Cambridge.

Davison, W., Zhang, H., 1994. In situ speciation measurements of trace components in natural waters using thin-film gels. Nature 367, 546-548.

Davison, W., Zhang, H., 2012. Progress in understanding the use of diffusive gradients in thin films (DGT) – back to basics. Environmental Chemistry 9, 1-13.

Deblonde, T., Cossu-Leguille, C., Hartemann, P., 2011. Emerging pollutants in wastewater: A review of the literature. International Journal of Hygiene and Environmental Health 214, 442-448.

Degryse, F., Smolders, E., Merckx, R., 2006. Labile Cd Complexes Increase Cd Availability to Plants. Environmental Science & Technology 40, 830-836.

Delle Site, A., 2001. Factors Affecting Sorption of Organic Compounds in Natural Sorbent/Water Systems and Sorption Coefficients for Selected Pollutants. A Review. Journal of Physical and Chemical Reference Data 30, 187-439.

Demars, K.R., Richardson, G.N., Soil, A.C.D.-o., Rock, Canada, C.E., Yong, R.N., Agency, U.S.E.P., Chaney, R.C., 1995. Dredging, Remediation, and Containment of

Contaminated Sediments. ASTM.

Diamanti-Kandarakis, E., Bourguignon, J.-P., Giudice, L.C., Hauser, R., Prins, G.S., Soto, A.M., Zoeller, R.T., Gore, A.C., 2009. Endocrine-Disrupting Chemicals: An Endocrine Society Scientific Statement. Endocrine Reviews 30, 293-342.

Doelman, P., Salomons, W., Schulin, R., Smidt, G.R.B., Stigliani, W.M., Van ser Zee, S., 1991. Chemical time bombs: definition, concepts, and examples. in: Stigliani, W.M. (Ed.). Interntional Institute For Applied Systems Analysis Laxenburg, Austria.

Donlan, R., 2002. Biofilms: Microbial Life on Surfaces. Emerging Infectious Disease Journal 8, 881.

Dueri, S., Castro-Jiménez, J., Comenges, J.-M.Z., 2008. On the use of the partitioning approach to derive Environmental Quality Standards (EQS) for persistent organic pollutants (POPs) in sediments: A review of existing data. Science of The Total Environment 403, 23-33.

Dunn, R.J.K., Teasdale, P.R., Warnken, J., Schleich, R.R., 2003. Evaluation of the Diffusive Gradient in a Thin Film Technique for Monitoring Trace Metal Concentrations in Estuarine Waters. Environmental Science & Technology 37, 2794-2800.

Eek, E., Cornelissen, G., Breedveld, G.D., 2010. Field Measurement of Diffusional Mass Transfer of HOCs at the Sediment-Water Interface. Environmental Science & Technology 44, 6752-6759.

Eismann, C.E., Menegário, A.A., Gemeiner, H., Williams, P.N., 2020. Predicting Trace Metal Exposure in Aquatic Ecosystems: Evaluating DGT as a Biomonitoring Tool. Exposure and Health 12, 19-31.

Endo, S., Matsuura, Y., 2018. Characterizing Sorption and Permeation Properties of Membrane Filters Used for Aquatic Integrative Passive Samplers. Environmental Science & Technology 52, 2118-2125.

Ernstberger, H., Davison, W., Zhang, H., Tye, A., Young, S., 2002. Measurement and Dynamic Modeling of Trace Metal Mobilization in Soils Using DGT and DIFS. Environmental Science & Technology 36, 349-354.

Ernstberger, H., Zhang, H., Tye, A., Young, S., Davison, W., 2005. Desorption Kinetics of Cd, Zn, and Ni Measured in Soils by DGT. Environmental Science & Technology 39, 1591-1597.

Escudero, J., Muñoz, J.L., Morera-Herreras, T., Hernandez, R., Medrano, J., Domingo-Echaburu, S., Barceló, D., Orive, G., Lertxundi, U., 2021. Antipsychotics as environmental pollutants: An underrated threat? Science of The Total Environment 769, 144634.

EU, 2012. Guidance on surface water chemical monitoring under the water framework directive. Guidance document No 19. Office for Official Publications of the European Communities: Luxembourg.

Fang, Z., Li, K., Li, Y., Zhang, H., Jones, K.C., Liu, X., Liu, S., Ma, L.Q., Luo, J., 2019. Development and Application of the Diffusive Gradients in Thin-Films Technique for Measuring Psychiatric Pharmaceuticals in Natural Waters. Environmental Science & Technology 53, 11223-11231.

Fang, Z., Li, Y., Li, Y., Yang, D., Zhang, H., Jones, K.C., Gu, C., Luo, J., 2021. Development and Applications of Novel DGT Passive Samplers for Measuring 12 Per- and

Polyfluoroalkyl Substances in Natural Waters and Wastewaters. Environmental Science & Technology 55, 9548-9556.

Fauvelle, V., Montero, N., Mueller, J.F., Banks, A., Mazzella, N., Kaserzon, S.L., 2017. Glyphosate and AMPA passive sampling in freshwater using a microporous polyethylene diffusion sampler. Chemosphere 188, 241-248.

Fedorova, G., Golovko, O., Randak, T., Grabic, R., 2014. Storage effect on the analysis of pharmaceuticals and personal care products in wastewater. Chemosphere 111, 55-60.

Feng, Z., Zhu, P., Fan, H., Piao, S., Xu, L., Sun, T., 2016. Effect of Biofilm on Passive Sampling of Dissolved Orthophosphate Using the Diffusive Gradients in Thin Films Technique. Analytical Chemistry 88, 6836-6843.

Ferguson, P.L., Chandler, G.T., Templeton, R.C., DeMarco, A., Scrivens, W.A., Englehart, B.A., 2008. Influence of Sediment−Amendment with Single-walled Carbon Nanotubes and Diesel Soot on Bioaccumulation of Hydrophobic Organic Contaminants by Benthic Invertebrates. Environmental Science & Technology 42, 3879-3885.

Fernandez, L.A., Lao, W., Maruya, K.A., Burgess, R.M., 2014. Calculating the Diffusive Flux of Persistent Organic Pollutants between Sediments and the Water Column on the Palos Verdes Shelf Superfund Site Using Polymeric Passive Samplers. Environmental Science & Technology 48, 3925-3934.

Fernandez, L.A., Lao, W., Maruya, K.A., White, C., Burgess, R.M., 2012. Passive Sampling to Measure Baseline Dissolved Persistent Organic Pollutant Concentrations in the Water Column of the Palos Verdes Shelf Superfund Site. Environmental Science & Technology 46, 11937-11947.

Fernandez, L.A., MacFarlane, J.K., Tcaciuc, A.P., Gschwend, P.M., 2009. Measurement of Freely Dissolved PAH Concentrations in Sediment Beds Using Passive Sampling with Low-Density Polyethylene Strips. Environmental Science & Technology 43, 1430-1436.

Fong, P.P., Hoy, C.M., 2012. Antidepressants (venlafaxine and citalopram) cause foot detachment from the substrate in freshwater snails at environmentally relevant concentrations. Marine and Freshwater Behaviour and Physiology 45, 145-153.

Forsberg, N.D., Smith, B.W., Sower, G.J., Anderson, K.A., 2014. Predicting Polycyclic Aromatic Hydrocarbon Concentrations in Resident Aquatic Organisms Using Passive Samplers and Partial Least-Squares Calibration. Environmental Science & Technology 48, 6291-6299.

Foster, G.D., Leahigh, A., 2021. Sediment–Water Distribution and Benthic Boundary Layer Fluxes of Pharmaceuticals and Personal Care Products near Wastewater Discharge into a Tidal River Shoal. ACS ES&T Water 1, 1447-1455.

Franquet-Griell, H., Pueyo, V., Silva, J., Orera, V.M., Lacorte, S., 2017. Development of a macroporous ceramic passive sampler for the monitoring of cytostatic drugs in water. Chemosphere 182, 681-690.

Ganser, G.H., Hewett, P., 2010. An Accurate Substitution Method for Analyzing Censored Data. Journal of Occupational and Environmental Hygiene 7, 233-244.

Gao, J., Pedersen, J.A., 2005. Adsorption of Sulfonamide Antimicrobial Agents to Clay Minerals. Environmental Science & Technology 39, 9509-9516.

Gasch, J., Leopold, C.S., Knoth, H., 2011. Drug retention by inline filters – Effect of positively

charged polyethersulfone filter membranes on drug solutions with low concentration. European Journal of Pharmaceutical Sciences 44, 49-56.

Gavrilescu, M., 2005. Fate of Pesticides in the Environment and its Bioremediation. Engineering in Life Sciences 5, 497-526.

Gaw, S.L., Sarkar, S., Nir, S., Schnell, Y., Mandler, D., Xu, Z.J., Lee, P.S., Reches, M., 2017. Electrochemical Approach for Effective Antifouling and Antimicrobial Surfaces. ACS Applied Materials & Interfaces 9, 26503-26509.

Geisler, A., Endo, S., Goss, K.-U., 2012. Partitioning of Organic Chemicals to Storage Lipids: Elucidating the Dependence on Fatty Acid Composition and Temperature. Environmental Science & Technology 46, 9519-9524.

Geissen, V., Mol, H., Klumpp, E., Umlauf, G., Nadal, M., van der Ploeg, M., van de Zee, S.E.A.T.M., Ritsema, C.J., 2015. Emerging pollutants in the environment: A challenge for water resource management. International Soil and Water Conservation Research 3, 57-65.

Gilliom, R.J., 2007. Pesticides in U.S. Streams and Groundwater. Environmental Science & Technology 41, 3408-3414.

Godoy, A.A., Kummrow, F., Pamplin, P.A.Z., 2015. Occurrence, ecotoxicological effects and risk assessment of antihypertensive pharmaceutical residues in the aquatic environment - A review. Chemosphere 138, 281-291.

Golovko, O., Rehrl, A.-L., Köhler, S., Ahrens, L., 2020. Organic micropollutants in water and sediment from Lake Mälaren, Sweden. Chemosphere 258, 127293.

Grimalt, J.O., Fernandez, P., Berdie, L., Vilanova, R.M., Catalan, J., Psenner, R., Hofer, R.,

Appleby, P.G., Rosseland, B.O., Lien, L., Massabuau, J.C., Battarbee, R.W., 2001. Selective Trapping of Organochlorine Compounds in Mountain Lakes of Temperate Areas. Environmental Science & Technology 35, 2690-2697.

Gschwend, P.M., MacFarlane, J.K., Reible, D.D., Lu, X., Hawthorne, S.B., Nakles, D.V., Thompson, T., 2011. Comparison of polymeric samplers for accurately assessing PCBs in pore waters. Environmental Toxicology and Chemistry 30, 1288-1296.

Guan, D.-X., 2019. Diffusive Gradients in Thin-Films (DGT): An Effective and Simple Tool for Assessing Contaminant Bioavailability in Waters, Soils and Sediments. in: Nriagu, J. (Ed.). Encyclopedia of Environmental Health (Second Edition). Elsevier, Oxford, pp. 111-124.

Guan, D., Li, Y., Yu, N., Yu, G., Wei, S., Zhang, H., Davison, W., Cui, X., Ma, L.Q., Luo, J., 2018. In situ measurement of perfluoroalkyl substances in aquatic systems using diffusive gradients in thin-films technique. Water Research 144, 162-171.

Guibal, R., Buzier, R., Charriau, A., Lissalde, S., Guibaud, G., 2017. Passive sampling of anionic pesticides using the Diffusive Gradients in Thin films technique (DGT). Analytica Chimica Acta 966, 1-10.

Guibal, R., Buzier, R., Lissalde, S., Guibaud, G., 2019. Adaptation of diffusive gradients in thin films technique to sample organic pollutants in the environment: An overview of o-DGT passive samplers. Science of The Total Environment 693, 133537.

Guo, C., Zhang, T., Hou, S., Lv, J., Zhang, Y., Wu, F., Hua, Z., Meng, W., Zhang, H., Xu, J., 2017a. Investigation and Application of a New Passive Sampling Technique for in Situ Monitoring of Illicit Drugs in Waste Waters and Rivers. Environmental Science &

Technology 51, 9101-9108.

Guo, W., Van Langenhove, K., Denison, M.S., Baeyens, W., Elskens, M., Gao, Y., 2017b. Estrogenic Activity Measurements in Water Using Diffusive Gradients in Thin-Film Coupled with an Estrogen Bioassay. Anal Chem 89, 13357-13364.

Guo, W., Van Langenhove, K., Vandermarken, T., Denison, M.S., Elskens, M., Baeyens, W., Gao, Y., 2019. In situ measurement of estrogenic activity in various aquatic systems using organic diffusive gradients in thin-film coupled with ERE-CALUX bioassay. Environment International 127, 13-20.

Gustavsson, P.-E., Son, P.-O., 2003. Chapter 6 - Monolithic Polysaccharide Materials. in: Švec, F., Tennikova, T.B., Deyl, Z. (Eds.). Journal of Chromatography Library. Elsevier, pp. 121-141.

Haham, H., Oren, A., Chefetz, B., 2012. Insight into the Role of Dissolved Organic Matter in Sorption of Sulfapyridine by Semiarid Soils. Environmental Science & Technology 46, 11870-11877.

Halpern, B.S., Walbridge, S., Selkoe, K.A., Kappel, C.V., Micheli, F., D'Agrosa, C., Bruno, J.F., Casey, K.S., Ebert, C., Fox, H.E., Fujita, R., Heinemann, D., Lenihan, H.S., Madin, E.M.P., Perry, M.T., Selig, E.R., Spalding, M., Steneck, R., Watson, R., 2008. A Global Map of Human Impact on Marine Ecosystems. Science 319, 948-952.

Han, J., Qiu, W., Gao, W., 2010. Adsorption of estrone in microfiltration membrane filters. Chemical Engineering Journal 165, 819-826.

Hao, C., Zhao, X., Yang, P., 2007. GC-MS and HPLC-MS analysis of bioactive pharmaceuticals and personal-care products in environmental matrices. TrAC Trends in Analytical

Chemistry 26, 569-580.

Hao, X., Zhang, R., Kravchenko, A., 2005. Effects of root density distribution models on root water uptake and water flow under irrigation. Soil Science 170, 167-174.

Harman, C., Allan, I.J., Vermeirssen, E.L.M., 2012. Calibration and use of the polar organic chemical integrative sampler—a critical review. Environmental Toxicology and Chemistry 31, 2724-2738.

Harman, C., Bøyum, O., Thomas, K.V., Grung, M., 2009. Small but Different Effect of Fouling on the Uptake Rates of Semipermeable Membrane Devices and Polar Organic Chemical Integrative Samplers. Environmental Toxicology and Chemistry 28, 2324-2332.

Harper, M.P., Davison, W., Tych, W., 2000. DIFS—a modelling and simulation tool for DGT induced trace metal remobilisation in sediments and soils. Environmental Modelling & Software 15, 55-66.

Harper, M.P., Davison, W., Zhang, H., Tych, W., 1998. Kinetics of metal exchange between solids and solutions in sediments and soils interpreted from DGT measured fluxes. Geochimica et Cosmochimica Acta 62, 2757-2770.

Hartnik, T., Jensen, J., Hermens, J.L.M., 2008. Nonexhaustive β-Cyclodextrin Extraction as a Chemical Tool To Estimate Bioavailability of Hydrophobic Pesticides for Earthworms. Environmental Science & Technology 42, 8419-8425.

Hayat, M.T., Xu, J., Ding, N., Mahmood, T., 2010. Dynamic Behavior of Persistent Organic Pollutants in Soil and Their Interaction with Organic Matter. in: Xu, J., Huang, P.M. (Eds.). Molecular Environmental Soil Science at the Interfaces in the Earth's Critical

Zone. Springer Berlin Heidelberg, Berlin, Heidelberg, pp. 217-222.

Hayduk, W., Laudie, H., 1974. Prediction of diffusion coefficients for nonelectrolytes in dilute aqueous solutions. AIChE Journal 20, 611-615.

Hayes, M.H., Swift, R., 1978. The chemistry of soil organic colloids. The chemistry of soil constituents, 179-320.

Hazlett, B.A., Rittschof, D., 1985. Variation in Rate of Growth in the Crayfish Orconectes Virilis. Journal of Crustacean Biology 5, 341-346.

He, K., Hain, E., Timm, A., Blaney, L., 2021. Bioaccumulation of estrogenic hormones and UV-filters in red swamp crayfish (Procambarus clarkii). Science of The Total Environment 764, 142871.

He, W., Yang, C., Liu, W., He, Q., Wang, Q., Li, Y., Kong, X., Lan, X., Xu, F., 2016. The partitioning behavior of persistent toxicant organic contaminants in eutrophic sediments: Coefficients and effects of fluorescent organic matter and particle size. Environmental Pollution 219, 724-734.

Hebig, K.H., Nödler, K., Licha, T., Scheytt, T.J., 2014. Impact of materials used in lab and field experiments on the recovery of organic micropollutants. Science of The Total Environment 473-474, 125-131.

Hendriks, A.J., van der Linde, A., Cornelissen, G., Sijm, D.T.H.M., 2001. The power of size. 1. Rate constants and equilibrium ratios for accumulation of organic substances related to octanol-water partition ratio and species weight. Environmental Toxicology and Chemistry 20, 1399-1420.

Higashino, M., O'Connor, B.L., Hondzo, M., Stefan, H.G., 2008. Oxygen transfer from flowing

water to microbes in an organic sediment bed. Hydrobiologia 614, 219-231.

Ho, Y.S., McKay, G., 1999. Pseudo-second order model for sorption processes. Process Biochemistry 34, 451-465.

Hofelt, C.S., Shea, D., 1997. Accumulation of Organochlorine Pesticides and PCBs by Semipermeable Membrane Devices and Mytilus edulis in New Bedford Harbor. Environmental Science & Technology 31, 154-159.

Hoffman, G.J., Van Genuchten, M.T., 1983. Soil Properties and Efficient Water Use: Water Management for Salinity Control. Limitations to Efficient Water Use in Crop Production, pp. 73-85.

Honeyman, B.D., Santschi, P.H., 1988. Metals in aquatic systems. Environmental Science & Technology 22, 862-871.

Huckins, J.N., Petty, J.D., Lebo, J.A., Almeida, F.V., Booij, K., Alvarez, D.A., Cranor, W.L., Clark, R.C., Mogensen, B.B., 2002. Development of the Permeability/Performance Reference Compound Approach for In Situ Calibration of Semipermeable Membrane Devices. Environmental Science & Technology 36, 85-91.

Iuele, H., Ling, N., Hartland, A., 2021. Characterization of a green expanded DGT methodology for the in-situ detection of emerging endocrine disrupting chemicals in water systems. Sustainable Chemistry and Pharmacy 22, 100450.

James, M.O., Boyle, S.M., 1998. Cytochromes P450 in crustacea1This article was invited by Guest Editors Dr John J. Stegeman and Dr David R. Livingstone to be part of a special issue of CBP on cytochrome P450 (Comp. Biochem. Physiol. 121 C, pages 1–412, 1998).1. Comparative Biochemistry and Physiology Part C: Pharmacology, Toxicology

and Endocrinology 121, 157-172.

Jannasch, H.W., Honeyman, B.D., Balistrieri, L.S., James W, M., 1988. Kinetics of trace element uptake by marine particles. Geochimica et Cosmochimica Acta 52, 567-577.

Jewell, C.S.E., Mayeaux, M.H., Winston, G.W., 1997. Benzo[a]pyrene Metabolism by the Hepatopancreas and Green Gland of the Red Swamp Crayfish, Procambarus clarkii, In Vitro. Comparative Biochemistry and Physiology Part C: Pharmacology, Toxicology and Endocrinology 118, 369-374.

Ji, X., Cantin, J., Cardenas Perez, A.S., Gong, Y., Giesy, J.P., Brinkmann, M., 2023. Combining passive sampling with fraction transfer and toxicokinetic modeling to assess bioavailability of organic pollutants in a benthic invertebrate, Lumbriculus variegatus. Journal of Hazardous Materials 441, 129986.

Ji, X., Challis, J.K., Brinkmann, M., 2022a. A critical review of diffusive gradients in thin films technique for measuring organic pollutants: Potential limitations, application to solid phases, and combination with bioassays. Chemosphere 287, 132352.

Ji, X., Challis, J.K., Cantin, J., Cardenas Perez, A.S., Gong, Y., Giesy, J.P., Brinkmann, M., 2022b. Desorption kinetics of antipsychotic drugs from sandy sediments by diffusive gradients in thin-films technique. Science of The Total Environment 832, 155104.

Ji, X., Challis, J.K., Cantin, J., Cardenas Perez, A.S., Gong, Y., Giesy, J.P., Brinkmann, M., 2022c. A novel passive sampling and sequential extraction approach to investigate desorption kinetics of emerging organic contaminants at the sediment−water interface. Water Research 217, 118455.

Jing, P., Rodgers, P.J., Amemiya, S., 2009. High Lipophilicity of Perfluoroalkyl Carboxylate

and Sulfonate: Implications for Their Membrane Permeability. Journal of the American

Chemical Society 131, 2290-2296.

Jon, A.A., Frank, A.P.C.G., 2006. A review of bioconcentration factor (BCF) and

bioaccumulation factor (BAF) assessments for organic chemicals in aquatic organisms.

Environmental Reviews 14, 257-297.

Jones, D.L., Willett, V.B., 2006. Experimental evaluation of methods to quantify dissolved

organic nitrogen (DON) and dissolved organic carbon (DOC) in soil. Soil Biology and

Biochemistry 38, 991-999.

Jorhem, L., Engman, J., Sundström, B., Thim, A.M., 1994. Trace elements in crayfish: Regional

differences and changes induced by cooking. Archives of Environmental

Contamination and Toxicology 26, 137-142.

Joyce, A.S., Portis, L.M., Parks, A.N., Burgess, R.M., 2016. Evaluating the Relationship

between Equilibrium Passive Sampler Uptake and Aquatic Organism Bioaccumulation.

Environmental Science & Technology 50, 11437-11451.

Kalichak, F., Idalencio, R., da Rosa, J.G.S., Barcellos, H.H.d.A., Fagundes, M., Piato, A.,

Barcellos, L.J.G., 2017. Psychotropic in the environment: risperidone residues affect

the behavior of fish larvae. Sci Rep 7, 14121.

Karickhoff, S.W., 1981. Semi-empirical estimation of sorption of hydrophobic pollutants on

natural sediments and soils. Chemosphere (Oxford) 10, 833-846.

Karlsson, M.V., Marshall, S., Gouin, T., Boxall, A.B.A., 2016. Routes of uptake of diclofenac,

fluoxetine, and triclosan into sediment-dwelling worms. Environmental Toxicology

and Chemistry 35, 836-842.

Ke, R., Xu, Y., Huang, S., Wang, Z., Huckins, J.N., 2007. Comparison of the uptake of polycyclic aromatic hydrocarbons and organochlorine pesticides by semipermeable membrane devices and caged fish (Carassius carassius) in Taihu Lake, China. Environmental Toxicology and Chemistry 26, 1258-1264.

Keilty, T.J., White, D.S., Landrum, P.F., 1988. Sublethal responses to endrin in sediment by Limnodrilus hoffmeisteri (Tubificidae), and in mixed-culture with Stylodrilus heringianus (Lumbriculidae). Aquatic Toxicology 13, 227-249.

Kell, D.B., Oliver, S.G., 2014. How drugs get into cells: tested and testable predictions to help discriminate between transporter-mediated uptake and lipoidal bilayer diffusion. Frontiers in Pharmacology 5, 231.

Khatri, N., Tyagi, S., 2015. Influences of natural and anthropogenic factors on surface and groundwater quality in rural and urban areas. Frontiers in Life Science 8, 23-39.

Kim, M.-K., Zoh, K.-D., 2016. Occurrence and removals of micropollutants in water environment. Environmental Engineering Research 21, 319-332.

Kingston, J.K., Greenwood, R., Mills, G.A., Morrison, G.M., Björklund Persson, L., 2000. Development of a novel passive sampling system for the time-averaged measurement of a range of organic pollutants in aquatic environments. Journal of Environmental Monitoring 2, 487-495.

Kleber, M., Eusterhues, K., Keiluweit, M., Mikutta, C., Mikutta, R., Nico, P.S., 2015. Chapter One - Mineral–Organic Associations: Formation, Properties, and Relevance in Soil Environments. in: Sparks, D.L. (Ed.). Advances in Agronomy. Academic Press, pp. 1-140.

Kot-Wasik, A., Zabiegała, B., Urbanowicz, M., Dominiak, E., Wasik, A., Namieśnik, J., 2007. Advances in passive sampling in environmental studies. Analytica Chimica Acta 602, 141-163.

Kukkonen, J., Landrum, P.F., 1994. Toxicokinetics and toxicity of sediment-associated pyrene to lumbriculus variegatus (oligochaeta). Environmental Toxicology and Chemistry 13, 1457-1468.

Kümmerer, K., 2008. Pharmaceuticals in the Environment: Sources, Fate, Effects and Risks. Springer, Berlin, Heidelberg.

Kupryianchyk, D., Noori, A., Rakowska, M.I., Grotenhuis, J.T.C., Koelmans, A.A., 2013. Bioturbation and Dissolved Organic Matter Enhance Contaminant Fluxes from Sediment Treated with Powdered and Granular Activated Carbon. Environmental Science & Technology 47, 5092-5100.

Kuroda, N., Hamada, S., Sakata, N., Jeon, B., Iijima, K., Yoshie, S., Ishizaki, T., Jin, X., Watanabe, T., Tamiya, N., 2019. Antipsychotic use and related factors among people with dementia aged 75 years or older in Japan: A comprehensive population-based estimation using medical and long-term care data. International Journal of Geriatric Psychiatry 34, 472-479.

Kwon, J.-W., Armbrust, K.L., 2006. Laboratory persistence and fate of fluoxetine in aquatic environments. Environmental Toxicology and Chemistry 25, 2561-2568.

Larsen, T.A., Lienert, J., Joss, A., Siegrist, H., 2004. How to avoid pharmaceuticals in the aquatic environment. Journal of Biotechnology 113, 295-304.

Le Bas, G., 1915. The molecular volumes of liquid chemical compounds, from the point of

view of Kopp. Longmans, Green.

Leggett, D.C., Parker, L.V., 1994. Modeling the Equilibrium Partitioning of Organic Contaminants between PTFE, PVC, and Groundwater. Environmental Science & Technology 28, 1229-1233.

Lehto, N.J., Sochaczewski, Ł., Davison, W., Tych, W., Zhang, H., 2008. Quantitative assessment of soil parameter (KD and TC) estimation using DGT measurements and the 2D DIFS model. Chemosphere 71, 795-801.

Leip, A., Billen, G., Garnier, J., Grizzetti, B., Lassaletta, L., Reis, S., Simpson, D., Sutton, M.A., de Vries, W., Weiss, F., Westhoek, H., 2015. Impacts of European livestock production: nitrogen, sulphur, phosphorus and greenhouse gas emissions, land-use, water eutrophication and biodiversity. Environmental research letters 10, 115004.

Leppänen, M.T., Kukkonen, J.V.K., 2000. Fate of sediment-associated pyrene and benzo[a]pyrene in the freshwater oligochaete Lumbriculus variegatus (Müller). Aquatic Toxicology 49, 199-212.

Levick, J.R., 1987. Flow through interstitium and other fibrous matrices. Quarterly Journal of Experimental Physiology 72, 409-437.

Li, H., Helm, P.A., Metcalfe, C.D., 2010. Sampling in the Great Lakes for pharmaceuticals, personal care products, and endocrine-disrupting substances using the passive polar organic chemical integrative sampler. Environmental Toxicology and Chemistry 29, 751-762.

Li, H., Qi, S., Li, X., Qian, Z., Chen, W., Qin, S., 2021a. Tetrafluoroterephthalonitrile-crosslinked β-cyclodextrin polymer as a binding agent of diffusive gradients in thin-

films for sampling endocrine disrupting chemicals in water. Chemosphere 280, 130774.

Li, J.-Y., Tang, J.Y.M., Jin, L., Escher, B.I., 2013a. Understanding bioavailability and toxicity of sediment-associated contaminants by combining passive sampling with in vitro bioassays in an urban river catchment. Environmental Toxicology and Chemistry 32, 2888-2896.

Li, J., Zhang, J., Li, C., Wang, W., Yang, Z., Wang, H., Gan, J., Ye, Q., Xu, X., Li, Z., 2013b. Stereoisomeric Isolation and Stereoselective Fate of Insecticide Paichongding in Flooded Paddy Soils. Environmental Science & Technology 47, 12768-12774.

Li, T., Di, Z., Yang, X., Sparks, D.L., 2011. Effects of dissolved organic matter from the rhizosphere of the hyperaccumulator Sedum alfredii on sorption of zinc and cadmium by different soils. Journal of Hazardous Materials 192, 1616-1622.

Li, W., Zhao, H., Teasdale, P.R., John, R., Wang, F., 2005. Metal speciation measurement by diffusive gradients in thin films technique with different binding phases. Analytica Chimica Acta 533, 193-202.

Li, Y., Chen, C.-E.L., Chen, W., Chen, J., Cai, X., Jones, K.C., Zhang, H., 2019. Development of a Passive Sampling Technique for Measuring Pesticides in Waters and Soils. Journal of Agricultural and Food Chemistry 67, 6397-6406.

Li, Y., Han, C., Luo, J., Jones, K.C., Zhang, H., 2021b. Use of the Dynamic Technique DGT to Determine the Labile Pool Size and Kinetic Resupply of Pesticides in Soils and Sediments. Environmental Science & Technology.

Liang, Y., Dutta, S.P., 2001. Application trend in advanced ceramic technologies. Technovation 21, 61-65.

Lick, W., 2006. The Sediment-Water Flux of HOCs Due to "Diffusion" or Is There a Well-Mixed Layer? If There Is, Does It Matter? Environmental Science & Technology 40, 5610-5617.

Lin, Y.-C., Panchangam, S.C., Liu, L.-C., Lin, A.Y.-C., 2019. The design of a sunlight-focusing and solar tracking system: A potential application for the degradation of pharmaceuticals in water. Chemosphere 214, 452-461.

Ling, W.T., Wang, H.Z., Xu, J.M., Gao, Y.Z., 2005. Sorption of dissolved organic matter and its effects on the atrazine sorption on soils. J Environ Sci (China) 17, 478-482.

Liu, S.-S., Li, J.-L., Ge, L.-K., Li, C.-L., Zhao, J.-L., Zhang, Q.-Q., Ying, G.-G., Chen, C.-E., 2021. Selective diffusive gradients in thin-films with molecularly imprinted polymer for measuring fluoroquinolone antibiotics in waters. Science of The Total Environment 790, 148194.

Liu, S., Jin, L., Yu, H., Lv, L., Chen, C.-E., Ying, G.-G., 2020. Understanding and predicting the diffusivity of organic chemicals for diffusive gradients in thin-films using a QSPR model. Science of The Total Environment 706, 135691.

Llorca, M., Gros, M., Rodríguez-Mozaz, S., Barceló, D., 2014. Sample preservation for the analysis of antibiotics in water. Journal of Chromatography A 1369, 43-51.

López-García, E., Postigo, C., Zonja, B., Barceló, D., López de Alda, M., 2018. Chapter Two - Analysis of Psychoactive Pharmaceuticals in Wastewater and Surface Water Using LC-MS. in: Cappiello, A., Palma, P. (Eds.). Comprehensive Analytical Chemistry. Elsevier, pp. 29-52.

Lydy, M.J., Harwood, A.D., Nutile, S.A., Landrum, P.F., 2015. Tenax extraction of sediments

to estimate desorption and bioavailability of hydrophobic contaminants: A literature review. Integrated Environmental Assessment and Management 11, 208-220.

Madrid, Y., Zayas, Z.P., 2007. Water sampling: Traditional methods and new approaches in water sampling strategy. TrAC Trends in Analytical Chemistry 26, 293-299.

Martin, H., Patterson, B.M., Davis, G.B., Grathwohl, P., 2003. Field Trial of Contaminant Groundwater Monitoring: Comparing Time-Integrating Ceramic Dosimeters and Conventional Water Sampling. Environmental Science & Technology 37, 1360-1364.

Martín, J., Camacho-Muñoz, D., Santos, J.L., Aparicio, I., Alonso, E., 2012. Occurrence of pharmaceutical compounds in wastewater and sludge from wastewater treatment plants: Removal and ecotoxicological impact of wastewater discharges and sludge disposal. Journal of Hazardous Materials 239-240, 40-47.

Martínez-Hernández, V., Meffe, R., Herrera, S., Arranz, E., de Bustamante, I., 2014. Sorption/desorption of non-hydrophobic and ionisable pharmaceutical and personal care products from reclaimed water onto/from a natural sediment. Science of The Total Environment 472, 273-281.

McClellan, K., Halden, R.U., 2010. Pharmaceuticals and personal care products in archived U.S. biosolids from the 2001 EPA national sewage sludge survey. Water Research 44, 658-668.

Mechelke, J., Vermeirssen, E.L.M., Hollender, J., 2019. Passive sampling of organic contaminants across the water-sediment interface of an urban stream. Water Research 165, 114966.

Megahan, W.F., 1999. Sediment pollution. Environmental Geology. Springer Netherlands,

Dordrecht, pp. 552-553.

Menezes-Blackburn, D., Sun, J., Lehto, N.J., Zhang, H., Stutter, M., Giles, C.D., Darch, T., George, T.S., Shand, C., Lumsdon, D., Blackwell, M., Wearing, C., Cooper, P., Wendler, R., Brown, L., Al-Kasbi, M., Haygarth, P.M., 2019. Simultaneous Quantification of Soil Phosphorus Labile Pool and Desorption Kinetics Using DGTs and 3D-DIFS. Environmental Science & Technology 53, 6718-6728.

Merkle, E.L., 1969. Home Range of Crayfish Orconectes juvenalis. The American Midland Naturalist 81, 228-235.

Metcalfe, C.D., Chu, S., Judt, C., Li, H., Oakes, K.D., Servos, M.R., Andrews, D.M., 2010. Antidepressants and their metabolites in municipal wastewater, and downstream exposure in an urban watershed. Environmental Toxicology and Chemistry 29, 79-89.

Meunier, C.L., Gundale, M.J., Sánchez, I.S., Liess, A., 2016. Impact of nitrogen deposition on forest and lake food webs in nitrogen-limited environments. Global change biology 22, 164-179.

Moermond, C.T.A., Roozen, F.C.J.M., Zwolsman, J.J.G., Koelmans, A.A., 2004. Uptake of Sediment-Bound Bioavailable Polychlorobiphenyls by Benthivorous Carp (Cyprinus carpio). Environmental Science & Technology 38, 4503-4509.

Momot, W.T., 1967. Population Dynamics and Productivity of the Crayfish, Orconectes virilis, in a Marl Lake. The American Midland Naturalist 78, 55-81.

Momot, W.T., Gowing, H., 1972. Differential Seasonal Migration of the Crayfish, Orconectes Virilis (Hagen) in Marl Lakes. Ecology 53, 479-483.

Mottaleb, M.A., 2015. Use of LC-MS and GC-MS Methods to Measure Emerging

Contaminants Pharmaceutical and Personal Care Products (PPCPs) in Fish. Journal of Chromatography & Separation Techniques 06.

Muijs, B., Jonker, M.T.O., 2011. Assessing the Bioavailability of Complex Petroleum Hydrocarbon Mixtures in Sediments. Environmental Science & Technology 45, 3554-3561.

Müller, A.-K., Markert, N., Leser, K., Kämpfer, D., Schiwy, S., Riegraf, C., Buchinger, S., Gan, L., Abdallah, A.T., Denecke, B., Segner, H., Brinkmann, M., Crawford, S.E., Hollert, H., 2021. Bioavailability and impacts of estrogenic compounds from suspended sediment on rainbow trout (Oncorhynchus mykiss). Aquatic Toxicology 231, 105719.

Muncaster, B.W., Hebert, P.D.N., Lazar, R., 1990. Biological and physical factors affecting the body burden of organic contaminants in freshwater mussels. Archives of Environmental Contamination and Toxicology 19, 25-34.

Mustajärvi, L., Eek, E., Cornelissen, G., Eriksson-Wiklund, A.-K., Undeman, E., Sobek, A., 2017. In situ benthic flow-through chambers to determine sediment-to-water fluxes of legacy hydrophobic organic contaminants. Environmental Pollution 231, 854-862.

Nannou, C.I., Kosma, C.I., Albanis, T.A., 2015. Occurrence of pharmaceuticals in surface waters: analytical method development and environmental risk assessment. International Journal of Environmental Analytical Chemistry 95, 1242-1262.

Nanseu-Njiki, C.P., Dedzo, G.K., Ngameni, E., 2010. Study of the removal of paraquat from aqueous solution by biosorption onto Ayous (Triplochiton schleroxylon) sawdust. Journal of hazardous materials 179, 63-71.

Navon, R., Hernandez-Ruiz, S., Chorover, J., Chefetz, B., 2011. Interactions of Carbamazepine

in Soil: Effects of Dissolved Organic Matter. Journal of Environmental Quality 40, 942-948.

Nelson, D.W., Sommers, L.E., 1996. Total Carbon, Organic Carbon, and Organic Matter. Methods of Soil Analysis, pp. 961-1010.

Noh, S., Kim, Y.-h., Kim, H., Seok, K.-s., Park, M., Bailon, M.X., Hong, Y., 2019. The performance of diffusive gradient in thin film probes for the long-term monitoring of trace level total mercury in water. Environmental Monitoring and Assessment 192, 66.

Northcott, G.L., Jones, K.C., 2000. Experimental approaches and analytical techniques for determining organic compound bound residues in soil and sediment. Environmental Pollution 108, 19-43.

Nunes, C.N., dos Anjos, V.E., Quináia, S.P., 2019. Are there pharmaceutical compounds in sediments or in water? Determination of the distribution coefficient of benzodiazepine drugs in aquatic environment. Environmental Pollution 251, 522-529.

Nye, P.H., 1983. The diffusion of two interacting solutes in soil. Journal of Soil Science 34, 677-691.

Öllers, S., Singer, H.P., Fässler, P., Müller, S.R., 2001. Simultaneous quantification of neutral and acidic pharmaceuticals and pesticides at the low-ng/l level in surface and waste water. Journal of Chromatography A 911, 225-234.

Omidvar, M., Soltanieh, M., Mousavi, S.M., Saljoughi, E., Moarefian, A., Saffaran, H., 2015. Preparation of hydrophilic nanofiltration membranes for removal of pharmaceuticals from water. Journal of Environmental Health Science and Engineering 13, 42.

Palomo, M., Bhandari, A., 2006. Impact of Aging on the Formation of Bound Residues after

Peroxidase-Mediated Treatment of 2,4-DCP Contaminated Soils. Environmental science & technology 40, 3402-3408.

Patel, N., Khan, M., Shahane, S., Rai, D., Chauhan, D., Kant, C., Chaudhary, V., 2020. Emerging Pollutants in Aquatic Environment: Source, Effect, and Challenges in Biomonitoring and Bioremediation- A Review. 6, 99-113.

Paulik, L.B., Smith, B.W., Bergmann, A.J., Sower, G.J., Forsberg, N.D., Teeguarden, J.G., Anderson, K.A., 2016. Passive samplers accurately predict PAH levels in resident crayfish. Science of The Total Environment 544, 782-791.

Payá-Pérez, A.B., Cortés, A., Sala, M.N., Larsen, B., 1992. Organic matter fractions controlling the sorption of atrazine in sandy soils. Chemosphere 25, 887-898.

Pelcová, P., Vičarová, P., Dočekalová, H., Poštulková, E., Kopp, R., Mareš, J., Smolíková, V., 2018. The prediction of mercury bioavailability for common carp (Cyprinus carpio L.) using the DGT technique in the presence of chloride ions and humic acid. Chemosphere 211, 1109-1112.

Pelcová, P., Vičarová, P., Ridošková, A., Dočekalová, H., Kopp, R., Mareš, J., Poštulková, E., 2017. Prediction of mercury bioavailability to common carp (Cyprinus carpio L.) using the diffusive gradient in thin film technique. Chemosphere 187, 181-187.

Pichette, C., Zhang, H., Davison, W., Sauvé, S., 2007. Preventing biofilm development on DGT devices using metals and antibiotics. Talanta 72, 716-722.

Pichette, C., Zhang, H., Sauvé, S., 2009. Using diffusive gradients in thin-films for in situ monitoring of dissolved phosphate emissions from freshwater aquaculture. Aquaculture 286, 198-202.

Pignatello, J.J., 1990. Slowly reversible sorption of aliphatic halocarbons in soils. II. Mechanistic aspects. Environmental Toxicology and Chemistry 9, 1117-1126.

Płotka-Wasylka, J., Szczepańska, N., de la Guardia, M., Namieśnik, J., 2015. Miniaturized solid-phase extraction techniques. TrAC Trends in Analytical Chemistry 73, 19-38.

Pluen, A., Netti, P.A., Jain, R.K., Berk, D.A., 1999. Diffusion of Macromolecules in Agarose Gels: Comparison of Linear and Globular Configurations. Biophysical Journal 77, 542-552.

Porte, C., Albaigés, J., 1994. Bioaccumulation patterns of hydrocarbons and polychlorinated biphenyls in bivalves, crustaceans, and fishes. Archives of Environmental Contamination and Toxicology 26, 273-281.

Poulier, G., Lissalde, S., Charriau, A., Buzier, R., Delmas, F., Gery, K., Moreira, A., Guibaud, G., Mazzella, N., 2014. Can POCIS be used in Water Framework Directive (2000/60/EC) monitoring networks? A study focusing on pesticides in a French agricultural watershed. Science of The Total Environment 497-498, 282-292.

Priha, O., Smolander, A., 1999. Nitrogen transformations in soil under Pinus sylvestris, Picea abies and Betula pendula at two forest sites. Soil Biology and Biochemistry 31, 965-977.

Raghav, S., Painuli, R., Kumar, D., 2019. Threats to Water: Issues and Challenges Related to Ground Water and Drinking Water. in: Naushad, M. (Ed.). A New Generation Material Graphene: Applications in Water Technology. Springer International Publishing, Cham, pp. 1-19.

Rainbow, P.S., 2002. Trace metal concentrations in aquatic invertebrates: why and so what?

Environmental Pollution 120, 497-507.

Ran, F., 2015. Polyethersulfone (PES). in: Drioli, E., Giorno, L. (Eds.). Encyclopedia of Membranes. Springer Berlin Heidelberg, Berlin, Heidelberg, pp. 1-2.

Rao, D.D., Sait, S.S., Reddy, A.M., Chakole, D., Reddy, Y.R., Mukkanti, K., 2010. Analysis of Duloxetine Hydrochloride and Its Related Compounds in Pharmaceutical Dosage Forms and In Vitro Dissolution Studies by Stability Indicating UPLC. Journal of Chromatographic Science 48, 819-824.

Rao, V.R., Mitz, S.V., Hadden, C.T., Cornaby, B.W., 1996. Distribution of Contaminants in Aquatic Organisms from East Fork Poplar Creek. Ecotoxicology and Environmental Safety 33, 44-54.

Rehberger, K., Wernicke von Siebenthal, E., Bailey, C., Bregy, P., Fasel, M., Herzog, E.L., Neumann, S., Schmidt-Posthaus, H., Segner, H., 2020. Long-term exposure to low 17α-ethinylestradiol (EE2) concentrations disrupts both the reproductive and the immune system of juvenile rainbow trout, Oncorhynchus mykiss. Environment International 142, 105836.

Reichert, J.F., Souza, D.M., Martins, A.F., 2019. Antipsychotic drugs in hospital wastewater and a preliminary risk assessment. Ecotoxicology and Environmental Safety 170, 559-567.

Ren, S., Wang, Y., Cui, Y., Wang, Y., Wang, X., Chen, J., Tan, F., 2020. Desorption kinetics of tetracyclines in soils assessed by diffusive gradients in thin films. Environmental Pollution 256, 113394.

Rezaee, M., Assadi, Y., Milani Hosseini, M.-R., Aghaee, E., Ahmadi, F., Berijani, S., 2006.

Determination of organic compounds in water using dispersive liquid–liquid microextraction. Journal of Chromatography A 1116, 1-9.

Rhind, S.M., 2009. Anthropogenic pollutants: a threat to ecosystem sustainability? Philosophical Transactions of the Royal Society B: Biological Sciences 364, 3391-3401.

Ribeiro, A.R., Pedrosa, M., Moreira, N.F.F., Pereira, M.F.R., Silva, A.M.T., 2015. Environmental friendly method for urban wastewater monitoring of micropollutants defined in the Directive 2013/39/EU and Decision 2015/495/EU. Journal of Chromatography A 1418, 140-149.

Ribeiro, C., Ribeiro, A.R., Tiritan, M.E., 2016. Occurrence of persistent organic pollutants in sediments and biota from Portugal versus European incidence: A critical overview. Journal of Environmental Science and Health, Part B 51, 143-153.

Roberts, T.R., 1984. Non-extractable pesticide residues in soils and plants. Pure and Applied Chemistry 56, 945-956.

Rodea-Palomares, I., Leganés, F., Rosal, R., Fernández-Piñas, F., 2012. Toxicological interactions of perfluorooctane sulfonic acid (PFOS) and perfluorooctanoic acid (PFOA) with selected pollutants. Journal of Hazardous Materials 201-202, 209-218.

Roulier, J.L., Tusseau-Vuillemin, M.H., Coquery, M., Geffard, O., Garric, J., 2008. Measurement of dynamic mobilization of trace metals in sediments using DGT and comparison with bioaccumulation in Chironomus riparius: First results of an experimental study. Chemosphere 70, 925-932.

Rusina, T.P., Smedes, F., Klanova, J., 2010. Diffusion coefficients of polychlorinated biphenyls

and polycyclic aromatic hydrocarbons in polydimethylsiloxane and low-density polyethylene polymers. Journal of Applied Polymer Science 116, 1803-1810.

Sabaliūnas, D., Ellington, J., Sabaliūnien±, I., 1999. Screening Bioavailable Hydrophobic Toxicants in Surface Waters with Semipermeable Membrane Devices: Role of Inherent Oleic Acid in Toxicity Evaluations. Ecotoxicology and Environmental Safety 44, 160-167.

Sabaliūnas, D., Södergren, A., 1997. Use of semi-permeable membrane devices to monitor pollutants in water and assess their effects: A laboratory test and field verification. Environmental Pollution 96, 195-205.

Sarrazin, F., Pianosi, F., Wagener, T., 2016. Global Sensitivity Analysis of environmental models: Convergence and validation. Environmental Modelling & Software 79, 135-152.

Scally, S., Davison, W., Zhang, H., 2006. Diffusion coefficients of metals and metal complexes in hydrogels used in diffusive gradients in thin films. Analytica Chimica Acta 558, 222-229.

Schäffer, A., Kästner, M., Trapp, S., 2018. A unified approach for including non-extractable residues (NER) of chemicals and pesticides in the assessment of persistence. Environmental Sciences Europe 30, 51.

Schilderman, P.A.E.L., Moonen, E.J.C., Maas, L.M., Welle, I., Kleinjans, J.C.S., 1999. Use of Crayfish in Biomonitoring Studies of Environmental Pollution of the River Meuse. Ecotoxicology and Environmental Safety 44, 241-252.

Schultz, M.M., Furlong, E.T., Kolpin, D.W., Werner, S.L., Schoenfuss, H.L., Barber, L.B.,

Blazer, V.S., Norris, D.O., Vajda, A.M., 2010. Antidepressant Pharmaceuticals in Two U.S. Effluent-Impacted Streams: Occurrence and Fate in Water and Sediment, and Selective Uptake in Fish Neural Tissue. Environmental Science & Technology 44, 1918-1925.

Schwab, K., Brack, W., 2007. Large volume TENAX® extraction of the bioaccessible fraction of sediment-associated organic compounds for a subsequent effect-directed analysis. Journal of Soils and Sediments 7, 178-186.

Schwarzenbach, R.P., Gschwend, P.M., Imboden, D.M., 2017. Environmental organic chemistry. Wiley-Interscience, New Jersey, USA.

Semple, K.T., Doick, K.J., Jones, K.C., Burauel, P., Craven, A., Harms, H., 2004. Defining bioavailability and bioaccessibility of contaminated soil and sediment is complicated. Environmental Science & Technology 38, 228a-231a.

Sherwood, C.R., Drake, D.E., Wiberg, P.L., Wheatcroft, R.A., 2002. Prediction of the fate of p,p′-DDE in sediment on the Palos Verdes shelf, California, USA. Continental Shelf Research 22, 1025-1058.

Shindell, O., Mica, N., Ritzer, M., Gordon, V.D., 2015. Specific adhesion of membranes simultaneously supports dual heterogeneities in lipids and proteins. Physical Chemistry Chemical Physics 17, 15598-15607.

Sijm, D., Kraaij, R., Belfroid, A., 2000. Bioavailability in soil or sediment: exposure of different organisms and approaches to study it. Environmental Pollution 108, 113-119.

Silveira, M.A.K., Caldas, S.S., Guilherme, J.R., Costa, F.P., Guimaraes, B.D., Cerqueira, M.B.R., Soares, B.M., Primel, E.G., 2013. Quantification of Pharmaceuticals and

Personal Care Product Residues in Surface and Drinking Water Samples by SPE and LC-ESI-MS/MS. Journal of the Brazilian Chemical Society 24, 1385-1395.

Simpson, S.L., Campana, O., Ho, K.T., 2016. Chapter 7 - Sediment Toxicity Testing. in: Blasco, J., Chapman, P.M., Campana, O., Hampel, M. (Eds.). Marine Ecotoxicology. Academic Press, pp. 199-237.

Skipper, H.D., Arthur G. Wollum, II, Turco, R.F., Duane, C.W., 1996. Microbiological Aspects of Environmental Fate Studies of Pesticides. Weed Technology 10, 174-190.

Sobol, I.M., 2001. Global sensitivity indices for nonlinear mathematical models and their Monte Carlo estimates. Mathematics and Computers in Simulation 55, 271-280.

Sochaczewski, Ł., Tych, W., Davison, B., Zhang, H., 2007. 2D DGT induced fluxes in sediments and soils (2D DIFS). Environmental Modelling & Software 22, 14-23.

Sorensen, J.P.R., Lapworth, D.J., Nkhuwa, D.C.W., Stuart, M.E., Gooddy, D.C., Bell, R.A., Chirwa, M., Kabika, J., Liemisa, M., Chibesa, M., Pedley, S., 2015. Emerging contaminants in urban groundwater sources in Africa. Water Research 72, 51-63.

Stein, K., Ramil, M., Fink, G., Sander, M., Ternes, T.A., 2008. Analysis and Sorption of Psychoactive Drugs onto Sediment. Environmental Science & Technology 42, 6415-6423.

Stroski, K.M., Challis, J.K., Wong, C.S., 2018. The influence of pH on sampler uptake for an improved configuration of the organic-diffusive gradients in thin films passive sampler. Analytica Chimica Acta 1018, 45-53.

Styszko, K., 2016. Sorption of emerging organic micropollutants onto fine sediments in a water supply dam reservoir, Poland. Journal of Soils and Sediments 16, 677-686.

Sugano, K., Kansy, M., Artursson, P., Avdeef, A., Bendels, S., Di, L., Ecker, G.F., Faller, B., Fischer, H., Gerebtzoff, G., Lennernaes, H., Senner, F., 2010. Coexistence of passive and carrier-mediated processes in drug transport. Nature Reviews Drug Discovery 9, 597-614.

Sun, H., Gao, B., Gao, L., Xu, D., Sun, K., 2019. Using diffusive gradients in thin films (DGT) and DGT-induced fluxes in sediments model to assess the dynamic release of copper in sediment cores from the Three Gorges Reservoir, China. Science of The Total Environment 672, 192-200.

Sun, N., Chen, Y., Xu, S., Zhang, Y., Fu, Q., Ma, L., Wang, Q., Chang, Y., Man, Z., 2018. Remobilization and bioavailability of polycyclic aromatic hydrocarbons from estuarine sediments under the effects of Nereis diversicolor bioturbation. Environmental Pollution 242, 931-937.

Talley, J.W., Ghosh, U., Tucker, S.G., Furey, J.S., Luthy, R.G., 2002. Particle-Scale Understanding of the Bioavailability of PAHs in Sediment. Environmental science & technology 36, 477-483.

Taylor, A.C., Fones, G.R., Mills, G.A., 2020. Trends in the use of passive sampling for monitoring polar pesticides in water. Trends in Environmental Analytical Chemistry 27, e00096.

ten Hulscher, T.E.M., Vrind, B.A., van den Heuvel, H., van der Velde, L.E., van Noort, P.C.M., Beurskens, J.E.M., Govers, H.A.J., 1999. Triphasic Desorption of Highly Resistant Chlorobenzenes, Polychlorinated Biphenyls, and Polycyclic Aromatic Hydrocarbons in Field Contaminated Sediment. Environmental Science & Technology 33, 126-132.

ter Laak, T.L., van Eijkeren, J.C.H., Busser, F.J.M., van Leeuwen, H.P., Hermens, J.L.M., 2009. Facilitated Transport of Polychlorinated Biphenyls and Polybrominated Diphenyl Ethers by Dissolved Organic Matter. Environmental Science & Technology 43, 1379-1385.

Thibodeaux, L.J., Valsaraj, K.T., Reible, D.D., 2001. Bioturbation-Driven Transport of Hydrophobic Organic Contaminants from Bed Sediment. Environmental Engineering Science 18, 215-223.

Thomann, R.V., 1989. Bioaccumulation model of organic chemical distribution in aquatic food chains. Environmental Science & Technology 23, 699-707.

Thomann, R.V., Connolly, J.P., Parkerton, T.F., 1992. An equilibrium model of organic chemical accumulation in aquatic food webs with sediment interaction. Environmental Toxicology and Chemistry 11, 615-629.

Thomann, R.V., Komlos, J., 1999. Model of biota-sediment accumulation factor for polycyclic aromatic hydrocarbons. Environmental Toxicology and Chemistry 18, 1060-1068.

Togola, A., Budzinski, H., 2007. Development of Polar Organic Integrative Samplers for Analysis of Pharmaceuticals in Aquatic Systems. Analytical Chemistry 79, 6734-6741.

Torri, S.I., CorrÊA, R.S., Renella, G., 2017. Biosolid Application to Agricultural Land—a Contribution to Global Phosphorus Recycle: A Review. Pedosphere 27, 1-16.

Tran, A.T.K., Hyne, R.V., Doble, P., 2007. Calibration of a passive sampling device for time-integrated sampling of hydrophilic herbicides in aquatic environments. Environmental Toxicology and Chemistry 26, 435-443.

Trimble, T.A., You, J., Lydy, M.J., 2008. Bioavailability of PCBs from field-collected sediments:

Application of Tenax extraction and matrix-SPME techniques. Chemosphere 71, 337-344.

Ugochukwu, U.C., 2019. Chapter 9 - Characteristics of clay minerals relevant to bioremediation of environmental contaminated systems. in: Mercurio, M., Sarkar, B., Langella, A. (Eds.). Modified Clay and Zeolite Nanocomposite Materials. Elsevier, pp. 219-242.

Uher, E., Zhang, H., Santos, S., Tusseau-Vuillemin, M.-H., Gourlay-Francé, C., 2012. Impact of Biofouling on Diffusive Gradient in Thin Film Measurements in Water. Analytical Chemistry 84, 3111-3118.

UN-Water, 2009. The United Nations World Water Development Report 3: Water in a changing world. Earthscan, Paris/New York.

Urík, J., Paschke, A., Vrana, B., 2020. Diffusion coefficients of polar organic compounds in agarose hydrogel and water and their use for estimating uptake in passive samplers. Chemosphere 249, 126183.

Urík, J., Vrana, B., 2019. An improved design of a passive sampler for polar organic compounds based on diffusion in agarose hydrogel. Environmental Science and Pollution Research 26, 15273-15284.

USEPA, 2000. Methods for measuring the toxicity and bioaccumulation of sediment-associated contaminants with freshwater invertebrates. Office of Health and Environmental Assessment Washington, DC, USA.

Valili, S., Siavalas, G., Karapanagioti, H.K., Manariotis, I.D., Christanis, K., 2013. Phenanthrene removal from aqueous solutions using well-characterized, raw, chemically treated, and charred malt spent rootlets, a food industry by-product. Journal

of Environmental Management 128, 252-258.

van Leeuwen, H.P., Town, R.M., Buffle, J., Cleven, R.F.M.J., Davison, W., Puy, J., van Riemsdijk, W.H., Sigg, L., 2005. Dynamic Speciation Analysis and Bioavailability of Metals in Aquatic Systems. Environmental Science & Technology 39, 8545-8556.

Vanderford, B.J., Pearson, R.A., Rexing, D.J., Snyder, S.A., 2003. Analysis of Endocrine Disruptors, Pharmaceuticals, and Personal Care Products in Water Using Liquid Chromatography/Tandem Mass Spectrometry. Analytical Chemistry 75, 6265-6274.

Vasquez, M.I., Lambrianides, A., Schneider, M., Kümmerer, K., Fatta-Kassinos, D., 2014. Environmental side effects of pharmaceutical cocktails: What we know and what we should know. Journal of Hazardous Materials 279, 169-189.

Verhougstraete, M.P., Martin, S.L., Kendall, A.D., Hyndman, D.W., Rose, J.B., 2015. Linking fecal bacteria in rivers to landscape, geochemical, and hydrologic factors and sources at the basin scale. Proceedings of the National Academy of Sciences 112, 10419.

Vermeirssen, E.L.M., Dietschweiler, C., Escher, B.I., van der Voet, J., Hollender, J., 2012. Transfer Kinetics of Polar Organic Compounds over Polyethersulfone Membranes in the Passive Samplers Pocis and Chemcatcher. Environmental Science & Technology 46, 6759-6766.

Vieno, N., Sillanpää, M., 2014. Fate of diclofenac in municipal wastewater treatment plant — A review. Environment International 69, 28-39.

Vodyanitskii, Y.N., Yakovlev, A.S., 2016. Contamination of soils and groundwater with new organic micropollutants: A review. Eurasian Soil Science 49, 560-569.

Voice, T.C., Weber, W.J., 1983. Sorption of hydrophobic compounds by sediments, soils and

suspended solids—I. Theory and background. Water Research 17, 1433-1441.

Vrana, B., Allan, I.J., Greenwood, R., Mills, G.A., Dominiak, E., Svensson, K., Knutsson, J., Morrison, G., 2005. Passive sampling techniques for monitoring pollutants in water. TrAC Trends in Analytical Chemistry 24, 845-868.

Vrana, B., Popp, P., Paschke, A., Schüürmann, G., 2001. Membrane-Enclosed Sorptive Coating. An Integrative Passive Sampler for Monitoring Organic Contaminants in Water. Analytical Chemistry 73, 5191-5200.

Wang, P., Challis, J.K., Luong, K.H., Vera, T.C., Wong, C.S., 2021. Calibration of organic-diffusive gradients in thin films (o-DGT) passive samplers for perfluorinated alkyl acids in water. Chemosphere 263, 128325.

Wang, Q., Kelly, B.C., 2018. Assessing bioaccumulation behaviour of hydrophobic organic contaminants in a tropical urban catchment. Journal of Hazardous Materials 358, 366-375.

Wang, R., Jones, K.C., Zhang, H., 2020a. Monitoring Organic Pollutants in Waters Using the Diffusive Gradients in the Thin Films Technique: Investigations on the Effects of Biofouling and Degradation. Environmental Science & Technology 54, 7961-7969.

Wang, R., Zou, Y., Luo, J., Jones, K.C., Zhang, H., 2019. Investigating Potential Limitations of Current Diffusive Gradients in Thin Films (DGT) Samplers for Measuring Organic Chemicals. Analytical Chemistry 91, 12835-12843.

Wang, W.W., Jiang, X., Zheng, B.H., Chen, J.Y., Zhao, L., Zhang, B., Wang, S.H., 2018. Composition, mineralization potential and release risk of nitrogen in the sediments of Keluke Lake, a Tibetan Plateau freshwater lake in China. Royal Society Open Science

5, 180612.

Wang, X.-C., Zhang, Y.-X., Chen, R.F., 2001. Distribution and Partitioning of Polycyclic Aromatic Hydrocarbons (PAHs) in Different Size Fractions in Sediments from Boston Harbor, United States. Marine Pollution Bulletin 42, 1139-1149.

Wang, Z., Elimelech, M., Lin, S., 2016. Environmental Applications of Interfacial Materials with Special Wettability. Environmental Science & Technology 50, 2132-2150.

Wang, Z., Walker, G.W., Muir, D.C.G., Nagatani-Yoshida, K., 2020b. Toward a Global Understanding of Chemical Pollution: A First Comprehensive Analysis of National and Regional Chemical Inventories. Environmental Science & Technology 54, 2575-2584.

Weber, W.J., Huang, W., 1996. A Distributed Reactivity Model for Sorption by Soils and Sediments. 4. Intraparticle Heterogeneity and Phase-Distribution Relationships under Nonequilibrium Conditions. Environmental Science & Technology 30, 881-888.

Wei, M., Yang, X., Watson, P., Yang, F., Liu, H., 2019. A cyclodextrin polymer membrane-based passive sampler for measuring triclocarban, triclosan and methyl triclosan in rivers. Science of The Total Environment 648, 109-115.

Weinberger, J., Klaper, R., 2014. Environmental concentrations of the selective serotonin reuptake inhibitor fluoxetine impact specific behaviors involved in reproduction, feeding and predator avoidance in the fish Pimephales promelas (fathead minnow). Aquatic Toxicology 151, 77-83.

Westrin, B.A., Axelsson, A., Zacchi, G., 1994. Diffusion measurement in gels. Journal of Controlled Release 30, 189-199.

Wetzel, J.E., 2002. Form Alternation of Adult Female Crayfishes of the Genus Orconectes

(Decapoda: Cambaridae). The American Midland Naturalist 147, 326-337.

White, D.S., Keilty, T.J., 1988. Burrowing avoidance assays of contaminated Detroit River sediments, using the freshwater OligochaeteStylodrilus heringianus (Lumbriculidae). Archives of Environmental Contamination and Toxicology 17, 673-681.

White, R.E., Torri, S.I., Corrêa, R.S., 2011. Biosolids Soil Application: Agronomic and Environmental Implications. Applied and Environmental Soil Science 2011, 928973.

Wilke, C.R., Chang, P., 1955. Correlation of diffusion coefficients in dilute solutions. AIChE Journal 1, 264-270.

Wilkinson, J., Hooda, P.S., Barker, J., Barton, S., Swinden, J., 2017. Occurrence, fate and transformation of emerging contaminants in water: An overarching review of the field. Environmental Pollution 231, 954-970.

Woessner, W.W., 2017. Chapter 8 - Hyporheic Zones. in: Hauer, F.R., Lamberti, G.A. (Eds.). Methods in Stream Ecology, Volume 1 (Third Edition). Academic Press, Boston, pp. 129-157.

Xie, H., Chen, Q., Chen, J., Chen, C.-E.L., Du, J., 2018. Investigation and application of diffusive gradients in thin-films technique for measuring endocrine disrupting chemicals in seawaters. Chemosphere 200, 351-357.

Xie, H., Dong, Y., Chen, J., Wang, X., Fu, M., 2021. Development and evaluation of a ceramic diffusive layer based DGT technique for measuring organic micropollutants in seawaters. Environment International 156, 106653.

Xing, B., Pignatello, J.J., Gigliotti, B., 1996. Competitive Sorption between Atrazine and Other Organic Compounds in Soils and Model Sorbents. Environmental Science &

Technology 30, 2432-2440.

Yamamoto, H., Liljestrand, H.M., Shimizu, Y., Morita, M., 2003. Effects of Physical−Chemical Characteristics on the Sorption of Selected Endocrine Disruptors by Dissolved Organic Matter Surrogates. Environmental Science & Technology 37, 2646-2657.

Yao, L., Steinman, A.D., Wan, X., Shu, X., Xie, L., 2019. A new method based on diffusive gradients in thin films for in situ monitoring microcystin-LR in waters. Sci Rep 9, 17528.

Yao, Y., Gao, B., Fang, J., Zhang, M., Chen, H., Zhou, Y., Creamer, A.E., Sun, Y., Yang, L., 2014. Characterization and environmental applications of clay–biochar composites. Chemical Engineering Journal 242, 136-143.

Yin, H., Cai, Y., Duan, H., Gao, J., Fan, C., 2014. Use of DGT and conventional methods to predict sediment metal bioavailability to a field inhabitant freshwater snail (Bellamya aeruginosa) from Chinese eutrophic lakes. Journal of Hazardous Materials 264, 184-194.

Yin, X., Guo, C., Lv, J., Hou, S., Zhang, Y., Jin, X., Teng, Y., Xu, J., 2019. Biomimetic Accumulation of Methamphetamine and Its Metabolite Amphetamine by Diffusive Gradients in Thin Films to Estimate Their Bioavailability in Zebrafish. Environmental Science & Technology Letters 6, 708-713.

You, J., Landrum, P.F., Trimble, T.A., Lydy, M.J., 2007. Availability of polychlorinated biphenyls in field-contaminated sediment. Environmental Toxicology and Chemistry 26, 1940-1948.

You, N., Li, J.-Y., Fan, H.-T., Shen, H., 2019. In-situ sampling of nitrophenols in industrial

wastewaters using diffusive gradients in thin films based on lignocellulose-derived activated carbons. Journal of Advanced Research 15, 77-86.

Yuan-Hui, L., Gregory, S., 1974. Diffusion of ions in sea water and in deep-sea sediments. Geochimica et Cosmochimica Acta 38, 703-714.

Zeng, Y.-H., Zhang, T.-T., Chena, Y.-R., 2019. Study about Hydrophilic Modification of PTFE Membrane. Journal of Fiber Bioengineering and Informatics 12, 73-80.

Zhang, C., Ding, S., Xu, D., Tang, Y., Wong, M.H., 2014. Bioavailability assessment of phosphorus and metals in soils and sediments: a review of diffusive gradients in thin films (DGT). Environmental Monitoring and Assessment 186, 7367-7378.

Zhang, H., Davison, W., 1995. Performance Characteristics of Diffusion Gradients in Thin Films for the in Situ Measurement of Trace Metals in Aqueous Solution. Analytical Chemistry 67, 3391-3400.

Zhang, H., Davison, W., 1999. Diffusional characteristics of hydrogels used in DGT and DET techniques. Analytica Chimica Acta 398, 329-340.

Zhang, H., Davison, W., Gadi, R., Kobayashi, T., 1998a. In situ measurement of dissolved phosphorus in natural waters using DGT. Analytica Chimica Acta 370, 29-38.

Zhang, H., Davison, W., Knight, B., McGrath, S., 1998b. In Situ Measurements of Solution Concentrations and Fluxes of Trace Metals in Soils Using DGT. Environmental Science & Technology 32, 704-710.

Zhang, H., Davison, W., Tye, A.M., Crout, N.M.J., Young, S.D., 2006. Kinetics of zinc and cadmium release in freshly contaminated soils. Environmental Toxicology and Chemistry 25, 664-670.

Zhang, H., Zhao, F.-J., Sun, B., Davison, W., McGrath, S.P., 2001. A New Method to Measure Effective Soil Solution Concentration Predicts Copper Availability to Plants. Environmental Science & Technology 35, 2602-2607.

Zhang, M., Tao, S., Wang, X., 2020. Interactions between organic pollutants and carbon nanomaterials and the associated impact on microbial availability and degradation in soil: a review. Environmental Science: Nano 7, 2486-2508.

Zhang, W., Ding, Y., Boyd, S.A., Teppen, B.J., Li, H., 2010. Sorption and desorption of carbamazepine from water by smectite clays. Chemosphere 81, 954-960.

Zhang, Y., Zhang, T., Guo, C., Hou, S., Hua, Z., Lv, J., Zhang, Y., Xu, J., 2018. Development and application of the diffusive gradients in thin films technique for simultaneous measurement of methcathinone and ephedrine in surface river water. Science of The Total Environment 618, 284-290.

Zhao, Z., Zhang, L., Wu, J., Fan, C., 2009. Distribution and bioaccumulation of organochlorine pesticides in surface sediments and benthic organisms from Taihu Lake, China. Chemosphere 77, 1191-1198.

Zheng, J.-L., Guan, D.-X., Luo, J., Zhang, H., Davison, W., Cui, X.-Y., Wang, L.-H., Ma, L.Q., 2015. Activated Charcoal Based Diffusive Gradients in Thin Films for in Situ Monitoring of Bisphenols in Waters. Analytical Chemistry 87, 801-807.

Zou, Y.-T., Fang, Z., Li, Y., Wang, R., Zhang, H., Jones, K.C., Cui, X.-Y., Shi, X.-Y., Yin, D., Li, C., Liu, Z.-D., Ma, L.Q., Luo, J., 2018. Novel Method for in Situ Monitoring of Organophosphorus Flame Retardants in Waters. Analytical Chemistry 90, 10016-10023.